Alma Mater Studiorum
Università di Bologna

Dottorato di ricerca in

SCIENZE FARMACEUTICHE

***Ciclo* XXIII**

***Settore scientifico-disciplinare di afferenza*: CHIM/06**

Title of Dissertation

SYNTHETIC STRATEGIES OF NEW MOLECULAR PARAMAGNETIC MECHANICALLY-INTERLOCKED COMPLEXES

Dissertation presented by

Dr.ssa Costanza Casati

Coordinatore Dottorato

Prof. Maurizio Recanatini

Relatore

Prof. Marco Lucarini

Esame finale anno 2010

ABSTRACT

Supramolecular chemistry is a multidisciplinary field which impinges on various other disciplines, referring to the area of chemistry beyond the molecules, which focuses on the chemical systems made up of a discrete number of assembled molecular subunits or components. The forces responsible for the spatial organization are intermolecular interactions (bonds), of a reversible nature, to form a supramolecular aggregate. These intermolecular bonds include electrostatic interactions, hydrogen bonding, π–π interactions, dispersion interactions and hydrophobic or solvophobic effects, so, while traditional chemistry focuses on the covalent bond, supramolecular chemistry examines the weaker and reversible noncovalent interactions between molecules.

It can be split into two broad categories; *host–guest chemistry* and *self-assembly*. The difference between these two areas is a question of size and shape. If one molecule is significantly larger than another and can wrap around it then it is termed the ‘host’ and the smaller molecule is its ‘guest’, which becomes enveloped by the host.

The supramolecular architectures I was interested in during my PhD are Rotaxanes and Catenanes; a rotaxane is a mechanically-interlocked molecular architecture consisting of a "dumbbell shaped molecule" which is threaded through a "macrocycle"; the stoppers at the end of the dumbbell are larger than the internal diameter of the ring and prevent disassociation (unthreading) of the components. A catenane consists of two or more interlocked macrocycles which cannot be separated without breaking the covalent bonds.

This Thesis, organized into six Chapters, describes mainly some synthetic strategies of new molecular paramagnetic mechanically interlocked complexes; the aim is actually to introduce one or more paramagnetic units: this allows to use the ESR spectroscopy to investigate complexation properties of these systems cause this technique works in the same time scale of supramolecular assemblies.

Chapter 1 underlines the main concepts upon which supramolecular chemistry is based, clarifying the nature of supramolecular interactions, the main principles of host-guest chemistry and the concept of molecular device, one of the possible applications of supramolecular chemistry within the field of nanochemistry.

In **chapter 2** it is pointed out the use of ESR spectroscopy to investigate the properties of purely organic non-covalent assemblies in liquid solution by spin labels and spin probes. Nitroxides are widely used as spin labels or spin probes thanks to the sensitivity of the nitroxide functionality to its surroundings; then magnitude of the ^{14}N hyperfine splitting constants, $a(N)$ and g-factor, depend on the polarity of the environment, while the lines shape of the EPR spectra reflect the probe’s

motional dynamics. Further advantages in using EPR spectroscopy are the sensitivity of the method, the possibility of obtaining kinetic information in the submicrosecond time range, the ability to measure tumbling rates on the nanosecond timescale and distances between spin labels in close proximity.

The **chapter 3** deals with the synthesis of a new class of π-electron-deficient tetracationic cyclophane ring, cyclobis(paraquat-*p*-phenylene), carrying one or two paramagnetic side-arms based on 2,2,6,6-tetramethylpiperidine-N-oxyl (TEMPO) moiety, by the clipping approach in the presence of 1,5-dimethoxynaphthalene (DMN), an electron-rich template which allows the isolation of the complex. The two new receptors based on CBPQT tetracation bringing one or two paramagnetic substituents on the paraphenylene units represent promising hosts in the synthesis of more complexed paramagnetic supramolecular architectures, rotaxanes or catenanes, employed as molecular magnetic devices.

In the **chapter 4**, the Huisgen 1,3-dipolar cycloaddition is exploited to synthesis of rotaxanes having paramagnetic α-cyclodextrins as wheels; the choice of a bulk sugar moiety (lactose) as an end cap group and a decane axle revealed to be essential to form radical rotaxanes as both the saccharidic group and the alkane chain length enhance the solubility in water of the half threads and the affinity for the host molecule, respectively, so the synthesis of the first diradical rotaxane was achieved, in which both the components of the assembly, macrocycle and axle, brought a TEMPO moiety. First ESR studies on the behavior of this new species indicate that the two radicals are spin exchanging and these results are in accord with a supramolecular structure which possesses features of a magnetic molecular switch.

In the **chapter 5**, the catalysis of Huisgen's cycloaddition by CB[6] is exploited to synthesize paramagnetic CB[6]-based [3]-rotaxanes having the TEMPO unit as stoppers. Firstly a [3]-rotaxane having an aromatic core was synthesized and the rigid structure, in which the movement of the rings upon the axle isn't allowed, made possible to obtain for the first time the exact distance between paramagnetic centers using PELDOR technique. The PELDOR trace is in agreement with a distance of 30.6 Å between the two terminal units. Then, in order to obtain a pH-driven reversibile molecular switch, a paramagnetic CB[6]-based [3]-rotaxane having a decyl spacer was synthesized. NMR spectra at different pH confirmed that this rotaxane behaves as a pH-driven reversible molecular switch and exhibits conformational changes caused by the movement of rings under base, acid and heat stimuli from one location to another.

In the **chapter 6** I reported the first preliminary studies of Actinoid series as a new class of templates in catenanes' synthesis; Metal ion templates played a key role in the development of macrocyclic ligand chemistry and its derivative chemistries, constituting a multifunctional center

about which molecular turns of various kinds are readily oriented. Metal ions with a range of different two- and three-dimensional coordination geometries have been used as a template for the synthesis of catenanes and rotaxanes; being *f-block elements*, so having the property of expanding the valence state, they constitute promising candidates as chemical templates offering the possibility of create a complex with coordination number beyond 6. Electron-rich ligands of the necessary geometry were synthesized and studied in their complexation properties with $Ti(Cl)_4$, a cation having similar electronic properties.

TABLE OF CONTENTS

Chapter 1. Concepts

1.1 Introduction

The desire to design, using functional small-molecule building blocks, new synthetic materials that feature even more useful ensemble properties emanating directly from nanoscale and microscale ordering and the need for improved miniaturization and device performance in the microelectronics industry has inspired many investigations into supramolecular chemistry, which deals with the chemistry and collective behaviour of organized ensembles of molecules.
As one of the modern frontiers in chemistry, supramolecular chemistry heralds many promises that range from biocompatible materials and biomimetic catalysts to sensors and nanoscale fabrication of electronic devices.

1.2 What is Supramolecular Chemistry?

Supramolecular chemistry[1] has been defined by one of its leading proponents, Jean-Marie Lehn, who won the Nobel Prize for his work in the area in 1987, as the 'chemistry of molecular assemblies and of the intermolecular bond'. More colloquially this may be expressed as 'chemistry beyond the molecule'. Other definitions include phrases such as 'the chemistry of the non-covalent bond' and 'non-molecular chemistry'. Originally supramolecular chemistry was defined in terms of the non-covalent interaction between a 'host' and a 'guest' molecule as highlighted in Figure 1.1, which illustrates the relationship between molecular and supramolecular chemistry in terms of both structures and function.
These descriptions, while helpful, are by their nature noncomprehensive and there are many exceptions if such definitions are taken too literally. The problem may be linked to the definition of organometallic chemistry as 'the chemistry of compounds with metal-to-carbon bonds'. This immediately rules out Wilkinson's compound, $RhCl(PPh_3)_3$, for example, which is one of the most important industrial catalysts for organometallic transformations known in the field. Indeed, it is often the objectives and thought processes of the chemist undertaking the work, as much as the work itself, which determine its field. Work in modern supramolecular chemistry encompasses not just host-guest systems but also molecular devices and machines, molecular recognition, so called 'self-processes' such as self-assembly and self-organisation and has interfaces with the emergence of complex matter and nanochemistry.

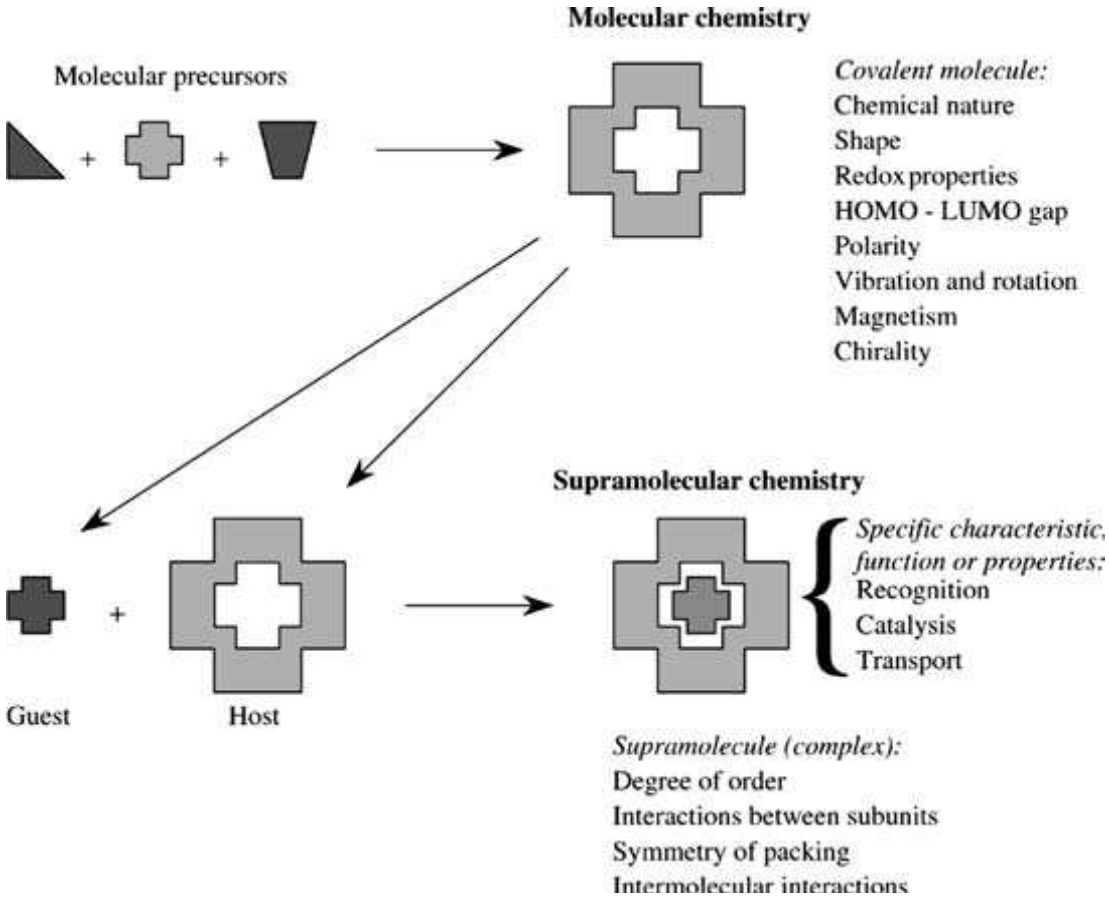

Figure 1.1. Comparison between the scope of molecular and supramolecular chemistry according to Lehn.

As a distinct area, supramolecular chemistry dates back to the late 1960s, although early examples of supramolecular systems can be found at the beginning of modern-day chemistry, for example, the discovery of chlorine clathrate hydrate, the inclusion of chlorine within a solid water lattice, by Sir Humphrey Davy in 1810.

So, *what is supramolecular chemistry*?[2] It has been described as 'chemistry beyond the molecule', whereby a 'supermolecule' is a species that is held together by non-covalent interactions between two or more covalent molecules or ions. It can also be described as 'lego™ chemistry' in which each lego™ brick represents a molecular building block and these blocks are held together by intermolecular interactions (bonds), of a reversible nature, to form a supramolecular aggregate. These intermolecular bonds include electrostatic interactions, hydrogen bonding, $\pi-\pi$ interactions, dispersion interactions and hydrophobic or solvophobic effects.†

Supramolecular chemistry is a multidisciplinary field which impinges on various other disciplines, such as the traditional areas of organic and inorganic chemistry, needed to synthesise the precursors

for a supermolecule, physical chemistry, to understand the properties of supramolecular systems and computational modelling to understand complex supramolecular behaviour. A great deal of biological chemistry involves supramolecular concepts and in addition a degree of technical knowledge is required in order to apply supramolecular systems to the real world, such as the development of *nanotechnological* devices.

Supramolecular chemistry can be split into two broad categories; *host–guest chemistry* and *self-assembly*. The difference between these two areas is a question of size and shape. If one molecule is significantly larger than another and can wrap around it then it is termed the 'host' and the smaller molecule is its 'guest', which becomes enveloped by the host (Figure 1.2(a)).

One definition of hosts and guests was given by Donald Cram, who said *The host component is defined as an organic molecule or ion whose binding sites converge in the complex… The guest component is any molecule or ion whose binding sites diverge in the complex*.[3] A *binding site* is a region of the host or guest that is of the correct size, geometry and chemical nature to interact with the other species. Thus, in Figure 1.2(a) the covalently synthesised host has four binding sites that converge on a central guest binding pocket. Host–guest complexes include biological systems, such as enzymes and their substrates, with enzymes being the host and the substrates the guest. In terms of coordination chemistry, metal–ligand complexes can be thought of as host–guest species, where large (often macrocyclic) ligands act as hosts for metal cations. If the host possesses a permanent

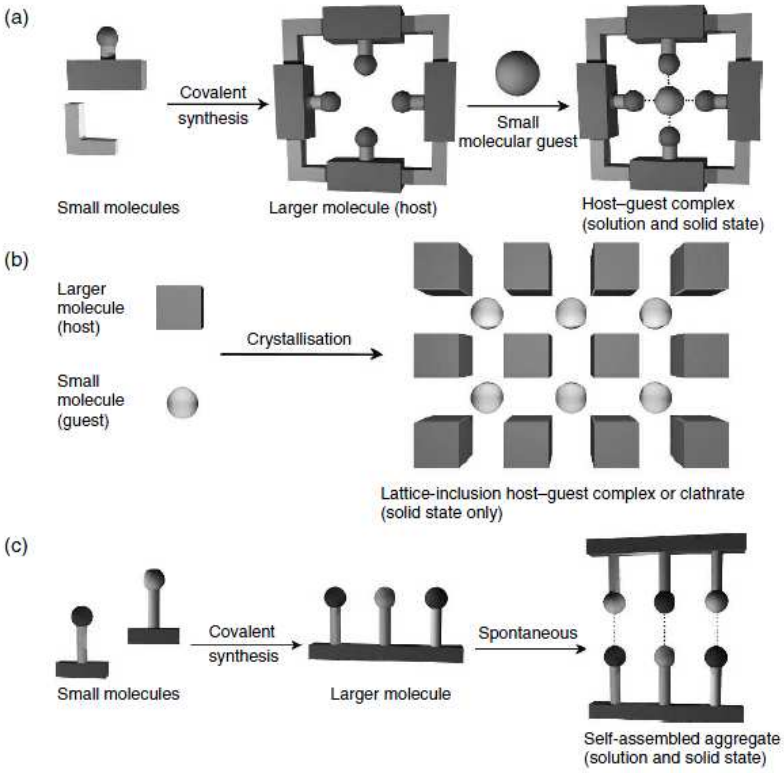

Figure 1.2. The development of a supramolecular system from molecular building blocks (binding sites represented by circles): (a) host–guest complexation; (b) lattice inclusion; (c) self-assembly between complementary molecules. (From reference 1)

molecular cavity containing specific guest binding sites, then it will generally act as a host both in solution and in the solid state and there is a reasonable likelihood that the solution and solid state structures will be similar to one another. On the other hand, the class of solid state inclusion compounds only exhibit host–guest behaviour as crystalline solids since the guest is bound within a cavity that is formed as a result of a hole in the packing of the host lattice. Such compounds are generally termed clathrates from the Greek klethra, meaning 'bars' (Figure 1.2(b)). Where there is no significant difference in size and no species is acting as a host for another, the non-covalent joining of two or more species is termed self-assembly. Strictly, self-assembly is an equilibrium between two or more molecular components to produce an aggregate with a structure that is dependent only on the information contained within the chimica building blocks (Figure 1.2(c)). This process is usually spontaneous but may be influenced by solvation or templation effects or in the case of solids by the nucleation and crystallisation processes.

Nature itself is full of supramolecular systems, for example, deoxyribonucleic acid (DNA) is made up from two strands which self-assemble via hydrogen bonds and aromatic stacking interactions to form the famous double helical structure (see Chapter 3, Section 3.2.4). The inspiration for many supramolecular species designed and developed by chemists has come from biological systems.

1.3. Supramolecular interactions

Non-covalent interactions represent the energies that hold supramolecular species together. Non-covalent interactions are considerably weaker than covalent interactions, which can range between ca. 150 kJ mol−1 to 450 kJ mol−1 for single bonds. Non-covalent bonds range from 2 kJ mol−1 for dispersion interactions to 300 kJ mol−1 for 'ion-ion' interactions. However, when these interactions are used in a co-operative manner a stable supramolecular complex can exist. The term 'non-covalent' includes a wide range of attractions and repulsions which are summarized in Table 1.1 and will be described in more detail in the following sub-sections.

Table 1.1 Summary of supramolecular interactions

Interaction	Strength (kJ mol^{-1})	Example
Ion–ion	200–300	Tetrabutylammonium chloride
Ion–dipole	50–200	Sodium [15]crown-5
Dipole–dipole	5–50	Acetone
Hydrogen bonding	4–120	(See Table 1.2)
Cation–π	5–80	K^+ in benzene
π–π	0–50	Benzene and graphite
van der Waals	< 5 kJ mol^{-1} but variable depending on surface area	Argon; packing in molecular crystals
Hydrophobic	Related to solvent–solvent interaction energy	Cyclodextrin inclusion compounds

1.3.1. Ionic and dipolar interactions[4]

Ionic and dipolar interactions can be split into three categories: (i) *ion-ion interactions*, (ii) *ion-dipole interactions*, and (iii) *dipole-dipole interactions*, which are based on the Coulombic attraction between opposite charges. The strongest of these interactions is the ion-ion (Figure 1.3(a)), comparable with covalent interactions. Ion-ion interactions are non-directional in nature, meaning that the interaction can occur in any orientation. Ion-dipole (Figure 1.3(b)) and dipole-dipole interactions (Figure 1.3 (c)), however, have orientation-dependant aspects requiring two entities to be aligned such that the interactions are in the optimal direction. Due to the relative rigidity of directional interactions, only mutually complementary species are able to form aggregates, whereas non-directional interactions can stabilise a wide range of molecular pairings. The strength of these directional interactions depends upon the species involved. Ion-dipole interactions are stronger than dipole-dipole interactions (50-200 and 5-50 kJ mol^{-1}, respectively) as ions have a higher charge density than dipoles. Despite being the weakest directional interaction, dipole-dipole interactions are useful for bringing species into alignment, as the interaction requires a specific orientation of both entities.

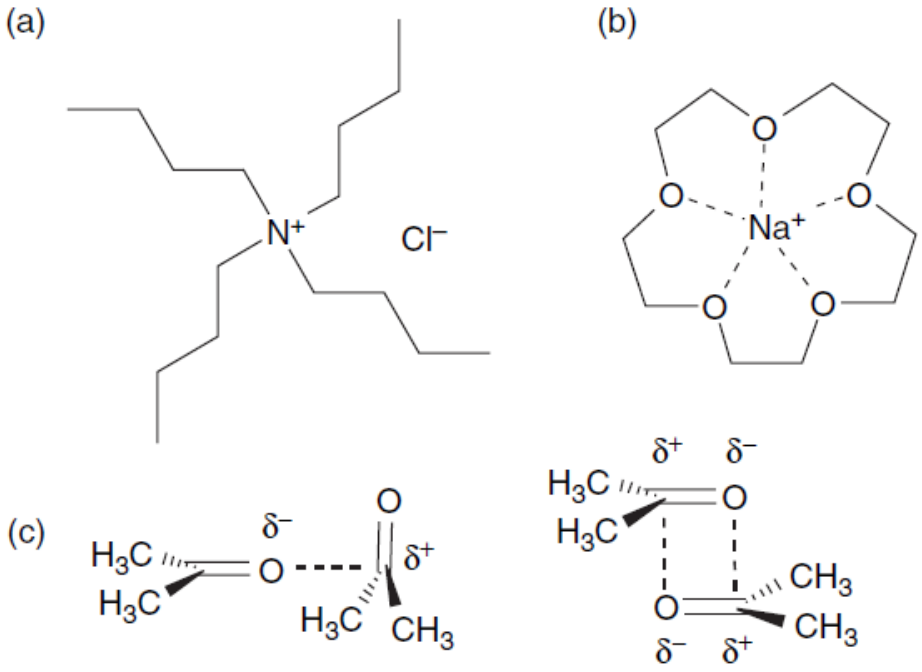

Figure 1.3. Examples of electrostatic interactions: (a) ion-ion interaction in tetrabutyilammonium chloride; (b) ion-dipole interactionin the sodium complex of [15]crown-5; (c) dipole-dipole interactions in acetone.

Electrostatic interactions play an important role in understanding the factors that influence high binding affinities, particularly in biological systems in which there is a large number of recognition processes that involve charge-charge interactions; indeed these are often the first interactions between a substrate and an enzyme.

1.3.2. Hydrogen bonding[5]

The *hydrogen bond* is arguably the most important non-covalent interaction in the design of supramolecular architectures, because of its strength and high degree of directionality. It represents a special kind of dipole-dipole interaction between a proton donor (D) and a proton acceptor (A). There are a number of naturally occurring 'building blocks' that are a rich source of hydrogen bond donors and acceptors (*e.g.* amino acids, carbohydrates and nucleo bases). Hydrogen bond donors are groups with a hydrogen atom attached to an electronegative atom (such as nitrose or oxygen), therefore forming a dipole with the hydrogen atom carrying a small positive charge. Hydrogen bond acceptors are dipoles with electron-withdrawing atoms by which the positively charge hydrogen atom can interact, for example, carbonyl moieties (Figure 1.4).

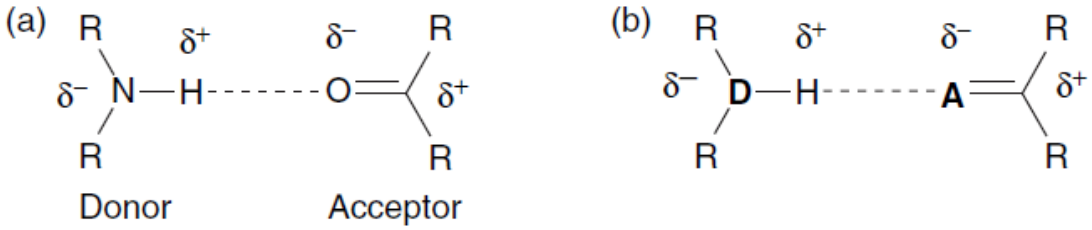

Figure 1.4. A carbonyl accepting a hydrogen bond from a secondary amine donor (a) and (b)

The strength of hydrogen bonds can be very different between various systems and is not necessarily correlated with the Brønstead acidity of the proton donor. It depends on the type of electronegative atom to which the hydrogen atom is attached and the geometry that the hydrogen bond adopts in the structure.

Typically, the strengths range from 4 to 120 kJ mol^{-1}, with the vast majority being under 60 kJ mol^{-1} and scales of hydrogen bond acidity and basicity have been developed.[6] The types of geometries that can be adopted in a hydrogen bonding complex are summarized in Figure 1.5.

The geometries displayed in Figure 1.5 are termed *primary hydrogen bond interactions* – this means that there is a direct interaction between the donor group and the acceptor group. There are also *secondary interactions* between neighbouring groups that must be considered. The partial

charges on adjacent atoms can either increase the binding strength by virtue of attraction between opposite charges or decrease the affinity due to repulsion between like charges.

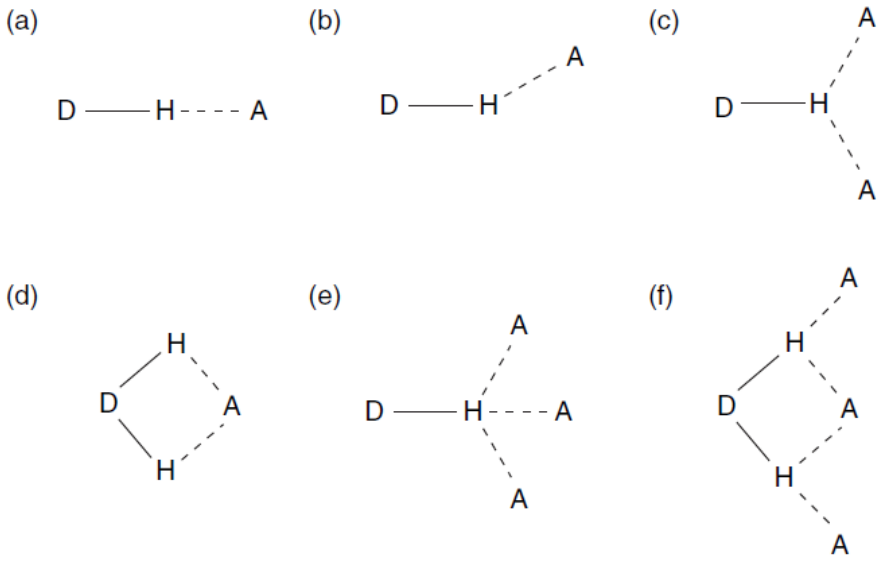

Figure 1.5. Various types of hydrogen bonding geometries: (a) linear; (b) bent; (c) donating bifurcated; (d) accepting bifurcated; (e) trifurcated; (f) three-centre bifurcated.

A real-life example of hydrogen bonding is the double helix of DNA. There are many hydrogen bond donors and acceptors holding base pairs together, as illustrated between the nucleobases cytosine I and guanine (G) in Figure 1.6.

The CG base pair has three primary interactions (*i.e.* traditional hydrogen bonds) and also has both attractive and repulsive secondary interactions.

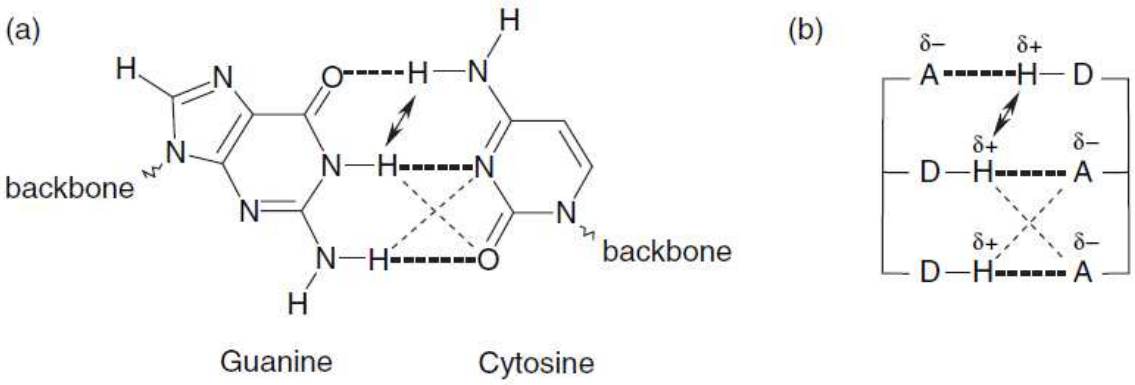

Figure 1.6. (a) Primary and secondary hydrogen bond interactions between guanine and cytosine base-pairs in DNA and (b) a schematic representation.

The highly directional nature of hydrogen bonding interactions, together with the specific alignment of hydrogen bond donors and acceptors, has proved to be a fruitful asset for the design of supramolecular systems.

1.3.3. π–Interactions

There are two main π-interactions that can be found in supramolecular systems, namely (i) cation–π interactions and (ii) π–π interactions. Cation–π interactions are well known in the field of organometallic chemistry, whereby olefinic groups are bound to transition metal centres, for example, ferrocene and Zeise's salt ($[PtCl_3(\eta^2\text{-}C_2H_4)]^-$), but these are not regarded as non-covalent interactions.[7]

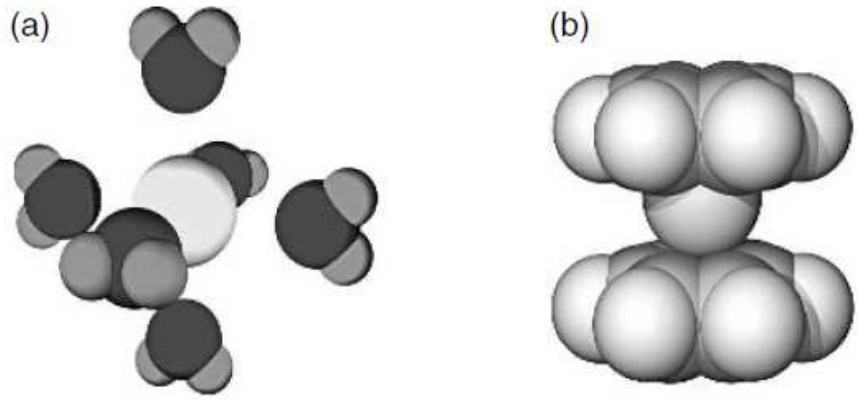

Figure 1.7 (a) Six or more water molecules can fit around K^+ whereas (b) there is space for only two benzene molecules.

However, alkaline- and alkaline-earth metals also form interactions with double-bond systems, typically between 5 and 80 kJ mol^{-1}. For example, the interaction of potassium ions with benzene has a similar energy to the K^+–OH_2 interaction. The potassium cation is more soluble in water than in benzene, however, as it is not sterically possible to fit as many benzene molecules around the metal ion as water molecules (Figure 1.7).

The two types of π–π interactions are *face-to-face*, whereby parallel ring-systems, separated by ca. 3.5 Å, are offset and the interaction is between the centre of one ring and the corner of another (Figure 1.8(a)), and *edge-to-face*, whereby a hydrogen atom from one ring interacts in a perpendicular orientation with respect to the centre of another ring (Figure 1.8(b)). These π–π interactions arise from the attraction between the negatively charge π-electron cloud of one conjugated system and the positively charged π-framework of a neighbouring molecule.[7]

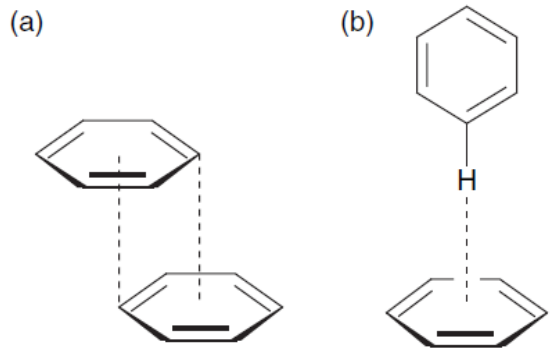

Figure 1.8 The two types of π–π interactions: (a) face-to-face; (b) edge-to-face.

The layered structure of graphite is held together by weak, face-to-face π-interactions and therefore feels 'slippery' (Figure 1.9). It is because of the slippage between layers that graphite can be used as a lubricant (albeit in the presence of oxygen). Interactions involving π-systems can be found in nature, for example, the weak face-to-face interactions between base-pairs along the length of the double helix are responsible for the shape of DNA.

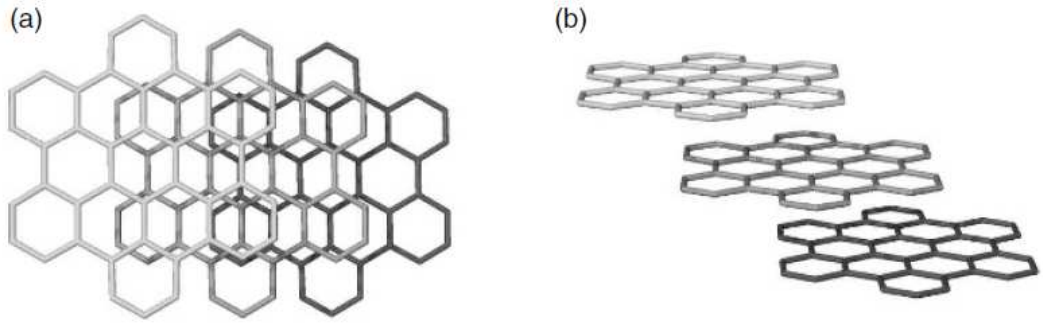

Figure 1.9 (a) Top and (b) side views of the layered structure of graphite, held together by face-to-face π-interactions.

1.3.4. van der Waals interactions[8]

Van der Waals interactions are dispersion effects that comprise two components, namely the *London interaction* and the *exchange and repulsion* interaction.

Van der Waals interactions arise from fluctuations of the electron distribution between species that are in close proximity to one another: as the electron cloud moves about a molecule's momentary location, an instantaneous dipole is formed within the molecule. This 'flickering' of electron distribution (or dipole) between two adjacent species will align the molecules such that a partial positive charge from one species will be attracted to a partial negative charge from another molecule (Figure 1.10); therefore, the two instantaneous dipoles attract one another and produce a London interaction whose strength is dependant on the polarisability of the molecule; the more

polarisable the species, then the greater the strength of the interaction. The potential energy of the London interaction decreases rapidly as the distance between the molecules increases (this depends on the reciprocal of the sixth power of the distance r – an r^{-6} dependence). These interactions are non-directional and do not feature highly in supramolecular design, but van der Waals interactions are important in the formation of inclusion compounds, in which small organic molecules are incorporated into a crystalline lattice, or where small organic molecules have been encapsulated into permanent molecular cavities.

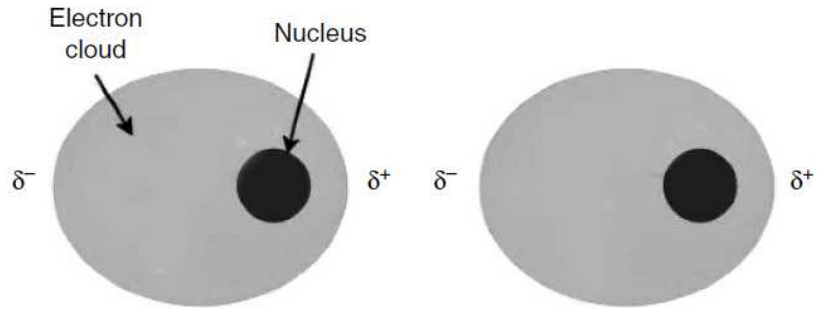

Figure 1.10 A London interaction between two argon atoms. The shift of the electron cloud around the nucleus produces instantaneous dipoles that attract each other.

In the solid state, species tend to align so there is a maximum number of interactions between each molecule, which minimises the lattice energy of the solid state structure. This close packing arrangement has been rationalized by Kitaigorodskii in a classic treatise.[9] As molecules 'grow' into a crystal, they arrange themselves so that all of the void space is occupied, to achieve the maximum interaction with their neighbours and hence the most stable lattice energy for the crystal. This close-packed arrangement is achieved by most solid state structures but there are a few examples were there is a void space, *i.e.* zeolites and channel coordination polymers, where the rigid framework is strong enough to withstand external forces.

1.3.5. Hydrophobic effects[10]

Hydrophobic effects arise from the exclusion of non-polar groups or molecules from aqueous solution.

Water molecules interact with themselves or with other polar groups or molecules preferentially (e.g. between dichloromethane and water which are immiscibile).and the organic solvent is forced away as the intersolvent interactions between the water molecules themselves are more favourable

than the ‘hole’ created by the dichloromethane. Hydrophobic interactions play an important role in some supramolecular chemistry, for example, the binding of organic molecules by cyclophanes and cyclodextrins in water.

Hydrophobic effects can be split into two energetic components, namely an enthalpic hydrophobic effect and an entropic hydrophobic effect.

Enthalpic hydrophobic interactions occur when a guest replaces the water within a cavity. This occurs quite readily as water in such systems does not interact strongly with the hydrophobic cavity of the host molecule and the energy in the system is high. Once the water has been replaced by a guest, the energy is lowered by the interaction of the former water guest with the bulk solvent outside the cavity (Figure 1.11). There is also an entropic factor to this process, in that the water that was previously ordered within the cavity becomes disordered when it leaves. An increase in entropy increases the favourability of the process.

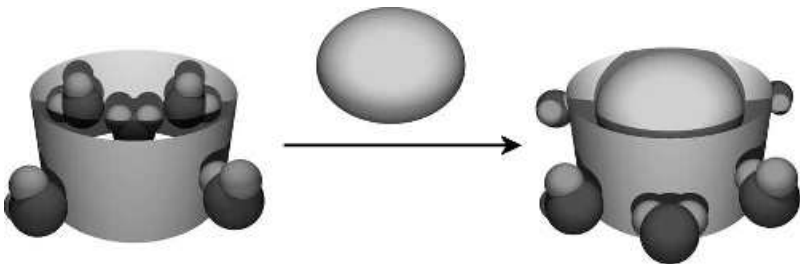

Figure 1.11 The displacement of water molecules from a hydrophobic cavity is responsible for the enthalpic hydrophobic effect.

Entropic hydrophobic interactions come about when there are two or more organic molecules in aqueous solution, the combination of which creates a hole in the water to form a supramolecular complex (Figure 1.12). There is less disruption (one hole in the aqueous phase instead of multiple holes) and hence an entropic gain, as the overall free energy of the system is lowered.

The hydrophobic effect is also very important in biological systems in the creation and maintenance of the macromolecular structure and supramolecular assemblies of the living cell or the formation of amphiphilic structures such as micelles, where hydrophilic ‘heads’ assemble in a roughly spherical geometry and lipid bilayers where the heads meet end-to-end.

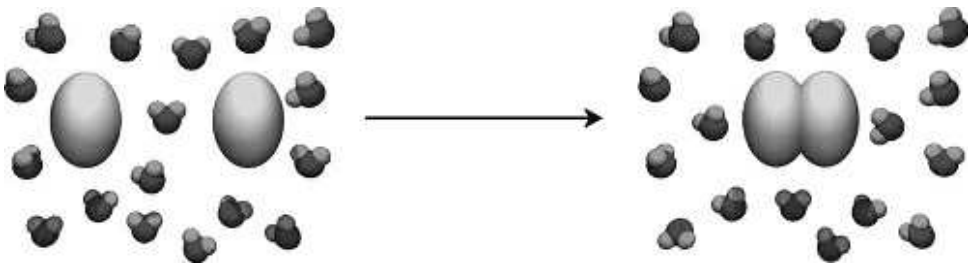

Figure 1.12 Two organic molecules creating a hole within an aqueous phase, giving rise to the entropic hydrophobic effect – one hole is more stable than two.

1.4. Solution host-guest chemistry

1.4.1. Binding constants

The binding of a guest by a host species, or the interaction of two or more species by non-covalent bonds, is an equilibrium process, whose equilibrium constant is called the *binding constant* or *association constant*.

The equilibrium that exists for a simple 1:1 host–guest system is shown in Figure 1.13 and the binding constant is calculated by Eq. (1.1), using the concentrations of the species present at equilibrium: host (H), guest (G) and the resulting complex (H·G). The final value, K, has units of mol dm^{-3} or M^{-1}. These values can range from near zero to very large and so for convenience a log scale is utilised and values are commonly seen quoted as log K. Binding constants are calculated from experimental data (from titrations monitored by NMR, UV–Vis or fluorescence spectroscopy, for example), which supply information about the position of the equilibrium.

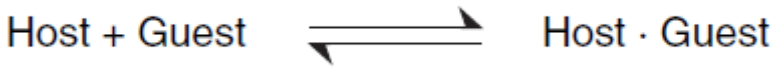

Figure 1.13. The equilibrium between a host–guest complex and the free species.

$$K = \frac{[H \cdot G]}{[H][G]} \quad \textbf{(1.1)}$$

Frequently, host–guest complexes do not form exclusively in a straightforward 1:1 ratio. In such cases, there is more than one binding constant as subsequent guests bind to the host.

1.4.2. Guests in solution

In the case of anion and cation binding, the two topics go hand-in-hand since the electrostatic charge on any ion must be balanced by a corresponding counter-ion. Thus a ‘cation’ or ‘anion’ host is always, in effect, a host for an ion pair (either contact or solvent-separated) unless the host itself bears a formal net charge.

So the binding equilibrium becomes a competition reaction between the existing counter-ion

and the host and the measured binding constant represents the competitiveness of the host over and above a specified counter-ion. In practice, the effect of the counter-ion is sometimes ignored or assumed to be negligible, particularly if weakly interacting counter-ions are used.

There are a number of successful ion-pair binding hosts; moreover, ion-pairing can be used to great effect in phasetransfer catalysis. In general, the selective inclusion of guests by a host molecule in solution is subject to an unprecedented level of design and control based on supramolecular principles. This allows the preparation of tailored systems for a wide range of applications, including sensing, food additives, drug delivery, imaging, biological modelling and in cosmetic therapy.

1.4.3. Macrocyclic and acyclic hosts

There are two major classes of host: acyclic (podands) and cyclic (macrocycles, macrobicycles or macrotricycles).

Acyclic hosts are linear or branching chain species with two or more sets of guest-binding functional groups positioned on the spacer unit in such a way as to chelate a target guest species to maximise guest affinity. Podands containing several rotatable bonds generally have less intrinsic affinity for their guests than hosts that are more rigidly preorganised because of the unfavourable enthalpic and entropic effects associated with the change in host conformation upon binding.

Podands generally have a high degree of flexibility and on binding to a guest the conformational change that occurs to produce a stable host–guest complex, may result in allosteric effects (the binding of a guest at one binding site that is influenced by the binding of a second guest).

In general, host flexibility is a very important feature, especially in biological systems, in which recognition of a substrate results in a conformational change that may be of major significance.

Flexible, podand-type hosts generally exhibit lower binding constants than cyclic analogues, which have binding sites positioned in a closed-ring arrangement.

As a result, cyclic systems are more preorganised and hence form more thermodynamically stable complexes because less conformational change is required upon binding.

1.5. Supramolecular architectures

1.5.1. Rotaxanes

The word “Rotaxane” is derived from the Latin word ‘*rota*’ meaning wheel and ‘*axis*’ meaning axle. [*n*]-Rotaxanes (Figure 1.14) are a class of molecole which consist f (*n-1*) macrocycles encircling a large linear component (referred to as thread) terminated by bulky stoppers which prevent the macrocycle from slipping out (unthreading), as they are larger than the internal diameter of the ring and this would require significant distortion of the covalent bonds. Rotaxanes without such physical barriers, in which the ‘thread’ can slip out of the ‘needle’, are termed pseudorotaxanes, which are frequently necessary precursors to both rotaxanes and catenanes.

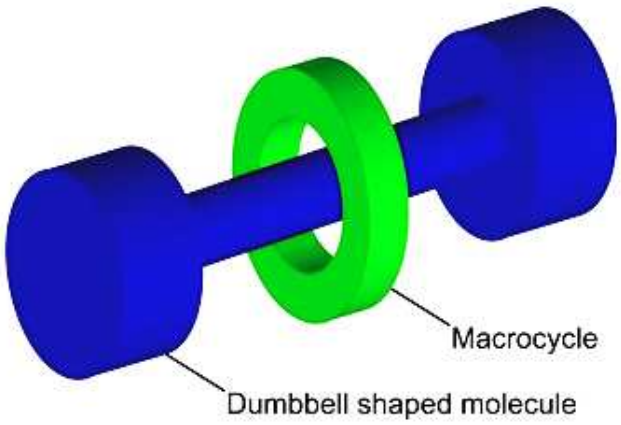

Figure 1.14. Graphical representation of a [2]-Rotaxane.

The two components of a rotaxane are kinetically trapped so it represents an example of a mechanically-interlocked molecular architecture.

Rotaxanes can behave as molecular shuttles because the macrocycle is free to glide over the thread: a non-covalent interaction (hydrogen bonding, metal-ligan complexation etc.) between the two components usually is the driving force for these synthesis and the macrocycle resides near a location on the thread called ‘*station*’; a rotaxane can have more than one station and in this case the macrocycle can switch between these two positions if they are both the same. If the two stations are different, the macrocycle is more likely to be on the station which has a greater interaction with it.

This movement can be controlled with external input like pH gradient (see chapter 5), light and electric current.

1.5.2. Catenanes

Catenane (Figure 1.15) is derived from the Latin '*catena*' meaning "chain" and it is another example of a mechanically-interlocked molecular architecture consisting of two or more interlocked macrocycles which cannot be separated without breaking the covalent bonds; generally they are named according to the number of interlocked rings; in catenane nomenclature, a number in square brackets precedes the word "catenane" in order to indicate how many rings are involved. Discrete catenanes up to a [7]catenane have been synthesized and isolated.

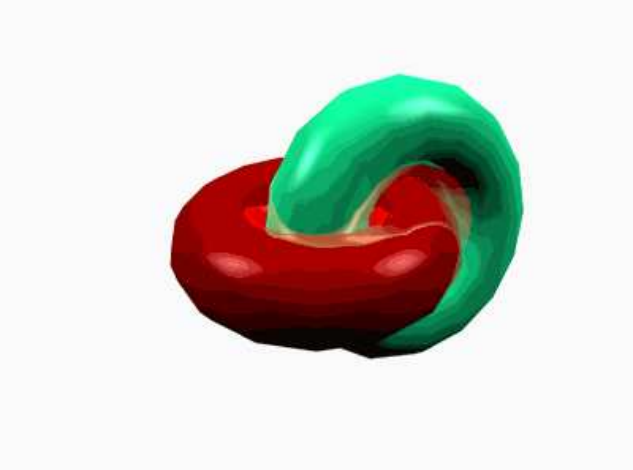

Figure 1.15. Graphical representation of a [2]-catenane

There are two primary approaches to the organic synthesis of catenanes. The first is to simply perform a ring-closing reaction with the hope that some of the rings will form around other rings giving the desired catenane product. This so-called "statistical approach" led to the first successful synthesis of a catenane; however, the method is highly inefficient, requiring high dilution of the "closing" ring and a large excess of the pre-formed ring, and is rarely used.

The second approach relies on supramolecular preorganization of the macrocyclic precursors utilizing non-covalent interactions like hydrogen bonding, metal coordination, hydrophobic forces, or coulombic interactions which offset some of the entropic cost of association and help position the components to form the desired catenane upon the final ring-closing. This "template-directed" approach (see chapter 6), together with the use of high-pressure conditions, can provide yields of over 90%, thus improving the potential of catenanes for applications

1.6. Conclusions

Supramolecular systems have a wide variety of uses, such as trapping molecules within solid state lattices, sensing and remediation of species from solution, understanding biological self-

assembly and nanotechnological devices and mechanically interlocked molecole (MIMs), which have been integrated into nanoelectromechanical systems (NEMs). Together, these topics form the core concepts upon which supramolecular chemistry is based.

For over 100 years, chemistry has focused primarily on understanding the behavior of molecules and their construction from constituent atoms. The new current level of understanding of molecules and chemical construction techniques has given the confidence to tackle the construction of virtually any molecule, be it biological or designed, organic or inorganic, monomeric or macromolecular in origin. During the last few decades, chemists have extended their investigations beyond atomic and molecular chemistry into the realm of supramolecular chemistry. Terms such as molecular self-assembly, hierarchical order, and nanoscience are often associated with this area of research.

Nanochemistry refers to the synthesis and study of chemical systems with features and functionality on the multi-nanometre length scale and materials with features of size of the order of 1–100 nm as *nanomaterials*. Very broadly there are two approaches to the nanoscale dimension – 'synthesising-up' and 'engineering-down'. The engineering down approach includes the latest in modern techniques for producing electronic components and originates in a bulk sense. Engineering down to the nanoscale (*nanotechnology*) involves doing the same sorts of things that an engineer or artisan does on a macroscopic scale but using specialised techniques in order to miniaturise. In contrast the synthesising-up approach (*nanochemistry*) is modelled on biology, particularly biological self-assembly, and aims to produce nanoscale functional components (perhaps with molecular device or molecular scale computing applications in mind) by chemical synthesis. Indeed the very first reports of functional molecular computing using supramolecular species have already begun to appear.

In summary, principles of supramolecular chemistry can be applied to the facile synthesis of new mesostructured assemblies featuring long-range order and displaying useful functional behavior (molecular recognition and sensing, biomimetic catalysis, size and shape selective molecular transport, etc.).

Moreover, the introduction of paramagnetic centers in the different supramolecular architectures (e.g. rotaxanes composed of different building blocks) offers the completely new possibility of using EPR spectroscopy for detecting these systems, being very sensible to the environment of paramagnetic centers and being able to follow processes in the nanoseconds scale, as for supramolecolar assemblies.

References

1. Steed, J. W.; Atwood, J. L. *Supramolecular Chemistry*, Wiley & Sons, Ltd, Chichester, UK, 2009.
2. Steed, J. W.; Turner, D. R.; Wallace, K. J. *Core Concepts in Supramolecular Chemistry and Nanochemistry*, Wiley & Sons, Ltd, Chichester, UK, **2007**.
3. Cram, D. J., *Angew. Chem., Int. Ed. Engl.* **1986**, *25*, 1039–1134.
4. Anslyn, E. V.; Dougherty, D. A. *Modern Physical Organic Chemistry*, University Science Books, Sausalito, CA, USA, **2006**, 162-168.
5. Jeffery, G. A., *An Introduction to Hydrogen Bonding*, Oxford University Press, Oxford, UK, **1997**.
6. Laurence, C and Berthelot, M., 'Observations on the strength of hydrogen bonding', *Persp. Drug Disc. Des.*, **2000**, *18*, 39-60.
7. Hunter, C. A. and Sanders, J. K. M., 'The nature of π–π interactions', *J. Am. Chem. Soc*., 1990, **112**, 5525–5534.
8. Schneider, H.-J., 'Van der Waals forces', in *Encyclopedia of Supramolecular Chemistry*, Vol. 2, Steed, J. W. and Atwood, J. L. (Eds), Marcel Dekker, New York, NY, USA, **2004**, pp. 1550–1556.
9. Kitaigorodskii, A. I., *Organic Chemical Crystallography*, Consultants Bureau, New York, NY, USA, **1961** (originally published in Russian by Press of the Academy of Sciences of the USSR, Moscow, USSR, 1955).
10. Southall, N. T., Dill, K. A. and Haymet, A. D. J., 'A view of the hydrophobic effect', *J. Phys. Chem.*, **2002**, *106*, 521–533.

Chapter 2. EPR investigations of organic non-covalent assemblies with spin labels and spin probes

2.1 Introduction

The object of the present chapter is to review the articles appeared in the literature in the last few years describing the use of EPR spectroscopy to investigate the properties of purely organic non-covalent assemblies in liquid solution by spin labels and spin probes.

2.1.1 Content and scope

Electron paramagnetic resonance (EPR) methods have been extensively used for detecting and identifying non covalent assemblies in solution and for clarifying their structure and properties. This body of work, which is usually based on the use of nitroxides as spin labels or spin probes, is largely driven by the sensitivity of the nitroxide functionality to its surroundings,[1] as the magnitude of the ^{14}N hyperfine splitting constants, a(N) and g-factor, depend on the polarity of the environment, while the lineshapes of the EPR spectra reflect the probe's motional dynamics. Further advantages in using EPR spectroscopy are the sensitivity of the method; the possibility of obtaining kinetic information in the submicrosecond time range; the ability to measure tumbling rates on the nanosecond timescale and distances between spin labels in close proximity.

The object of the present report is to review EPR experiments that have been used for, and are relevant to, pure organic non-covalent assemblies in liquid solution published in the last few years. For less recent works on this field, the reader is invited to read previously published reviews.[2]

Very recently a review regarding the use of EPR spectroscopy to investigate the properties of self-assembled monolayers protecting gold nanoparticles has also been reported.[3]

2.2 Host-guest Chemistry: Cyclodextrins

α, β, and γ-Cyclodextrins (CDs) are cyclic oligosaccharides made up of 6, 7, or 8 D-glucose units, respectively, bonded through α–(1–4)-linkages (see Figure 1). The oligosaccharide ring forms a torus, with primary OH groups of the glucose residues positioned at the narrower end of these tube-shaped molecules, while the secondary glucopyranose OH groups are located around

the wider opening. The chiral internal cavity of a CD is hydrophobic, while the external surface of the torus is hydrophilic. In aqueous solution, CDs form a broad range of complexes with guest molecules fitting, at least partially, into the hydrophobic cavity. For this reason, CDs are regarded as practical enzyme models and have found applications in the pharmaceutical science as well as in the area of separation science.[4]

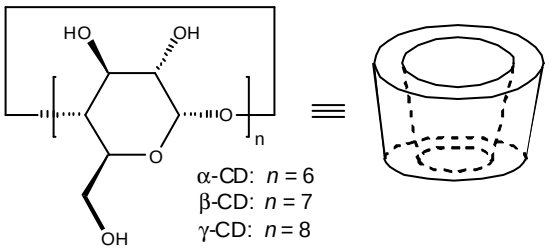

Figure 1 Cyclodextrins structure

In the last 40 years, many EPR studies, providing important structural and thermodynamic information, have been reported on supramolecularcomplexes between CDs and various nitroxide spin probes. [2] To expand the range of inclusion complexes that can be studied by EPR spectroscopy, two different approaches have been followed in the last years: the use of very sensitive spin probes based on *N*-benzyl-*tert*-butyl nitroxide and the synthesis of of several spin-labelled cyclodextrins, in which one or two nitroxide functionalities are attached to the CD molecule.[‡]

2.2.1 *N*-benzyl-*tert*-butyl nitroxide (BTBN).

BTBN has been largely used as paramagnetic guest species for studying complexation behaviour of CDs and related host systems, because, due to the sensitivity of its spectroscopic parameters (in water: a(N) = 16.69 G, $a(2H_\beta)$ = 10.57 G, g = 2.0056),[§] to the polarity of the environment, and to conformational changes, after inclusion in the β-CD cavity, it shows large variations of the hyperfine splitting constants at both nitrogen and benzylic protons, (a(N) = 15.74 G, $a(2H_\beta)$ = 7.88 G, g = 2.0058).[5] Thus, EPR spectra of this radical in the presence of a suitable host system show signals clearly different for the free and included species, and their ratio provides the value of equilibrium constant for the formation of the inclusion complex. In addition, because the lifetimes of the two species are comparable to the time scale of EPR spectroscopy, as suggested by the strong dependence on the temperature of the spectral line width, this technique permits one to obtain information on the kinetics of association and

dissociation of the inclusion complex.

With the aim to broaden the range of observations reported in the literature on the behaviour of binary complexes between cyclodextrins and organic substrates in the presence of alcohols of different size and lipophilicity and in particular to determine their influence, barely investigated in the past, on the dynamics of the inclusion process, a systematic study was undertaken on the effects of 14 different alcohols (linear, cyclic, and branched) on the inclusion in aqueous solutions of the radical guest N-benzyl *tert*-butyl-d_9-nitroxide (BTBN-d_9) in CDs, by using EPR.[6] In this study, the *tert*-butyl hydrogens were deuterated to improve the spectral resolution and, thus, to get more accurate values of the kinetic rate constants. Figure 2 shows the increasing resolution of the EPR lines of the free and included species observed upon deuteration of BTBN.

Global analysis of EPR data allowed the authors to explain the CDs binding behaviour: the formation of a ternary complex, where alcohol and radical guest are co-included into CD cavity was discarded in all cases, while EPR data were found more consistent with the formation of a binary complex alcohol@CD competing with the monitored complex nitroxide@CD.

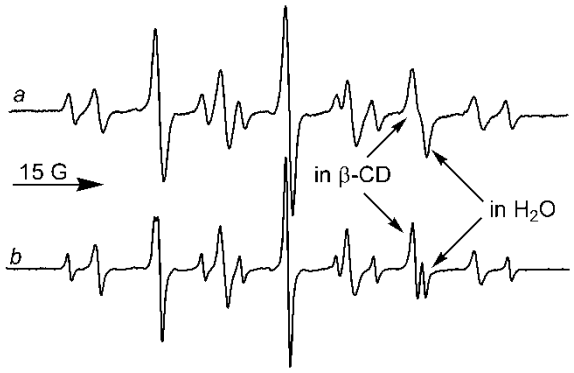

Figure 2 EPR spectra of *N*-benzyl-*tert*-butyl nitroxide (a) and *N*_benzyl-*tert*-butyl-d_9-nitroxide, (b), both recorded in water at 298 K in the presence of β-CD (8.2 mM) and cyclohexanol (14mM). Reproduced from *J. Phys. Chem. A*, 2008, **112**, 8706, with permission of American Chemical Society.

Both kinetic and thermodynamic analyses of the experimental results revealed that the presence of alcohols affects to a larger extent the dissociation rather than the association of radical probe and CD and that the former process is of greater importance in determining the stability of the complex, this confirming the reliability of the competition model proposed. This competition has been used for the indirect determination of the stability constants of complexes between CD and examined alcohols. By using a similar approach, it was shown that EPR spectroscopy can be considered a rapid and accurate technique to investigate the CDs binding behaviour toward different nonradical guests.

The combined use of BTBN and EPR spectroscopy has also been proved to be suitable for

studying the partitioning rate of a given substrate in CD–micelle systems. The method is based on the significant differences in the EPR parameters shown by BTBN when it experiences water, CD cavity or sodium dodecyl sulfate (SDS) micellar environments (see Figure 3).[7]

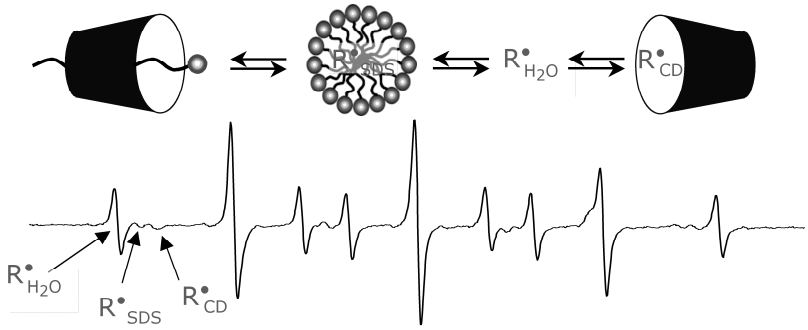

Fig. 3 EPR spectrum of BTBN recorded in water at room temperature in the presence of β-CD and SDS micelles.

Actually, the partitioning of nitroxide probes in the hydrophobic environment of SDS micelles gives rise to a reduction of the value of both nitrogen and β-protons splittings, respect to the values of the nitroxide dissolved in water. However, these differences are more pronounced when BTBN is included in the cavity of CD due to both polar and conformational changes occurring upon complexation. Because of these differences in the EPR parameters it was possible, for the first time, the direct and simultaneous measurement of the concentration of an organic spin probe in the three different ‘‘pseudo-phases’’ (namely SDS micelles, CDs and water).[7]

From an applicative point the residence time of the probe in each environment determined by EPR was employed to predict the electrophoretic behaviour of the diamagnetic carbonylic analogue of BTBN, benzyl-*tert*-butyl ketone, in CD-micellar systems when the anionic SDS micelle acts as a carrier and the inclusion of the solutes into the neutral CD cavity is a process in competition with the partitioning into the micelle.[8]

2.2.2 Spin-labelled cyclodextrins

Attaching a paramagnetic moiety to cyclodextrin makes it possible to expand the scope of EPR studies to complexes of CDs with unlabelled molecules. Except for one early study which did not probe host–guest complexation,[9] spin labelling of cyclodextrins has been explored only in the last few years.

Ionita and Chechik reported the synthesis and the EPR characterisation of new spin-labelled

cyclodextrins which were prepared in two or three steps starting from β-CD (see Figure 4).[10] In particular, β-CD was monotosylated at the C6 position and the resulting 6-*O*-*p*-toluenesulfonyl-β–CD was converted into 6-deoxy-6-mercapto-β-CD in order to obtain compound **1** (by reaction with 4-(2-bromoacetamido)–TEMPO; TEMPO is 2,2,6,6-tetramethylpiperidine-1-oxyl) and **2** (by reaction with 4-maleimido–TEMPO). CD-labelled **3** was obtained by direct substitution reaction of 6-*O*-*p*-toluensulfonyl–β-CD with 4-NH_2–TEMPO.

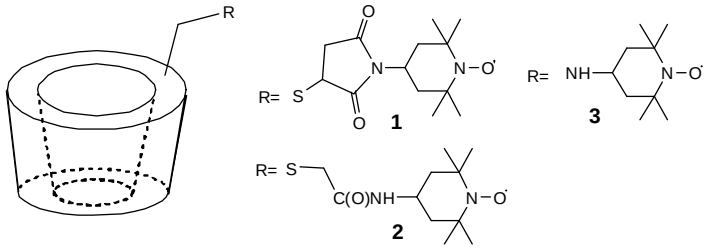

Figure 4 Schematic representation of spin-labelled CDs **1**-**3**.

The aqueous solutions of the above spin-labelled CDs shows typical nitroxide EPR spectra with the high field line broadened due to restricted tumbling. Although the EPR parameters of these materials are not very sensitive to the complexation of small molecules, formation of large host–guest complexes leads to substantial reduction of the rate of tumbling. Complexation of **3** with an adamantane functionalised dendrimer leads to an increase of rotational correlation time τ from 5.87×10^{-10} to 13.48×10^{-10} s (at dendrimer and **3** concentrations of 5.4×10^{-3} and 5×10^{-3} M, respectively) this being an indication that spin-labelled cyclodextrins are suitable probes for studying formation of large supramolecular assemblies by measuring lineshape variations in the corresponding EPR spectra.

By using an approach similar to that one used to probe supramolecular complexation with resorcinarenes[11] and calixarenes[12] Ionita and Chechik synthesized and characterised by EPR two spin-labelled CD biradicals in which two 4-carboxy-TEMPO groups were attached to adjacent glucose units (**4**) or separated by two glucose units (**5**).[13]

As expected, the presence of two paramagnetic moieties in bis-labelled CDs **4** and **5** lead to the appearance of additional lines due to a spin–spin exchange interaction (characterised by exchange coupling constant *J*). For both **4** and **5** isomers, *J* is much greater than *a*(N), and the EPR spectra of biradicals in a dichloromethane solution show five lines (Fig. 5b and 5c). On the contrary, the biradical spectra do not show the spin–spin exchange interaction in aqueous solution (Fig. 5d and 5e). Because the strength of the exchange depends on the rate of collisions between the radicals, the absence of such interaction has been attributed to a more open

conformation adopted by the biradicals in water solution. By increasing temperature (which leads to reduced viscosity and increased mobility), spin–spin interactions were observed for **4** in water (Fig. 5f), while for **5** were still not present.

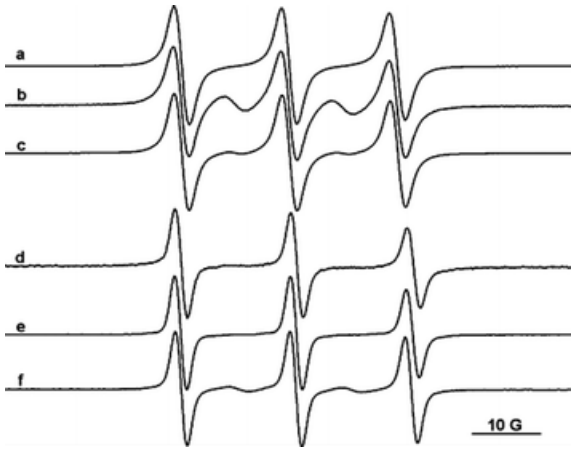

Figure 5 EPR spectra of: a mono spin-labelled CD (a), **4** (b) and **5** (c) in dichloromethane, **4** (d) and **5** (e) in water at room temperature, **4** (f) in water at 350 K. Reproduced from *New J. Chem.*, 2007, **31**, 1726, with permission of Royal Society of Chemistry.

At room temperature, addition of known strong guests for CDs such as adamantane derivatives or methyl orange did not lead to any significant changes in EPR spectra of **4** and **5**. However, at temperatures higher than 323 K, that is at temperature at which exchange lines are visible (*vide supra*), the formation of inclusion complexes of **4** in water can be monitored by following changes in the spin–spin interactions. Actually, host–guest interactions between the CD biradicals and small-sized guests is expected to increase the conformational rigidity of the assembly, which in turn would affect the strength of exchange. Spin–spin interactions for **4** in water at 323 K, however, were not affected by the presence of adamantane derivatives (adamantane amine, adamantane carboxylic acid) or oligoethylene oxides (containing 1–4 repeat units). It can be conceived that binding of these guests does not significantly change the steric environment around the lower rim of the cavity; this lack of conformational change upon complexation means that EPR could not detect the formation of inclusion complexes between **4** and small guests. The spin–spin interactions in **4** was strongly affected only in the presence of an adamantane end-capped diethylene glycol. The almost complete disappearance of the exchange lines in this case suggests that the frequency of collisions between the TEMPO units is significantly reduced upon complexation, presumably due to steric hindrance in the complex.

Complexation properties of spin labelled CDs **1-5** have also investigated by electron spin-echo envelope modulation (ESEEM) spectroscopy.[14] This method, which is usually used in colloidal

or biological systems, is in principle highly suitable for structural studies of supramolecular assemblies. Actually, when used with nitroxide labels/probes, ESEEM reports on the number of nuclear spins around the nitroxide group and the nuclear spin-nitroxide distances.[15] This sensitivity to local concentration of nuclear spins can be exploited to probe the accessibility of the nitroxide group to the solvent molecules. For instance, accessibility can be assessed by monitoring interactions of the nitroxide group with the solvent ^{2}H nuclei if the spin-labeled structure is dissolved in a deuterated solvent. Inclusion of a nitroxide probe inside the cavity of a CD give rises to reduction in the number of solvent magnetic nuclei in the vicinity. The complexed nitroxide will therefore give ESEEM traces with reduced modulations as compared to the uncomplexed one. The modulation depth can hence provide quantitative structural information about the environment around the spin probe.

During this investigation[14] it was shown that ESEEM provided complementary information to cw-EPR and was proved more sensitive to the host-guest complexation. Nonetheless, the requirement for frozen samples introduces a complication for systems in equilibrium, in terms of the uncertainty of the temperature at which the equilibrium has been broken. Moreover, ESEEM traces report on solvent accessibility in a frozen solution, and hence cannot provide information about the dynamics of complexation, or conformational changes that do not significantly change solvent accessibility.

Bardelang et al. also reported the synthesis of a mono spin-labelled permethylated CD (**6**) and analysed the self-inclusion process of the paramagnetic moiety covalently attached to the CD core.[16-18]

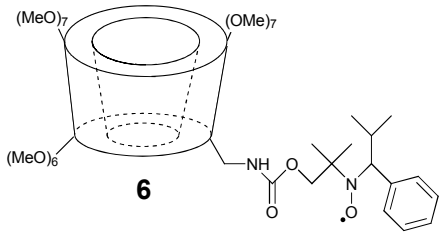

Figure 6. Spin labelled methylated cyclodextrin **6**.

In aqueous solution, the EPR spectrum of **6** shows a very pronounced asymmetric shape due to a strong broadening of the two lines resonating at higher magnetic field. A good simulation of this spectrum could be achieved only by assuming the existence of two nearly equally populated species that are undergoing a fast exchange. This species were identified as those having the nitroxide moiety outside of the inner cavity or the nitroxide moiety located amidst the methoxy crown of the narrow rim of the CD cavity, as illustrated in Figure 7.

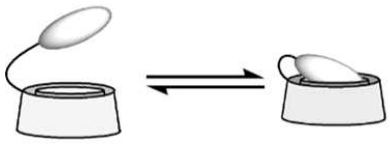

Figure 7. Two possible geometries for nitroxide **6**.

It is important to note that, nitroxide **6** represented a good model for the development and the synthesis of nitrone-appended cyclodextrins characterised by spin adduct with improved stability.[17,19-20]

While in all previously examined cases, the paramagnetic label was found to be located outside the ring cavity or weakly included in the CD cavity, Franchi et al.[21] reported the first example of a spin labelled cyclodextrin in which the nitroxide functionality is mechanically trapped inside the cavity of CD by a covalent link with one of the CD rims, that is, by formation of [1]rotaxane.[22]

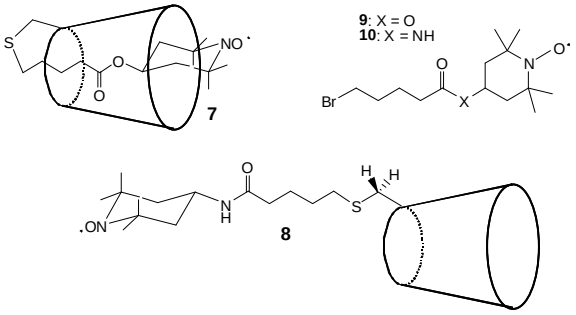

Figure 8 Spin-labels **7**-**10**

The structurally assignment of [1]rotaxane **7** was made possible by comparing its EPR spectra with those of the spin-labelled CD **8** having the paramagnetic arm located outside the cavity (see Figure 8). Actually, the 0.45 G Δa(N) decrease between **7** and the corresponding free thread **9** measured in water was considered compatible with a geometry in which the piperidine ring is strongly self-included within the hydrophobic cavity of the β-CD with the nitroxyl pointing toward the bulk water. On the other hand, the smaller Δa(N) (0.20 G) between **8** and **10** does not agree with an interlocked radical species but, with a weak self-complexing nitroxide similarly to what found by Bardelang *et al.*[16]

This hypothesis was also supported by the analysis of the EPR spectra variation observed after the addition of 2,6-di-*O*-Me-β-cyclodextrin (DM-β-CD) or SDS as external competing

host or guest, respectively. Whereas the EPR spectrum of **8** recorded in the presence of DM-*β*-CD 0.1 M showed a significant decrease in the *a*(N) value, that recorded in the presence of SDS is characterized by *a*(N) value comparable to that of the free thread. This indicated that in **8** the nitroxide fragment can be reversibly trapped by another host or displaced by guest competing for the CD cavity (Figure 9). Differently, the spectrum of **7** did not show any variation in the presence of the competing species, thus confirming the irreversible nitroxide trapping inside the cavity of CD.

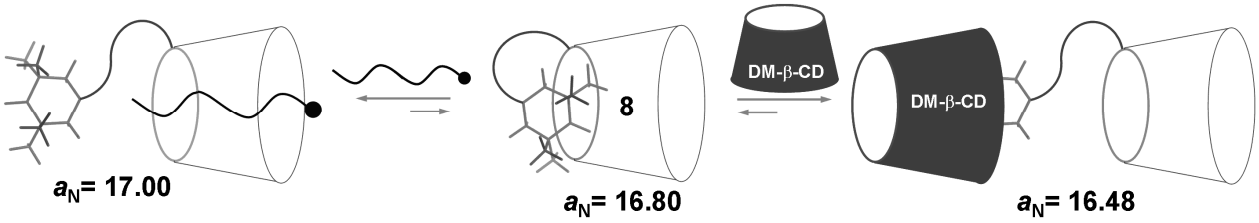

Figure 9 Schematic representation of equilibria involving nitroxide **8**, SDS and DM-*β*-CD

2.3 Host-guest Chemistry: Cucurbit[n]urils

Cucurbit[n]urils[23-27] (CBn, n = 5–8, 10) are a family of macrocycles made from the condensation reaction of glycoluril and formaldehyde in acid. Their hydrophobic cavity and hydrophilic carbonyl portals allow the macrocycles to form a range of host–guest complexes with organic and inorganic compounds. Similar to CDs, the hydrophobic interior of CBn provides an inclusion of various small molecules, including pharmaceuticals;[28] unlike CDs, the polar carbonyl groups at the portals also allow to bind ions through charge–dipole interactions, so providing a significant increase of the generally poor CB solubility in water solution.

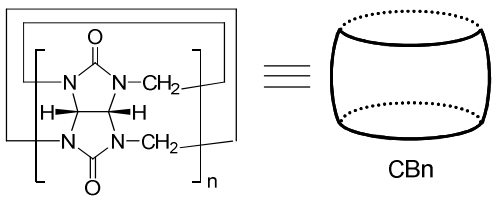

Fig. 10 Cucurbit[*n*]uril structure

The first EPR investigation exploring the binding properties of this relatively new class of macrocyclic hosts was conducted on CB7, by using *N*-benzyl-*tert*-butyl nitroxide(BTBN).[29] The EPR spectrum at 298 K of BTBN recorded in the presence of CB7 (Figure 11) was

characterized by the presence of additional signals, beside those due to the free species, which were attributed to the radical included in the host cavity (BTBN@CB7).

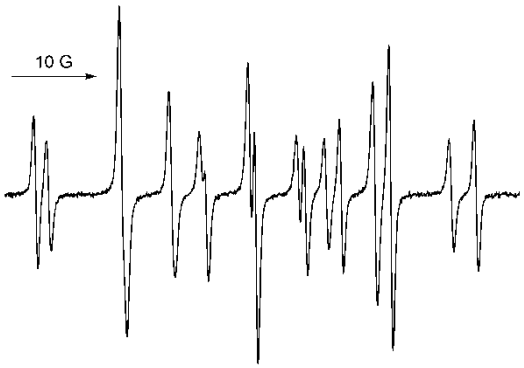

Figure 11 EPR spectrum of BTBN at 298 K recorded in water in the presence of CB7 7.0 mM.

The values of the nitrogen splitting, a(N), and of β-proton splitting, $a(2H_\beta)$, decrease significantly upon inclusion into the less polar environment of the CB7 host cavity, giving rise to the remarkable differences in the resonance frequencies for the $M_I(2H_\beta) = \pm 1$ lines of the included and free species. Because of this difference it was concluded that the nitroxide is included in the CB7 cavity from the *tert*-butyl side. Actually, this geometry results in a deeply inclusion of the NO group in the internal apolar environment of the host cavity, while inclusion from the phenyl side is expected to leave the NO group exposed to water. The EPR results were corroborated by ^{1}H NMR studies carried out on *tert*-butyl benzyl ketone, the diamagnetic analogue of BTBN.

Unexpected EPR results were observed for the complexation of BTBN with CB7 in the presence of alkali cations (Table 1). Addition of an alkali chloride, MCl (M=Li, Na, K or Cs) to a solution containing 10 mM CB7 caused the appearance of signals of a new species (Figure 12) and a significant decrease of the EPR signals of free and BTBN@CB7 complex. The unpredicted species was identified as the radical hosted in the CB7 cavity in which one metal cation is in close contact with the nitroxidic oxygen and two neighbouring portal oxygen atoms with the *tert*-butyl group of the guest included inside the host cavity, BTBN(M^+)@CB7.

Table 1. EPR parameters of BTBN at 298 K in water.

Nitroxide	a(N) / G	a(2H$_\beta$) / G	g factor
BTBN	16.80	10.70	2.0056
BTBN@CB7	15.60	9.57	2.0061
BTBN(Li^+)@CB7	17.12	14.82	2.0058
BTBN(Na^+)@CB7	17.08	15.28	2.0059
BTBN(K^+)@CB7	16.64	14.65	2.0060
BTBN(Cs^+)@CB7	16.52	13.90	2.0061

The formation of the coordination complex results in a substantial increase in the electron spin density on the nitrogen in inverse order with respect to the size of the cation owing to increased localisation of negative charge on the oxygen atom from bonding to the alkali cation. The EPR spectra showed selective line-broadening effects as a result of metal exchange between bulk water and the coordination complex. Analysis of the EPR linewidth variations allowed to measure, for the first time, the corresponding kinetic rate constants (Figure 12).

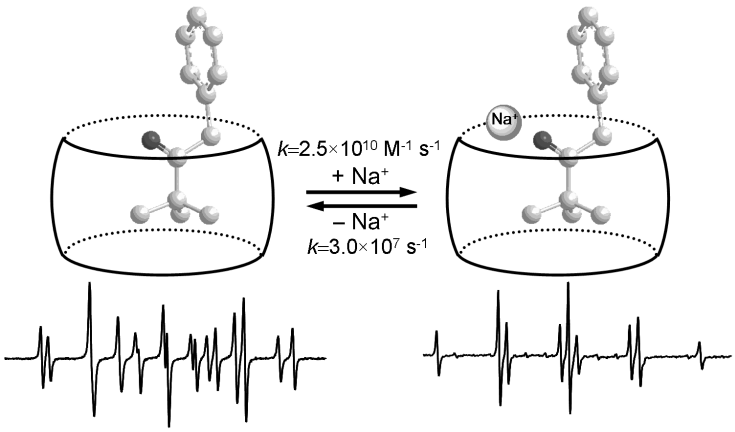

Figure 12. Schematic representation of Na^+ exchange between bulk water and the coordination complex. The EPR spectra of BTBN at 298 K were recorded in water in the presence of CB7 7.0 mM in the absence (left) and in the presence (right) of NaCl 0.4 M. Rate constants were determined by theoretical simulation of spectra recorded in the presence of variable amount of NaCl.

Taking CB7 as a model host, these results led to a general picture describing the interplay between the association of metal ions and the complexation of organic guests - included those

having a coordinating lone pair which form stable ternary metal̃guest–CB complexes generated by a template effect of the cation - which must be taken into account when discussing the complexation behaviour of cucurbituril derivatives in the presence of salts.

In order to study possible applications of CB7 as a host for pH-sensitive nitroxides probes, inclusion complexes of CB7 with different nitroxides reported in Figure 13 were investigated.[30]

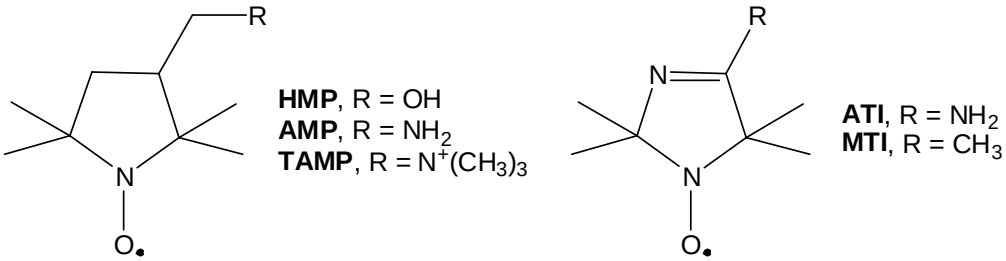

Figure 13 pH sensitive and related nitroxides investigated in ref 30.

Mixing of ATI and MTI with CB7 gave rise to EPR spectra that were found to be pH dependent. At pH close to the p*K* value, the EPR spectra of ATI in the presence of CB7 showed the superposition of signals of three nitroxides (Figure 14c).

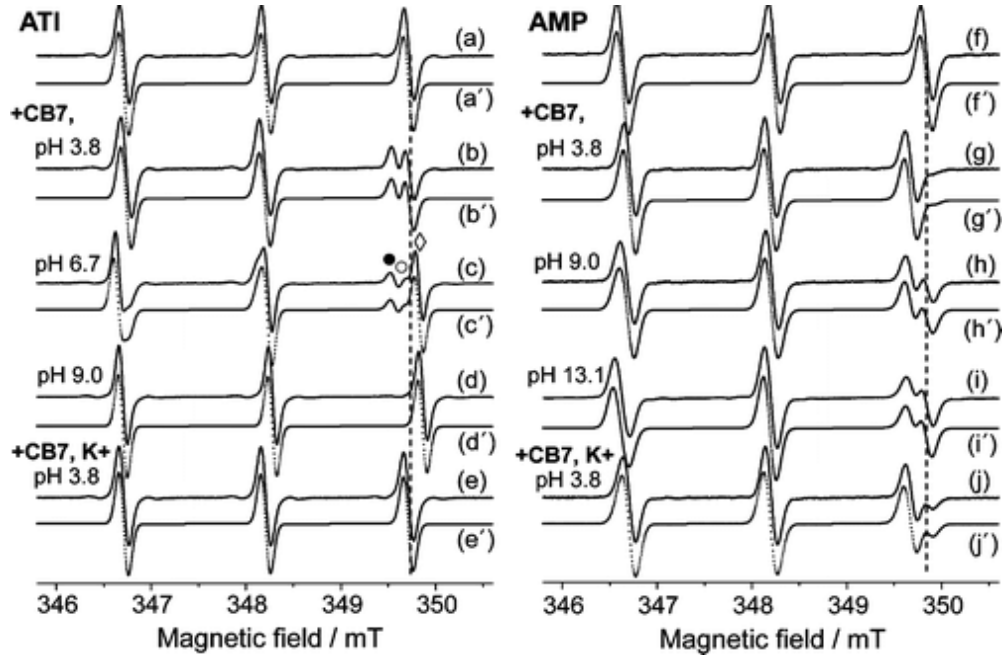

Figure 14 EPR spectra of nitroxide ATI or AMP (0.25 mM) at 298 K recorded in deionized water: (a,f) nitroxides in the absence of CB7 at pH 3.8. ATI in the presence of 0.5 mM CB7 at (b) pH 3.8, (c) pH 6.7, (d) pH 9.0, and (e) pH 3.8, and the addition of 0.1 M KI. AMP in the presence of 0.5 mM CB7 at (g) pH 3.8, (h) pH 9.0, (i) pH 13.1, and (j) pH 3.8, and addition of KI (0.1 M). Simulated spectra are displayed with dotted lines. Reproduced from *J. Phys. Chem. B,* 2010, **114**, 1719, with permission of American Chemical Society.

Two of them were clearly assigned to the protonated and nonprotonated forms of the nitroxide. The third one having lower hyperfine interaction (HFI) constant than the protonated form $ATIH^+$, and the rotational correlation time obtained from simulation of the EPR line close to those observed for the HMP@CB7 complex, was attributed to the $ATIH^+$@CB7 complex.

Similarly to HMP, the EPR spectrum of AMP was found to be sensitive to CB7 addition at any pH in the pH range of 2-14. However, the EPR parameters of the complexes formed in strongly basic and in neutral or acidic solutions were different. In strongly basic medium the formation of AMP@CB7 occurs, whereas at pH $\lesssim$9 another complex is formed ($AMPH^+$@CB7). Formation of both complexes was accompanied by similar increase in correlation time.

As a general behaviour it was found that reversible formation of inclusion complexes AMP@CB7, $AMPH^+$@CB7, HMP@CB7, $ATIH^+$@CB7, and $MTIH^+$@CB7 is accompanied by a decrease of a(N) of the nitroxide group, and by a 5-7-fold increase of rotational correlation time monitored by EPR. The binding constants of nitroxide@CB7 complexes were determined, and the influence of alkali metal ions and pH on the equilibrium between free and encapsulated nitroxides was studied. The EPR spectra of CB7 mixtures with protonable nitroxides were found to be more sensitive to pH changes than the spectra of pure nitroxides, and the apparent pK of these mixtures was found to increase with CB7 concentration. In agreement with the general pattern of CB7 complexation with organic substances, the nitroxides with cationic functional groups show much stronger binding than similar uncharged compounds, owing to the considerable dipolar interaction of CB carbonyl portals with ammonium ions. Interaction with CB7 stabilizes the protonated form of the nitroxide, increasing the apparent pK of the mixture.

EPR has also used to investigate the complex formation between cucurbit[8]uril (CB8), a larger component of cucurbituril family, and sterically hindered nitroxides.[31] The results were compared with those previously reported for the complexes with CB7.[29] Unexpectedly, the change of the cavity size gives rise to completely different results.

CB8 is known to be essentially insoluble in water. On the contrary mixing an aqueous solution containing **13** and CB8 caused the complete dissolution of the host in water, while treatment of **11**, **14** or benzyl-*tert*-butyl nitroxide with CB8 did not give rise to any EPR signal from the radical included in the macrocycle ligand, which remained as an undissolved solid.

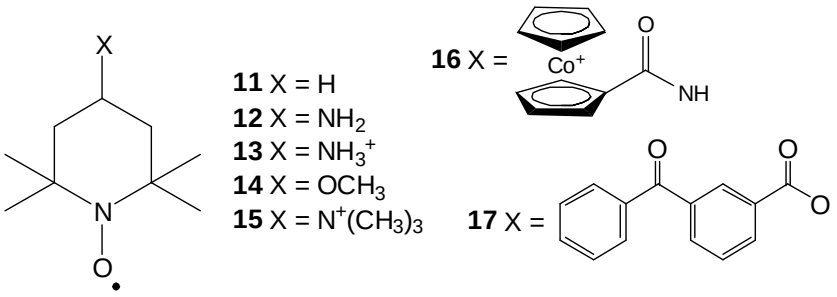

Figure 15 Nitroxides **11-17**

The formation of a strong complex between nitroxide **13** and CB8 is expected on the basis of the strong interaction between the ammonium site and the carbonyl oxygen atoms of CB8, as already found with protonated amines.[32] It is very likely that this complex is much more soluble than free CB8, thereby "pulling" CB8 into solution. The EPR spectrum of this solution given in Figure 16b, was nicely simulated by assuming the presence of three different species, the first species due to the radical dissolved in bulk water ($\mathbf{13}_{water}$) and the second species ascribed to the 1:1 inclusion complex of the radical with the macrocycle ($\mathbf{13}_{CB8}$). The signals due to the third species were instead completely unexpected and consisted of seven equally spaced hyperfine lines separated by 5.1 G (g=2.0063) with a relative intensity of 1:3:6:7:6:3:1. This species, never observed with the smaller macrocycle CB7, was assigned to a nitroxide triradical in which each electron divides its time equally between three nitrogen nuclei ($\mathbf{13}_{trimer}$). Since the three radicals are not directly linked through a C=C π-system framework, it was assumed that the spin exchange between the three nitroxide units is operating through space due to the formation of a noncovalent supramolecular organisation.

The supramolecular assembly was confirmed by the formation of a long fibrous millimetres sized network obtained by slow cooling the aqueous solution of CB8 and **13** from room temperature to 5 °C. Cucurbiturils are known to form fibres. Kim and co-workers showed that intermolecular CH···O interactions were responsible for self-assembly of CB7 in acidic solutions, leading to water gelation,[33] while Bardelang *et al.* have reported that molecules of CB8 are able to form water-filled channels consisting of one-dimensional macrocycle nanotubes.[34] In the same way, it was supposed that mixing of **13** with CB8 may lead to the formation of a supramolecular organisation of the macrocyclic hosts containing radical units that assemble into a long fibril, in which the nitroxide behaves as glue to form non covalent building unit.

The noncovalent and reversible nature of the triradical was evidenced by following the EPR spectral variations observed by addition of anilinium chloride in the pH range from 3 to 7, as illustrated in Figure 16. Around pH 3 the EPR spectrum of a solution containing CB8 and anilium chloride (Figure 16c) showed only the signals due to the radical dissolved in water, this being an indication that the radicals are completely displaced from the macrocyclic cavity by the aromatic ammonium cation. Increasing the basicity of the solution to pH 7 with NaOH, the signal due to the radical in water was suppressed and the spectra of the monoradical complex and of the triradical were instead observed (see Figure 16a). This observation strongly suggests that the deprotonated aniline is released from the cavity being replaced by the nitroxide guests.

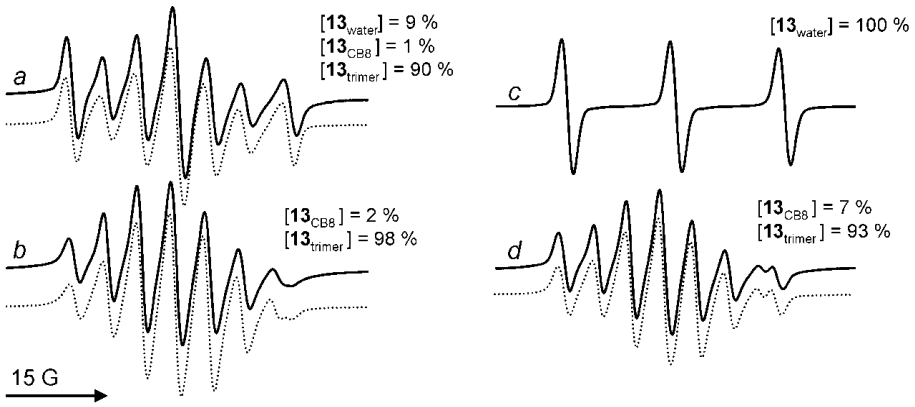

Figure 16 Experimental (solid lines) and simulated (dotted lines) EPR spectra of **13** in the presence of CB8: *a*) initial solution; *b*) fibers (see text) redissolved in water containing 1 mM NaCl; *c*) spectrum *a* in the presence of anilium chloride at pH 3 showing the displacement of the free radical **13** and *d*) spectrum *a* in the presence of anilium chloride at pH 7. The simulations were obtained by using the reported relative amounts of nitroxidic species.

This spectrum consisting of seven lines is compatible with a radical showing three electron spin exchanges (J_{12}, J_{13} and J_{23}) in which the three spins are placed either in a symmetric triangular arrangement ($J_{12} = J_{13} = J_{23}$) or in linear fashion ($J_{12} = J_{13} \neq J_{23}$). Attempts to obtain structural informations of the triradical in the solid state failed because slow evaporation of solution of **13** with CB8 did not afford suitable crystals for X-ray crystal structure determination. In the main time, by using nitroxide **14** having a methoxy group as substituent at 4 position, Tordo and co-workers[35] were able to obtain the X-ray crystal structure of the complex (Figure 17). Orange prismatic crystals suitable for X-ray crystallography were grown from a solution of **14** and CB8 in water over a period of one month. The asymmetric unit of **14**@CB8 contains six cucurbiturils, and the nitroxide inside each appeared to be disordered. The host-guest couples are arranged in supramolecular equilateral triangles (Figure 17) to form layers with water molecules in between. In each triangle, the distances between the oxygen atoms of the three

nitroxides are in the range 8.4-9.0 Å, with an average value of 8.7 Å; this is expected to lead to three almost equivalent spin-spin interactions with large *J* values.

When **14**@CB8 crystals were dissolved in pure water, an X-band EPR signal was observed composed of the superposition of the expected three-line spectrum from free **14** and a seven-line spectrum. This additional spectrum exhibited a 1:3:6:7:6:3:1 seven-line pattern with a hyperfine coupling constant *a*(N) of 5.13 G, in agreement with the "trinitroxide" supraradical [**14**@CB8]$_3$.

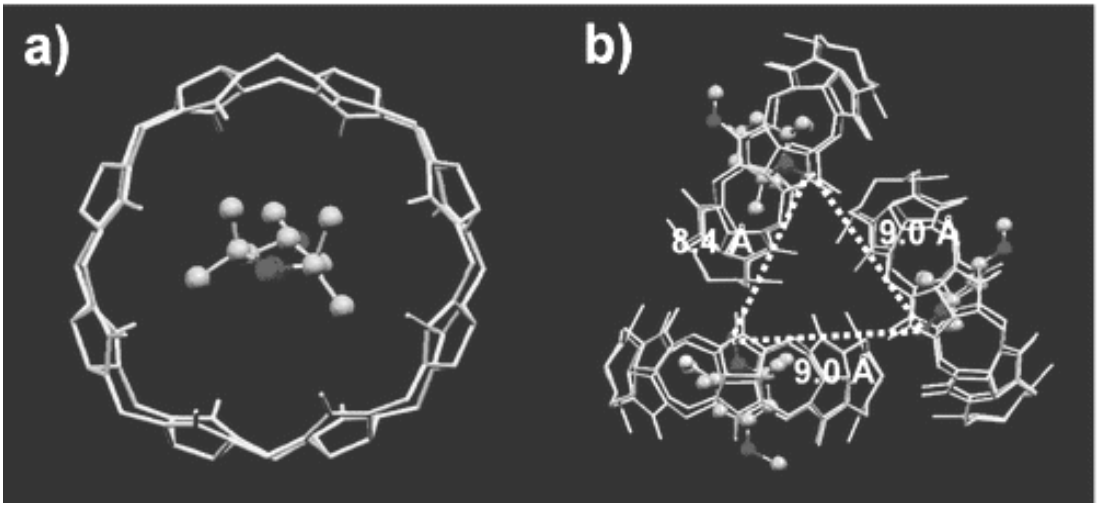

Figure 17 a) X-ray structure of the **14**@CB8 inclusion complex; b) supramolecular triangle showing a three-spin-system interaction in the solid state. Reproduced from *J. Am. Chem. Soc.*, 2009, **131**, 5402, with permission of American Chemical Society.

The high stability of nitroxide@cucurbituril complex prompted Tordo and coworkers to investigate the effect of CB7 on the nitroxide reduction process by sodium ascorbate.[35] A very high resistance was observed, with a half-life ($t_{1/2}$) of ca. 254 min (i.e., a 60-fold increase respect to the free nitroxide), in the presence of 2 mM ascorbate anion with CB7, in agreement with a slow kinetics of decomplexation. For comparison, using β-CD as the host led to an increase by a factor of less than 2. CB8 also showed significant activity toward **14** protection, albeit to a lesser extent, presumably because of a weaker binding constant and the axial orientation of the nitroxide inside the cavity.

Supramolecular complexation behaviour of CB7 and CB8 was investigated also in the presence of cationic probes, i.e. 4-(*N*,*N*,*N*-trimethylammonium)-2,2,6,6-tetramethylpiperidinyl-N-oxyl bromide (**15**), and related nitroxides, and the aggregation characteristics of host-guest complexes in water were examined by ^{1}H NMR and EPR.[36] Both CB7 and CB8 form a 1:1 complex with **15**. The structure of the complexes in the solid state were inferred by X-ray diffraction studies (Figure 18) and in the gas phase by computation (B3LYP/6-31G(d)). In solid state, both complexes display the nitroxide placed at the center of the cavity with the nitroxide N-O group inside the portals of the macrocycle and the pendant trimethyl ammonium group of **15** exposed outside the portals of the host. Such geometries were confirmed by computational results which highlighted the differences between the dimension of the two portals of the complexes with the top (toward which the nitroxide group was oriented) being larger than the bottom oxygen portals.

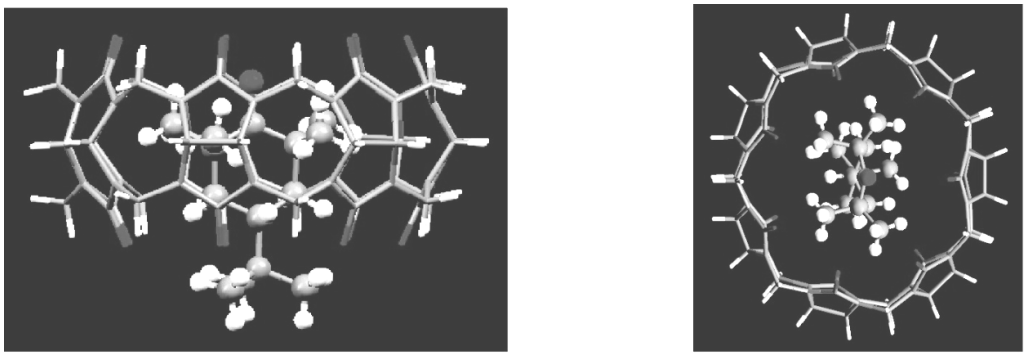

Figure 18. Side and front views of **15**@CB7 obtained from X-ray crystal structure solution. Reproduced from *Langmiur*, 2009, **25**, 13820, with permission of American Chemical Society.

The EPR spectrum of **15**@CB8 consists mainly of three lines being characteristic of a single nitroxide radical, similarly to that of the **15**@CB7 complex.

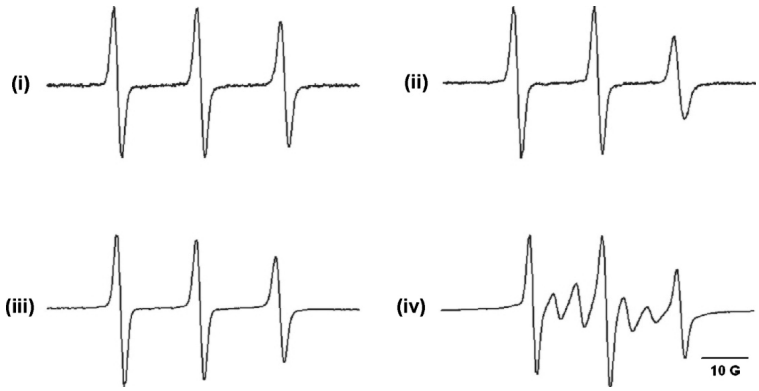

Figure 19. EPR spectra of the **15@**CB8 (1:1) complex at different concentrations: (i) 1×10^{-5}, (ii) 5×10^{-5}, (iii) 1×10^{-4}, and (iv) 1×10^{-3} M. Reproduced from *Langmiur*, 2009, **25**, 13820, with permission of American Chemical Society.

In the case of CB8, however, in addition to the expected three-line spectrum, an additional spectrum consisting of seven lines was recorded (Figure 19), the contribution of the seven-line spectrum to the total spectrum being dependent on the concentration of the complex and added salt (NaCl) to the aqueous solution. Similarly to what found with nitroxides **13** and **14** in the presence of CB8,[31,35] the spectra are consistent with the presence of a triradical [**15**@CB8]$_3$. The only manner which reproduces the observed spectra by simulation is by assuming a spin exchange among three nitroxide radicals included within CB8 interacting in a triangular geometry that leads to spin exchange between the three radical centres. The authors[36] established, with the help of 13 additional examples, that this was a general phenomenon.

2.4 Non covalent interactions: halogen bonding

Interest in nitroxide radicals stems from their prominent role as spin labels in biology, biochemistry, and biophysics to monitor the structure and the motion of biological molecules and membranes, as well as nanostructures.[1] As mentioned before, labeling of specific sites by nitroxide probes allows effective structural and dynamic analyses by means of EPR spectroscopy, thanks to the sensitivity of some magnetic parameters (e.g., *g*-factor and nuclear hyperfine tensors) to interactions with the surrounding molecules and to the polarity of the local environment.

In this contest, the ability of the NO moiety to interact with hydrogen-bond donors is particularly significant, since it leads to a fine-tuning of the physicochemical properties of nitroxides under controlled conditions.[37-38] The hydrogen atom is the most common electron-acceptor site, and hydrogen bonding (HB) is the most frequently occurring noncovalent interaction in chemical and biological processes. Halogen atoms equally work as acceptors and the interaction, which they give rise to, is characterized by several properties similar to those of the hydrogen bond.[39] The term halogen bond (XB) is generally used for defining such noncovalent interaction involving halogens as electron acceptors. The general scheme D···X-Y thus applies to XB, in which X is the halogen (Lewis acid, XB donor), D is any electron donor (Lewis base, XB acceptor), and Y is carbon, nitrogen, halogen, etc.: halogen bonding to different XB donors can show a strength comparable to hydrogen bonding (in terms of equilibrium constants and other thermodynamic parameters).

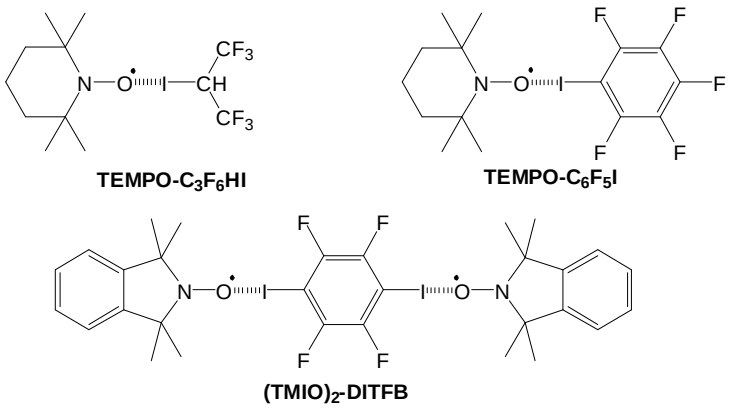

Figure 20 Some of X̃-bonded nitroxides investigated by EPR.

The interaction of the stable TEMPO radical (2,2,6,6-tetramethylpiperidine-*N*-oxyl) with several iodine-substituted fluoroalkanes and fluorobenzenes in solution has been recently investigated by EPR spectroscopy.[40] Such an approach complements other analytical methods used till now to detect XB formation, to define its nature, to establish its strength and structure, and to reveal the similarities between XB and HB. In this paper[40] the presence of a X-bonded nitroxide is demonstrated by analysis of the corresponding EPR spectrum. In particular, the formation of a X-bonded TEMPO was manifested primarily as an increase in the isotropic nitrogen hyperfine coupling a(N) (see Figure 21), with a minimal effect on the g value (g_{iso}). The substantial increase of the nitrogen splitting (e.g., 15.37 G in C_8F_{18}, 16.17 G in $C_8F_{17}I$), is consistent with an increase in spin density at the nitrogen nucleus of the nitroxide, because the ionic resonance structure of TEMPO becomes slightly more stable through the halogen bonding of the N-O• moiety with the iodine nucleus.

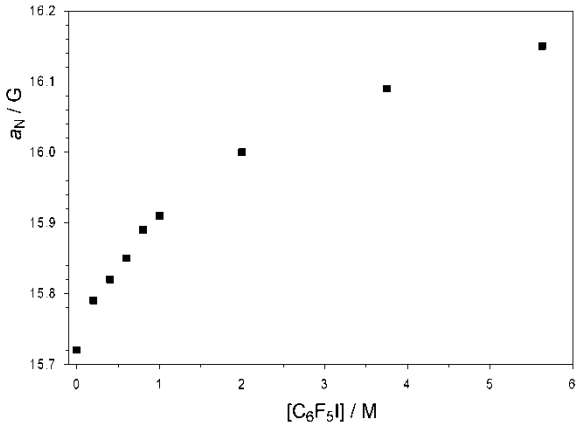

Figure 21. Experimental dependence of a(N) for solutions of TEMPO in hexafluorobenzene at 298 K, as a function of iodopentaflurobenzene (C_6F_5I) concentration.

The isotropic *g*-value of TEMPO was also slightly affected, increasing from 2.00597 to 2.00619. Interestingly, the experimental *g* values of the TEMPO complexes with iodine derivatives are larger than those generally shown by nitroxides dissolved in hydrogen bonding donor solvents. This behaviour can be related to the change in the distribution of the spin-density between three atoms: nitrogen, oxygen, and iodine. The electronic *g* tensor is dominated by contributions from the amount of unpaired electron on a given atom and from spin-orbit coupling. Since the spin-orbit coupling constant for the iodine atom (4303 cm^{-1}) is much larger than for nitrogen (73.3 cm^{-1}) and oxygen (151 cm^{-1}), a small transfer of the unpaired spin density from the nitroxidic moiety to the iodine atom is expected to increase the *g* tensor value as demonstrated by DFT computations.[41]

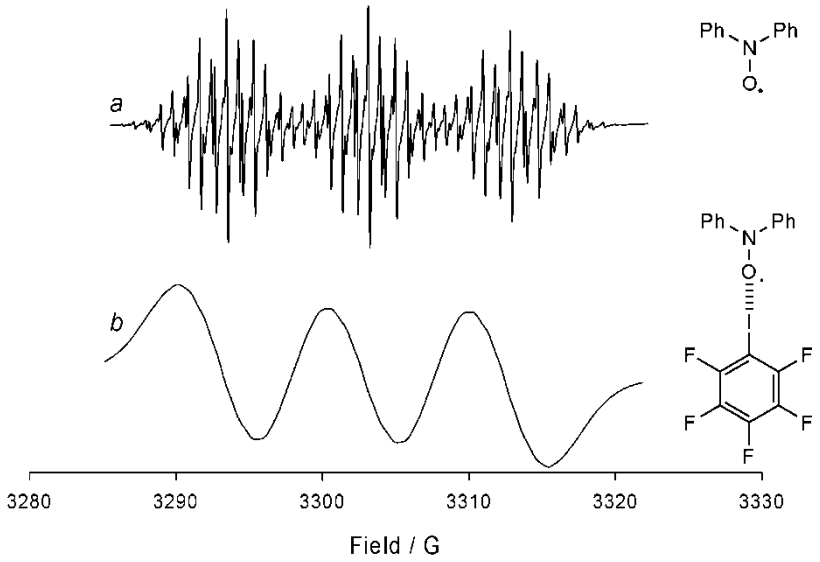

Figure 22. EPR spectra of DPNO recorded in C_6F_6 (a) and in C_6F_5I (b). In the latter case the nitroxide concentration has been raised to get a better signal to noise ratio.

A more convincing evidence for the formation of the halogen-bonded complex was provided by the marked broadening of the EPR lines observed when the nitroxide spectra were recorded in iodoperfluorocarbon solvents. This effect is particularly evident in the EPR spectra of diphenylnitroxide (DPNO), whose hyperfine structure completely disappears upon addition of the iodoperfluoro derivatives (see Fig. 22). The origin of the line broadening may result either from unresolved iodine (^{127}I; I=5/2) hyperfine coupling or/and an increase in the rotational correlation time, a consequence of the increased hydrodynamic radius of the X-bonded nitroxide species.

In a following[42] paper Micallef and coworkers investigated the EPR beahviour of an isoindoline nitroxide (1,1,3,3-tetramethylisoindolin-2-yloxyl, TMIO) in the presence of pentafluoroiodobenzene. Also in this case, the EPR spectrum obtained in the X-bonding donor

pentafluoroiodobenzene exhibited a dramatic increase in line width, with a concomitant reduction in signal intensity. Estimation of the hydrodynamic radii of TMIO (6.78 Å) and TMIO-pentafluoroiodobenzene (15 Å) from the crystal structure of $(TMIO)_2$-diiodotetrafluorobenzene, produces a value of α', which is very similar to the value determined by simulating the experimental spectrum by using Kivelson's line width model.[42] This would suggest that the line broadening arises from a larger rotational correlation time, a consequence of an increased hydrodynamic radius of the TMIO·pentafluoroiodobenzene X-bonded species. If this is correct, then the delocalization of the nitroxide unpaired electron onto the iodine atom (^{127}I; I=5/2) of the solvent through X-bonding interactions must be small, although not negligible.

Since the rate of formation and breakdown of XB is very fast in the time scale of EPR spectroscopy, the experimental spectrum represents the concentration-weighted average of the spectra due to the free and halogen-bonded nitroxides. Under these conditions, the ratio between the free and the complexed species and thus, the equilibrium constants for the formation of the complex, can be obtained by simulation of the experimental spectra in the fast exchange regime by using the intrinsic EPR line shape for the X-bonded nitroxide.[40] The strength of the XB between TEMPO and the different iodoperfluoro derivatives was obtained for the TEMPO/$C_8F_{17}I$ complex, by measuring the variation of the equilibrium constant determined by EPR spectra analysis, in the temperature range between 298 and 328 K. The corresponding thermodynamic parameters were obtained as $\Delta H° = 7.0 \pm 0.4$ kcal/mol and $\Delta S° = 18.1 \pm 1.4$. The EPR value of enthalpy of formation (7 kcal/mol) is quite remarkable and indicates that iodoperfluoro compounds form with TEMPO interactions whose strength is similar to those formed with strong HB donors. For instance, a value of 5.75 kcal/mol has been measured for the formation of TEMPO-hexafluropropanol hydrogen-bonded complex.

2.5 Self-organised architectures investigated by EPR spin probes

Self-assembly is a powerful tool for the preparation of assemblies of well-defined (nano)architecture and for obtaining materials with tailored physicochemical properties (in particular, electronic and optical properties).[43] This approach has been used to obtain different materials, for example, gels, liquid crystals and discrete assemblies, with potential broad practical applications. A great effort has been devoted to the investigation of self-organised architectures based on directional, multiple hydrogen-bonding interactions. In particular Rebek and colleagues[44] have pioneered the use of self-assembly to produce molecular capsules seamed

together by hydrogen bonds. In most cases the basic building blocks of capsules are hosts related to resorcinarenes, which are bowl-shaped tetrameric macrocycles formed by the condensation of resorcinol derivatives with aldehydes in an acidic medium.[45]

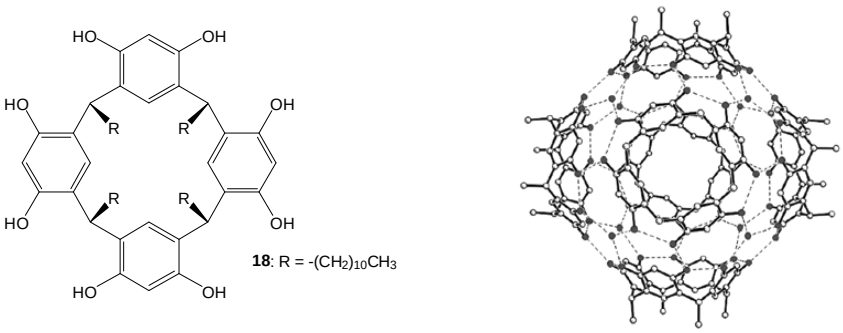

Figure 23. Strucure of the resorcinare host **18** (left) and crystal structure of hexamer $\mathbf{18}_6 \cdot 8H_2O$ in a ball and stick representation (right). Reproduced from *J. Am. Chem. Soc.*, 2004, **126**, 2939 with permission of American Chemical Society.

Kaifer and co-workers[46-47] have applied EPR techniques to investigate the formation and properties of large molecular capsules that result from the self-assembly of resorcinarenes **18** in nonpolar media, such as chloroform and dichloromethane solutions. They used nitroxide spin probes (TEMPO or derivatives) as potential guests for encapsulation by resorcinarene **18**. The EPR spectra were recorded in water-saturated CH_2Cl_2 solutions in order to provide the water molecules that are necessary to complete the hydrogen-bond network required for capsule formation.

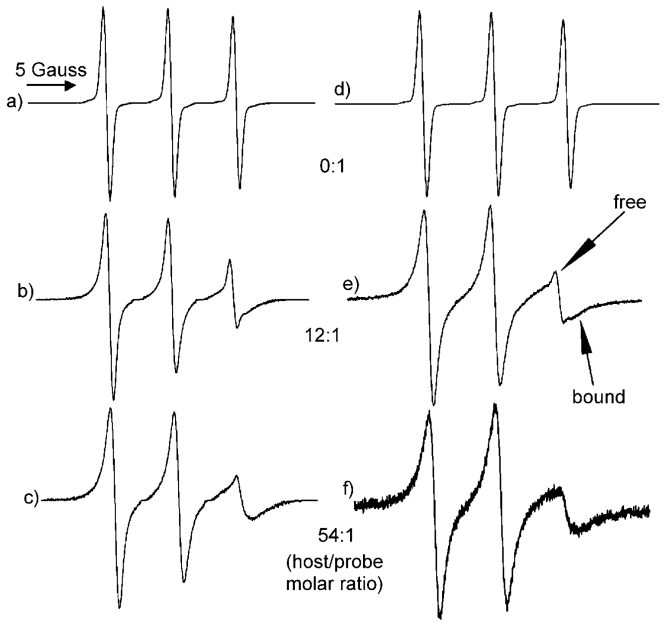

Figure 24. Experimental EPR spectra in water-saturated CH_2Cl_2 at 293 K. a) **12** 0.10 mM, b) **12** 0.10 mM + **18** 1.20 mM, c) **12** 0.05 mM + **18** 2.70 mM d) **15** 0.10 mM, e) **15** 0.10 mM + **18** 1.20 mM, f) **12** 0.05 mM + **18** 2.70 mM. Reproduced from E. Mileo, S. Yi, P. Bhattacharya and A. E. Kaifer, Probing the Inner Space of Resorcinarene Molecular Capsules with Nitroxide Guests, *Angew. Chem. Int. Ed.*, 2009, **48**, 5337. Copyright Wiley-VCH Verlag GmbH & Co. KGaA.

The addition of increasing amounts of resorcinarene **18** to 4-amino-TEMPO (**12**)/CH_2Cl_2 solution leads to significant changes in the EPR spectra (figure 24). In the region that corresponds to the high-field line, two different, superimposed signals are present: a sharp signal, due to the free nitroxide probe that undergoes fast motion, and a much broader line (Figure 24b) due to the encapsulated radical. This reflects the decreasing tumbling rate of the nitroxide probe upon encapsulation inside the hexameric assembly. Similar results were also obtained for nitroxides **15** and **16**, while EPR spectra of tempone were substiantially unaffected by the presence of resorcinarene.

The EPR spectroscopic data collected in this work supported the hypothesis that encapsulation of guests with $\mathbf{18}_6$ is affected by the electrostatic nature of the guests involved. Electrostatic surface potential plots of the nitroxide probes revealed that their encapsulation is enhanced by surfaces with positive charge density, such as those of nitroxide **12**, **15**, and **16**. In contrast, a probe such as tempone, whose surface is predominantly laced with negative charge density, fails to undergo encapsulation. This failure is probably due to the electrostatic complementarity between positively charged guests and the mostly aromatic, inner walls of the resorcinarene capsules.

In order to assess to what extent the motion of the trapped probes may reflect the overall motion of the entire assembly, the approximate molecular volumes were calculated from the rotational correlation times for the encapsulated nitroxide probes. Molecular volumes of 4700, 19000, and 39000 $Å^3$ for encapsulated nitroxides **12**, **15**, and **16**, respectively were estimated. Since the overall volume of the hexameric molecular capsule is expected to remain constant regardless of the sequestered guest, these values reflect the relative levels of probe motion inside the capsule.

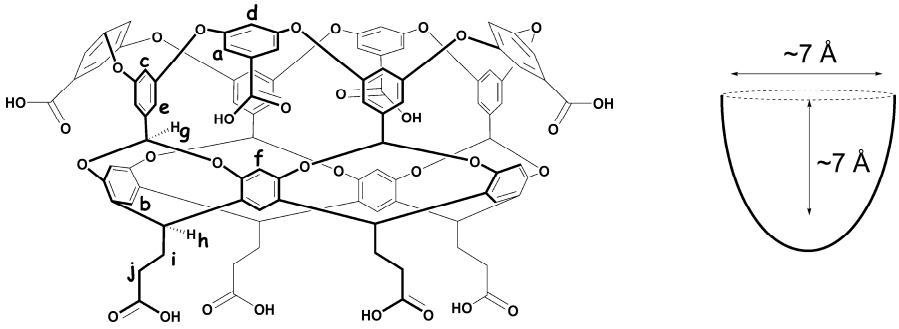

Figure 25. Structure of the host investigated in ref.s 48-49. Reproduced from *Langmuir*, 2009, **25**, 3473, with permission of American Chemical Society.

The Turro and Ramamurthy research groups have shown that spin probes yield very interesting data on the properties of dimeric molecular capsules formed by a deep-cavity cavitand in

aqueous solution.[48-49] In particular, the cavitand studied, reported in Figure 25, has shown to readily form dimeric capsule in water.[50]

The walls of molecular flasks are not necessarily completely insulating, and interactions between incarcerated guests and external molecules can occur through the phenomenon of superexchange. Enabled by employing a ^{15}N-labeled incarcerated nitroxide **17** and a ^{14}N-labeled free nitroxide **15** in the external aqueous phase, Ramamurthy and Turro reported an example of the simultaneous observation, by EPR spectroscopy, of the electron spin-spin superexchange between an incarcerated paramagnetic nitroxide molecule and a nitroxide molecule present in the external aqueous phase.[48] In this example, no new host–guest or guest–guest interactions occur, but the host instead facilitates interactions of the enclathrated guest with the outside environment. They showed how this communication between an incarcerated guest and molecules in the bulk solvent can be controlled by supramolecular factors such as Coulombic attraction and repulsion between a charged guest@host complex and charged molecules in the bulk aqueous phase. In addition to observation of electron spin-spin interactions, the EPR data provide direct information on the motion and the polarity of a ^{15}N-labeled incarcerated guest and ^{14}N-labeled free molecule in the bulk solvent.

2.6. Switching of the spin-spin interactions.

One valuable feature of supramolecular self-assembly is its dynamic nature, due to the reversibility of the non-covalent interactions. This dynamic nature leads to the preparation of functional materials, the physical properties of which can be tuned and controlled by external stimulii, for example, light.[51]

Switching of the spin-spin interactions in organic radicals is of particular interest for the development of molecular-scale magnetic devices. When the spin exchange occurs only through-space, complete control of this interaction can be obtained by modifying the spatial arrangement of radical centres.[52] Whereas spin-spin coupling via covalent bonds has been well studied, strong through-space interactions between organic radicals are more difficult to achieve because unpaired spins have to be located at a short distance.

2.6.1 Self-assembled cages

In an unconventional approach, Fujita and co-workers utilized cage **19** to organize and

manipulate the through-space interactions of organic radicals.[53] In solution, free nitronyl nitroxides **20** exhibit no particular intermolecular interaction, being characterised by a sharp EPR signal, which is split into a 1:2:3:2:1 quintet due to coupling with two nucleus spins of nitrogen atoms (Figure 27a). When an excess of powdered **19** was suspended in an aqueous solution of **20** at 20 °C for 1 h the clathrate compound, **19**•(**20**)$_2$, containing in the molecular cage two nitroxidic units is formed.

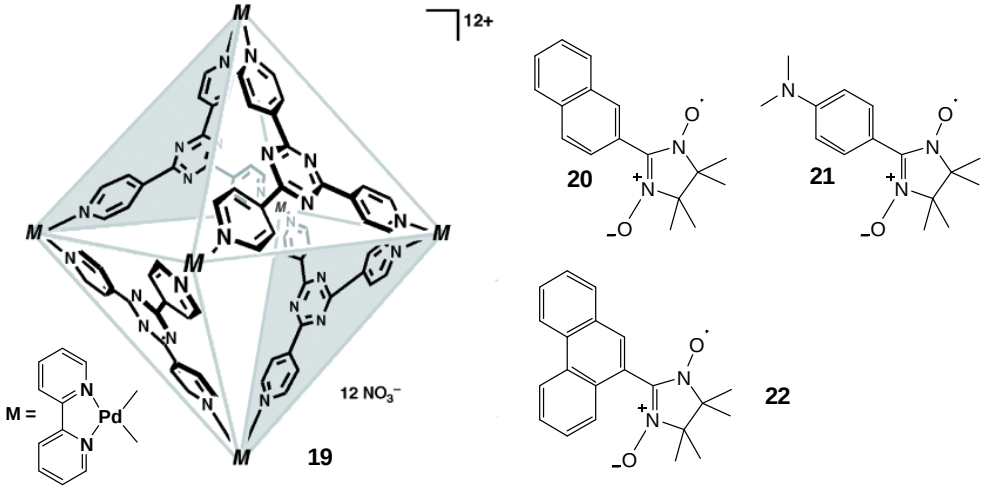

Figure 26 Molecular cage **19** and nitroxides **20**-**22** investigated by Fujita et al.

The remarkable feature is that the enclathration inside the cage induces intermolecular spin-spin interaction between two guests, which is clearly observed by EPR. Actually, the spectrum of **19**•(**20**)$_2$ in solution at 293 K is characterised by an additional broad signal assigned to a dimeric aggregate of radical **20** in a triplet state that stems from intermolecular spin-spin interaction (Figure 27). A reliable evidence for the intermolecular spin-spin interaction comes from the clear observation of a forbidden transition, $\Delta m_s=2$, at half the magnetic field of $\Delta m_s=1$ (1600 G). The distance between radical centers was estimated by point–dipole approximation to be 5.9 Å. X-ray crystallographic analysis confirmed that the two radical centers of **20** are held in proximity, with an average intermolecular distance of 5.8 Å.

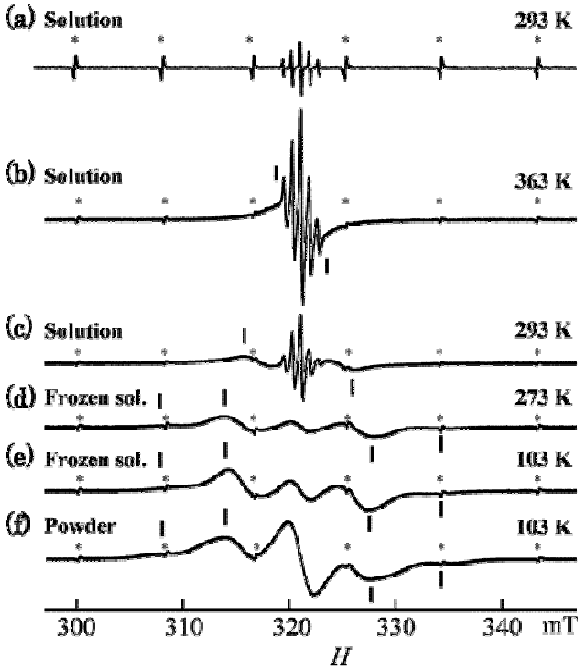

Figure 27. EPR spectra of (a) radical **20** (saturated) and (b-e) clathrate complex **19**•(**20**)$_2$ (5 mM) in water at various temperatures. (f) Powder EPR spectra of clathrate complex **19**•(**20**)$_2$ at 103 K. Signals with an asterisk are of a Mn^{2+} external reference. Reproduced from *J. Am. Chem. Soc.* 2004, **126**, 16694, with permission of American Chemical Society.

The use of the dimethylamino derivative **21** led to a pH-responsive host–guest system, and the spin–spin interactions could be controlled by adjusting the pH value.[54] The two guest radicals interact in neutral solution, and the EPR of the clathrate shows a triplet state. When the pH value is lowered by the addition of acid (HNO_3), the dimethylamino group is protonated and the cationic nitroxide has a lower affinity for the highly positive cage **19**. The radical guests exit the host cavity and the EPR triplet signal is replaced by a doublet, which indicates no intermolecular interactions. This process is reversible: neutralization with K_2CO_3 results in re-encapsulation and the reappearance of the triplet signal. This pH-controlled switching of a spin-spin coupling between two organic radicals placed in a self-assembled cage represented the first example of reversible control by an external stimulus over an intermolecular spin-spin interaction in solution.

Radical cages with unpaired electron spins in their frameworks are seldom prepared and their properties - with the exception of cagelike cluster compounds that have unpaired electrons at metal centers[55] - particularly the interactions with radical guests, are largely unexplored. This is mainly because of difficulties in introducing stable organic radicals at the core of the host frameworks. Only very recently, Fujita and coworkers[56] reported the self-assembly of a radical cage containing multiple spin centres around a cavity suitable for guest inclusion. They showed

that verdazyl radical-cored ligand **23** is quantitatively self-assembled into the large spin cage **24** upon treatment with a Pd(II) complex (Figure 28).

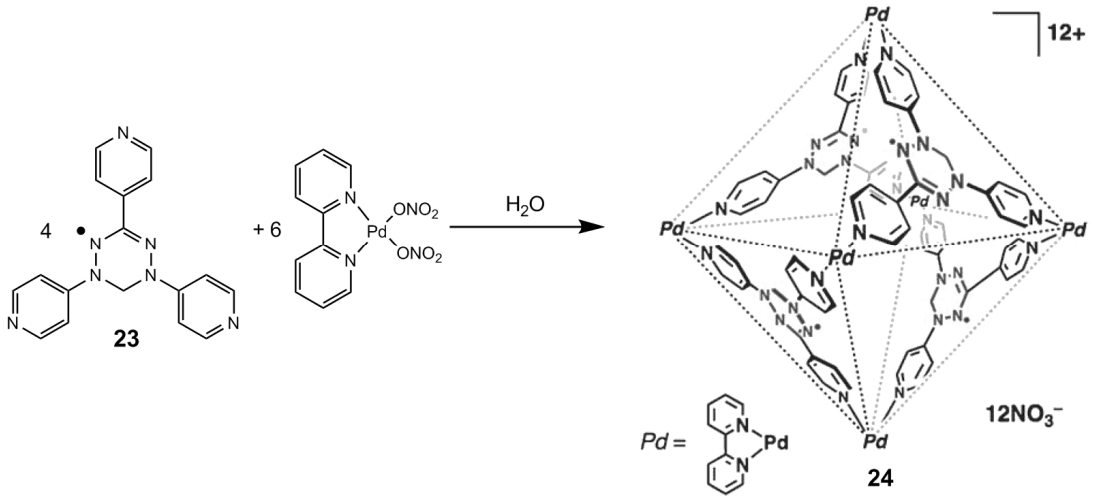

Figure 28 Schematic representation of spin cage **24** formation.

The four spin centres of spin cage **24** show intramolecular magnetic interactions. While ligand **23** shows nine sharp signals derived from four nitrogen nuclei (Figure 29a), which indicates that intermolecular exchange interactions are considerably weak compared to the hyperfine interaction (a(N)=5.6 G), the EPR spectrum of **24** shows only one broad signal (Figure 29b).

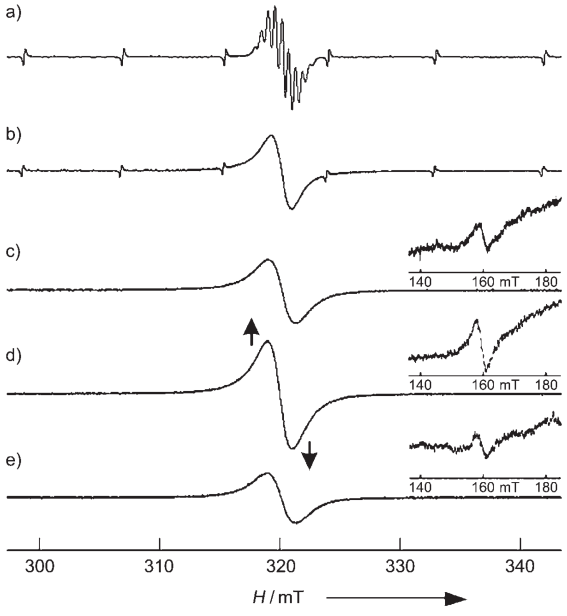

Figure 29. EPR spectra of a) ligand **23** (295 K, $CHCl_3$/MeOH 4/1), b) cage **24** (293 K, H_2O); c) cage **24** (113 K, frozen H_2O); d) complex **22**·**24** (113 K, frozen H_2O); e) recovered **24** after extraction of **22** with $CHCl_3$ from **22**·**24** (113 K, frozen H_2O). The insets show the forbidden transition (Δm_s=2). Spectra are normalized. Reproduced from K. Nakabayashi, Y. Ozaki, M. Kawano and M. Fujita, A Self-Assembled Spin Cage, *Angew. Chem. Int. Ed.*, 2008, **47**, 2046. Copyright Wiley-VCH Verlag GmbH & Co. KGaA.

The broadening of the signal is independent of concentration and temperature, and thus

intermolecular interactions and motional broadening can be discounted. The signal broadening was ascribed to the proximity of the four spin centres on the ligands within the framework of **24**. The observation of a Δm_s=2 transition also supports the presence of intramolecular spin–spin interactions.

Similar to the analogous triazine-cored **19** complexes,[53] spin cage **24** is capable of binding neutral guests within the cavity in aqueous media. When radical guests are accommodated in the cavity of **24**, spin–spin interactions between the host and the guest are observed by EPR and the magnetic character of the spin cage is affected by the enclathration. Actually, when an excess of powdered nitrosyl radical **22** was suspended in an aqueous solution of **24** at 20°C for 1 h it gave, after filtration of surplus radical guest, the clathrate compound **22·24**. This complex showed a considerably enhanced Δm_s=2 transition, compared to empty cage **24**, and thus indicates the proximity of spin centres on the host and the guest in the cavity (Figure 29d). The original EPR spectrum of the cage was reproduced by removing the radical guest (Figure 29e). Thus, a unique spin cage whose magnetic properties can be modulated by inclusion of a radical guest, was obtained. The water solubility of the spin cage will allow studies on organic radicals in aqueous media to enable the development of guest-tunable spin materials, such as new spin probe reagents and MRI contrast agents, that work in water.

2.6.2 Lipophilic Guanosines.

A different example of open-shell moieties ordered by a supramolecular architecture showing new magnetic properties and based on lipophilic guanosines has been reported by Graziano *et al.*[57]

Lipophilic guanosines are very versatile self-assembling units. In the presence of alkali cations they spontaneously self-associate to give quartet-based columnar structures.[58] As it is possible to functionalise the guanosines in the 8 position and/or at the sugar hydroxy functions, they are ideal scaffolds to locate functional units in pre-programmed positions, inside highly ordered architectures.

Graziano et al.[57] showed that the scaffolding of the persistent radical unit 4-carbonyl-2,2,6,6-tetramethylpiperidine-1-oxyl, can be achieved by taking advantage of the K^+-templated self-assembly of the guanosine derivative **25** into highly directional hydrogen bonded networks. By combining NMR, CD and EPR data it was shown that in the presence of potassium ions this compound can form in fact a D_4-symmetric octameric assembly $\mathbf{25}_8@K^+$ in which the nitroxyl moieties show a weak electron spin–spin exchange interaction. Reversible interconversion

fuelled by cation release and complexation allows the switching between discrete quartet-based assemblies and molecularly dissolved **25**, thus controlling the intermolecular weak spin–spin interactions (Figure 30).

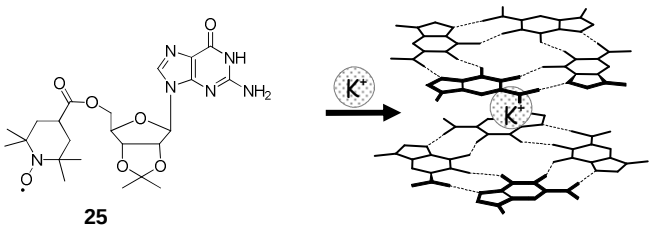

25

Figure 30. Schematic representation of D_4-symmetric octamer formed from paramagnetic guanosine **25**.

The next step was that to increase the spin exchange difference between the two states to obtain drastic magnetic changes before and after addition of the metal cation. Neviani *et al.*[59] reported on the self-assembly properties of derivative **26** where two TEMPO units are connected to the guanosine deoxynucleoside at the O5′ and O3′ positions (Figure 31). This target molecule was simply chosen because in the metal templated assembled species of **26** the number of paramagnetic units doubles, possibly leading to significant enhancement of magnetic coupling.

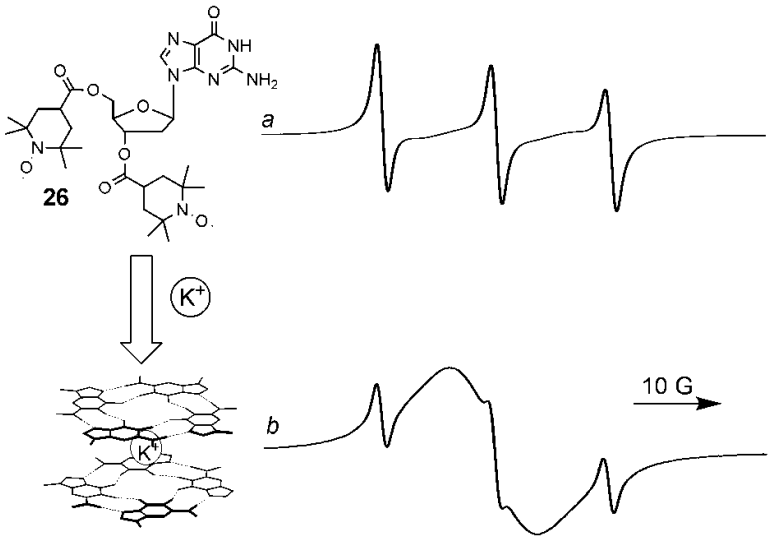

Figure 31 Room temperature EPR spectra of **26** (0.5 mM) before (a) and after (b) K-Picrate extraction.

In the absence of metal cations, the spectrum is characterized by three equally spaced lines with a broadening between them, this being an indication that intramolecular spin exchange is occurring (Figure 31a). In sharp contrast, the EPR spectrum recorded after solid-liquid extraction of potassium picrate shows mainly one broad signal whose integrated intensity corresponds to the initial amount of radicals (Figure 31b). The broadening (peak to peak line width = 12 G) of the signal is independent of concentration and temperature, and thus

interassembly interactions and motional broadening can be discounted. This spectrum is reminiscent of those obtained from very concentrated nitroxide solutions (>0.05 M). Since the spectrum was obtained at 0.5 mM concentration, the signal broadening is ascribed to the proximity of spin centers of **26** within the framework of the octamer. This signal may contain not only a triplet transition but also other multiplet transitions from higher spin states arising from multiple interactions between the 16 radical units. At 77 K in CH_2Cl_2 glass, the spectrum of the octamer showed only a featureless single peak in the g ≈ 2 region and a weak $|\Delta ms| = 2$ peak at 1660 G. The observation of a $|\Delta ms| = 2$ transition also support the presence of intermolecular spin-spin interaction. However, the signal of $|\Delta ms| = 2$ transition is very weak, indicating that these transition probabilities are extremely small as a result of a small *D*-value of the high spin-spin states from the octamer. Accordingly to previous investigation[60] on symmetric tetraradical, this feature was attributed the lack of resolvable zero field splitting to the time-averaged symmetry of the complex.

Although metal-induced magnetic exchange coupling in paramagnetic azacrowns have also been reported,[61] the above work should be regarded as the first example of a radical-armed self-assembling scaffold showing drastic magnetic changes by addition-removal of diamagnetic alkali metal cations.

2.7. Conclusions

The reported examples showed that EPR has proved to be an important tool for the investigation of non-covalent assemblies and we expect that this technique will continue to represent an important tool in the field of supramolecular chemistry. In particular, the characterisation of sophisticated spin traps based on the coupling of nitrones with macrocyclic will require extensive use of EPR spectroscopy. EPR will remain also the fundamental tool to follow the reversible introduction-suppression of spin-spin exchange in a self-recognizing and self assembling stable free radicals. A development of pulsed or multi-frequency experiments (at the moment largely unexplored) for the characterisation of host-guest complexes is also desired in the next few years.

References

‡ Formation of inclusion complexes between cyclodextrin derivatives and TEMPO or DOXYL-based spin probes has also recently reported: S. Rossi, M. Bonini, P. Lo Nostro and P. Baglioni, *Langmuir*, 2007, **23**, 10959; G. Ionita, A. Caragheorgheopol, H. Caldararu, L. Jones and V. Chechik, *Org. Biomol. Chem.*, 2009, **7**, 598; B. Dzikovski, D. Tipikin, V. Livshits, K. Earleac and J. Freed, *Phys. Chem. Chem. Phys.*, 2009, **11**, 6676.

1. 'Nitroxides: Applications in Chemistry, Biomedicine, and Materials Science', ed. Likhtenshtein, G. I.; Yamauchi, J.; Nakatsuji, S.; Smirnov, A. I.; Tamura, R. Wiley-VCH, Weinheim, **2008**.
2. Franchi, P.; Lucarini, M.; Pedulli, G. F. *Curr. Org. Chem.,* **2004**, *8*, 1831; Martini, G.; Ciani, L. *Phys. Chem. Chem. Phys.*, **2009**, *11*, 211.
3. Lucarini, M.; Pasquato, L. *Nanoscale*, **2010**, *2*, 668.
4. 'Cyclodextrins and their Complexes', ed. H. Dodziuk, Wiley-VCH, Weinheim, **2006**.
5. Lucarini, M.; Luppi, B.; Pedulli, G. F.; Roberts, B. P. *Chem. Eur. J.*, **1999**, *5*, 2048.
6. Franchi, P.; Pedulli, G. F.; Lucarini, M. *J. Phys. Chem. A,* **2008,** *112*, 8706.
7. Mileo, E.; Franchi, P.; Gotti, R.; Bendazzoli, C.; Mezzina, E.; Lucarini, M. *Chem. Comm.*, **2008**, 1311.
8. Lin, C.-E.; Huang, H.-C.; Weng, H.-W. *J. Chromatogr. A*, **2001**, *917*, 297.
9. Paton, R. M.; Kaiser, E. T. *J. Am. Chem. Soc.*, **1970**, *92*, 4723.
10. Ionita, G.; Chechik, V. *Org. Biomol. Chem.,* **2005**, *3*, 3096; V. Chechik and G. Ionita, *Org. Biomol. Chem.* **2006**, *4*, 3505;
11. Krock, L.; Shivanyuk, A.; Goodin, D. B.; Rebek, J. *Chem. Commun.*, **2004**, 272.
12. Araki, K.; Nakamura, R.; Otsuka, H.; Shinkai, S. *J. Chem. Soc.,Chem. Commun.*, **1995**, 2121.
13. Chechik, V.; Ionita, G. *New J. Chem.*, **2007**, *31*, 1726.
14. Ionita, G.; Florent, M.; Goldfarb, D.; Chechik, V. *J. Phys. Chem. B,* **2009,** *113*, 5781.
15. Carmieli, R.; Papo, N.; Zimmermann, H.; Potapov, A.; Shai, Y.; Goldfarb, D. *Biophys. J.*, **2006**, *90*, 492.
16. Bardelang, D.; Rockenbauer, A.; Jicsinszky, L.; Finet, J.-P.; Karoui, H.; Lambert, S.; Marque, S. R. A.; Tordo, P. *J. Org. Chem.,* **2006**, *71*, 7657.
17. Bardelang, D.; Finet, J.-P.; Jicsinszky, L.; Karoui, H.; Marque, S. R. A.; Rockenbauer, A.; Rosas, R.; Charles, L.; Monnier, V.; Tordo, P. *Chem. Eur. J.*, **2007**, *13*, 9344.

18. Bagryanskaya, E. G.; Bardelang, D.; Chenesseau, S.; Finet, J.-P.; Jicsinszky, L.; Karoui, H.; Marque, S. R. A.; Mobius, K.; Polovyanenko, D.; Savitsky, A.; Tordo, P. *Appl. Magn. Reson.*, **2009**, *36*, 181.

19. Hardy, M.; Bardelang, D.; Karoui, H.; Rockenbauer, A.; Finet, J.-P.; Jicsinszky, L.; Rosas, R.; Ouari, O.; Tordo, P. *Chem. Eur. J.*, **2009**, *15*, 11114.

20. Han, Y.; Tuccio, B.; Lauricella, R.; Villamena, F. A.; *J. Org. Chem.*, **2008**, *73*, 7108; Han, Y.; Liu, Y.; Rockenbauer, A.; Zweier, J. L.; Durand, G.; Villamena, F. A. *J. Org. Chem.*, **2009**, *74*, 5369.

21. Franchi, P.; Fanì, M.; Mezzina, E.; Lucarini, M. *Org. Lett.*, **2008**, *10*, 1901.

22. Hiratani, K.; Kaneyama, M.; Nagawa, Y.; Koyama, E.; Kanesato, M. *J. Am. Chem. Soc.*, **2004**, *126*, 13568.

23. Mock, W. L. in 'Comprehensive Supramolecular Chemistry', ed. F. Vögtle, Pergamon, Oxford, **1996**, Vol. 2, p. 477.

24. Kim, K.; Kim, H. J. in 'Encyclopedia of Supramolecular Chemistry', ed. J. L. Atwood and J. W. Steed, Marcel Dekker, New York, **2004**, p. 390.

25. Lee, J. W.; Samal, S.; Selvapalam, N.; Kim, H. J.; Kim, K. *Acc. Chem. Res.*, **2003**, *36*, 621.

26. Kim, K. *Chem. Soc. Rev.*, **2002**, *31*, 96.

27. Lagona, J.; Mukhopadhyay, P.; Chakrabarti, S.; Isaacs, L. *Angew. Chem., Int. Ed.*, **2005**, *44*, 4844.

28. Uzunova, V. D.; Cullinane, C.; Brix, K.; Nau, W. M.; Day, A. I. *Org. Biomol. Chem.*, **2010**, *8*, 2037.

29. Mezzina, E.; Cruciani, F.; Pedulli, G. F.; Lucarini, M. *Chem. Eur. J.*, **2007**, *13*, 7223.

30. Kirilyuk, I.; Polovyanenko, D.; Semenov, S.; Grigor'ev, I.; Gerasko, O.; Fedin, V.; Bagryanskaya, E. *J. Phys. Chem., B* **2010**, *114*, 1719.

31. Mileo, E.; Mezzina, E.; Grepioni, F.; Pedulli, G. F.; Lucarini, M. *Chem. Eur. J.*, **2009**, *15*, 7859.

32. Marquez, C.; Hudgins, R. R.. Nau, W. M. *J. Am. Chem. Soc.*, **2004**, *126*, 5806.

33. Hwang, I.; Jeon, W. S.; Kim, H.-J.; Kim, D.; Kim, H.; Selvapalam, N.; Fujita, N.; Shinkai, S.; Kim, K. *Angew. Chem., Int. Ed.* **2007**, *46*, 210.

34. Bardelang, D.; Udachin, K. A.; Leek, D. M.; Ripmeester, J. A. *Cryst. Eng.Comm.*, **2007**, *9*, 973.

35. Bardelang, D.; Banaszak, K.; Karoui, H.; Rockenbauer, A.; Waite, M.; Udachin, K.; Ripmeester, J. A.; Ratcliffe, C. I.; Ouari, O.; Tordo, P. *J. Am. Chem. Soc.*, **2009**, *131*, 5402.

36. Jayaraj, N.; Porel, M.; Ottaviani, M. F.; Maddipatla, M. V. S. N.; Modelli, A.; Da Silva, J. P.; Bhogala, B. R; Captain, B.; Jockusch, S.; Turro, N. J.; Ramamurthy, V. *Langmuir*, **2009**, *25*, 13820.

37. Improta, R.; Barone, V. *Chem. Rev.*, **2004**, *104*, 1231.

38. Franchi, P.; Lucarini, M.; Pedrielli, P.; Pedulli, G. F. *Chem. Phys. Chem.*, **2002**, *3*, 789.

39. Metrangolo, P.; Meyer, F.; Pilati, T.; Resnati, G.; Terraneo, G. *Angew. Chem. Int. Ed.*, **2008**, *47*, 6114.

40. Mugnaini, V.; Punta, C.; Liantonio, R.; Metrangolo, P.; Recupero, F.; Resnati, G.; Pedulli, G. F.; Lucarini, M. *Tetrahedron Lett.*, **2006**, *47*, 3265.

41. Cimino, P.; Pavone, M.; Barone, V. *J. Phys. Chem. A*, **2007**, *115*, 8482.

42. Hanson, G. R.; Jensen, P.; McMurtrie, J.; Rintoul, L.; Micallef, A. S. *Chem. Eur. J.*, **2009**, *15*, 4156.

43. Hoeben, F. J. M.; Jonkheijm, P.; Meijer, E. W.; Schenning, A. P. H. *Chem. Rev.*, **2005**, *105*, 1491; Lawrence, D. S.; Jiang, T.; Levett, M. *Chem. Rev.*, **1995**, *95*, 2229; Ajayaghosh, A.; George,. S. J.; Schenning, A. P. H. *Top. Curr. Chem.*, **2005**, *258*, 83.

44. Conn, m. M.; Rebek, J. Jr, *Chem Rev.*, 1997, **97**, 1647; J. Rebek, Jr, *Chem. Commun.*, **2000**, 637.

45. Sliwa, W.; Kozlowski, C.. 'Calixarenes and Resorcinarenes: Synthesis, Properties and Applications', Wiley-VCH, Weinheim, **2009**.

46. Mileo, E.; Yi, S.; Bhattacharya, P.; Kaifer, A. E. *Angew. Chem. Int. Ed.*, **2009**, *48*, 5337.

47. Yi, S.; Mileo, E.; Kaifer, A. E. *Org. Lett.*, **2009**, *11*, 5690.

48. Chen, J. Y.-C.; Jayaraj, N.; Jockusch, S.; Ottaviani, M. F.; Ramamurthy, V.; Turro, N. J. *J. Am. Chem. Soc.*, **2008**, *130*, 7206.

49. Kulasekharan, R.; Jayaraj, N.; Porel, M.; Choudhury, R.; Sundaresan, A. K.; Parthasarathy, A.; Ottaviani, M. F.; Jockusch, S.; Turro, N. J.; Ramamurthy, V. *Langmuir*, **2010**, *26*, 6943.

50. Porel, M.; Jayaraj, N.; Kaanumalle, L. S.; Maddipatla, M. V. S. N.; Parthasarathy, A.; Ramamurthy, V. *Langmuir*, **2009**, *25*, 3473.

51. Feringa, B. L.; van Delden, R. A.; Koumura, N.; Geertsema, E. M. *Chem. Rev.*, **2000**, *100*, 1789; Kinbara, K.; Aida, T. *Chem. Rev.*, **2005**, *105*, 1377; Yagai, S.; Kitamura, A. *Chem. Soc. Rev*. **2008**, *37*, 1520.

52. Fujita, W.; Awaga, K. *Science* **1999**, *286*, 261. Itkis, M. E.; Chi, X.; Cordes, a. W.; Haddon, R. C. *Science* **2002**, *296*, 1443.

53. K. Nakabayashi, M. Kawano, M. Yoshizawa, S. Ohkoshi and M. Fujita, *J. Am. Chem. Soc.*, **2004**, *126*, 16694.

54. Nakabayashi, K.; Kawano, M.; Fujita, M. *Angew. Chem. Int. Ed.*, **2005**, *44*, 5322.

55. For a review on cagelike compounds with spins at metal centers see: McInnes, E. J. L.; Piligkos, S.; Timco, G. A.; Winpenny, R. E. P. *Coord. Chem. Rev.*, **2005**, *249*, 2577.

56. Nakabayashi, K.; Ozaki, Y.; Kawano, M.; Fujita, M. *Angew. Chem. Int. Ed.*, **2008**, *47*, 2046.

57. Graziano, C.; Pieraccini, S.; Masiero, S.; Lucarini. M.; Spada, G. P. *Org. Lett.*, **2008**, *10*, 1739.

58. Lena, S.; Masiero, S.; Pieraccini, S.; Spada, G. P. *Chem. Eur. J.*, **2009**, *15*, 7792.

59. Neviani, P.; Mileo, E.; Masiero, S.; Pieraccini, S.; Lucarini, M.; Spada, G. P. *Org. Lett.*, **2009**, *11*, 3004.

60. Rajca, A.; Mukherjee, S.; Pink, M.; Rajca, S. *J. Am. Chem. Soc.* **2006**, *128*, 13497; Kirste, B.; Grimm, M.; Kurreck, H. *J. Am. Chem. Soc.* **1989**, *111*, 108.

61. Igarashi, K.; Nogamia, T.; Ishida, T. *Chem. Comm.*, **2007**, 501.

Chapter 3. Synthesis and characterization of a paramagnetic receptor based on cyclobis(paraquat-*p*-phenylene) tetracation

The majority of this chapter has been published in:

-A. Margotti, C. Casati, M. Lucarini, E. Mezzina, *Tetrahedron Lett.*, **2008**, *49*, 4784-87.

3.1. Introduction

The term *cyclophane* includes all molecules that contain a bridged aromatic ring. Many types of bowl-shaped molecules fall into this category, such as carcerands and hemicarcerands, cryptophanes and hemicryptophanes and calixarenes, resorcinarenes and rigidified recorcinarenes. One of the first examples of a cyclophane molecule was [2.2]metacyclophane (**1a**), which was synthesized in 1899 by Pellegrin (Figure 1). Cram and Steinberg introduced the modern concept of a cyclophane in 1951 by re-synthesizing cyclophane **1a**, along with **1b**, termed *meta and paracyclophanes*, respectively, in which two aromatic rings are held together rigidly by ethylene bridging groups.

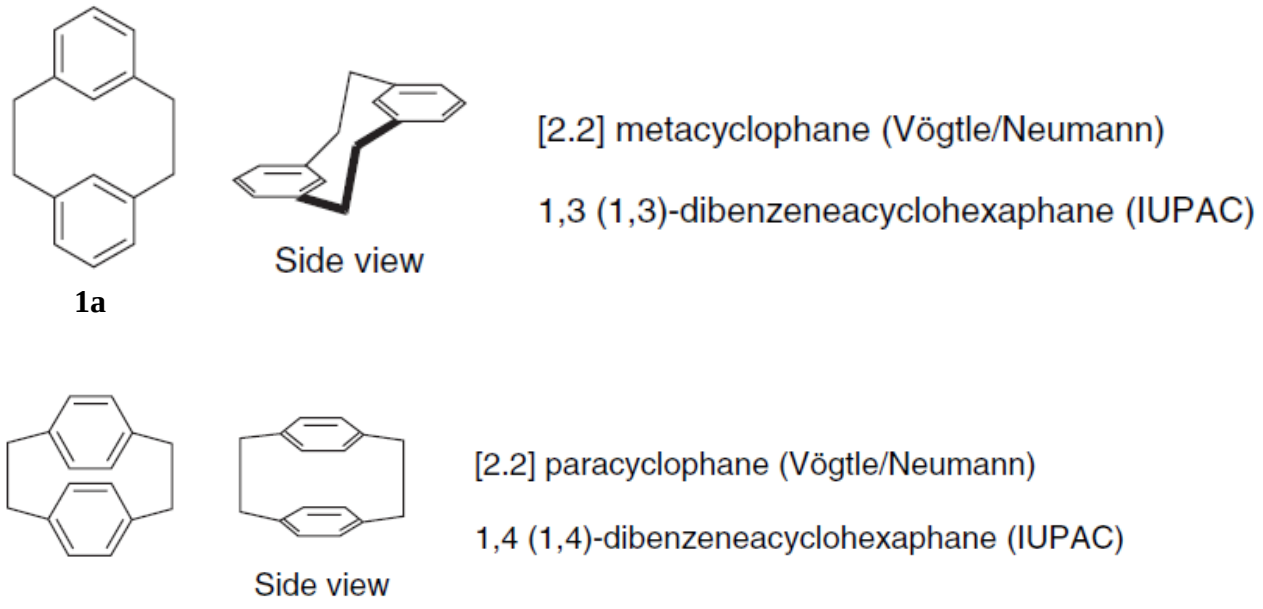

Figure 1. The cyclophanes, [2,2]metacyclophane (**1a**) and [2,2]paracyclophane (**1b**), showing the original (Vögtle and Neumann) and IUPAC nomenclatures.

Vögtle and Neumann broadened the definition of cyclophanes to include every molecule that contains one aromatic ring and at least one *n*-membered bridged group, with $n > 0$. In 2003, IUPAC produced other rules for the definition of highly complex molecular ring systems, as follows:

1. A cyclophane is a compound that has a MANCUDE ring system, that is to say, a **MA**ximium number of **N**on**CU**mulative **D**oubl**E** bonds, or assemblies of MANCUDE ring systems.
2. Cyclophanes contain atoms and/or saturated or unsaturated chains as alternate components of larger ring systems (*cf.* compounds **1a** and **1b**).

3.2 Charge-transfer cyclophanes

In addition to cyclophane hosts based on hydrophobic and hydrogen bonding recognition, a wide range of cyclophanes and cages have been prepared based on charge-transfer interactions. A series of electron-rich cyclophanes-benzo crown ether derivatives was demonstrated to be able to form attractively coloured charge transfer complexes with the herbicide paraquat (*N*,*N*′-dimethyl-4,4′-bipyridinium) and related electron deficient pyridinium type compounds. The host-guest interactions arise from face-to-face charge transfer π-stacking and CH···O hydrogen bonding.

We can readily turn the polarity of this interaction on its head to give an electron deficient paraquat-derived cyclophane **2** capable of binding electron rich aromatic guests such as derivatives of *p*-dimethoxybenzene.

Compound **2**, prepared by the group of Sir J. Fraser Stoddart of Northwestern University, USA, is perhaps one of the most famous cyclophanes in supramolecular chemistry. It is known as the ‘blue box’ because of Stoddart’s colour coding system of filled blue circles for electron deficient and red for electron rich aromatic rings (Figure 2). Blue is an appropriate choice because of the violet-blue colour of the radical cation formed upon one-electron reduction of many paraquat derivatives; a colour that gives them the name ‘viologens’. The blue box has proved to be an amazingly versatile component of many supramolecular assemblies, notably catenanes and rotaxanes. It forms host-guest complexes with a wide range of electron-rich guests, it has extensive redox chemistry involving both one- and two-electron reduction of both paraquat moieties (Scheme 1a), and useful photophysical properties making it a handy probe of electron transfer theory, a useful photosynthesis mimic, and a component of light and redox-activated molecular devices. The blue box has been developed further by incorporation of extra recognition sites as in the chiral **3**. Compound **3** is capable of shape-selective molecular recognition of a single enantiomer of DOPA [3-(3,4-dihydroxyphenyl)-DL-alanine].[1]

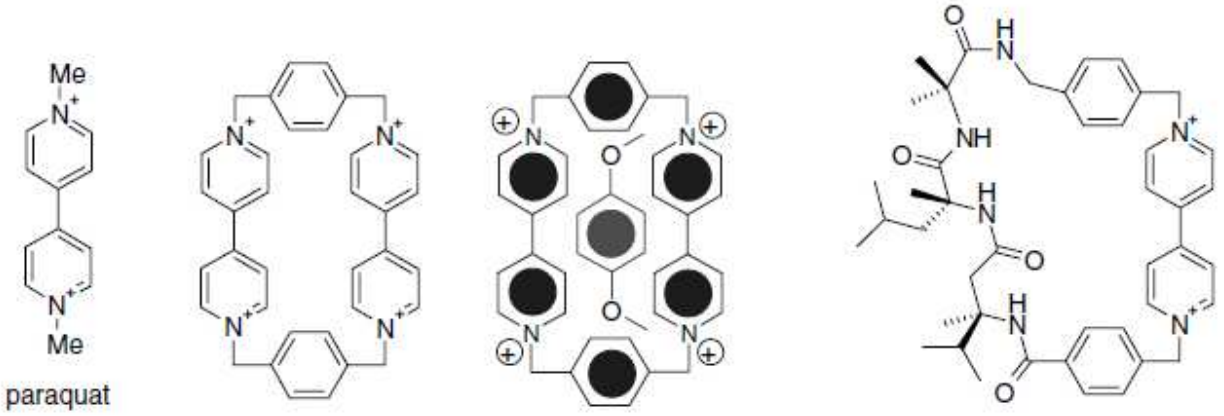

2 Stoddart representation**:** **3**

"blue box" with included

p-dimethoxy benzene

Figure 2 Paraquat, the electron deficient 'blue box' developed by Stoddart and co-workers and a later derivative. Electron deficient aromatic rings are coloured blue, red is used for electron rich rings, neutral hydrocarbons are coloured black while green is used for other moieties such as tetrathiafulvalene.

DOPA resolution is important because L-DOPA is used as a drug in the management of Parkinson's disease.

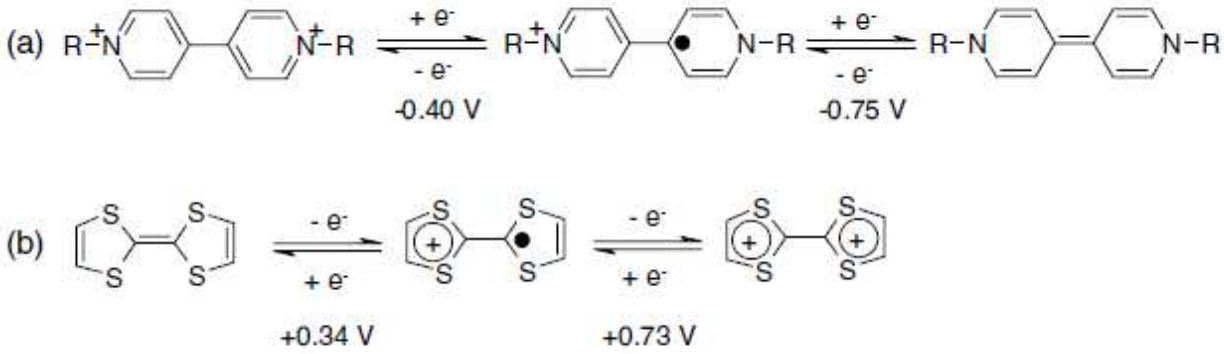

Figure 3. Redox chemistry of (a) viologens and (b) tetrathiafulvalene

Another very versatile cyclophane component capable of forming charge-transfer compounds is the tetrathiafulvalene (TTF) moiety. Like paraquat, TTF has an extensive redox chemistry summarised in Figure 3b, however TTF is an electron donor not an electron acceptor. This redox activity means that it has been incorporated into a range of organic molecular electronic devices.

In terms of cyclophane chemistry, TTF-derived cyclophanes and cages are well known and have interesting properties.[2]

3.3. Content and scope

The present chapter deals with the synthesis of a new class of π-electron-deficient tetracationic cyclophane ring, cyclobis(paraquat-*p*-phenylene), carrying one or two paramagnetic side-arms based on 2,2,6,6-tetramethylpiperidine-N-oxyl (TEMPO) moiety, which has been achieved in five steps starting from 2,5-dimethyl benzoic acid. The possibility of exploiting the proposed cyclophanes as hosts in rotaxane-like structures was tested preparing the monoradical receptor by the clipping procedure in the presence of 1,5-dimethoxynaphthalene (DMN). The addition of template allows the isolation of the monoradical complex with DMN.

3.4. A new paramagnetic $CBPQT^{4+}$-based host

Many areas of chemistry take advantage of the information obtained by the combination of molecules of open-shell configuration and chemical stability, owing to the properties displayed by long lifetime radicals to be isolated as pure compounds and observed by conventional spectroscopic methods. Stable radicals[3] have been used to obtain structural, dynamic and reactivity information using electron paramagnetic resonance (EPR) spectroscopy, and for this reason have been introduced in techniques such as spin labelling,[4] spin trapping[5] and EPR imaging,[6] as well as in the development of new materials displaying magnetic and conductivity properties,[7] or in metal-radical hybrid solid investigation towards molecule-based magnets.[8]

Amongst the open-shell species, nitroxides $R_2NO^{\cdot}$ represent the most well-known class of stable radicals.[9] The versatility of these radicals is further due to the opportunity of behaving like a 'normal' diamagnetic compound, with the possibility of performing diverse organic reactions on molecules carrying a nitroxide group without affecting the radical site itself. Supramolecular chemistry[12] and host–guest chemistry[11] may benefit by this possibility, since introduction of a paramagnetic centre into a molecule acting as a component of the 'supermolecule' is potentially attractive to modulate the behaviour of molecular devices. Recent literature examples of macrocycles carrying paramagnetic centres are represented by paramagnetic calix[4]arenes[10] or cyclodextrin-labelled nitroxides.[13]

In this section there is the synthetic procedure for the preparation of a new class of π-electron-deficient tetracationic cyclophane ring, cyclobis(paraquat-*p*-phenylene) $(CBPQT)^{4+}$, carrying one or two paramagnetic side-arms (**1a**$^{\bullet}$ and **1b**$^{\bullet\bullet}$, respectively) based on 2,2,6,6-tetramethylpiperidine-N-oxyl (TEMPO) moiety as depicted in Figure 1.[14] The electron-deficient macrocycle was chosen

because of its use as ‘molecular shuttle’ in most of the molecular devices proposed by Stoddart and co-workers.[15] The reported radical-armed $(CBPQT)^{4+}$ macrocycle represents a promising host for the preparation of paramagnetic supramolecular architectures, in which spin-spin interactions can be reversibly switched on–off by the movement of the paramagnetic shuttle.

In order to obtain the new macrocycles the bis-pyridinium precursors salts, either in the unsubstituted (**6a**) or in the one-armed (**6b**) form, were linked with a benzylic dibromide **5** containing the nitroxide functionality.

Scheme 1 outlines the synthesis of **5**. Ester **2**, obtained by the acid-catalyzed treatment of 2,5-dimethylbenzoic acid with ethanol,[16] was subjected to an NBS radical bromination with AIBN as the initiator to afford the benzylic dibromide **3**. Reduction of **3** using diisobutylaluminium hydride (DIBAL-H) as the reducing agent, gave the corresponding alcohol **4** in good yields. Subsequent esterification of **4** with 4-carboxy-TEMPO (4-COOH-TEMPO) afforded the dibromide radical **5**.

The modified dipyridinium salt **6b** was prepared by stirring **5** with 2 equiv of 4,4’-bipyridine in DMF at room temperature according to the reaction conditions reported in the Scheme 1.

Chromatography by silica gel column ($MeOH/NH_4Cl/MeNO_2$) afforded **6b** as a reddish solid in good yield. Formation of the cyclophanes shown in Figure 4 was achieved using the clipping methodology consisting in mixing **5** and salt **6a** or **6b** in refluxing acetonitrile for 24–48 h (Scheme 2).

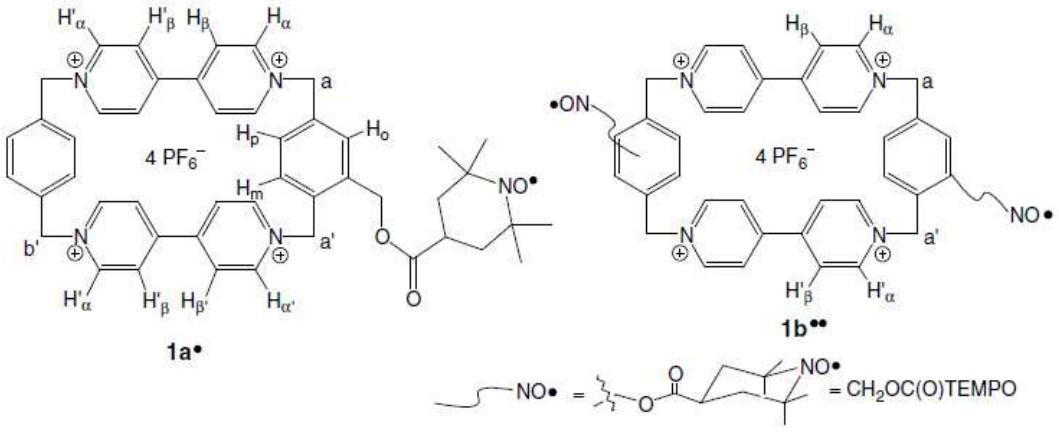

Figure 4. Structure of the paramagnetic macrocycles **1a**$^{\bullet}$ and **1b**$^{\bullet\bullet}$.

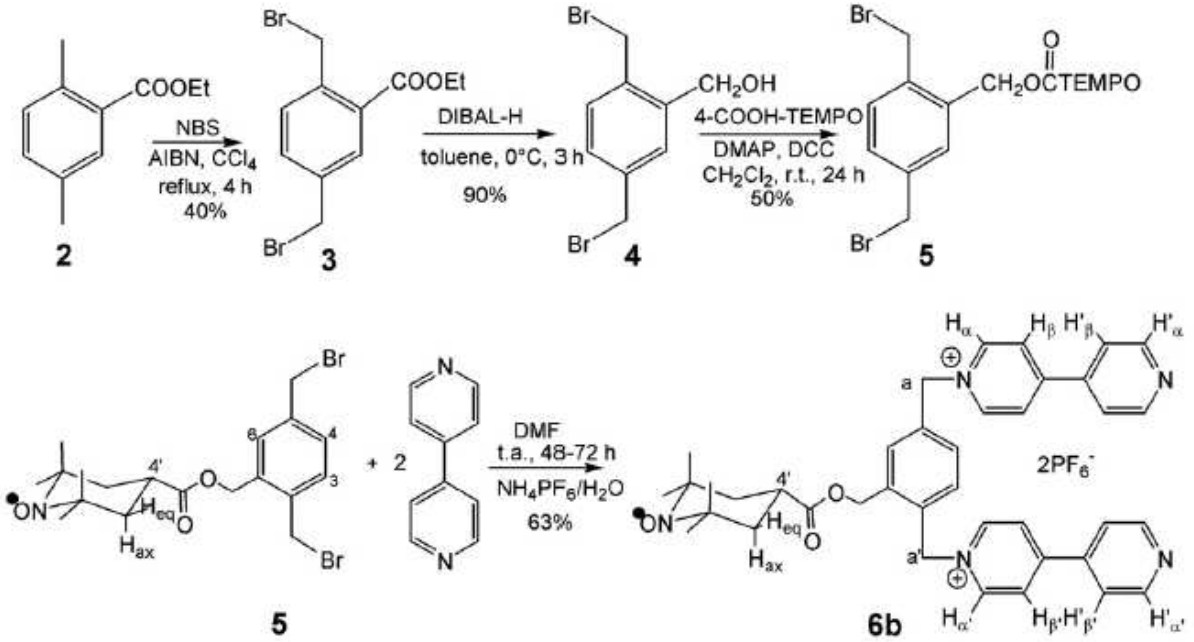

Scheme 1.

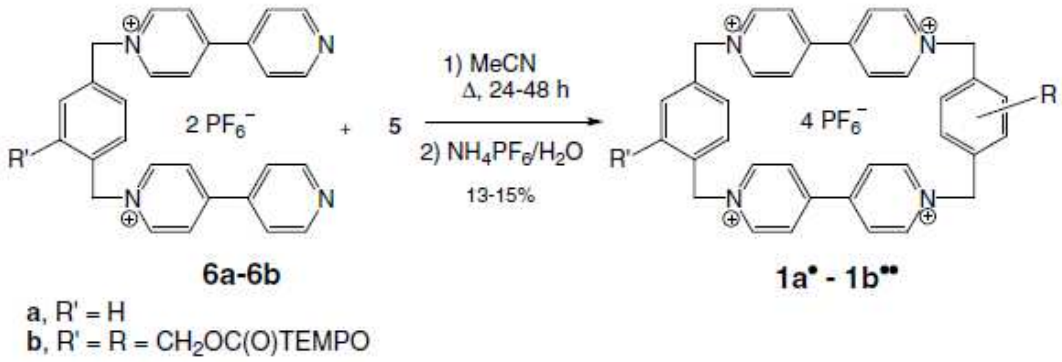

Scheme 2.

Compounds **1a**$^{\bullet}$ and **1b**$^{\bullet\bullet}$ were recovered by precipitation from the reaction mixture, and isolated without chromatography after exchanging the Cl^- counterions of the cyclophane with saturated aqueous NH_4PF_6, as an orange-brown solid.

Structural assignment of the new CBPQT-based macrocycles **1a**$^{\bullet}$ and **1b**$^{\bullet\bullet}$ was justified on the basis of ESI-MS (Figure 8) and 1D, 2D NMR analyses. In Figure 5, the ^{1}H NMR spectrum of **1a**$^{\bullet}$ (trace a) is reported.

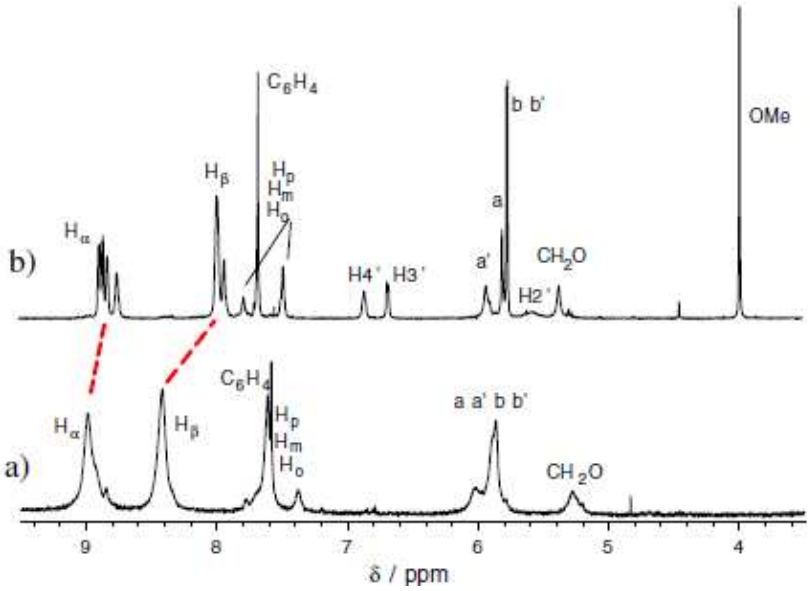

Figure 5. ^{1}H NMR spectra (600 MHz, CD_3CN, 298 K) of the monoradical host **1a•** (a) and its complex with 1,5-dimethoxynaphthalene **7•** (b). The signals were assigned on the basis of 2D ROESY experiments using the labels reported in Figure 4. The dashed lines indicate the most pronounced signal shifts of the complex relatively to the free host.

Because of the paramagnetic units the NMR spectrum shows a very low spectral resolution. In particular, the spectrum is characterized by the lack of the radical heterocyclic signals, and by very broad signals due to the CBPQT protons. In order to render the paramagnetic host suitable for a complete characterization by NMR, it was necessary to quantitatively convert it to the analogous N-hydroxy amine derivatives (**1a-OH**) by adding directly inside the NMR sample stoichiometric amounts of phenylhydrazine.[17]

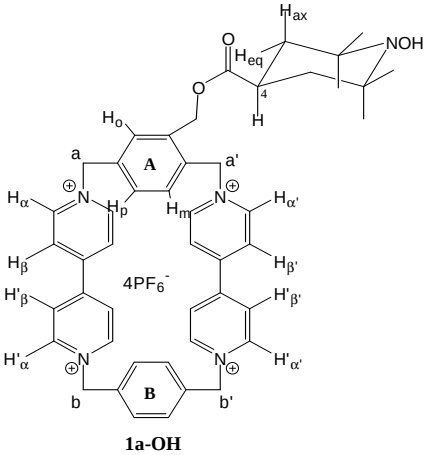

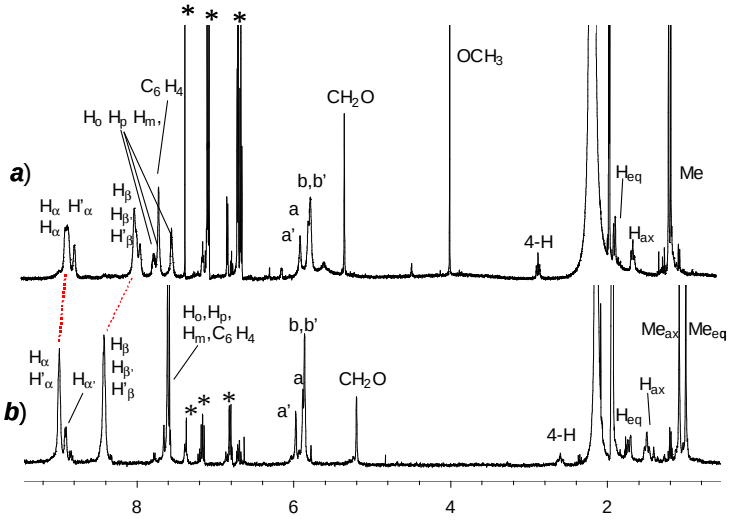

Figure 6. ^{1}H NMR spectra (600 MHz, CD_3CN, 298 K) (a) of the complex with DMN **7a-OH** , (b) **1a-OH** obtained after in situ reduction of **7a•** and **1a•** with phenylhydrazine, respectively. Star symbols refer to the signals of phenylhydrazine. The signals were assigned on the basis of 2D ROESY experiments by using the labels reported in the molecular structure. The dashed lines indicate the signal shifts of the complex relatively to the free host.

The spectrum of **1a-OH** (see Fig. 6, trace b) shows well resolved signals for the viologen protons (H_α and H_β); the presence of the radical arm in the structure is evident by the peak shift of H'_α close to the substituent (assigned by 2D ROESY experiments, Fig. 7), and by the splittings of the methylene signals (a and a') of the 1,4-*para*-phenylene unit (see contour plots in Fig. 7), as a consequence of the arm-modified symmetry of $CBPQT^{4+}$. Detection of new sharp signals relative to the piperidine moiety emerging after radical reduction allows the complete ^1H picture of the macrocycle.

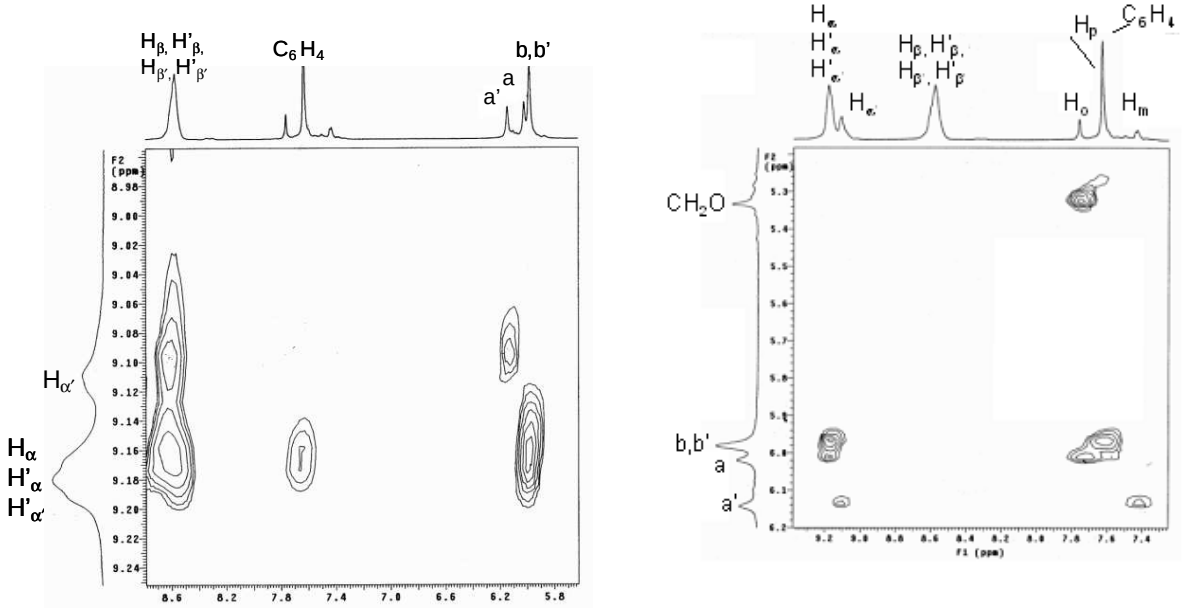

Figure 7. Partial 2D ROESY (600 MHz, D_2O, 298 K) spectra of **1a-OH** · **4Cl**. The contour plot shows the region of intramolecular connections involving the cyclophane ring which allowed the assignment of the *para*-phenilene methylene protons (a and a') and the protons of the viologen ring $H_{\alpha'}$ next to the radical-substituted phenyl ring (ring A). The signals were assigned by using the labels reported in the molecular structure.

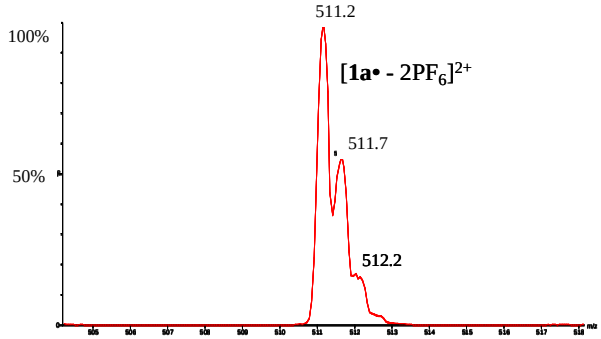

Figure 8. Positive ESI spectrum of a MeCN solution containing **1a•**. The spectrum has been recorded by using the following instrumental settings: positive ions; desolvation gas (N_2) 230 L/h; cone gas (skimmer): 50 L/h; desolvation temp. 120° C; capillary voltage: 3.0 kV; cone voltage: 30 V.

In Figure 9 (trace a) is instead reported the spectrum of the diradical CBPQT **1b$^{\bullet\bullet}$.** It should be noted that it exhibits separate signals of H_α and H'_α per viologen unit, and a couple of methylene proton resonances (a and a'), due to the presence of a radical substituent in each phenyl ring of the tetracationic cyclophane. In the spectrum of the paramagnetic host appears also one set of peaks belonging to the nitroxyl heterocyclic ring, despite the existence of a paramagnetic centre.[18]

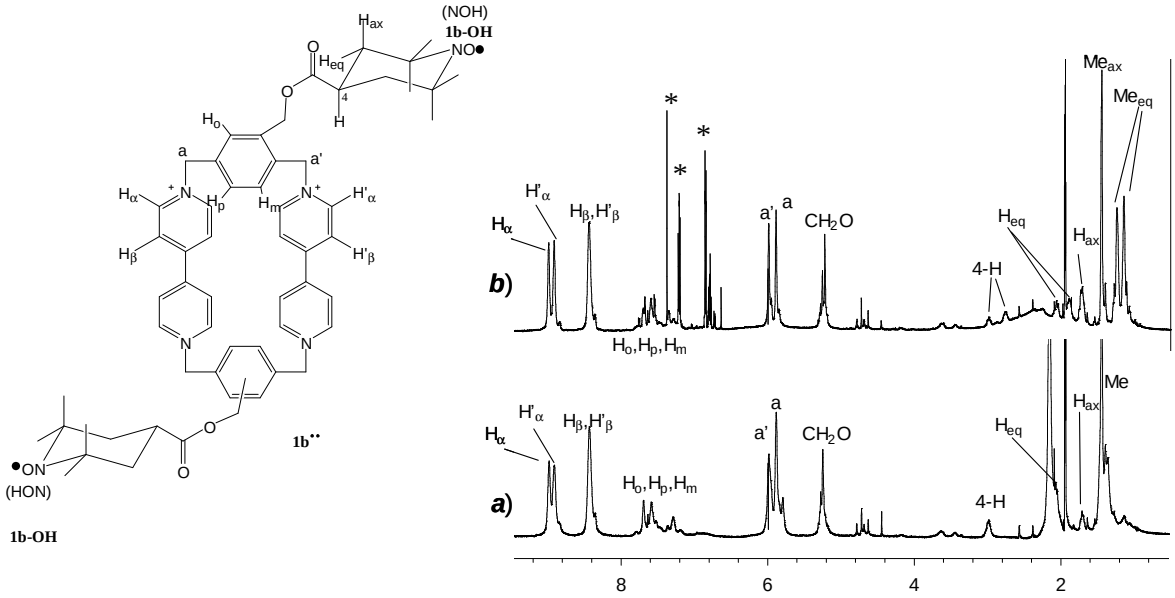

Figure 9. ^{1}H NMR spectra (600 MHz, CD3CN, 298 K) (a) of **1b••** · **4PF6**, (b) of **1b-OH** obtained after in situ reduction of **1b••** with phenylhydrazine. Star symbols refer to the signals of phenylhydrazine. The signals were assigned on the basis of 2D ROESY experiments by using the labels reported in the molecular structure. In CD3CN sample of **1b-OH** most of proton peaks of *N*-hydroxypiperidine moiety are splitted into couples of signals, while in the diradical (spectrum a) **1b••** only one set of signals is detected for the corresponding protons. The same behaviour is found in samples of **1b-OH** recorded in DMSO-d^6.

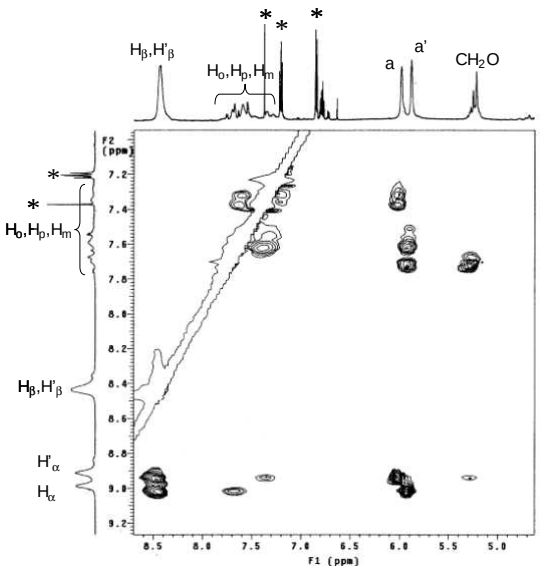

Figure 10. Partial 2D ROESY (600 MHz, CD_3CN, 298 K) spectra of **1b-OH** · **4PF$_6$**. The contour plot shows the region of intramolecular connections involving the cyclophane ring which allowed the assignment of the *para*-phenilene methylene protons (a and a') and the protons of the viologen ring H'$_\alpha$ next to the radical-substituted phenyl ring. Star symbols refer to the signals of phenylhydrazine. The signals were assigned by using the labels reported in the molecular structure.

The possibility of using the proposed receptors as a component in rotaxane-like structure was verified by repeating the clipping procedure for preparation of the macrocycles in the presence of 1,5-dimethoxynaphthalene (DMN), as it is well established that the latter is an effective guest for electron-deficient $CBPQT^{4+}$-based cyclophanes.[19] Actually, addition of the template favours the clippage at room temperature between the bis-pyridinium salt **6a** and the radical dibromide **5** in DMF, and affords a powder after 5 days.[15] Separation of the TLC purple spots of the crude on a silica gel column ($MeOH/NH_4Cl$ (2M)/CH_3NO_2 4:4:2) and product isolation after treatment with saturated aqueous NH_4PF_6 give [1a_DMN] (**7**$^{\cdot}$) complex as a purple solid in 33% yield. The schematic representation[19] of **7**$^{\cdot}$ is reported in Figure 7.

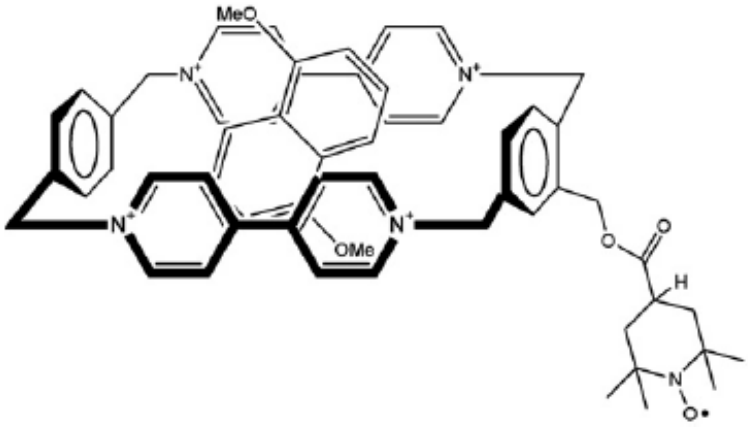

Figure 11. Schematic complex structure

Proof of the formation of the host-guest complexation has been attained by UV–Vis and NMR measurements. The absorption spectrum of **7**$^{\cdot}$ (Figure 12) recorded in water at 298 K shows a broad band in the visible region (λ_{max} = 530 nm, ε = 275 M^{-1} cm^{-1}) resulting from charge transfer interaction between DMN and the π-electron-deficient bipyridinium units of the cyclophane **1a**$^{\bullet}$ and DMN.

Two main features may be outlined looking at the ^{1}H NMR spectrum of the radical complex (Figure 5, trace b). (*i*) The viologen host signals (H_α and H_β) are significantly shifted towards lower frequencies ($\Delta\delta$ = 0.2, 0.45 ppm). The most pronounced shifts are recorded for H_β, which owing to their central location in the macrocycle are most affected from the inclusion of the guest. Also the guest undergoes proton displacements after involvement in the complex, substantial upfield shifts being measured for all the aromatic protons. (*ii*) All the radical host signals in the complete form (trace b) show much better resolution than those of the free macrocycle (trace a), the signals of H_α and H_β being splitted in four and two sets of resonances, respectively. Because line broadening of nuclear magnetic resonances in spin-labelled molecules is distance dependent,[20] the last observation

must be related to the position assumed by the radical arm in the free macrocycle and in the complex.

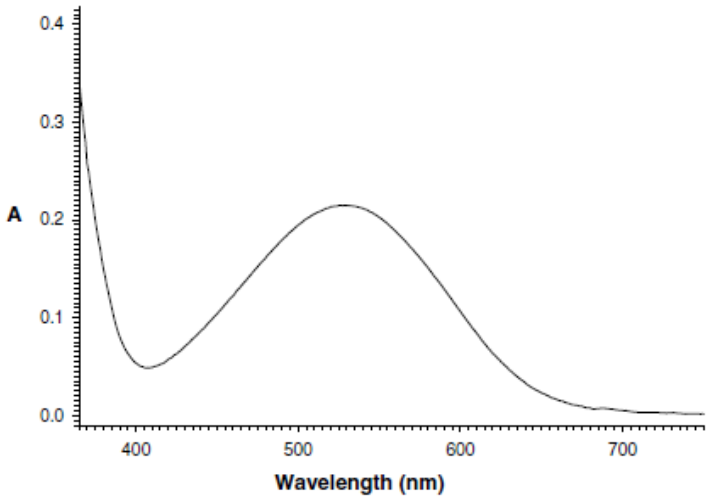

Figure 12. Spectrum UV–Vis of the complex **[7a$^{\bullet}$]·4Br** in H_2O (0.8 mM). In the same spectral region **1a$^{\bullet}$** does not show any significant absorption.

In the former case, the broadening of the lines indicates that the nitroxide could be located in a position close to the macrocyclic receptor[21] similar to that found by Cooke et al. in their armed $CBPQT^{4+}$ derivative containing a pyrrole moiety.[22] Reasonably, complexation displaces the radical substituent from its original position to a new position in which the free radical part is farther from the macrocycle, thus resulting in an improvement of spectral resolution.

Further support for the hypothesis that the heterocycle position changes upon complexation comes from the observation of downfield shifts for the piperidine protons when passing from the reduced free macrocycle **1a-OH** to the corresponding diamagnetic complex **7-OH** (the NMR signals due to the heterocylic protons are too broad to be detected in the spectrum of **1a$^{\bullet}$** and **7a$^{\bullet}$**).

EPR spectra of CH_3CN solutions containing **1a$^{\bullet}$** or **7a$^{\bullet}$** were also recorded. The spectra show typical nitroxide EPR signals with the high field line slightly broadened due to restricted tumbling. Quite unexpected, the two radicals show very similar ^{14}N hyperfine splittings, a_N (15.82 G for **1a$^{\bullet}$** and 15.75 G for **7a$^{\bullet}$**), indicating that the complexation does not significantly affect the spin distribution on the nitroxide moiety.

a)

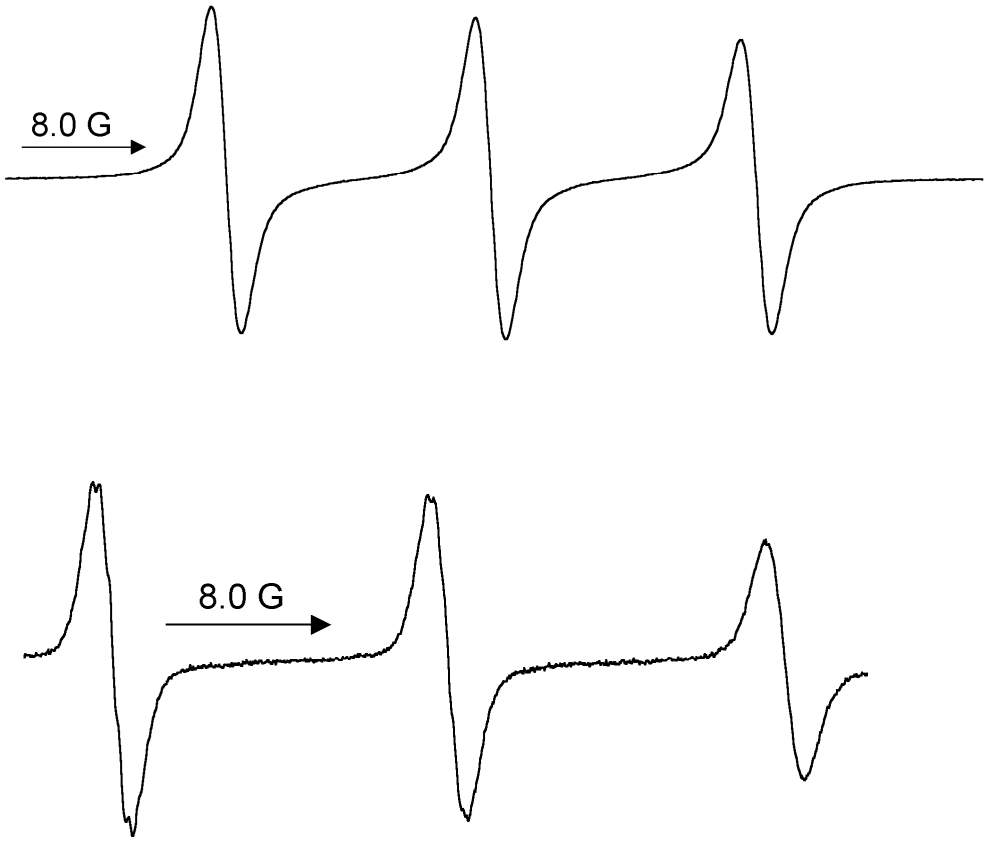

b)

Figure 13. ESR spectra of monoradical **1a•** (a) and diradical **1b••** (b) recorded at 298 K in MeCN and in DMSO, respectively.

Attempts to isolate the complex between the diradical $CBPQT^{4+}$ (**1b$^{\bullet\bullet}$**) with DMN were unsuccessful, thus indicating that formation of host–guest complex with DMN is considerably less favourable in this case, presumably owing to the steric hindrance of the two arms opposing to the insertion of the guest.

3.5. Conclusions

The two new receptors based on CBPQT tetracation bringing one or two paramagnetic substituents on the paraphenylene units represent promising hosts in the synthesis of more complexed paramagnetic supramolecular architectures, rotaxanes or catenanes, employed as molecular magnetic devices.

Moreover, the monoradical receptor **1a**$^{\cdot}$is able to complex eletron-rich molecules. The complex with DMN, isolated by flash chromatography, provides evidence that replacement of the radical arm with DMN in the complex imparts a drastic change upon the spectral proton signals of the cavity, that appear well resolved and separated, contrary to what happens in the free receptor which displays broad signals, therefore, the radical arm could even act as a probe to detect inclusion complex formation.

3.6. Experimental section

All reagents were commercially available and were used without further purification. Compounds **2**,[25] **3**,[26] **4**,[27] **6a**[26] were prepared according to literature procedures. Solvents were used as purchased unless otherwise noted. Analytical TLC was performed on silica gel plates 60-F_{254}. Column chromatography was performed using silica gel 60.

Synthesis of 5. A solution of the alcohol **4** (0.86 g, 2.92 mmol), 4-carboxy-TEMPO (0.585 g, 2.92 mmol), 1,3-dicyclohexylcarbodiimide (DCC) (0.602 g, 2.92 mmol), and 4-dimethylaminopyridine (DMAP, catalytic amount) (0.071 g, 0.584 mmol) in CH_2Cl_2 (100 mL) was stirred for 12 h at room temperature under nitrogen atmosphere. The resulting suspension was filtered, and the filtrate was evaporated and subjected to column chromatography (SiO_2, 7:3 petroleum ether/ethyl acetate) to furnish **5** as a thick orange-brown oil in 50% yield. ^{1}H NMR (400 MHz, $CDCl_3$, 298 K): δ = 7.40-7.60 (m, 3H, H-3, H-4, H-6), 5.37 (br s, 2H, CH_2O), 4.64 (br s, 2H, CH_2Br), 4.54 (br s, 2H, CH_2Br); Positive ESI-MS: *m/z* 498.8 $[M+Na]^+$.

Synthesis of 6b. *Method A:* A solution of **5** (0.178 g, 0.37 mmol) in anhydrous acetonitrile (7 ml) was added dropwise to a refluxing solution of 4,4'-bipyridine (0.142 g, 0.91 mmol) in anhydrous acetonitrile (5 ml), and heating was continued for 24 h under nitrogen. After the solution was cooled to room temperature, the brown precipitate was filtered off and washed with acetonitrile (5 ml) and Et_2O (5 ml) before being dissolved in water. The aqueous solution was subjected to silica gel chromathography (lenght 10 cm, i.d. 2 cm) eluting with MeOH-H_2O-saturated aqueous NH_4Cl solution (5:4:1). The salt-containing fractions were combined, and the solvent was removed in vacuo. The residue was dissolved in water, and a saturated aqueous solution of NH_4PF_6 was added until no further precipitation was observed. After filtration, the precipitate was washed with water and dried, yielding an orange-brown solid. Yield: 22%. ^{1}H NMR (400 MHz, CD_3OD, 298 K): δ = 9.06-9.16 (m, 2H, H_α), 8.94-9.05 (m, 2H, $H_{\alpha'}$), 8.76-8.86 (m, 4H, H'_α, $H'_{\alpha'}$), 8.45-8.60 (m, 4H, H_β, $H_{\beta'}$), 7.90-8.04 (m, 4H, H'_β, $H'_{\beta'}$), 7.78-7.84 (m, 1H, H_{ar}), 7.64-7.70 (m, 1H, H_{ar}), 7.48-7.54 (m, 1H, H_{ar}), 6.05-6.20 (br s, 2H, a'), 5.90-6.00 (br s, 2H, a), 5.30-5.45 (br s, 2H, CH_2O; Positive ESI-MS: *m/z* 774.2 $[M-PF_6]^+$, 314.1 $[M - 2\ PF_6]^{2+}$.

Treatment of the NMR sample containing **6b** with phenylhydrazine gave **6b-OH**: ^{1}H NMR (400 MHz, CD_3OD, 298 K): δ = 9.25 (d, *J* = 6.8 Hz, 2H, H_α), 9.12 (d, *J* = 6.6 Hz, 2H, $H_{\alpha'}$), 8.80-8.88 (m, 4H, H'_α, $H'_{\alpha'}$), 8.55-8.65 (m, 4H, H_β, $H_{\beta'}$), 7.90-8.10 (m, 4H, H'_β, $H'_{\beta'}$), 7.82 (bs s, 1H, H_{ar}), 7.70-7.78 (m, 1H, H_{ar}), 7.48-7.55 (m, 1H, H_{ar}), 6.14 (s, 2H, a'), 6.02 (s, 2H, a), 5.33 (s, 2H, CH_2O), 2.54-2.66 (m, 1H, 4'-H), 1.70 (br d, *J* = 10.8 Hz, 2H, H_{eq}), 1.52 (br t, *J* = 10.8 Hz, H_{ax}), 1.11 (s, 6H, Me), 1.01 (s, 6H, Me).

Method B: A solution of **5** (0.3 g, 0.63 mmol) and 4,4'-bipyridine (0.242 g, 1.55 mmol) in dry DMF (30 ml) was stirred at room temperature for 48-72 h under nitrogen. The solvent was removed in vacuo and the residue subjected to column chromatography (SiO_2, 4:4:2 MeOH/NH_4Cl (2 M)/CH_3NO_2) (length 10 cm, i.d. 3 cm). The fractions containing the product were combined together and concentrated under vacuo. The residue was dissolved in water and a saturated aqueous solution of NH_4PF_6 was added to furnish **6b**. The precipitate was washed with water and dried, affording the salt in 65% yield.

Synthesis of 1a$^{\bullet}$. A solution of **6a** (0.240 g, 0.34 mmol) and **5** (0.164 g, 0.34 mmol) in dry acetonitrile (50 ml) was heated under reflux for 24 h. More dibromide **5** (0.071 g, 0.14 mmol) was added and the reaction mixture was refluxed for an additional 24 h. After the solution was cooled down to room temperature, the precipitate was filtered off and washed with acetonitrile (10 ml) and Et_2O (10 ml). The solid was dissolved in water and treated with a saturated aqueous solution of NH_4PF_6 until no further precipitation was observed. The precipitate was filtered off and washed with water, MeOH, Et_2O and dried, affording a reddish powder (0.058 g, 0.044 mmol) in 13% yield.
Elemental Analysis : calcd (%) for $C_{47}H_{50}F_{24}N_5O_3P_4$: C 43.00%, H 3.84%, N 5.33%; found C 43.35%, H 3.68%, N 5.16%.
^{1}H NMR (600 MHz, CD_3CN, 298 K): δ = 8.80–9.20 (m, 8H, H_α, H'$_\alpha$, $H_{\alpha'}$), 8.30–8.50 (m, 8H, H_β, H'$_\beta$, $H_{\beta'}$), 7.40–7.80 (m, 7H, H_{Ar}, C_6H_4), 5.75–6.10 (m, 8H, a, a', b, b'), 5.20–5.35 (br s, 2H, CH_2O); positive ESI-MS: *m/z* 1167.7 $[M\text{-}PF_6]^+$, 511.2 $[M\text{-}2PF_6]^{2+}$.
Reduction of the NMR sample containing **1a•** in CD_3CN by addition of equimolar amount of phenylhydrazine gave the *N*-hydroxy derivative **1a-OH**.
1a-OH: ^{1}H NMR (600 MHz, CD_3CN, 298 K): δ = 8.99 (bs s, 6H, H_α, H'$_\alpha$), 8.91 (d, *J* = 6.0 Hz, 2H, $H_{\alpha'}$), 8.42 (br s, 8H, H_β, H'$_\beta$, $H_{\beta'}$), 7.56-7.68 (m, 7H, H_o, H_m, H_p, C_6H_4), 5.97 (s, 2H, a'), 5.88 (s, 2H, a), 5.86 (s, 4H, b, b'), 5.20 (s, 2H, CH_2O), 2.54-2.66 (m, 1H, 4-H), 1.72 (br d, *J* = 14.0 Hz, 2H, H_{eq}), 1.50 (br t, *J* = 14.0 Hz, H_{ax}), 1.09 (s, 6H, Me), 1.00 (s, 6H, Me). ^{13}C NMR (145 MHz, CD_3CN, 298 K) (see Fig.): δ = 175.58, 151.49, 146.88, 146.68, 145.97, 137.95, 135.50, 135.25, 133.64, 132.65, 132.23, 131.30, 128.53, 64.97, 64.35, 64.24, 62.10, 58.71, 42.20, 35.45, 32.56, 19.66.

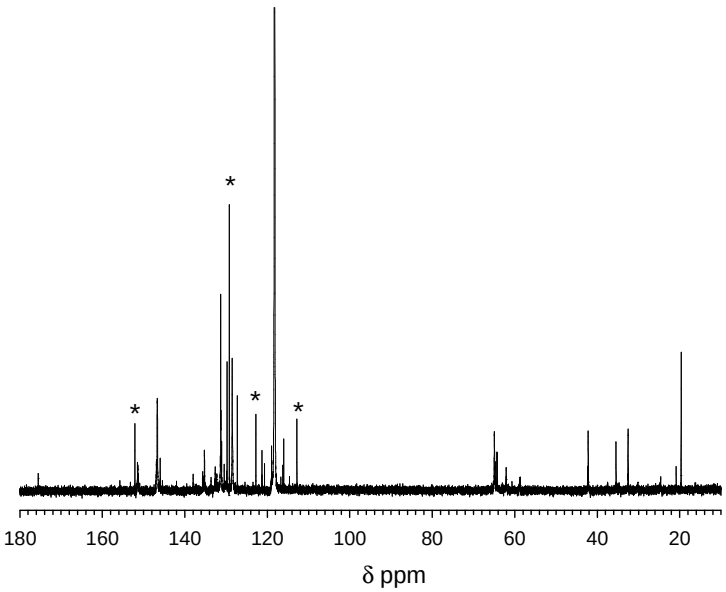

Figure. ^{13}C NMR spectrum of **1a-OH** obtained after in situ reduction of **1a•** with phenylhydrazine. Star symbols refer to the signals of phenylhydrazine.

Compound [**1a•]** · **4Cl**$^-$ was analyzed also in D_2O before PF_6^-cation exchange: ^{1}H NMR (600 MHz, D_2O, 298 K): δ = 9.00-9.20 (m, 8H, H_α, H'$_\alpha$, $H_{\alpha'}$, H'$_{\alpha'}$), 8.40-8.80 (m, 8H, H_β, H'$_\beta$, H_β', H'$_\beta$'), 7.40-7.80 (m, 7H, H_{Ar}, C_6H_4), 5.80-6.30 (m, 8H, a, a', b, b'), 5.20-5.35 (m, 2H, CH_2O).
Reduction of the NMR sample containing **1a•** in D_2O by addition of $Na_2S_2O_4$ gave the *N*-hydroxy derivative **1a-OH**. ^{1}H NMR (600 MHz, D_2O, 298 K): δ = 9.18 (bs s, 6H, H_α, H'$_\alpha$, H'$_{\alpha'}$), 9.11 (s, 2H, $H_{\alpha'}$), 8.58 (br s, 8H, H_β, H'$_\beta$, $H_{\beta'}$, H'$_{\beta'}$), 7.76 (s, 1H, $H_o^\dagger$), 7.63 (br s, 4H, C_6H_4), 7.63 (m, 1H, $H_p^\dagger$), 7.43 (m, 1H, $H_m^\dagger$), 6.14 (s, 2H, a'), 6.02 (s, 2H, a), 5.98 (s, 4H, b, b'), 5.33 (s, 2H, CH_2O), 3.00-3.08 (m, 1H, 4-H), 2.05 (d, *J* = 13.5 Hz, 2H, H_{eq}), 1.63 (t, *J* = 13.5 Hz, 2H, H_{ax}), 1.39 (s, 6H, Me), 1.38 (s, 6H, Me).

Synthesis of 1b$^{\bullet\bullet}$. A solution of **6b** (0.140 g, 0.15 mmol) and **5** (0.071 g, 0.15 mmol) in dry acetonitrile (23 ml) was heated under reflux for 24 h. After the solution was cooled down to room temperature, the precipitate was filtered off and washed with aceto nitrile (10 ml) and Et_2O (10 ml). The solid was dissolved in water and treated with a saturated aqueous solution of NH_4PF_6 until no further precipitation was observed. The precipitate was filtered off and washed with water, MeOH, Et_2O and dried, affording a brown powder (0.036 g, 0.023 mmol) in 15% yield.
Elemental Analysis of **1b••**: calcd (%) for $C_{58}H_{68}F_{24}N_6O_6P_4$: C 45.68%, H 4.49%, N 5.51%; found C 45.36%, H 4.60%, N 5.60%.
^{1}H NMR (600 MHz, CD_3CN, 298 K): δ = 8.98 (br s, 4H, Hα), 8.90 (br s, 4H, H'$_\alpha$), 8.43 (br s, 8H, H_β, H'$_\beta$), 7.20–7.80 (m, 6H, H_{Ar}), 5.75–6.10 (m, 8H, a, a'), 5.10–5.40 (br s, 4H, CH_2O), 2.92–3.20 (m, 1H, 4-H), 2.02–2.12 (m, 2H, H_{eq}), 1.64–1.76 (m, 2H, H_{ax}), 1.44 (s, 12H, Me).
Reduction of the NMR sample containing **1b••** in CD_3CN by addition of equimolar amount of phenylhydrazine gave the *N*-hydroxy derivative **1b-OH**. ^{1}H NMR (600 MHz, CD_3CN, 298 K): δ = 8.98 (s, 4H, H_α), 8.91 (s, 4H, H'$_\alpha$), 8.43 (br s, 8H, H_β, H'$_\beta$), 7.50-7.72 (m, 4H, H_o, H_p), 7.24-7.38 (m, 2H, H_m), 5.98 (s, 4H, a'), 5.88 (s, 4H, a), 5.15-5.30 (m, 4H, CH_2O), 2.92-3.02 (m, 1H, 4-H), 2.70-2.82 (m, 1H, 4-H), 2.02-2.12 (m, 2H, H_{eq}), 1.82-1.90 (m, 2H, H_{eq}), 1.64-1.76 (m, 4H, H_{ax}), 1.44 (s, 12H, Me), 1.23 (s, 6H, Me), 1.14 (s, 6H, Me). ^{13}C NMR (145 MHz, CD_3CN, 298 K) (Fig.): δ = 173.66, 152.13, 151.87, 151.64, 151,49, 146.99, 146.70, 137.24, 135.28, 131.43, 128.54, 64.75, 62.06, 59.23, 37.53, 30.25, 24.57, 20.92.

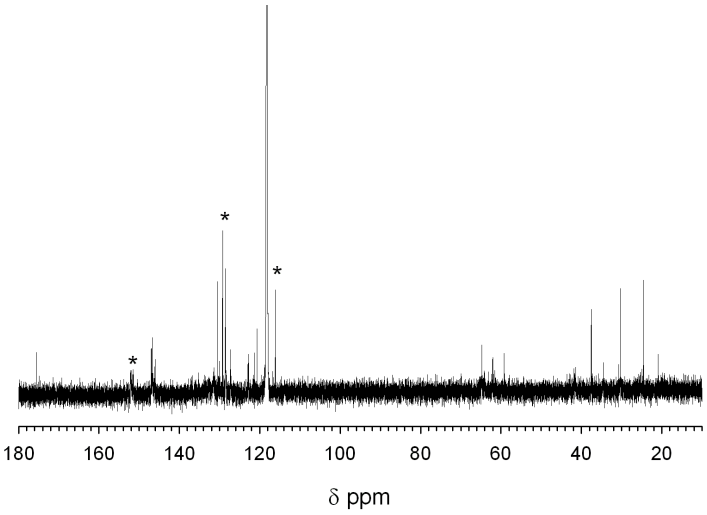

Figure. ^{13}C NMR spectrum of **1b-OH** obtained after in situ reduction of **1b••** with phenylhydrazine. Star symbols refer to the signals of phenylhydrazine.

Compound [**1b••]** $^{\cdot}$ **4Cl**$^{-}$ was analyzed also in D_2O before PF_6^-cation exchange: ^{1}H NMR (600 MHz, D_2O, 298 K): δ = 8.90-9.20 (m, 8H, H_α, H'_α), 8.40-8.60 (m, 8H, H_β, H'_β), 7.20-7.70 (m, 6H, H_o, H_m, H_p), 5.80-6.10 (m, 8H, a, a'), 5.10-5.35 (m, 4H, CH_2O).
Reduction of the NMR sample containing **1b••** by addition of $Na_2S_2O_4$ gave the *N*-hydroxy derivative **1b-OH**. ^{1}H NMR (600 MHz, D_2O, 298 K): δ = 9.20 (bs s, 4H, H_α), 9.12 (s, 4H, H'_α), 8.58 (br s, 8H, H_β, H'_β), 7.20-7.70 (m, 6H, H_o, H_m, H_p[†]), 6.14 (s, 4H, a'), 6.02 (s, 4H, a), 5.33 (s, 4H, CH_2O), 2.95-3.15 (m, 2H, 4-H), 2.00-2.15 (m, 4H, H_{eq}), 1.64 (m, 4H, H_{ax}), 1.41 (s, 12H, Me), 1.39 (s, 12H, Me).

[†] The H_o, H_m, and H_p refer to the position of the phenyl protons relatively to the radical substituent.

Synthesis of 7a•. A solution containing **6a** (0.1 g, 0.14 mmol), **5** (0.066 g, 0.14 mmol), DMN (0.079 g, 0.42 mmol) and NaI (0.007 g) in dry DMF (10 ml) was stirred at room temperature for 5 days under nitrogen. The solvent was removed under vacuum and the residue was chromatographed over a silica gel column (length 6 cm, i.d. 1.5 cm) using a mixture of MeOH/NH_4Cl (2M)/CH_3NO_2 (4:4:2) as eluent. The fractions containing the complex, indicated by purple spots of TLC analysis (Rf 0.40), were combined together and concentrated in vacuo. The residue was dissolved in water and a saturated aqueous solution of NH_4PF_6 was added to afford **7a**$^{\cdot}$. The precipitate was washed with water and dried, furnishing the complex as a purple solid in 33% yield. ^{1}H NMR (600 MHz, CD_3CN, 298 K): δ = 8.88 (d, *J* = 4.8 Hz, 2H, H'$_\alpha$), 8.86 (d, *J* = 4.8 Hz, 2H, H'$_\alpha$), 8.83 (s, 2H, H_α), 8.75 (s, 2H, $H_{\alpha'}$), 7.99 (s, 6H, H_β, H'$_\beta$), 7.93 (s, 2H, $H_{\beta'}$), 7.78 (br s, 1H, H_o) 7.67 (s, 4H, C_6H_4), 7.48 (br s, 2H, H_m, H_p), 6.86 (m, 2H, H-3'), 6.67 (d, *J* = 7.2 Hz, 2H, H-2'), 5.88–5.98 (m, 2H, a'), 5.80 (s, 2H, a), 5.77 (s, 2H, b) 5.76 (s, 2H, b), 5.50–5.65 (m, 2H, H-4'), 5.37 (br s, 2H, CH_2O), 3.98 (s, 6H, OMe).
Reduction of the NMR sample containing **7a•** in CD_3CN by addition of equimolar amount of phenylhydrazine gave the *N*-hydroxy derivative **7a-OH**. ^{1}H NMR (600 MHz, CD_3CN, 298 K): δ = 8.80-8.95 (m, 6H, H_α, H'_α), 8.77 (br s, 2H, H_α'), 7.90-8.05 (m, 8H, H_β, H'_β, $H_{\beta'}$), 7.72-7.80 (m, 1H, H_o), 7.69 (s, 4H, C_6H_4), 7.50-7.56 (m, 2H, H_m, H_p), 5.89 (br s, 2H, a'), 5.78 (br s, 2H, a), 5.76 (br s, 4H, b), 5.32 (s, 2H, CH_2O), 3.98 (s, 6H, OMe), 2.85 (m, 1H, 4-H), 1.87 (br d, *J* = 13.7 Hz, 2H, H_{eq}), 1.64 (br t, *J* = 13.7 Hz, H_{ax}), 1.18 (s, 6H, Me), 1.15 (s, 6H, Me).

References

1. Chen, G. Y., Lean, J. T., Alcala, M., Mallouk, T. E., Modular synthesis of π-acceptor cyclophanes derived from 1,4,5,8-naphthalenetetracarboxylic diimide and 1,5-dinitronaphthalene. *J. Org. Chem.* **2001**, *66*, 3027–3034.
2. Jeppesen, J. O., Nielsen, M. B., Becher, J., Tetrathiafulvalene cyclophanes and cage molecules. *Chem. Rev.* **2004**, *104*, 5115–5131.
3. For a recent review see: Hicks, R. G. *Org. Biomol. Chem*. **2007**, *5*, 1321–1338.
4. Berliner, L. J. *Spin Labelling*; Academic Press: New York, **1979**.
5. (a) Perkins, M. J. *Adv. Phys. Org. Chem*. **1980**, *17*, 1; (b) Rehorek, D. *Chem. Soc. Rev*. **1991**, *20*, 341–353; (c) Beckwith, A. L. J.; Bowry, V. W.; Ingold, K. U. *J. Am. Chem. Soc*. **1992**, *114*, 4983–4992; (d) Bowry, V. W.; Ingold, K. U. *J. Am. Chem. Soc.* **1992**, *114*, 4992–4996.
6. Zweier, J. L.; Kuppusamy, P. *Proc. Natl. Acad. Sci. U.S.A.* **1988**, *85*, 5703–5707.
7. (a) Amabilino, D. B.; Veciana, J. *In Magnetism, Molecules to Materials II*; Miller, J. S., Drillon, M., Eds.; Wiley-VCH: Weinheim, 2001; Vol. 2, pp 1–60; (b) *Magnetic* Lahti, P. M., Ed.; Marcel Dekker: New York, 1999; (c) Rawson, J. M.; Alberala, A.; Whalley, A. J. *Mater. Chem*. **2006**, *16*, 2560–2575.
8. (a) Caneschi, A.; Gatteschi, D.; Sessoli, R. *Acc. Chem. Res*. **1989**, *22*, 392–398; (b) Manriquez, J. M.; Yee, G. T.; McLean, R. S.; Epstein, A. J.; Miller, J. S. *Science* **1991**, *252*, 1415–1417; (c) Inoue, K.; Hayamizu, T.; Iwamura, H.; Hashizume, D.; Ohashi, Y. *J. Am. Chem. Soc*. **1996**, *118*, 1803–1804; (d) Ise, T.; Ishida, T.; Hashizume, D.; Iwasaki, F.; Nogami, T. *Inorg. Chem*. **2003**, *42*, 6106–6113.
9. (a) Forrester, A. R.; Hay, J. M.; Thomson, R. H. *Organic Chemistry of Stable Free Radicals*; Academic Press: London, 1968; (b) Rozanstev, E. G. *Free Nitroxyl Radicals*; Plenum: New York, 1970; (c) Rozantsev, E. G.; Sholle, V. D. *Synthesis* **1971**, 401; (d) Rozantsev, E. G.; Sholle, V. D. *Synthesis* **1971**, 190; (e) Keana, J. F. W. *Chem. Rev*. **1978**, *78*, 37–64.
10. Lehn, J.-M. *Supramolecular Chemistry*; Wiley-VCH: Weinheim, 1995.
11. (a) Cram, D. J. *Angew. Chem., Int. Ed. Engl*. **1988**, *27*, 1009–1020; (b) Cram, D. J. *Science* **1983**, *219*, 1177–1183.
12. Rajca, A.; Mukherjee, S.; Pink, M.; Rajca, S. *J. Am. Chem. Soc*. **2006**, *128*, 13497–13507.
13. (a) Ionita, G.; Chechik, V. *Org. Biomol. Chem*. **2005**, *3*, 3096–3098; (b) Bardelang, D.; Rockenbauer, A.; Jicsinszky, L.; Finet, J.-P.; Karoui, H.; Lambert, S.; Marque, S. R. A.; Tordo,

P. *J. Org. Chem.* **2006**, *71*, 7657–7667; (c) Franchi, P.; Fanì, M.; Mezzina, E.; Lucarini, M. *Org. Lett*. **2008**, *10*, 1901–1904.

14. The synthesis of mono- and bis-nitroxides derived from [2,2]-paracyclophane has been already reported: Forrester, A. R.; Ramasseul, R. *J. Chem. Soc. (B)* **1971**, 1638–1644.
15. Balzani, V.; Credi, A.; Raymo, F. M.; Stoddart, J. F. *Angew. Chem., Int. Ed.* **2000**, *39*, 3349–3391.
16. Benniston, A. C.; Harriman, A. *Synlett* **1993**, 223–226.
17. Mezzina, E.; Fanì, M.; Ferroni, F.; Franchi, P.; Menna, M.; Lucarini, M. *J. Org. Chem*. **2006**, *71*, 3773–3777.
18. From the spectral data it is not possible to gain information on the possible isomers, which can be formed in the biradical respect to the relative orientation of the radical arms both in the paraphenylene portions (pseudo-*meta*, o pseudo-*para*) and in the macrocycle (*sin* or *anti*). For a discussion on the possible isomers in disubstituted paracyclophanes see Ref. 12.
19. (a) Odell, B.; Reddington, M. V.; Slawin, A. M. Z.; Spencer, N.; Stoddart, J. F.; Williams, D. J. *Angew. Chem., Int. Ed. Engl*. **1988**, *27*, 1547–1550; (b) Ashton, P. R.; Odell, B.; Reddington, M. V.; Slawin, A. M. Z.; Stoddart, J. F.; Williams, D. J. *Angew. Chem., Int. Ed. Engl*. **1988**, *27*, 1550 1553.
20. Ref. 2, pp 339–372.
21. The formation of a self-complexing system having the radical inside the cavity cannot be proved by NMR because of the lack of the nitroxide heterocyclic signals in the spectrum.
22. Cooke, G.; Woisel, P.; Bria, M.; Delattre, F.; Garety, J. F.; Hewage, S. G.; Rabani, G.; Rosair, G. M. *Org. Lett*. **2006**, *8*, 1423–1426.

Chapter 4. The application of CuAAC 'click' chemistry to α-Cyclodextrin-based paramagnetic 2-Rotaxanes' synthesis

4.1. Introduction[1]

Examination of nature's favorite molecules reveals a striking preference for making carbon-heteroatom bonds over carbon-carbon bonds, surely no surprise given that carbon dioxide is nature's starting material and that most reactions are performed in water.

Taking the cue from nature's approach, great attention was focused on the development of a set of powerful, highly reliable, and selective reactions for the rapid synthesis of useful new compounds and combinatorial libraries through heteroatom links (C-X-C), an approach called 'click chemistry'.

Click chemistry is a modular synthetic strategy towards the assembly of new molecular entities which relies mainly upon the construction of carbon–heteroatom bonds using spring-loaded reactants. Its growing number of applications are found in nearly all areas of modern chemistry from drug discovery to materials science.

In 2001, Kolb, Finn and Sharpless published a Landmark review describing a new strategy for organic chemistry, or as the authors also put it ''the reinvigoration of an old style of organic synthesis''. The name click chemistry (CC) was coined to describe this 'guiding principle' - a principle born to meet the demands of modern day chemistry and in particular, the demands of drug discovery.

Since the foundations of CC were laid, there has been an explosive growth in publications describing a wealth of applications of this practical and sensible chemical approach.

The copper(I)-catalysed 1,2,3-triazole forming reaction between azides and terminal alkynes has become the gold standard of click chemistry due to its reliability, specificity and biocompatibility.

4.2. The Click chemistry philosophy

Examination of the molecules created by nature (the quintessential chemist), reveals an overall preference for carbon–heteroatom bonds over carbon–carbon bonds; for example, nucleic acids, proteins and polysaccharides are condensation polymers of subunits linked through carbon–heteroatom bonds. This strategy of making large oligomers from relatively simple building blocks can be described as nature's way of performing combinatorial chemistry with remarkable modularity and diversity. All proteins are created from 20 building blocks that are joined via reversible heteroatom links.

Following nature's lead, the aim is to generate substances by joining small units together with heteroatom links (C-X-C). The goal is to develop an expanding set of powerful, selective, and modular 'blocks' that work reliably in both small- and large-scale applications.

Click chemistry serves as a powerful strategy in the quest for function, and can be summarised neatly in one sentence: ''*all searches must be restricted to molecules that are easy to make*''.

The definition of a set of stringent criteria that a process must meet to be useful in this context termed the foundation of this approach whose the focus rests exclusively on highly energetic 'spring loaded' reactants.

The reaction must be *modular, wide in scope,* give *very high yields,* generate only *inoffensive byproducts,* and be *stereospecific* (but not necessarily enantioselective).

The required process characteristics include *simple reaction conditions* (ideally, the process should be insensitive to oxygen and water), *readily available starting materials and reagents,* the use of *no solvent or a solvent that is benign* (such as water) *or easily removed,* and *simple product isolation.* Purification, if required, must be by non-chromatographic methods, such as crystallization or distillation, and the product must be stable under physiological conditions.

Click reactions achieve their required characteristics by having a high thermodynamic driving force, usually greater than 20 kcal mol^{-1}. Such processes proceed rapidly to completion and also tend to be highly selective for a single product being governed by kinetic control and being highly reliable and selective processes. (these reactions are 'spring-loaded' for a single trajectory).

Ideally, starting materials and reagents for 'click' reactions should be readily available, and it is a convenient coincidence that unsaturated-hydrocarbon based organic synthesis is currently at the heart of this powerful approach, since these materials are readily available from nature or can be obtained by steam cracking of alkanes in the petrochemical industry.

Although meeting the requirements of a 'click' reaction is a tall order, several processes have been identified which step up to the mark (Scheme 1):

* cycloadditions of unsaturated species, especially 1,3-dipolar cycloaddition reactions, but also the Diels–Alder family of transformations;

* nucleophilic substitution chemistry, particularly ring-opening reactions of strained heterocyclic electrophiles such as epoxides, aziridines, aziridiniumions, and episulfoniumions;

* carbonyl chemistry of the 'non-aldol' type, such as formation of ureas, thioureas, aromatic heterocycles, oxime ethers, hydrazones, and amides; and

* additions to carbon-carbon multiple bonds, especially oxidative cases such as epoxidation, dihydroxylation, aziridination, and sulfenyl halide addition, but also Michael additions of Nu-H reactants.

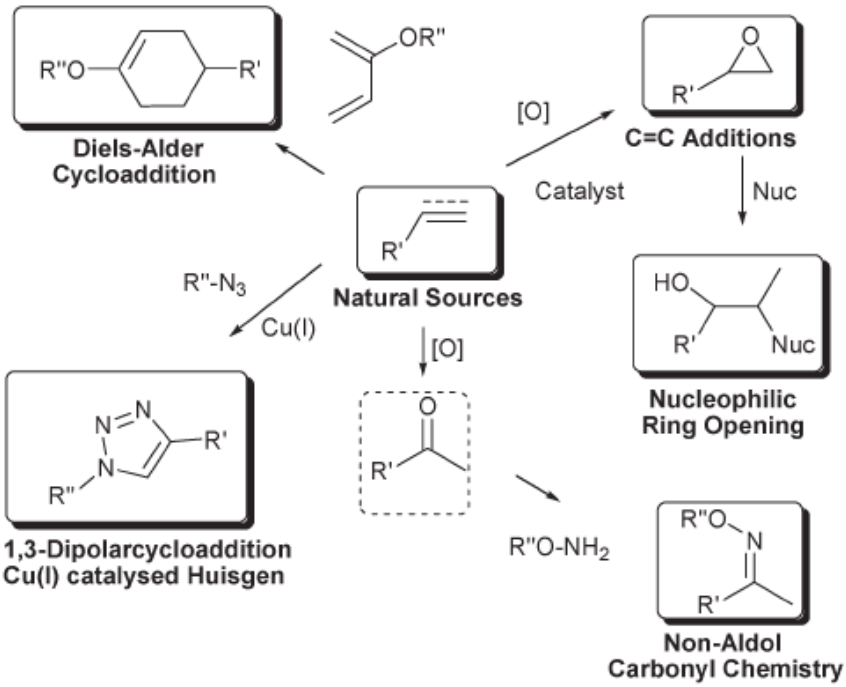

Scheme 1. A selection of reactions which match the Click Chemistry criteria.

4.2.1. The cream of the crop: the Huisgen 1,3-dipolar cycloaddition[2]

Huisgen 1,3-dipolar cycloadditions[3] are exergonic fusion processes that unite two unsaturated reactants and provide fast access to an enormous variety of five-membered heterocycles.[4]

Of all the reactions which achieve 'click status', the Huisgen 1,3-dipolar cycloaddition of alkynes and azides (the CuAAC reaction) to yield 1,2,3-triazoles[5] is undoubtedly the first example of a click reaction and the most useful member of this family.

The ease of synthesis of the alkyne and azide functionalities, coupled with their kinetic stability and tolerance to a wide variety of functional groups and reaction conditions, make these complementary coupling partners particularly attractive. Since efforts to control this 1,4- versus 1,5-regioselectivity problem have so far met with varying success,[6] it was the recent discovery of the dramatic rate acceleration of the azide–alkyne coupling event under copper(I) catalysis and the beneficial effects of water that have placed this reaction at the 'center stage' of click chemistry (Scheme 2). This new reaction process requires no protecting groups, and proceeds with almost complete conversion and selectivity for the 1,4-disubstituted 1,2,3-triazole (anti-1,2,3-triazole). No purification is generally

required. This ‘near perfect’ reaction has become synonymous with click chemistry, and is often referred to as ‘The Click Reaction’.

This powerful bondforming process has proven extremely versatile, and has driven the concept of CC from an ideal to a reality.

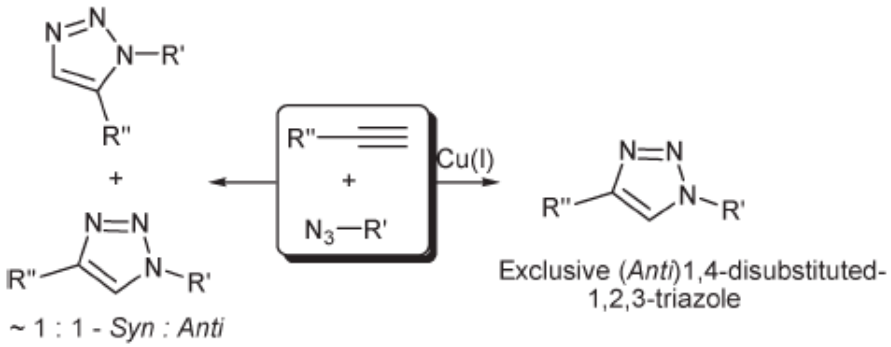

Scheme 2. The Cu(I) catalysed Huisgen ‘click reaction’ results in exclusive formation of the 1,4-triazole, whilst the thermally induced Huisgen cycloaddition usually results in an approximately 1-1 mixture of 1,4- and 1,5-triazole stereoisomers.

Ironically, what makes azides unique for click chemistry purposes is their extraordinary stability toward H_2O, O_2, and the majority of organic synthesis conditions.[7] The spring-loaded nature of the azide group remains invisible unless a good dipolarophile is favorably presented.[8]

Even if a number of copper(I) sources can be used directly, the catalyst is better prepared in situ by reduction of Cu(II) salts, which are less costly and often purer than CuI salts ($CuSO_4 \cdot 5H_2O$ serves well). As the reductant, ascorbic acid and/or sodium ascorbate proved to be excellent[9] allowing the preparation of a broad spectrum of 1,4-triazole products in high yields and purity at 0.25-2 mol% catalyst loading.

The triazole formed is essentially chemically inert to reactive conditions, e.g. oxidation, reduction, and hydrolysis, and has an intermediate polarity with a dipolar moment of 5 D.[10] The basis for the unique properties and rate enhancement for triazole formation under Cu(I) catalysis should be found in the high ΔG of the reaction in combination with the low character of polarity of the dipole of the noncatalyzed thermal reaction, which leads to a considerable activation barrier.

The reaction appears to be very forgiving and does not require any special precautions, proceeding to completion in 6 to 36 hours at ambient temperature in a variety of solvents, including aqueous tert-butyl alcohol or ethanol and, very importantly, water with no organic co-solvent. Although most experiments were performed at near neutral pH values, the catalysis seems to proceed well at pH values ranging from approximately 4 to 12.

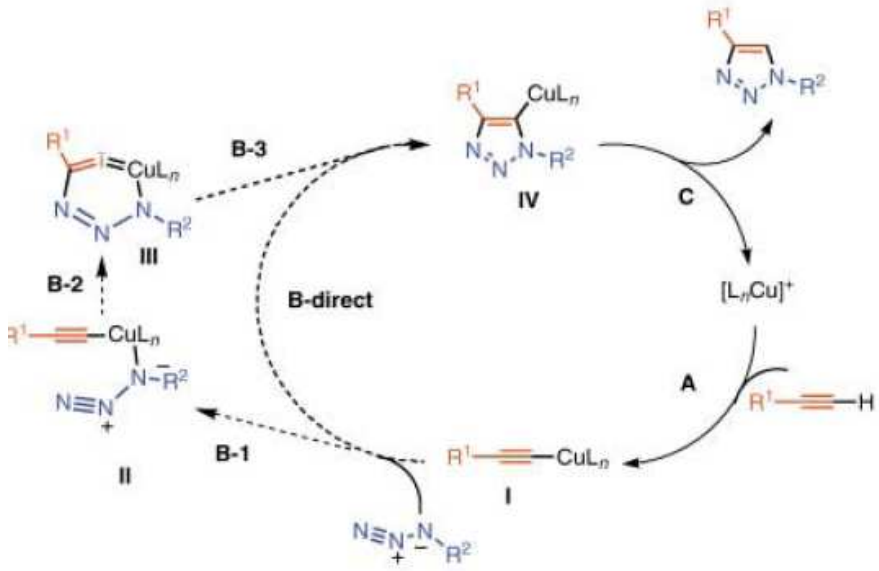

Scheme 3. Proposed catalytic cycle for the CuI-catalyzed ligation.

The mechanistic proposal for the catalytic cycle is shown in Scheme 1. It begins unexceptionally with formation of the copper(I) acetylide I[11] (as expected, no reaction is observed with internal alkynes); extensive density functional theory calculations[12] offer compelling evidence which strongly disfavors–by about 12-15 kcal– the concerted [2+3] cycloaddition (B-direct) and points to a stepwise, annealing sequence (B-1 then B-2 then B-3, hence the term 'ligation'), which proceeds via the intriguing six-membered copper-containing intermediate III.[13]

4.3. The application of CuAAC 'click' chemistry to rotaxane synthesis[14]

The copper(I)-catalysed azide–alkyne cycloaddition (the CuAAC 'click' reaction) is proving to be a powerful new tool for the construction of mechanically interlocked molecular-level architectures because of the high selectivity for the functional groups involved (terminal alkynes and azides) and the mild experimental conditions which are compatible with the weak and reversible intermolecular interactions generally used to template the assembly of interlocked structures.

Since the CuAAC reaction was introduced as a means of making rotaxanes by an 'active template' mechanism in 2006, it has proven effective for the synthesis of numerous different types of rotaxanes, catenanes and molecular shuttles by passive as well as active template strategies.

4.3.1. Synthetic strategies

A quarter of a century after the first template synthesis of a mechanically interlocked molecule,[15] there now exists a lot of strategies for the construction of mechanically bonded molecular-level structures.

Rotaxanes, catenanes, knots and links have all been accessed via template methods using a diverse range of recognition motifs, such as electron-rich–electron-poor π-stacking systems, hydrogen bonding and metal ion coordination.[16] These molecules, in which some of the components are connected mechanically rather than by covalent bonds, could potentially find application in the modification of physical and chemical properties,[15] encapsulating and delivering substrates (such as dyes and drugs),[17,18] as smart materials with switchable surface properties[19,20] and in molecular electronics[21,22] and other types of molecular machinery.[23]

Three distinct approaches[24] have been devised for the template synthesis of rotaxanes and catenanes (Scheme 4):

(i) The capping (or threading-followed-by-stoppering) method[25] involves the covalent capture of a threaded supramolecular complex (a pseudorotaxane) by attachment of two bulky units at each end of the linear thread to give the corresponding rotaxane. The bulky 'stoppers' prevent disassociation (dethreading) of the macrocycle and, since the breaking of a covalent bond is then required to disassemble the structure, the rotaxane is a molecule not a supramolecular complex.[24]

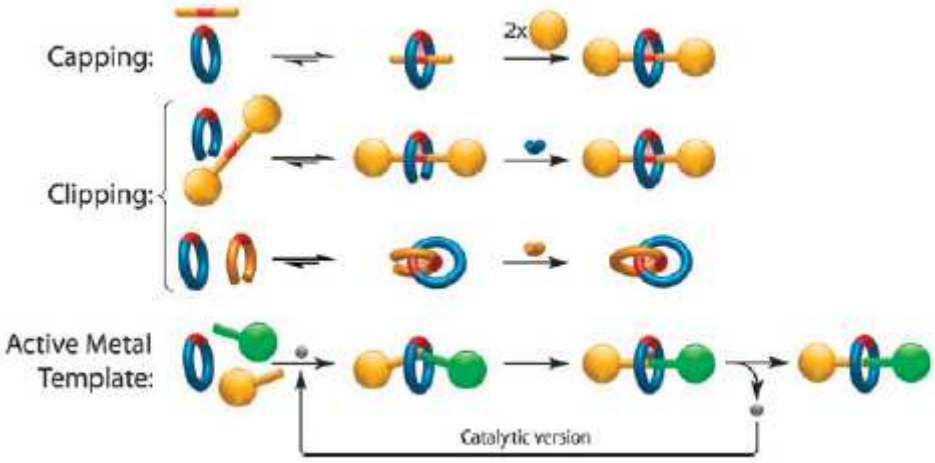

Scheme 4. Template strategies for the synthesis of rotaxanes and catenanes.

(ii) The clipping approach,[26] in which the interlocked structure is obtained by macrocyclisation of an acyclic ligand around the template site of an already stoppered thread (rotaxane) or another macrocycle (catenane).

(iii) The active metal template strategy,[27] where the substrate used as a template also plays an active role in promoting the crucial covalent bond formation used to capture the interlocked structure.

To date the CuAAC reaction has been used in catenane and rotaxane synthesis in four different ways: to build hard-toobtain structures by linking together small fragments into bigger and more complex structures or covalently capturing threaded supramolecular complexes, the modification of pre-existing structures (including decoration and postsynthetic functionalisation), the combination of both of these approaches where the CuAAC is used to link building blocks and as a functionalisation tool, and finally the use of preformed triazole rings as ligands for the assembly of, and to play a role in controlling the dynamics of, mechanically interlocked architectures.

4.4. Cyclodextrins: Introduction[28]

Cyclodextrins are a class of chiral, cyclic oligosaccharides that have molecule-sized cavities. They are preorganised and have a defined bowl shape that is held together by an intramolecular hydrogen bonding network.

4.4.1 Properties and applications

The most common, most studied and cheapest commercially available hosts, the cyclodextrins are the most widely used receptors in host–guest inclusion chemistry, with a broad range of applications and industrial production of over a thousand tons per annum. They are used in the food and cosmetics industries and the pharmaceutical sector as stabilising agents, and for the slow release of drugs. Their existence has been known for a long time, but they were merely scientific curiosities until the latter part of the 20th Century. The explosion in their use in recent years is due to a number of factors. Cyclodextrins are semi-natural compounds – they are synthesised from starch *via* a simple enzymatic conversion. As a consequence, the technology employed to synthesise cyclodextrins on a multi-ton scale is both cheap and environmentally friendly. Cyclodextrins are effective complexing agents for a wide range of molecular guests but have negligible toxicity which can be eliminated by selecting the appropriate derivative for a particular application. The importance of cyclodextrins is such that a magazine, *Cyclodextrin News*, is dedicated to all areas of research on cyclodextrins. The total number of cyclodextrin related papers is over 30 000 as of July 2005 – averaging 4.4 publications per day between 2004 and 2005 alone.

Cyclodextrins are cyclic oligosaccharides comprising (usually) six to eight D-glucopyranoside units (Figure 1a), linked by a 1,4-glycosidic bond (Figure 1b). The three most important members of the cyclodextrin family are α-cyclodextrin (α-CD), β-cyclodextrin (β-CD) and γ-cyclodextrin (γ-CD), which possess, respectively, six, seven and eight glucopyranoside units. Several other (minor) cyclodextrins are known, including δ-cyclodextrin and ε-cyclodextrin (nine and ten units,

respectively), and the five-membered pre-α-cyclodextrin. The α, β, γ nomenclature serves to distinguish the different ring sizes of the homologous series and is essentially historical in nature.

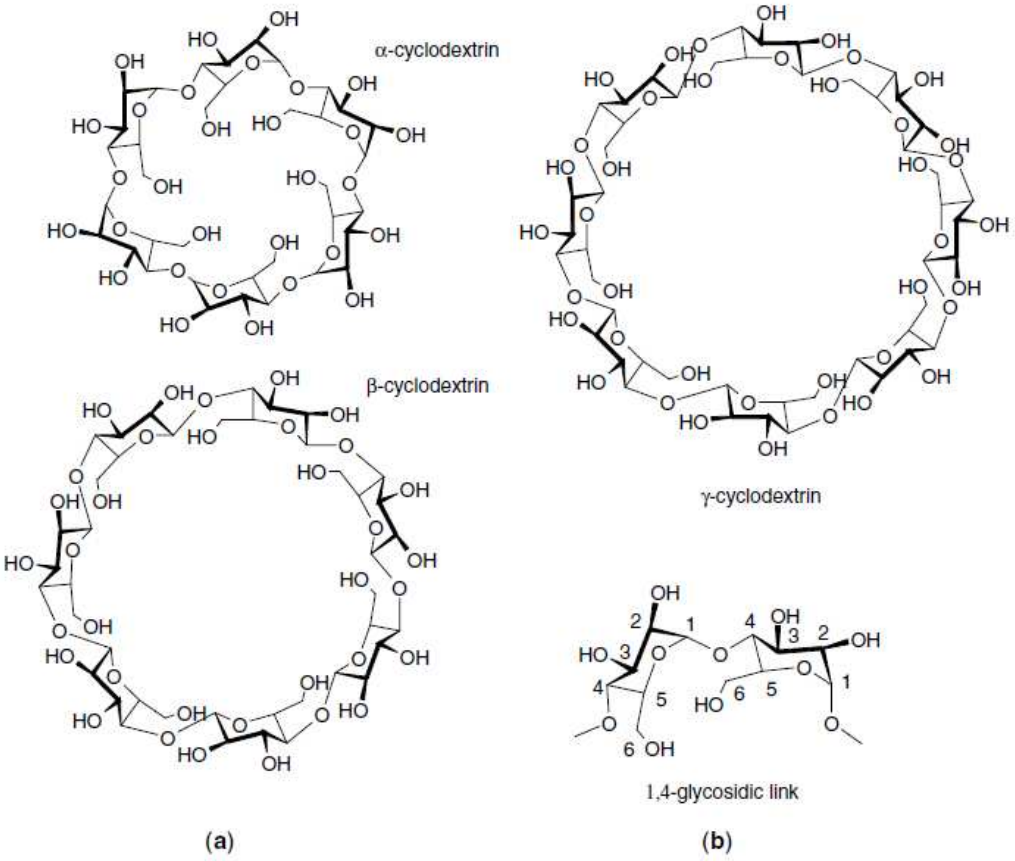

Figure 1. (a) The three most important cyclodextrins. (b) The 1,4-glycosidic link that joins adjacent D-glucopyranoside units.

It is very widely used, however, despite the fact that it does not distinguish the ring size explicitly. This is unsurprising, since systematic names for the cyclodextrins are extremely cumbersome. Other terms for β-cyclodextrin include cyclomaltoheptose, cycloheptaglucan and cycloheptaamylose, with analogous terms for the other members of the family. The cyclodextrin portion of the name comes from dextrose, an early synonym for glucose. Other cyclic oligosaccharides derived from mannose and galactose are also known, but are much less studied.

The shape of a cyclodextrin is often represented as a tapering torus or truncated funnel and, like the upper and lower rims of calixarenes, there are two different faces to the cyclodextrins, referred to as the primary and secondary faces. The primary face is the narrow end of the torus, and comprises the primary hydroxyl groups. The wider secondary face contains the -CH_2OH groups (Figure 2).

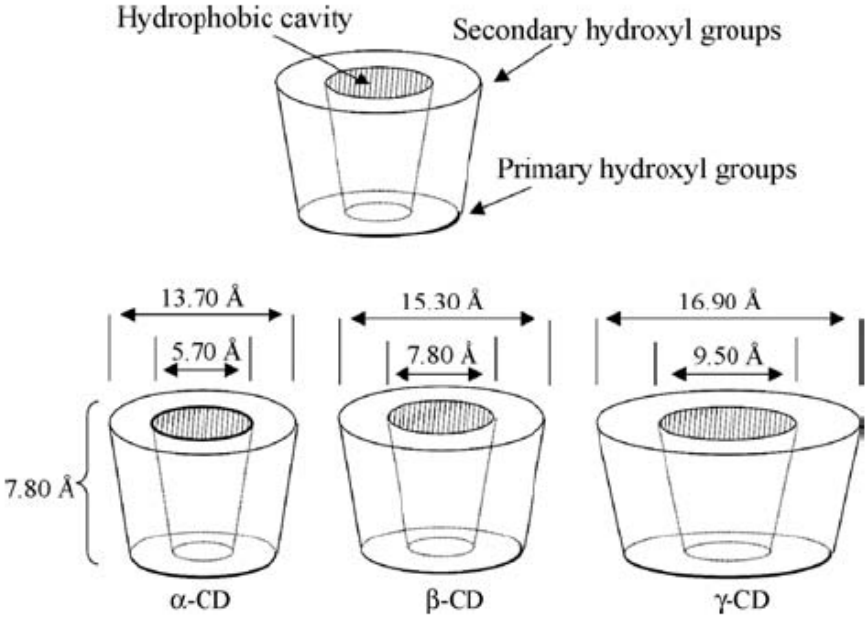

Figure 2. Anatomy of the cyclodextrins

The six-membered D-glucopyranoside rings are linked edge to edge, with their faces all pointing inwards towards a central hydrophobic cavity of varying dimensions. It is this cavity, coupled with the water solubility derived from the hydrophilic alcohol functionalities, that gives the cyclodextrins their unique complexation ability in aqueous solution. Important parameters are given in Table 1.

	α	β	γ
Number of glucose units	6	7	8
Ring size	30	35	40
Internal cavity centre diameter (Å)	5.0	6.2	8.0
Solubility in water (g L^{-1},25°C)	145	18.5	232
ΔH^{o} solution (kJ mol^{-1})	32.1	34.7	32.3
ΔS^{o} solution (J K^{-1} mol^{-1})	57.7	48.9	61.4
$[\alpha]_D$25°C	150.5	162.0	177.4
Cavity volume ($Å^3$)	174	262	427
Cavity volume in 1 g cyclodextrin (cm^3)	0.10	0.14	0.20
Crystalline water (wt. %)	10.2	13.2–14.5	8.13–17.7
pK_a (25°C, by potentiometry)	12.33	12.20	12.08
Rate of hydrolysis by *A. oryzae* α-amylase	Negligible	Slow	Rapid
Common guests	Benzene, phenol	Napthalene, 1-anilino-8-napthalenesulfonate	Anthracene, crown ethers, 1-anilino-8-napthalene-sulfonate

Table 1. Characteristics of α-, β- and γ-Cyclodextrins.

4.5. Cyclodextrin-based [2]-, [3]- and higher rotaxanes using CuAAC as a capping and linking reaction[29]

The spontaneous threading of CDs onto a linear aliphatic thread in aqueous solution can provide [*n*]pseudorotaxanes in a facile and efficient way, the corresponding [*n*]rotaxanes being obtained by aqueous-tolerant stoppering reactions.

In 2009, Sébastien Fort and co-workers demonstrated that the inclusion complex formed by a lactosyl-α-CD conjugate and a decane axle carrying a lactosyl stopper at one extremity and an azido group at the other end could be dimerized by bis-propargyl spacers of different lengths to provide oligorotaxanes having adjustable threading ratios, introducing saccharidic ligands on rotaxanes both as a biological recognition element and as a capping group (scheme 5).[30]

In recent years, polyrotaxanes have emerged as novel and promising scaffolds for the preparation of high affinity polyvalent ligands.[31] Polyrotaxanes are supramolecular assemblies in which cyclic molecules (cyclodextrin, but also calixarene, cucurbituril or crown ether) are threaded onto a linear polymer chain capped with bulky end groups.[32] The cylindrical host molecules are able to spin around the polymer axle as well as to move back and forth along the chain, offering the advantage of polymeric features such as the ability to span nanometer lengths as well as the dynamic presentation of biological ligands.

Stoddart *et al.* have developed a self-assembled pseudopolyrotaxane consisting of lactosyl-substituted cyclodextrins threaded onto a linear polyviologen.[33]

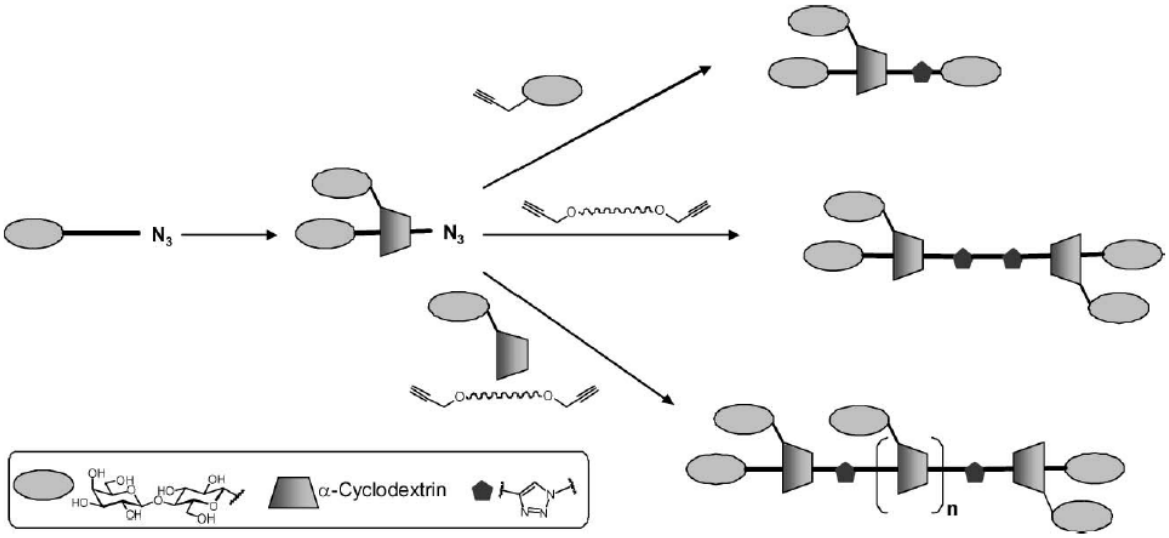

Scheme 5. Synthetic approach towards click-assembled oligorotaxanes.

α-CD-based [2]-, [3]- and higher order rotaxanes could all be prepared from pseudorotaxane **3** (assembled from monostoppered axle **1** and lactose-derivatised α-CD **2**) under CuAAC reaction conditions ($CuSO_4 \cdot 5H_2O$, Na ascorbate, H_2O) with various mono- and di-alkyne linkers and stoppers in modest to good yields (Scheme 6). [2]Rotaxane **5** was synthesised in 54% yield by reacting **3** with alkyne stopper **4** (Scheme 5a).

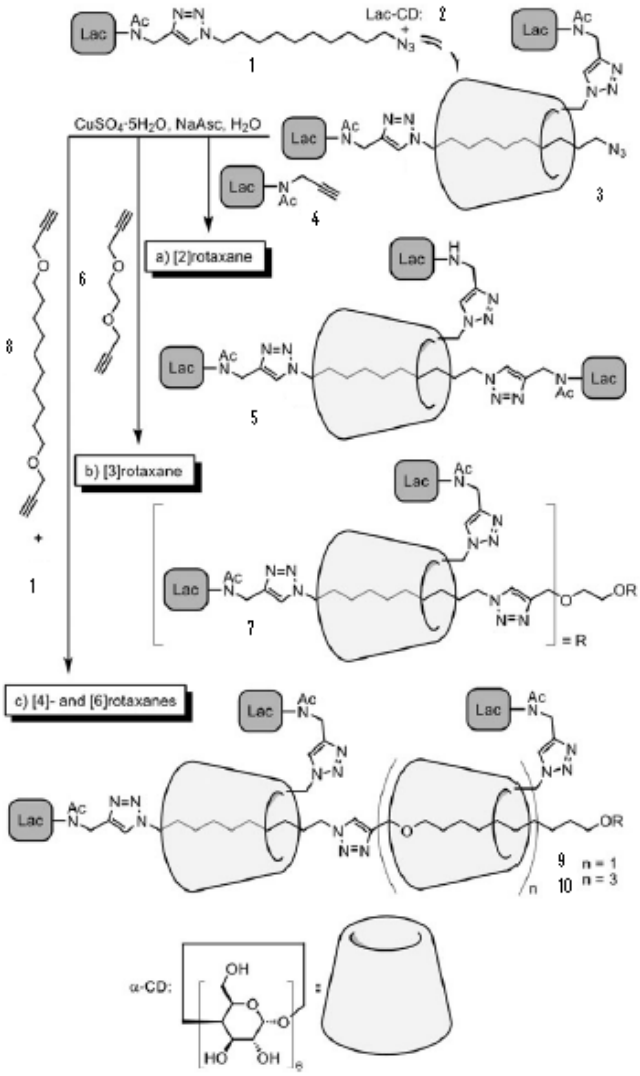

Scheme 6. Lactose-derivatised α-CD-based rotaxanes accessed via CuAAC capping and linking reactions. (a) [2]Rotaxane 5, (b) [3]rotaxane 7 and (c) [4]rotaxane 9 and [6]rotaxane 10.

Replacing **4** with dialkyne thread **6** under these reaction conditions gave [3]rotaxane **7** (24%) as the major product, together with smaller amounts of the corresponding [2]- and [4]-rotaxanes (Scheme 6b). [4]Rotaxane **9** (27%) and [6]rotaxane **10** (67%) were obtained by reacting **1** and extended dialkyne thread **3** with 3 and 15 equivalents of Lac-CD **2**, respectively (Scheme 6c). The average number of CDs threaded were determined by ^{1}H NMR and MS experiments.

4.6. Results and Discussion:
Paramagnetic Cyclodextrin-based [2]rotaxanes using CuAAC as capping reaction

The starting idea was to consider radical or diamagnetic half threads (**A**) having an azide moiety at one extremity and some TEMPO derivatives (**B**) bearing a terminal alkyne functionality (Figure 3) as suitable substrates to apply the 'click chemistry' in the preparation of persistent radical-appended rotaxanes.

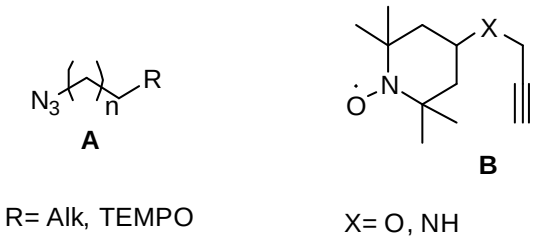

Figure 3

Supposing an initial complexation of the azide by the cyclodextrin, it should have been possible to synthesize various dumbbells for open shell [2]-rotaxanes through CuAAC reaction with a radical alkyne (Scheme 7).

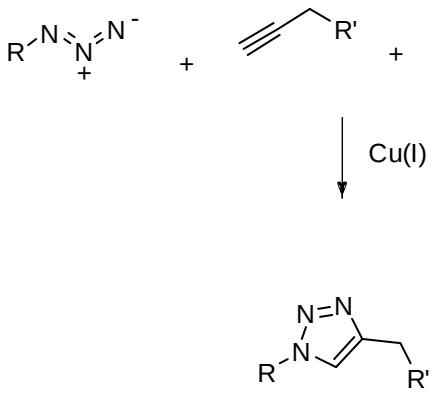

Scheme 7

To this aim, several half thread azides were prepared, differing in alkane chain length and TEMPO linkage (ester or amide), and the click approach was tested on two alkynes containing as blocking reagent the radical TEMPO and a bulky aromatic moiety, respectively, in the presence of native α-cyclodextrin. All these compounds were obtained in good yields, according the synthetic procedures displayed in Scheme 8.

AZIDES

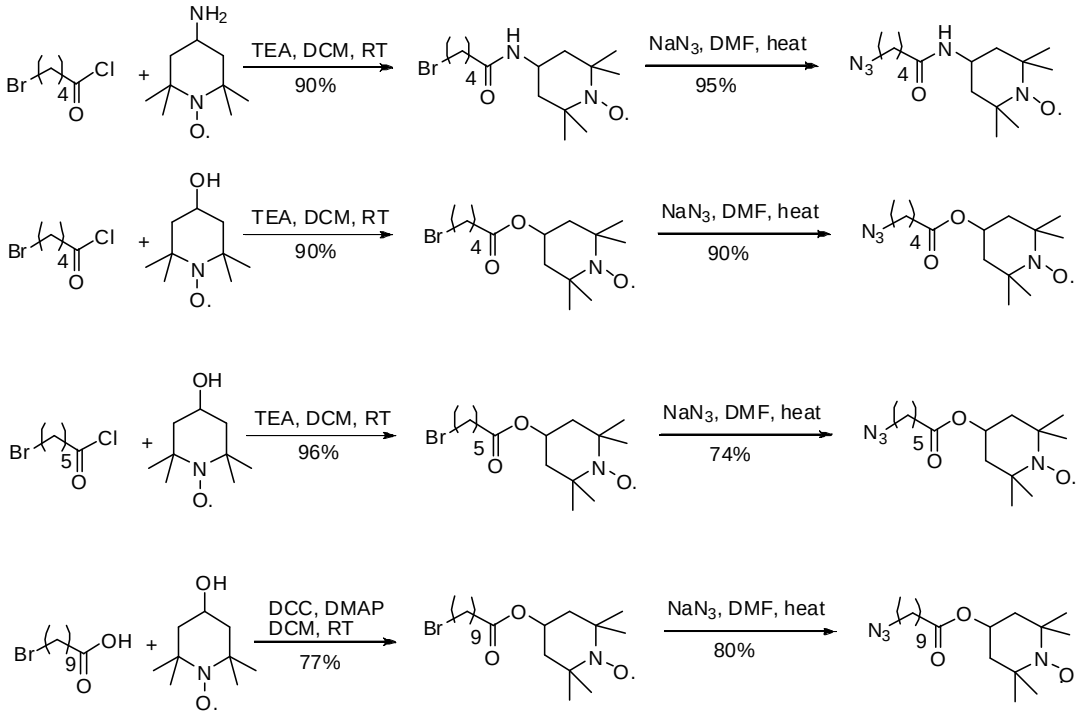

ALKYNES

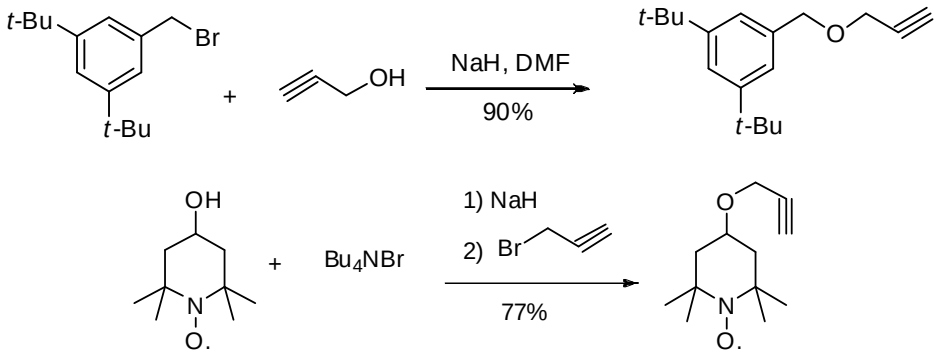

Scheme 8

Unfortunately, first attemps to obtain useful results from radical azides and the diamagnetic alkyne reported above were unsuccessful (Scheme 9). In almost all cases the click reaction was carried out in the presence of α-CD, except that where the bead component was a mercapto derivative of β-CD. The reactions, performed in water and at room temperature, were followed by ESI-MS analysis which showed the presence of the corresponding cycloaddition products (thread) together with starting unreacted material, but did not evidence any peak corresponding to interlocked assemblies.

On the basis of these experiments some considerations were outlined on the complexation of the azide by CD, and on the environment wherein the click reaction occurs, *i.e.* the cyclodextrin could interacts with the half thread azide wrapping the alkyl chain and not the azide moiety and the CuAAC reaction occurs outside the CD cavity in the bulk solvent.

As a consequence, failure to obtain rotaxanation led to consider some critical factors emerged in the performed reactions: *i*) solubility in reaction's conditions; *ii*) affinity for the inner cavity of the α-CD; *iii*) length of the half-thread.

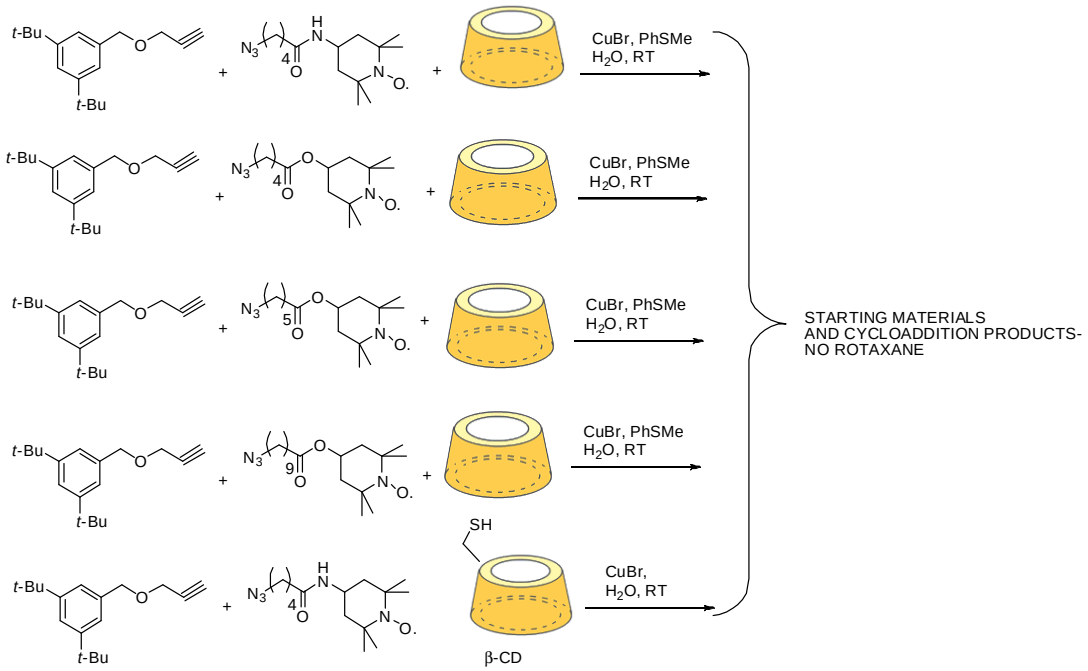

Scheme 9

To answer the items above, the approach relied on the formation and assembly by click reaction of a pseudorotaxane composed by α-CD and a C-10 alkane chain blocked at one end by a saccharidic stopper and carrying an azido group at the other end.

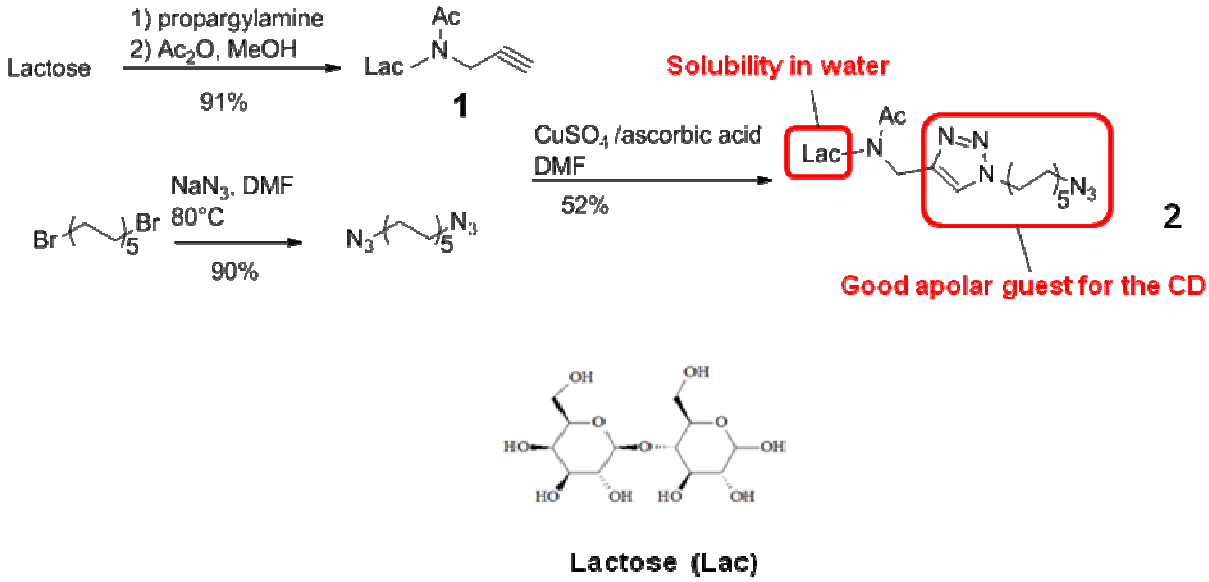

Scheme 10

The use of a lactosyl moiety as blocking agent aimed at solubilizing the guest part in aqueous media, thus allowing complexation to proceed with α-CD; in addition the size and hydrophilicity of

the sugar (see structure **2** in Scheme 10) were both expected to prevent unthreading of the CD from the rotaxane. The guest part consisted of decane backbone is expected to favor the complexation process and form 1:1 complex with the macrocycle leaving the azide moiety exposed to solvent.

With this assumptions, lactosyl-decane-azide (**2**) was prepared (Scheme 10) starting by commercially available 1,10-dibromodecane, which was converted into the corresponding diazide by action of sodium azide in nearly quantitative yield. Monofunctionalization of diazide by lactosyl derivative **1** was conducted in DMF with the $CuSO_4$/sodium ascorbate system. Using a 15 fold excess of diazide, a single addition of lactosyl unit was favored, affording compound **2** with a satisfactory yield of 57%.

Using the half thread azide **2** in the click conditions with the radical alkine 4-propargyloxy-TEMPO[34c] (Scheme 11), in the presence of α-cyclodextrin, a new monoradical rotaxane **3** was recovered in 22% yield.

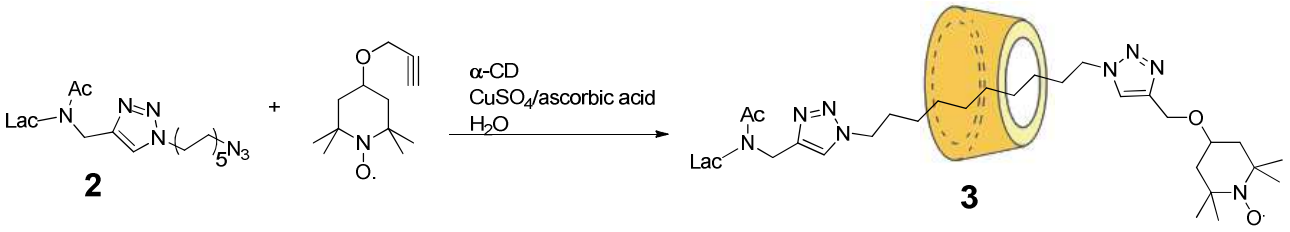

Scheme 11

ESI-MS analysis and NMR spectroscopy were used to provide evidence of the threading processes. On one hand electrospray spectrometry gave information either on the presence of the pseudorotaxane formed by the macrocycle and the lactosyl-azide **2** obtained before addition of the stopper TEMPO alkyne or the appearance of the peak corresponding to the rotaxane **3** after cycloaddition of the end cap radical (Figure 4).

From the other side NMR spectra allow a complete characterization of the supramolecular structure. In particular ^1H spectra of the dumbbell and of the rotaxane were achieved after $Na_2S_2O_4$ *in situ* reduction of the NMR sample to obtain the corresponding N-hydroxy forms (Figure 5). Although spectra *a* and *b* of Figure 5 seem very similar with little chemical shift changes of the thread when involved in the mechanical bond with the macrocycle, the 2D ROESY spectrum gave evidence of the interlocked structure. Actually the detection of important cross peaks involving the alkane chain of the thread (G zone) with the inner proton of α-CD falling in the range 3.7-4.0 ppm (D zone) are indicative of a host-guest spatial interaction; it should be noted that this correlation is absent in the 2D ROESY spectrum of the thread (spectrum *a*, Figure 5), indicating that the lactosyl proton falling in the same range of CD protons are too far from decane protons.

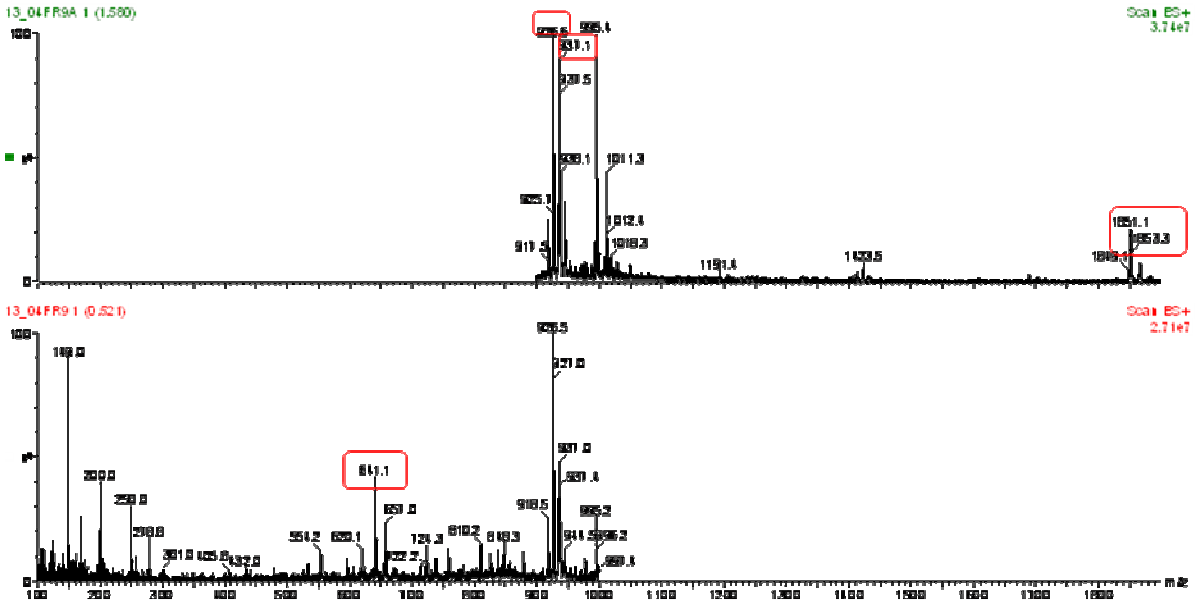

Figure 4. ESI-MS spectra of rotaxane **3** showing the peaks (in the squares) present as mono and double charged (up) and triple charged forms (bottom).

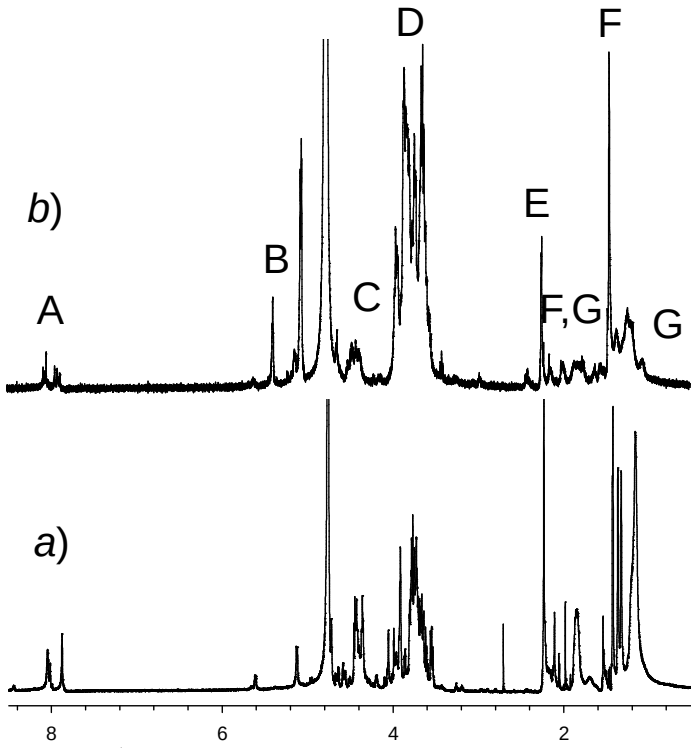

Figure 5. ^{1}H NMR spectra (600 MHz, 298 K, D_2O, 2 mM) of (*a*) dumbbell lactosyl-C10-TEMPOH, (*b*) rotaxane **3-OH**. A: H triazolyl moiety; B: H1 CD; C: H1 Gal, N-C*H*$_2$-triazolyl and H decane; D: H-2,3,4,5 lactosyl moiety and CD; E: CH_3-CO; F: TEMPOH; G: H decane. Signal assignments was achieved by measuring the 2D ROESY spectrum of rotaxane **3-OH**.

The success in the synthesis of this α-CD-based paramagnetic rotaxane containing lactosyl and TEMPO moieties as stoppers put the basis for the preparation of new rotaxanes in which the bead component consisted of a radical TEMPO-α-CD conjugate. In particular I was interested in the synthesis of rotaxanes in which both the linear and the cyclic component bring a persistent radical

moiety, in order to study by Electron Spin Resonance possible interactions between the two radicals in a mechanical bonded supramolecular structure.

To this purpose the syntheses of two TEMPO-monofunctionalized α-cyclodextrins were undertaken, bringing the radical arm in the larger secondary rim (Scheme 12b) and at the 6 position of the minor rim (Scheme 12b), respectively.

The reactions for the functionalization of the primary rim were realized by selective tosylation of α-CD according to the procedure described by Melton and Slessor[34a] affording pure 6-*O*-Ts-α-CD in 20% yield. Tosyl displacement by sodium azide in DMF gave the azido derivative[34a] in 90% yield. Coupling of 4-propargyloxy-TEMPO onto the cyclodextrin in the presence of a catalytic amount of copper sulfate and sodium ascorbate as reducing agent afforded the single 6-triazolyl-TEMPO-α-CD in 48 % yield after purification by gel filtration over a Sephadex G-15 column.

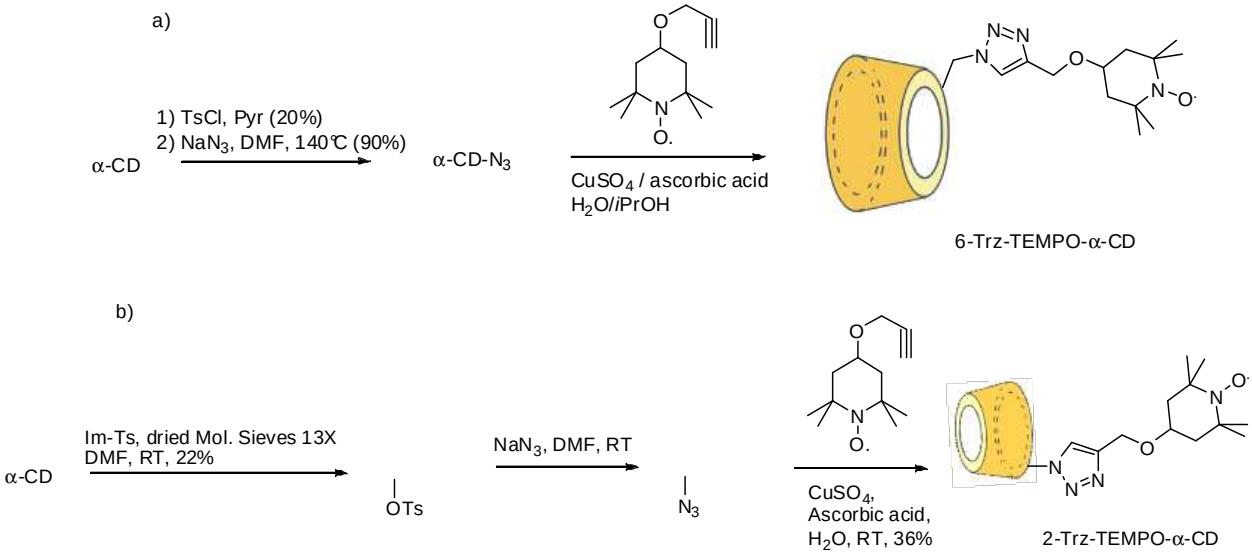

Scheme 12

The functionalization of the secondary edge of α-CD was realized according the reaction sequence reported in Scheme 12b.[34b]

The 'click' rotaxanation of lactosyl azide **2** with TEMPO alkine in the presence of the monofuntionalized CDs in the condition of the reaction reported in Scheme 11, provided good results only for the 6-armed macrocycle (Scheme 13, up), giving rise to the first supramolecular species **4** in which two radical components, bead and axle, are mechanically bonded.

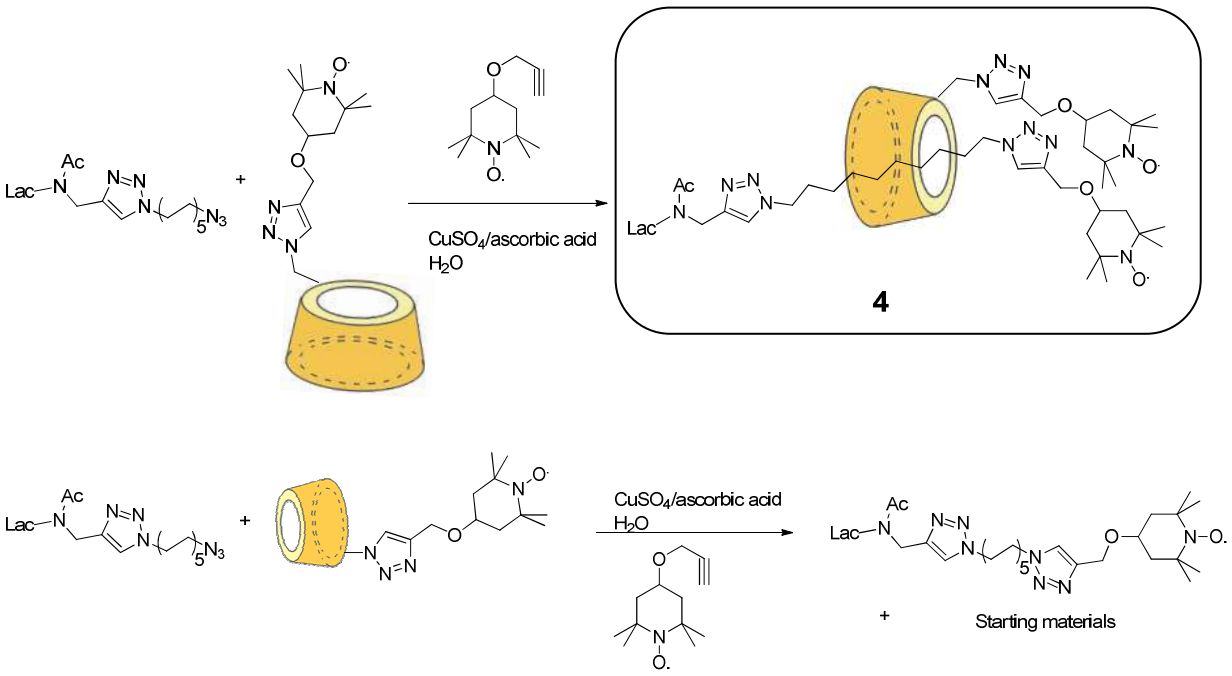

Scheme 13

Structural determination of the new diradical rotaxane **4** was provided by ESI-MS (Figure 6) and NMR data (Figure 7).

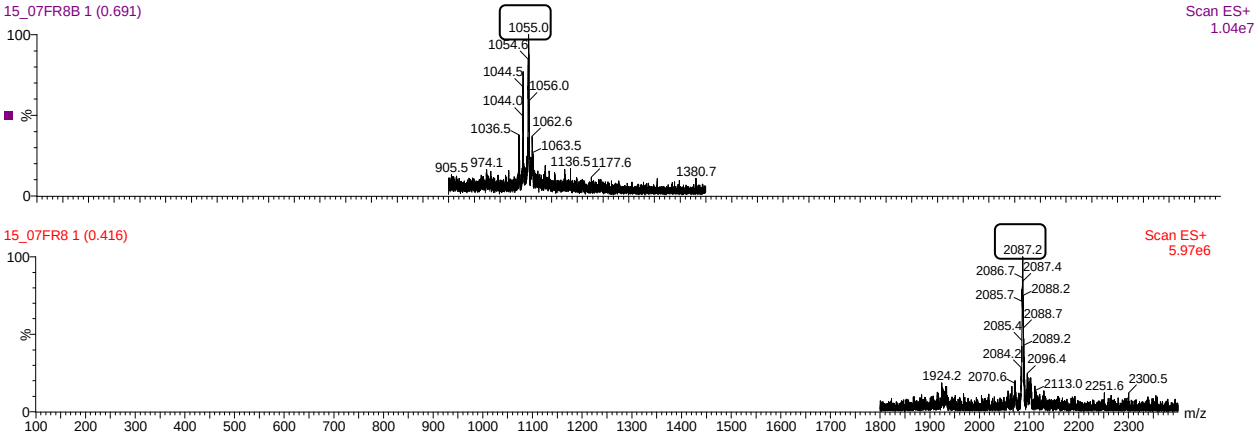

Figure 6. ESI-MS spectra of of rotaxane **4** showing the peak (in the squares) present as a double charged (up) and a mono charged form (bottom).

The discussion on the NMR data of rotaxane **4** resembles that above reported for the previously sinthesised α-CD-based rotaxane **3**.

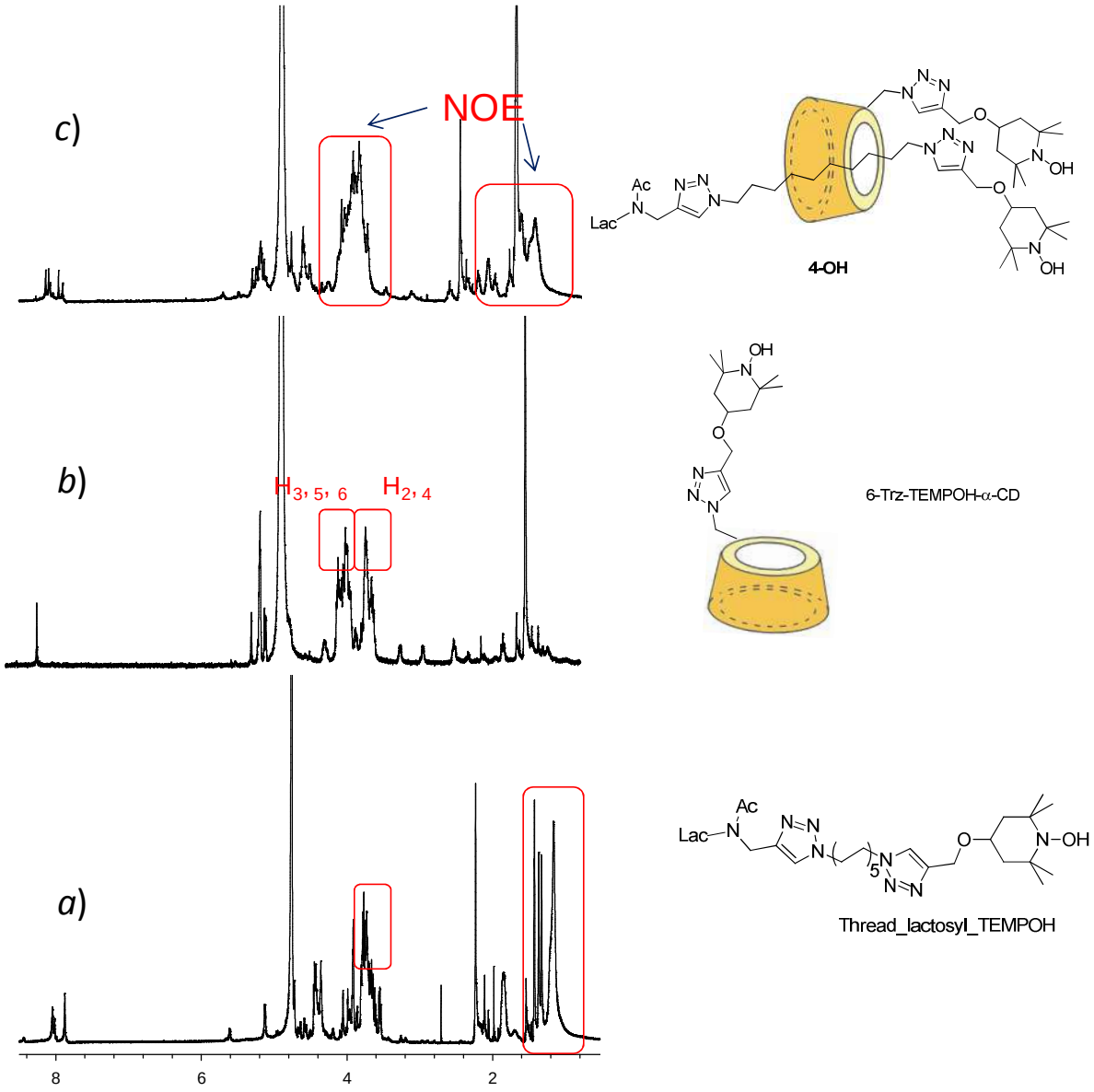

Figure 7. ^{1}H NMR spectra (600 MHz, 298 K, D_2O, 1.5 mM) of (*a*) dumbbell lactosyl-C10-TEMPOH, (*b*) 6-Trz-TEMPOH-α-CD, (*c*) rotaxane **4-OH**.

The unsymmetrical structure of both the 6-functionalized cyclodextrin and the axle can lead in principle to a mixture of orientational isomers in which the orientation of the CD along the axle depends on molecular structure of the guest and the host. Actually, the lack of rotaxane formation in the case of the branched CD functionalized in the major rim (Scheme 13, below) indicates that the substitution of CD in the secondary rim may hamper the inclusion and the threading process of the decane part into the cavity of the host, and suggests that the inclusion direction of the azide occurs from the secondary edge of CD. Consequently, the 6-funtionalized CD may form a single pseudorotaxane isomer and the represented structure **4** should prefigure the exact cyclodextrin orientation along the chain in which two radical centres are spatially close each other. As a matter of fact, ESR data corroborates this hyphothesis. The room temperature ESR spectrum of rotaxane **4**

in water (Figure 8) consists five lines, as expected when the electrons are coupled (*J*) more strongly to each other than to either nitrogen nucleus, that is, when $J >> a_N$.[35]

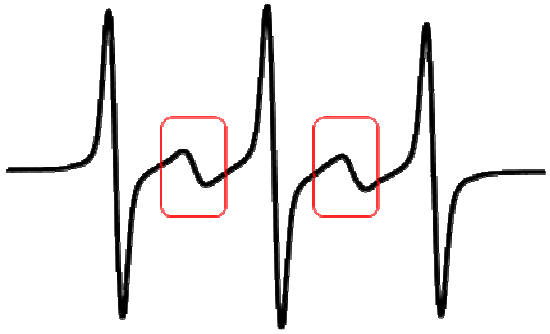

Figure 8. ESR spectrum of rotaxane **4** in water at room temperature. The red squares evidence the lines arising from spin exchange between the two spatially closed nitroxide units.

While in the absence of spin exchange, the biradical behaves as two single nitroxide radicals and the ESR spectrum consists of three lines due to the individual spins coupled with the nitrogen nucleus with a hyperfine splitting constant a_N, in the presence of spin exchange occurring between the two paramagnetic centers a five-lines system is usually observed. Thus, the ESR spectrum is consistent with a geometry in which the two nitroxides must be relatively close in space. Further studies based on pulsed ESR experiments are in progress to fully characterize the rotaxane structure and to exploit the possibility of using the diradical α-CD-6-functionalized-based rotaxane **4** as a magnetic molecular switch.

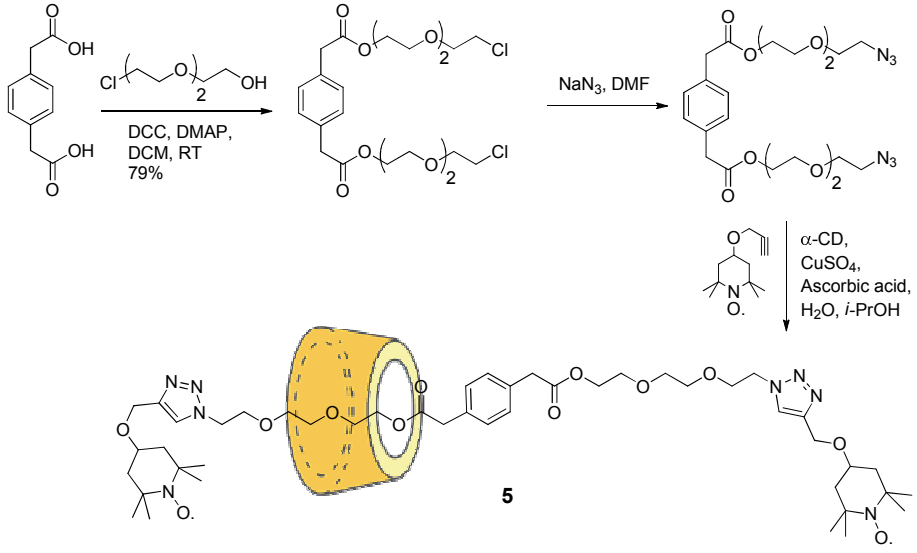

Scheme 14

In the last period of my Ph.D I studied the possibility to prepare new paramagnetic threads containing one *para*–disubstituted phenyl station with two polyether chains with the purpose of increasing the affinity of the guest for the CD cavity, and extending the length of the axle to study the movement of the macrocycle in the rotaxane assembly. In this study the paramagnetic end cap

groups are again TEMPO units. The synthesis reported in Scheme 14 starts from 1,4-phenylendiacetic acid, which, after condensation with 2-(2-(2-chloroethoxy)ethoxy)ethanol and treatment with sodium azide, affords the corresponding diazide in good yield.

After click reaction with the TEMPO alkine in the presence of α-CD, compound **5** was isolated in 5-10 % yield. The new rotaxane was identified by the usual spectroscopic techniques, but the synthesis is still under investigation in order to improve reaction conditions and yields. This result is promising owing to the possible entrapment of the diradical thread into the 6-Trz-TEMPO-α-cyclodextrin, which could generate the first example of a rotaxane triradical.

4.7. Conclusions

In this section some recent results regarding the synthesis of radical supramolecular structures in the form of α-CD-based rotaxane assemblies have been obtained and discussed.

The choice of a bulk sugar moiety (lactose) as an end cap group and a decane axle revealed to be essential to form radical rotaxanes as both the saccharidic group and the alkane chain length enhance the solubility in water of the half threads and the affinity for the host molecule, respectively.

With these assumptions the synthesis of the first diradical rotaxane was achieved, in which both the components of the assembly, macrocycle and axle, brought a TEMPO moiety. First ESR studies on the behavior of this new species indicate that the two radicals are spin exchanging, condition which realizes when two radicals are in close proximity. Addition of β-CD to a solution of **4** completely suppress spin communication between the two radical centres by complexation of the nitroxide.

These results are in accord with a supramolecular structure which possesses features of a magnetic molecular switch.

4.8. Experimental Section

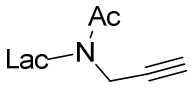

1

***N*-(4-*O*-b-D-Galactopyranosyl-b-D-glucopyranosyl)-3-acetamido-1-propyne (1).** A solution of lactose (1.2 g, 3,3 mmol) in neat propargylamine (3.7 mL, 67 mmol) was stirred for 48 h at room temperature. After evaporation under reduced pressure, the residue was taken up in MeOH (24 cm3) and acetic anhydride (3.8 ml, 40 mmol) was added. The solution was stirred overnight, concentrated and coevaporated three times with toluene. Purification by column chromatography (CH_3CN/H_2O/30 % NH_3 9:1:0.1) afforded **1** (1.28 g, 91%). δ_H (D_2O, 353 K, 400 MHz) 2.27 (s, 3 H), 3.58 (dd, *J* 10 and 8 Hz, 1 H), 3.65–3.84 (m, 8 H), 3.94 (m, 2 H), 4.48 (d, *J* 8 Hz, 1 H); ESI-MS $[M+Na]^+$: 444.14.

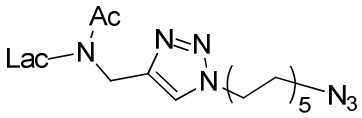

2

Lactosyl-decane-azido conjugate (2).
Sodium ascorbate (321 mg, 2 mmol) and copper sulfate (400 mg, 2 mmol) in water (4 mL each) were added to a solution of compound **1** (0.85 g, 2 mmol) and 1,10-diazidodecane (6.8 g, 30 mmol) in DMF (120 mL). The reaction mixture was stirred or 3h and concentrated under reduced pressure. The residue was purified by column chromatography (CH_3CN/H_2O 95:5 to 75:25) affording **2** (0.75 g, 57%). δ_H (D_2O, 353 K, 400 MHz) 1.26 (m, 12 H), 1.59 (quint, *J* 7,Hz, 2 H), 1.87 (m, 2 H), 2.22 (brs, 3 H), 3.30 (t, *J* 7, 2 H), 3.58 (dd, *J* 10 and 8 Hz, 1 H), 3.63–3.81 (m, 10 H), 3.89 (d, *J* 12, 1 H), 3.94 (d, *J* 3 Hz, 1 H), 4.29 (m, 2 H), 4.46 (d, *J* 8, 1 H), 4.60 (m, 2 H), 7.90 (brs, 1 H); ESI-MS: *m*/*z*=668 $[M+Na]^+$, 646 $[M+H]^+$.

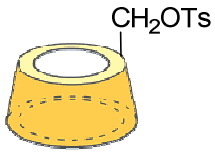

6-*O*-*p*-Toluenesulfonyl-α-cyclodextrin.[34,36] Tosyl chloride (9.8 g, 51 mmol) was added to a stirred solution of α-cyclodextrin (5 g, 5 mmol) in pyridine (160 mL). After 15 min, the reaction was quenched by addition of water (30 ml). The solution was evaporated under reduced pressure. The crude residue was purified by column chromatography (CH_3CN/H_2O, 9:1) to give **2** (1.5 g, 26%). δ_H(D_2O, 298 K, 400 MHz) 2.52 (s, 3 H), 3.53 (t, *J* 9 Hz, 1H), 3.64 (m, 12H), 3.81–4.07 (m, 22 H), 4.42 (dd, *J* 11 and 6 Hz, 1 H), 4.52 (d, *J* 11 Hz, 1 H), 4.99 (br s, 2 H), 5.08 (br d, *J* 4 Hz, 4 H), 7.58 (d, *J* 8 Hz, 2 H), 7.90 (d, *J* 8 Hz, 2 H); MS-ESI: *m*/*z* = 1150 $[M+Na]^+$.

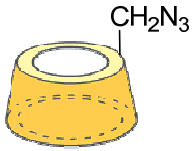

6-Azido-6-deoxy-α-cyclodextrin.[34,36] Sodium azide (0.88 g, 14 mmol) was added to a solution of mono-tosyl-α-CD (1.5 g, 1.3 mmol) in DMF (30 mL). The solution was stirred at 140 °C overnight and evaporated under reduced pressure. The crude residue was purified by column chromatography (CH_3CN/H_2O, 8:2) affording the product (1.2 g, 93%). MS-ESI: *m*/*z* = 1020 $[M+Na]^+$.

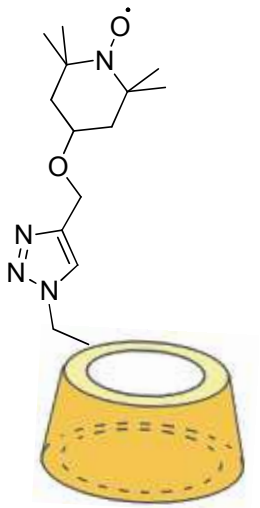

α-CD-Trz-TEMPO

α-CD-Trz-TEMPO. Ascorbic acid (0.032 g, 0.18 mmol) and copper sulfate (0.017 g, 0.07 mmol) were added to a solution of azido cyclodextrin **3** (0.35 g, 0.35 mmol) and 4-propargyloxy-TEMPO (0.074 g, 0.35 mmol) in 2:1 H_2O/*i*PrOH (10 mL). The reaction mixture stirred at room temperature overnight and evaporated under reduced pressure. The crude residue was purified by column chromatography (silica gel, eluent CH_3CN/H_2O, 85:15) and gel exclusion over Sephadex column G15 (0.2 g, 48.5%). The ^1H NMR spectrum was measured after $Na_2S_2O_4$ in situ reduction of the sample containing the nitroxide.
δ_H (D_2O, 298 K, 600 MHz) 1.35 (s, 6 H), 1.40 (s, 6 H), 1.45 (t, *J* 12 Hz, 2 H), 2.14 (t, *J* 12 Hz, 2 H), 2.86 (d, *J* 12 Hz, 1 H), 3.15 (d, *J* 12 Hz, 1 H), 3.50-4.10 (m, 34 H), 4.19 (m, 1 H), 4.60-4.70 (m, 2 H), 4.95-5.19 (m, 8 H), 8.07 (s, 1 H). ESI-MS *m*/*z* = 1208.3 $[M+H]^+$, 1230.3 $[M+Na]^+$.

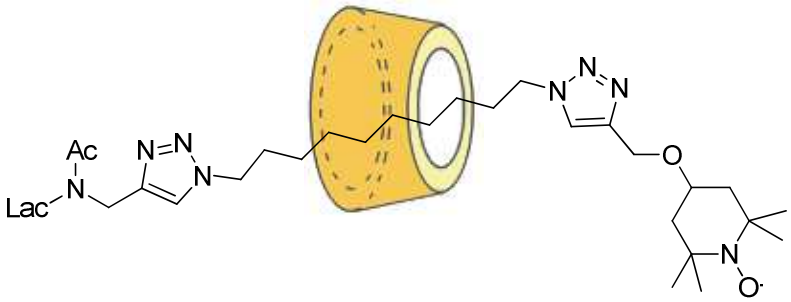

3

Rotaxane 3. To an aqueous solution (5 mL) of α-CD (0.06 g, 0.062 mmol) and lactosyl azide (**2**) (0.04 g, 0.062 mmol) stirred for 15 min, 4-propargyloxy-TEMPO (0.015 g, 0.073 mmol), ascorbic acid (0.005 g, 0.025 mmol) and copper sulfate (0.003 g, 0.012 mmol) were added and the mixture was stirred for 72 h at room temperature. After evaporation under reduced pressure the crude was purified by column chromatography (silica gel, eluent CH_3CN/H_2O, 9:1 to CH_3CN/H_2O/30% NH_3 8:2:1) and gel exclusion over Sephadex column G15 (0.024 g, 22%).
The ^1H NMR spectrum was measured after $Na_2S_2O_4$ in situ reduction of the sample containing the nitroxide.
δ_H (D_2O, 298 K, 600 MHz) 1.00-1.40 (m, 12 H), 1.44 (brs, 12 H), 1.50-1.65 (m, 4 H) 1.70-1.90 (m, 4 H), 1.95-2.03 (m, 2 H), 2.10-2.26 (m, 5 H), 3.50-4.10 (m, 49 H), 4.25-4.58 (m, 6 H), 4.59-4.63 (m, 2 H), 5.02-5.11 (m, 8 H), 7.90-8.10 (m, 2 H). ESI-MS *m/z* = 1851.6 $[M+Na]^+$.

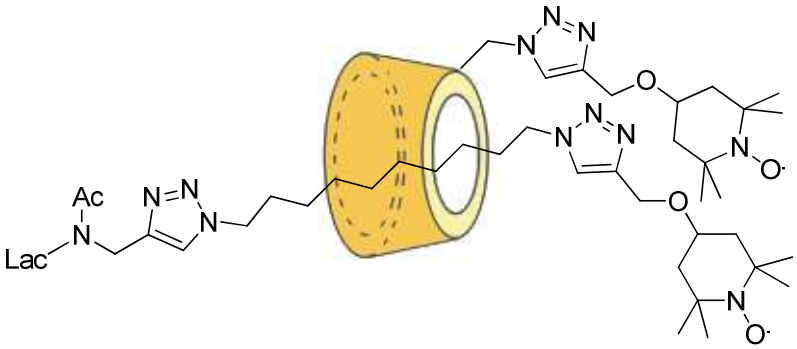

4

Rotaxane 4. To an aqueous (3 mL) solution of 6-Trz-TEMPO-α-CD (0.05 g, 0.041 mmol) and lactosyl azide (**2**) (0.026 g, 0.041 mmol) stirred for 15 min, 4-propargyloxy-TEMPO (0.01 g, 0.05 mmol), ascorbic acid (0.003 g, 0.016 mmol) and copper sulfate (0.002 g, 0.008 mmol) were added and the mixture was stirred for 72 h at room temperature. After evaporation under reduced pressure the crude was purified twice by gel exclusion over Sephadex column G15 (0.025 g, 29%).
The ^1H NMR spectrum was measured after $Na_2S_2O_4$ in situ reduction of the sample containing the nitroxide.
δ_H (D_2O, 298 K, 600 MHz) 1.08-1.38 (m, 12 H), 1.44 (brs, 12 H), 1.70-1.78 (m, 2 H) 1.80-1.90 (m, 4 H), 1.95-2.03 (m, 2 H), 2.10-2.26 (m, 5 H), 2.35-2.42 (m, 2 H), 2.93 (m, 1 H), 3.29 (m, 1 H), 3.50-4.20 (m, 47 H), 4.30-4.58 (m, 8 H), 4.59-4.65 (m, 2 H), 4.92-5.21 (m, 6 H), 7.85-8.15 (m, 3 H). ESI-MS *m/z* = 2085.98 $[M+Na]^+$.

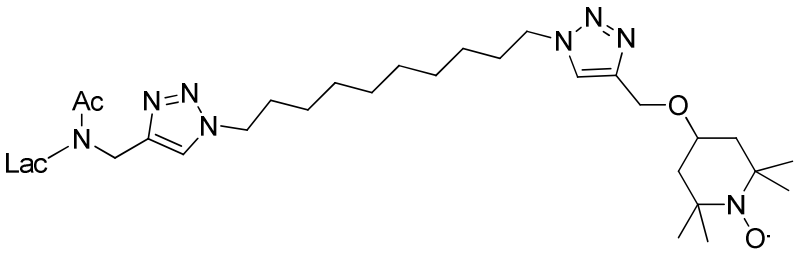

Thread lactosyl-TEMPO. This product was obtained by purification of rotaxane 3 or 4 as secondary by-product. The sample was identified by NMR after in situ reduction of the sample. δ_H (D_2O, 298 K, 600 MHz) 1.08-1.28 (m, 12 H), 1.30-1.42 (m, 12 H), 1.60-1.78 (m, 2 H), 1.80-1.95 (m, 4 H) 2.10-2.26 (m, 5 H), 3.55-4.05 (m, 13 H), 4.30-4.70 (m, 10 H), 5.12 (m, 1 H), 7.87(s, 1 H), 8.07 (s, 1 H). ESI-MS m/z = 878.67 $[M+Na]^+$.

References

1. Kolb, H. C; Finn, M. G.; Sharpless, K. B. *Angew. Chem. Int. Ed*. **2001**, *40*, 2004 – 2021
2. a)Rostovtsev, V. V.; Green, L. G.; Fokin, V. V.; Sharpless, K. B. *Angew. Chem. Int. Ed.*, **2002**, *41*, 2596-99; b) Moses, J. E., Moorhouse A. D. *Chem. Soc. Rev*., **2007**, *36*, 1249–1262.
3. a) Huisgen, R. *1,3-Dipolar Cycloaddition Chemistry* (Ed.: A. Padwa), Wiley, New York, **1984**, 1-176; b) Padwa, A. *Comprehensive Organic Synthesis*, (Ed.: B. M. Trost), Pergamon, Oxford, **1991**, *4*, 1069 - 1109; c) for a review of asymmetric 1,3-dipolar cycloaddition reactions, see Gothelf, K. V.; Jorgensen, K. A. *Chem. Rev*. **1998**, *98*, 863 - 909; d) for a review of synthetic applications, see Mulzer, J. *Org. Synth*. *Highlights* **1991**, 77 - 95.
4. a) Fan, W.-Q.; Katritzky, A. R. in *Comprehensive Heterocyclic Chemistry II*, (Eds.: A. R. Katritzky, C. W. Rees, E. F. V. Scriven), Pergamon, Oxford, **1996**, *4*, 101-126; b) Butler, R. N. in *Comprehensive Heterocyclic Chemistry II*, (Eds.: A. R. Katritzky, C. W. Rees, E. F. V. Scriven), Pergamon, Oxford, **1996**, *4*, 621-678; c) Banert, K. *Chem. Ber*. **1989**, *122*, 911-918.
5. a) Huisgen, R. *Pure Appl. Chem*. **1989**, *61*, 613-628; b) Huisgen, R.; Szeimies, G.; Moebius, L. *Chem. Ber*. **1967**, *100*, 2494-2507; c) W. Lwowski *1,3-Dipolar Cycloaddition Chemistry*, (Ed.: A. Padwa), Wiley, New York, **1984**, *1*, chap. 5; d) Bastide, J.; Hamelin, J.; Texier, F.; Ven, V. Q.;*Bull. Soc. Chim. Fr*. **1973**, 2555-2579; Bastide, J.; Hamelin, J.; Texier, F.; Ven, V. Q.; *Bull. Soc. Chim. Fr*. **1973**, 2871-2887.
6. Zanirato, P. *J. Chem. Soc. Perkin Trans. 1* **1991**, 2789-2796; Hlasta, D. J.; Ackerman, J. A. *J. Org. Chem.* **1994**, *59*, 6184-6189; Booth, C. A.; Philp, D. *Tetrahedron Lett.* **1998**, *39*, 6987-6990; Howell, S. J.; Spencer, N.; Philp, D. *Tetrahedron* **2001**, *57*, 4945-4954; Mock, W. L.; Irra, T. A.; Wepsiec, J. P.; Adhya, M. *J. Org. Chem*. **1989**, 54, 5302-5308; Mock, W. L. *Top. Curr.*

Chem. **1995**, *175*, 1-24; Chen, J.; Rebek, J. Jr., *Org. Lett.* **2002**, *4*, 327-329; Wijnen, J. W.; Steiner, R. A.; Engberts, J. B. F. N. *Tetrahedron Lett.* **1995**, *36*, 5389-5392; Repasky, M. P.; Jorgensen, W. L. *Faraday Discuss.* **1998**, *110*, 379-389.

7. Organic azides, particularly in the aliphatic series, are exceptionally stable toward the common reactive chemicals on the Earth×s surface, which range from dioxygen and water to the aqueous solutions of highly functionalized organic molecules which make up living cells: Saxon, E.; Bertozzi, C. R. *Science* **2000**, *287*, 2007-2010; Kiick, K. L.; Saxon, E.; Tirrel, D. A.; Bertozzi, C. R. *Proc. Natl. Acad. Sci. USA*, **2002**, *99*, 19-24.
8. In fact, it was the razor sharp reactivity window for this cycloaddition process which spawned our “in situ click chemistry” ideas–an approach which recently resulted in the discovery of the most potent noncovalent inhibitor of acetylcholinesterase known to date: Lewis, W. J.; Green, L. G.; Grynszpan, F.; Radic, Z.; Carlier, P. R.; Taylor, P.; Finn, M. G.; Sharpless, K. B. *Angew. Chem.* **2002**, *114*, 1095-1099; *Angew. Chem. Int. Ed.* **2002**, *41*, 1053-1057.
9. For a review of reactions of _-ascorbic acid with transition metals, see M. B. Davies, *Polyhedron* **1992**, *11*, 285-321, and references therein; redox properties of ascorbic acid are summarized in Creutz, C. *Inorg. Chem.* **1981**, *20*, 4449.
10. Wu, P.; Fokin, V. V. *Aldrich Chim. Acta* **2007**, *40*, 7.
11. van Koten, G.; Noltes, J. G. *Comprehensive Organometallic Chemistry*(Ed.: G. Wilkinson), Pergamon, Oxford, **1982**, *2*, chap. 14, 720.
12. Himo, F.; Lovell, T.; Rostovtsev, V.; Fokin, V. V.; Sharpless, K. B.; Noodleman, L. unpublished results.
13. Doyle, M. P.; McKervey, M. A; Ye, T. *Modern Catalytic Methods for Organic Synthesis with Diazo Compounds*, Wiley, New York, **1997**, 163- 248.
14. Hanni, K. D.; Leigh, D. A. *Chem. Soc. Rev.*, **2010**, *39*, 1240-51.
15. Dietrich-Buchecker, C. O.; Sauvage, J.-P.; Kintzinger, J.-P. *Tet. Lett.*, **1983**, *24*, 5095–5098.
16. Sauvage, J.-P.; Dietrich-Buchecker, C. O. *Molecular Catenanes, Rotaxanes and Knots* Wiley-VCH, Weinheim, **1999**.
17. Craig, M. R.; Hutchings, M. G.; Claridge, T. D. W.; Anderson, H. L. *Angew. Chem., Int. Ed.*, **2001**, *40*, 1071–1074.
18. Fernandes, A.; Viterisi, A.; Coutrot, F.; Potok, S.; Leigh, D. A.; Aucagne, V.; Papot, S. *Angew. Chem., Int. Ed.*, **2009**, *48*, 6443–6447.
19. Berna´, J.; Leigh, D. A.; Lubomska, M.; Mendoza, S. M.; Pe´rez, E. M.; Rudolf, P; Teobaldi, G.; Zerbetto, F.; *Nat. Mater.*, **2005**, *4*, 704–710.

20. Liu, Y.; Flood, A. H.; Bonvallet, P. A.; Vignon, S. A.; Northrop, B. H.; Tseng, H.-R.; Jeppesen, J. O.; Huang, T. J.; Brough, B.; Baller, M.; Magonov, S.; Solares, S. D.; Goddard, W. A.; Ho C.-M.; Stoddart, J. F. *J. Am. Chem. Soc.*, **2005**, *127*, 9745–9759.

21. Collier, C. P.; Mattersteig, G.; Wong, E. W.; Luo,Y.; Beverly, K.; Sampaio, J.; Raymo, F. M.; Stoddart, J. F.; Heath, J. R. *Science*, **2000**, *289*, 1172–1175.

22. Green, E.; Choi, J. W.; Boukai, A.; Bunimovich, Y.; Johnston-Halprin, E.; DeIonno, E.; Luo, Y.; Sheriff, B. A.; Xu, K.; Shin, Y. S.; Tseng, H.-R.; Stoddart J. F.; Heath, J. R. *Nature*, **2007**, *445*, 414–417.

23. Kay, E. R.; Leigh, D. A.; Zerbetto, F. *Angew. Chem., Int. Ed*., **2006**, *46*, 72–191.

24. Structures formed by ‘slippage’ are formally not rotaxanes, rather they are pseudorotaxanes that are kinetically stable under some conditions. Rotaxanes are ‘molecules in which a ring encloses another, rod-like molecule having end-groups too large to pass through the ring opening and thus holds the rod-like molecule in position without covalent bonding’. [A. D. McNaught and A. Wilkinson, The IUPAC Compendium of Chemical Terminology, Blackwell Science, Oxford, 2nd edn, 1997]. A structure obviously cannot be said to have ‘end-groups too large to pass through the ring opening’ if they have passed through in order to form it.

25. Ashton, P. R.; Chrystal, E. J. T.; Glink, p. T.; Menzer, S.; Schiavo, C.; Spencer, N.; Stoddart, J. F.; Tasker, P. A.; White, A. J. P.; Williams, D. J.; *Chem.–Eur. J*., **1996**, *2*, 709–728.

26. Ashton, P. R.; Goodnow, T. T.; Kaifer, A. E.; Reddington, M. V.; Slawin, A. M. Z.; Spencer, N.; Stoddart, J. F.; Vicent, C.; Williams, D. J.; *Angew. Chem., Int. Ed. Engl*., **1989**, *28*, 1396–1399.

27. Crowley, j. D.; Goldup, S. M.; Lee, A.-L.; Leigh, D. A.; McBurney, R. T.; *Chem. Soc. Rev*., **2009**, *38*, 1530–1541.

28. Szejtli, J. ‘Introduction and overview of cyclodextrin chemistry’, *Chem. Rev.*, **1998**, *98*, 1743–1753.

29. Hanni, K. D.; Leigh, D. A. *Che. Soc. Rev.*, **2010**, *39*, 1240-1251.

30. Chwalek, M.; Auzély, R.; Fort, S. *Org. Biomol. Chem.*, **2009**, *7*, 1680-1688.

31. Yui, N.; Ooya, T.; *Chem. Eur. J*., **2006**, *12*, 6730–6737.

32. (*a*) Harada, A. *Acc. Chem. Res.*, **2001**, *34*, 456–464; (*b*) Wenz, G.; Han, B.-H.; Muller, A. *Chem. Rev.*, **2006**, *106*, 782–817; (*c*) Nepogodiev, S. A.; Stoddart, J. F. *Chem. Rev.*, **1998**, *98*, 1959–1976; (*d*) *Molecular Catenanes, Rotaxanes and Knots*, J.-P. Sauvage, C. O. Dietrich-Buchecker, eds., Wiley-VCH, Weinheim, 1999; (*e*) Takata, T.; Kihara, N. *Rev. Heteroatom Chem.*, **2000**, *22*, 197–218; (*f*) Mahan, E.; Gibson, H. W. *Cyclic Polymers*, 2nd ed., J. A. Semlyen, ed., Kluwer Publishers, Dordrecht, **2000**, pp. 415–560; (*g*) Cantrill, S. J.; Pease, A. R.;

Stoddart, J. F. *J. Chem. Soc., Dalton Trans.*, **2000**, 3715–3734; (*h*) Hubin, T. J.; Busch, D. H. *Coord. Chem. Rev.*, **2000**, *200–202*, 5–52; (*i*) Panova Topchieva, I. N. *Russ. Chem. Rev.*, **2001**, *70*, 23–44; (*j*) Lucci, R.; Ciani, G.; Proserpio, D. M. *Coord. Chem. Rev.*, **2003**, *246*, 247–289.

33. Nelson, A.; Belitsky, J. M.; Vidal, S.; Joiner, C. S.; Baum, L. G.; Stoddart, J. F. *J. Am. Chem. Soc.*, **2004**, *126*, 11914–11922.

34. (*a*) Melton, L. D.; Slessor, K. N. *Carbohydr. Res.*, **1971**, *18*, 29–37. (*b*) Teranishi, K.; Watanabe, K.; Hisamatsu, M; Yamada, T. *J. Carbohydrate Chem.*, **1998**, *17*, 489-494. (*c*) Luo, J.; Pardin, C.; Lubell, W. D.; Zhu, X. X. *Chem. Commun.*, **2007**, 2136-2138.

35. Luckurst, G. R.; Pedulli, G. F. *J. Am. Chem. Soc.* **1970**, *92*, 4738-4739.

36. W. Tang and S.-C. Ng, *Nature Protocols*, 2008, **3**(4), 691–697.

Chapter 5. pH Responsive Paramagnetic 3-Rotaxanes Synthesis Through Cucurbit[6]uril Catalyzed 1,3-Dipolar Cycloaddition

5.1. Introduction[1]

In 1981, the macrocyclic methylene-bridged glycoluril hexamer (CB[6]) was dubbed "cucurbituril" by Mock and co-workers because of its resemblance to the most prominent member of the cucurbitaceae family of plants, the pumpkin. In the intervening years, the fundamental binding properties of CB[6] (high affinity, selectivity and constrictive binding interactions) have been delineated by the pioneering work of the research groups of Mock, Kim, and Buschmann, leading to their actual applications.

More recently, the cucurbit[*n*]uril family has grown to include homologues (CB[5]–CB[10]), derivatives, congeners, and analogues whose sizes span and exceed the range available with the α-, β-, and γ-cyclodextrins.

5.2. Historical background

In 1905, contemporaneous with the pioneering work of Schardinger on the cyclodextrins, Behrend et al. reported that the condensation of glycoluril (acetyleneurea) and formaldehyde in concentrated HCl yields an insoluble polymeric crystalline substance, now known as Behrend's polymer,[2] in good yield (40–70%) by recrystallization from concentrated H_2SO_4 and which is able to form cocrystals (complexes) with a variety of substances like $KMnO_4$, $AgNO_3$, H_2PtCl_6, $NaAuCl_4$, congo red, and methylene blue.

In 1981 Mock reinvestigated the report by Behrend et al. and disclosed the remarkable macrocyclic structure, unclear until there, comprising six glycoluril units and twelve methylene bridges; resembling to a pumpkin, the compound was dubbed cucurbituril, the most prominent member of the cucurbitaceae family (Figure 1).[3]

Interest in the CB[n] family has increased dramatically in the new millennium following the preparation of four new CB[n] homologues (CB[5], CB[7], CB[8], and CB[10]·CB[5]) by the research groups of Kim and Day[4-6], thanks to the great advances in many areas of fundamental and

applied science (chemistry, biology, materials science and nanotechnology) that rely on the ability to employ and control noncovalent interactions between molecules. CB[5]–CB[8] are now even available commercially. In contrast to the host–guest chemistry of α-, β-, and γ-cyclodextrin which has developed steadily over the past century, the supramolecular chemistry of CB[6] only began to develop in the 1980s and 1990s as a result of the pioneering work of Mock,[7] Buschmann and co-workers,[8] and Kim and co-workers.[9-10]

5.3. Synthesis of CB [*n*]

In the condensation of glycoluril and formaldehyde, neither Behrend *et al*. nor Mock detected any macrocyclic compounds (homologues) composed of a different number of glycoluril rings (for example, CB[5], CB[7], and CB[8]). 20 years later, when this reaction was conducted under milder, kinetically controlled conditions by the research groups of Kim and Day, CB[5]–CB[8] and CB[5]@CB[10] were detected and isolated (Figure 1).[4-6,11]

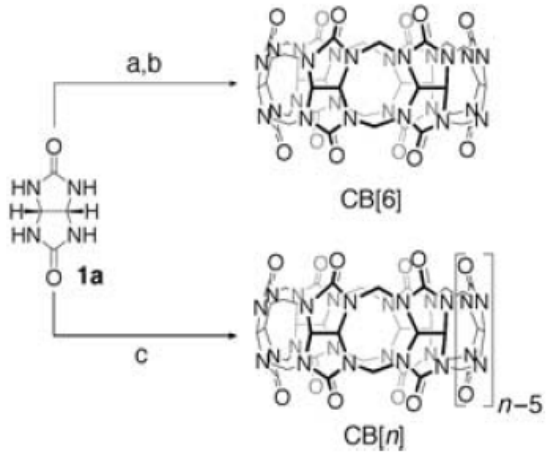

Figure 1. Synthesis of CB[6] from glycoluril under forcing conditions and a mixture of CB[n] under milder conditions. a) CH_2O, HCl, heat; b) H_2SO_4; c) CH_2O, HCl, 100°C, 18 h.

5.4. Fundamental properties of CB[*n*]

5.4.1. Dimensions

CB[*n*] are cyclic methylene-bridged glycoluril oligomers whose shape resembles a pumpkin. The defining features of CB[5]–CB[10] are their two portals lined by ureido carbonyl groups that provide entry to their hydrophobic cavity.[12] Similar to the cyclodextrins, the various CB[*n*] have a common depth (9.1×10^{-9} m), but their equatorial, annular widths *a*, and volumes vary systematically

with ring size (Table 1). The portals guarding the entry to CB[*n*] are approximately 2×10^{-9} m narrower than the cavity itself which results in constrictive binding producing significant steric barriers to guest association and dissociation.[13] The cavity sizes available in the CB[*n*] family span and exceed those available with the cyclodextrins. Figure 2 shows the X-ray crystal structures for CB[5]–CB[8] and CB[5]@CB[10].

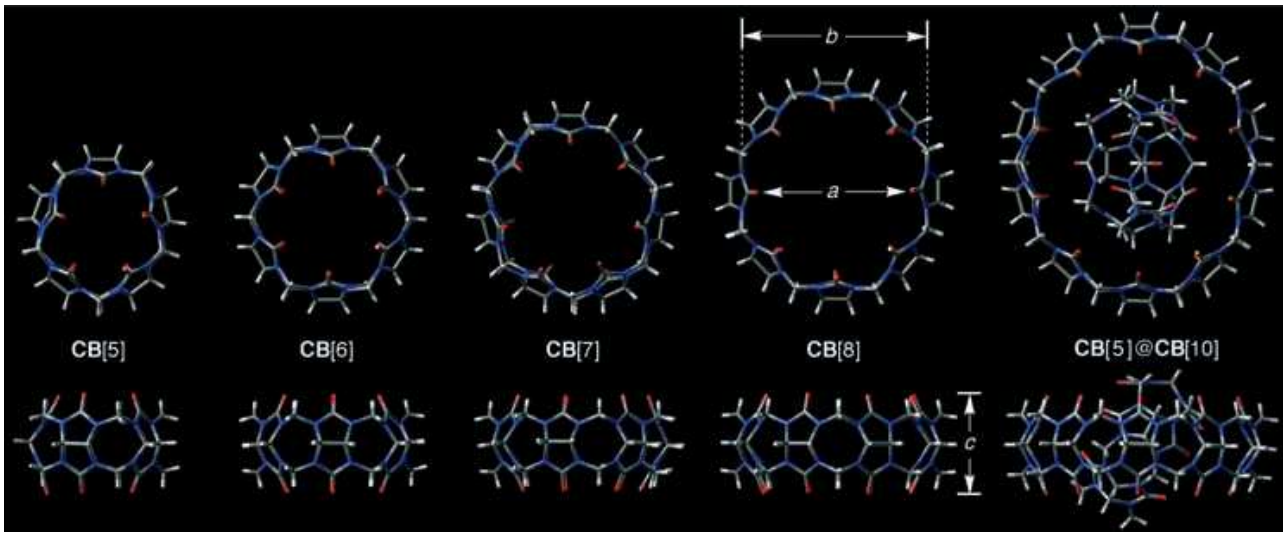

Figure 2. Top and side views of the X-ray crystal structures of CB[5],[4] CB[6],[3] CB[7],[4] CB[8],[4] and CB[5]@CB[10].[6] The various compounds are drawn to scale.

5.4.2. Solubility, stability, acidity

One of the limitations of the CB[*n*] family is their relatively poor solubility in water, lower than the cyclodextrins: CB[6] and CB[8] are essentially insoluble, whereas CB[5] and CB[7] possess modest solubility in water (Table 1).

	M_r	a [Å][a]	b [Å][a]	c [Å][a]	V [Å^3]	s_{H_2O} [mM]	Stability [°C]	pK_a
CB[5]	830	2.4[5]	4.4[5]	9.1[5]	82[5]	20–30[5]	>420[5]	
CB[6]	996	3.9[5]	5.8[5]	9.1[5]	164[5]	0.018[61]	425[62]	3.02[63]
CB[7]	1163	5.4[5]	7.3[5]	9.1[5]	279[5]	20–30[5]	370[5]	
CB[8]	1329	6.9[5]	8.8[5]	9.1[5]	479[5]	<0.01[5]	>420[5]	
CB[10][b]	1661	9.0–11.0	10.7–12.6	9.1	–	–	–	–
α-CD	972	4.7[64]	5.3[64]	7.9[64]	174[64]	149[64]	297[65]	12.332[64]
β-CD	1135	6.0[64]	6.5[64]	7.9[64]	262[64]	16[64]	314[65]	12.202[64]
γ-CD	1297	7.5[64]	8.3[64]	7.9[64]	427[64]	178[64]	293[65]	12.081[64]

[a] The values quoted for a, b, and c for CB[*n*] take into account the van der Waals radii of the relevant atoms. [b] Determined from the X-ray structure of the CB[5]@CB[10] complex.[9]

Table 1: Dimensions and physical properties of CB[*n*] and the cyclodextrins.

However, the carbonyl groups lining the portals of CB[*n*] are weak bases (like urea): the pK_a value of the conjugate acid of CB[6] is 3.02 and the pK_a values for CB[5], CB[7], and CB[8], although

not measured, are likely to be similar to that of CB[6], so the solubility of CB[5]–CB[8] increase dramatically in concentrated aqueous acid (for example, 61 mM for CB[6] in HCO_2H/H_2O (1:1), about 60 mM for CB[5], about 700 mM for CB[7], and about 1.5 mM for CB[8] in 3M HCl).[14-16] Another outstanding feature of CB[5]–CB[8] is their high thermal stability: thermal gravimetric analysis shows this to exceed 370°C in all cases.

5.4.3. Electrostatic potential

Although similar in shape, β- CD and CB [7] exhibit different electrostatic potential, which can play a crucial role in molecular recognition events in both aqueous and organic solution.[17]
The electrostatic potential at the portals and within the cavity of CB[7] is significantly more negative than for β-CD, so CB[*n*] show a pronounced preference to interact with cationic guests whereas β-CD prefers to bind to neutral or anionic guests (Figure 3).

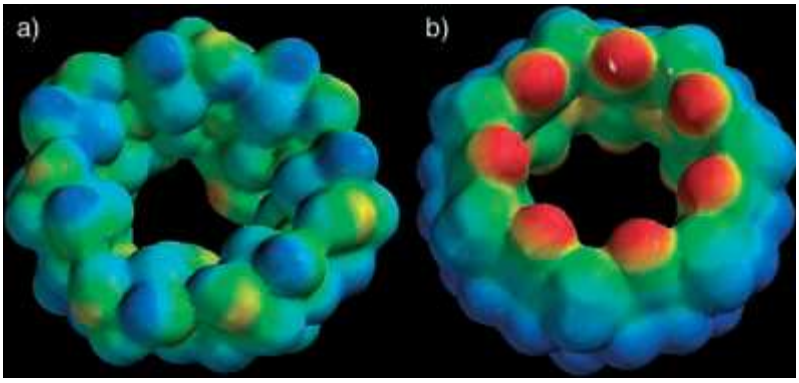

Figure 3. Electrostatic potential maps for a) β-CD and b) CB[7]. The red to blue color range spans -80 to 40 kcal mol^{-1}. Adapted from Kim and co-workers.[9]

5.5. Host-guest chemistry of CB[*n*]

Houk et al. recently reviewed the binding affinities for a wide variety of systems including synthetic host-guest, antibody-antigen, receptor-drug, and enzyme-substrate complexes.[18]
Table 2 compares the affinity of α-CD and CB[6] toward a series of alcohols, modest guests for both hosts. Despite its preference to interact with positively charged guests, CB[6] binds more tightly to the alcohols (except hexanol) than does α-CD but in a non selective manner: generally CB[6] binds with higher affinity and selectivity toward its guest than do the cyclodextrins

	CH_3CH_2OH	$CH_3(CH_2)_2OH$	$CH_3(CH_2)_3OH$	$CH_3(CH_2)_4OH$	$CH_3(CH_2)_5OH$
CB[6]	2.64	2.61	2.53	2.73	2.71
α-CD	0.99	1.46	1.91	2.51	2.90

Table 2. Calorimetrically determined log K values for the complexation of alcohols with CB[6] in HCO_2H/H_2O (1:1) at 25°C and with α-CD in H_2O.[19-20]

In table 3 there is a similar comparison between the affinity of CB [6] and [18]crown-6 toward several monovalent and divalent cations: CB[6] shows higher affinity toward all cations except Ba^{2+}, whose radius is a good match for the cavity of [18]crown-6.

These examples clearly illustrate that the binding ability of CB[6] generally equals or exceeds those of other well-known host molecole such as cyclodextrins and crown ethers.

	Li^+	Na^+	K^+	Rb^+	Ca^{2+}	Sr^{2+}	Ba^{2+}
CB[6]	2.38	3.23	2.79	2.68	2.80	3.18	2.83
[18]crown-6	–	0.80	2.03	1.56	<0.5	2.72	3.87

Table 3. Calorimetrically determined log *K* values for the complexation of monovalent and divalent cations with CB[6] in HCO_2H/H_2O (1:1) at 25°C and with [18]crown–6 in H_2O.[14-21]

5.5.1. Protonation of CB[6] at the carbonyl groups lining the portals

Being a weak base (pK_a=3.02), CB[6] can be protonated in moderately acidic media, so, when binding studies are conducted with CB[6] in strongly acidic media (for example, HCO_2H/H_2O (1:1)), H^+ competes with guest binding (Figure 4, red equilibria). Comparisons between binding constants measured in different media must, therefore, be treated with caution.

5.5.2. Binding of metal ions by CB[6]

As CB[6] binds H^+ at the ureido carbonyl groups of the portals, it also binds alkali-metal, alkaline-earth, transition-metal, and lantanide cations in homogenous solution (Figure 4, blue equilibrium).[8, 22, 14, 15, 23-26]

Table 3 shows the binding constants determined by Buschmann *et al.* for CB[6] with a variety of monovalent and divalent cations. The selectivity between the different cations is less than tenfold. The low selectivity observed and the lack of a simple trend in log*K* values is attributed to a

mismatch between the ionic radii of the cations and the annular radius of the relatively rigid CB[6] ionophore. The metal-binding equilibria (Figure 4, blue equilibria) are in competition with protonation (red equilibrium); thus, as the acidity of the solution is increate, the observed logK values for metal binding should decrease.

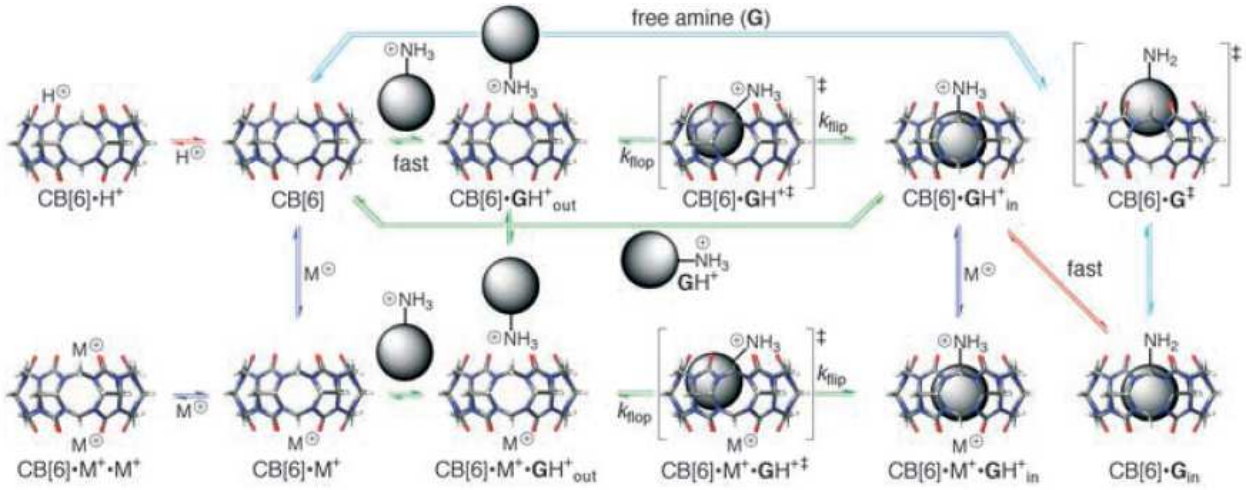

Figure 4. Comprehensive mechanistic scheme for molecular recognition by CB[6]. Red arrow: protonation; blue arrow: cation binding, green arrow: ammonium ion binding, light blue arrow: amine binding.

5.5.3. Preference of CB[6] for positively charged organic guests-ion-dipole interactions

Mock and co-workers observed by a series of ^{1}H NMR competition experiments that alkylammonium ions bind tightly to CB[6] in HCO_2H/H_2O (1:1) and measured binding constants of 10^{1}-10^{7} M^{-1}. These experiments were facilitated by two characteristics of the host–guest complexes of CB[6]:

a) The interior of CB[6] constitutes a ^{1}H NMR shielding region (upfield shifts of 1 ppm are common). The regions just outside the portals lined with carbonyl groups are weakly deshielding.

b) Dynamic exchange processes between free and bound guest are often slow on the NMR time scale, thus allowing a direct observation of the free and bound guest simultaneously.

To establish the importance of ion–dipole interactions relative to hydrogen bonds in the formation of CB[6] complexes (Figure 5), Mock and Shih considered the relative binding affinities of hexylamine and hexyldiamine. “Formal replacement of the terminal hydrogen of *n*-hexylamine with another amino group enhances binding 1200-fold. […]

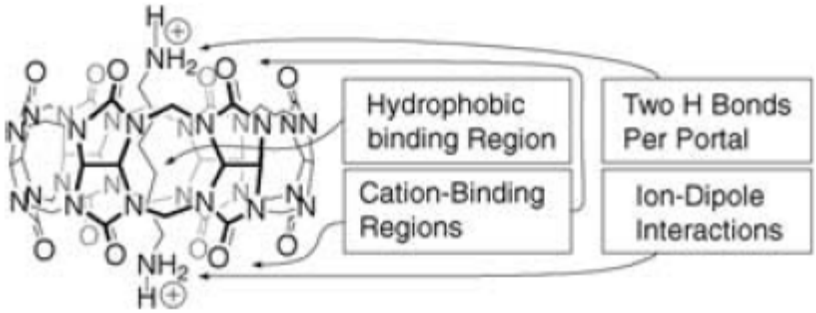

Figure 5. Representation of the different binding regions of CB[6] and the geometryof the complex between CB[6] and the hexanediammonium ion

However,replacement of this hydrogen by a hydroxyl group contributes nothing to the stabilization of the complex. […] While the alcohol (and ammonium ions)may be hydrogen bonded in the complex, in the absence of CB[6] they would also be fully hydrogen bonded. […] The consequential feature of ammonium ions is that they are charged. […] Hence, it is our understanding that the high specificity for ammonium ions is largely an electrostatic ion–dipole attraction."[27] The preference of CB[6] for charged guests will transfer to the other members of the CB[*n*] family, but the relative importance of electrostatic interactions versus the hydrophobic effect may change as the cavity size increases. Blatov and coworkers recently developed a computational technique based on crystallographic data to identify suitable guests for each member of the CB[*n*] family.[28]

5.6. Applications of CB[*n*] in Rotaxanes' synthesis

Mechanically interlocked molecules assembled through host-guest chemistry, such as rotaxanes and catenanes, containing more than one recognition site, are proving to have great potential for the construction of molecular switches and motors.

The circular shape and outstanding binding properties of CB[6] suggested its use as the wheel in the synthesis of a wide variety of rotaxanes, which have assumed important roles in supramolecular chemistry and nanotechnology because of their ability to undergo controlled motions with respect to one another in response to environmental stimuli.

5.6.1. The stoppering approach

Most commonly, rotaxanes are prepared from pseudorotaxanes -non-interlocked wheel and axle complexes- through the addition of bulky stoppers by reactions that result in the formation of covalent bonds (Figure 6).

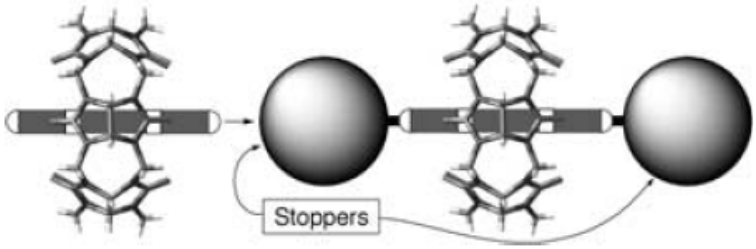

Figure 6. The stoppering approach to rotaxane formation

Any CB[n] complex which extends past the rim of the cavity can be considered a pseudorotaxane starting material for reactions leading to the formation of rotaxane, polyrotaxane, and polypseudorotaxanes.[29] CB[6]-based rotaxanes have been prepared in solution by dipolar cycloadditions,[30, 31-33, 34] stoppering with dinitrophenyl groups,[35] amide-bond formation,[36-40] ionic interactions,[41] and coordination of alkylcobaloximes.[42, 43] A variety of polymer backbones and side chains have been threaded with CB[6] beads including polyacrylamides and polystyrenes,[44] poly(hexamethyleneimine),[32, 45] di- and polyviologen,[46, 47] and poly(propyleneimine)dendrimers.[48]

5.6.2. Catalysis of Huisgen's cycloaddition

Mock et al. recognized that, in CB[6], the two portals lined with carbonyl groups can potentially recognize two ammonium ions, thus forming a termolecular complex that orients and compresses those substrates for chemical reaction.[30, 49]

They studied the dipolar cycloaddition between azide **2** and alkyne **1** catalyzed by CB[6] in an elegant example of click chemistry (Figure 7)[48] and found that the CB[6]-catalyzed reaction of **1** and **2** is a rare example of what is known as the Pauling principle of catalysis, which states that "the complementarity between an enzyme and the transition state for its conducted reaction ought to be greater than that between enzyme and the reactants".[30]

Remarkably, CB[6] accelerates this reaction by a factor of 5.5×10^4 compared to the bimolecular reaction and renders it highly regioselective.

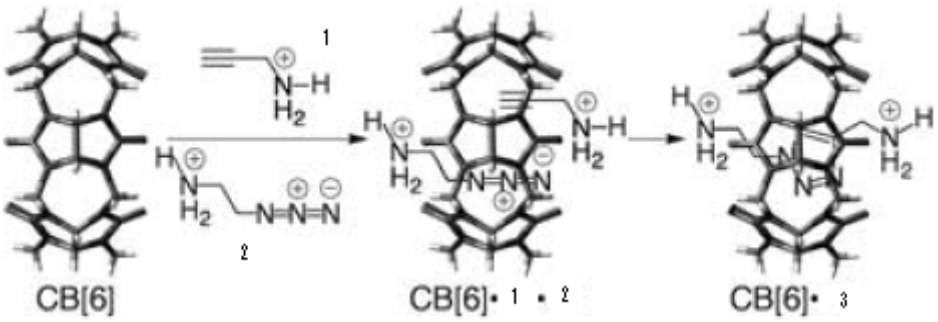

Figure 7. Catalysis of a [3+2] dipolar cycloaddition inside CB[6].

The reaction also displays several enzimelike features, namely:

1) reaching a limit in the reaction rate at high concentrations of **1** and **2**,

2) product release from CB[6]·**3** is rate-limiting,

3) inhibition of the substrate through formation of nonproductive termolecular complex CB[6]·**1** **2**,

4) competitive inhibition by nonreactive substrate analogues.

Steinke's research group used the CB[6]-promoted dipolar cycloadditon of azides and terminal acetylenes for the preparation of catalytically selfthreading rotaxanes,[31, 32] [2]-, [3]-, and [4]-rotaxanes and pseudorotaxanes,[33] as well as oligotriazoles.[50]

5.7. Nitroxide biradicals as thread units in paramagnetic cucurbituril-based rotaxanes[51]

With the polar carbonyl groups lining the rims of the cucurbiturils, the end groups on the threads can prevent dissociation of the rotaxanes into their cyclic bead and linear thread components through steric and/or electrostatic means.

In principle, as already reported with α-cyclodextrin,[52] complexation of a nitroxide biradical can be exploited for the preparation of mechanically-interlocked paramagnetic aggregates, in which the properties of such assemblies can be merged with the use of nitroxides in materials science and their applications in the study of biological processes.[53] While the inclusion of mononitroxide radicals by CB[*n*] has been already reported,[54-58] preparation of nitroxide biradical-based rotaxane with CB[*n*] has never been reported. The behaviour of CB[6], CB[7] and CB[8] was investigated in the presence of nitroxide biradical**s** containing tetramethylpiperidine-*N*-oxyl (TEMPO) units to form host–guest complexes in the forms of paramagnetic pseudorotaxanes and rotaxane.

5.7.1. Is the TEMPO a stopper?

To verify if the TEMPO unit stopper is bulky enough to act as an end-cap group of a rotaxane consisting of CB [*n*], the ESR behaviour of diradical **1a** was investigated (Scheme 1) in the presence of CB[*n*] having different sizes (*n*= 6,.7, 8).

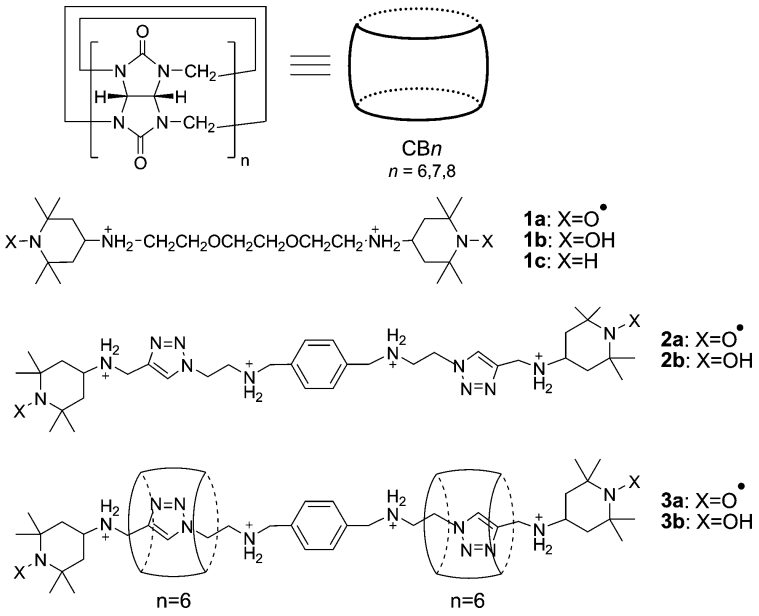

Scheme 1

The ESR spectrum of **1a** recorded in water (a_N = 16.90 G, g = 2.0056) is reported in Figure 8 and is characterized by five lines, due to the exchange interaction between the paramagnetic fragments linked by the polyether chain, as the exchange coupling constant between unpaired electrons, *J*, is greater than the hyperfine splitting, a_N.[59]

This exchange interaction, which leads to the appearance of extra lines in the ESR spectra, is operating through space and depends on the frequency of collisions between the paramagnetic moieties. The complexation of the biradicals with the CB is expected to significantly reduce the probability of collisions of the nitroxide termini giving rise to the disappearance of the exchange peaks in the ESR spectra.[60] Thus, besides following a_N changes as usually done with mononitroxide, with biradicals monitoring of the variation in the intensity of exchange peaks as a function of host concentration could provide extra information on complexation behaviour.

In Figure 8, ESR spectral variations of **1a** observed by adding increasing amount of CB[*n*] are reported. The exchange lines in the spectra of **1a** decrease continuously with increased CB[*n*]

concentration until complete disappearance at around 2 mM with CB[7] and CB[8] and *ca.* 20 mM with CB[6]. This is consistent with the complexation with the CB[*n*] units which reduces the exchange interaction.

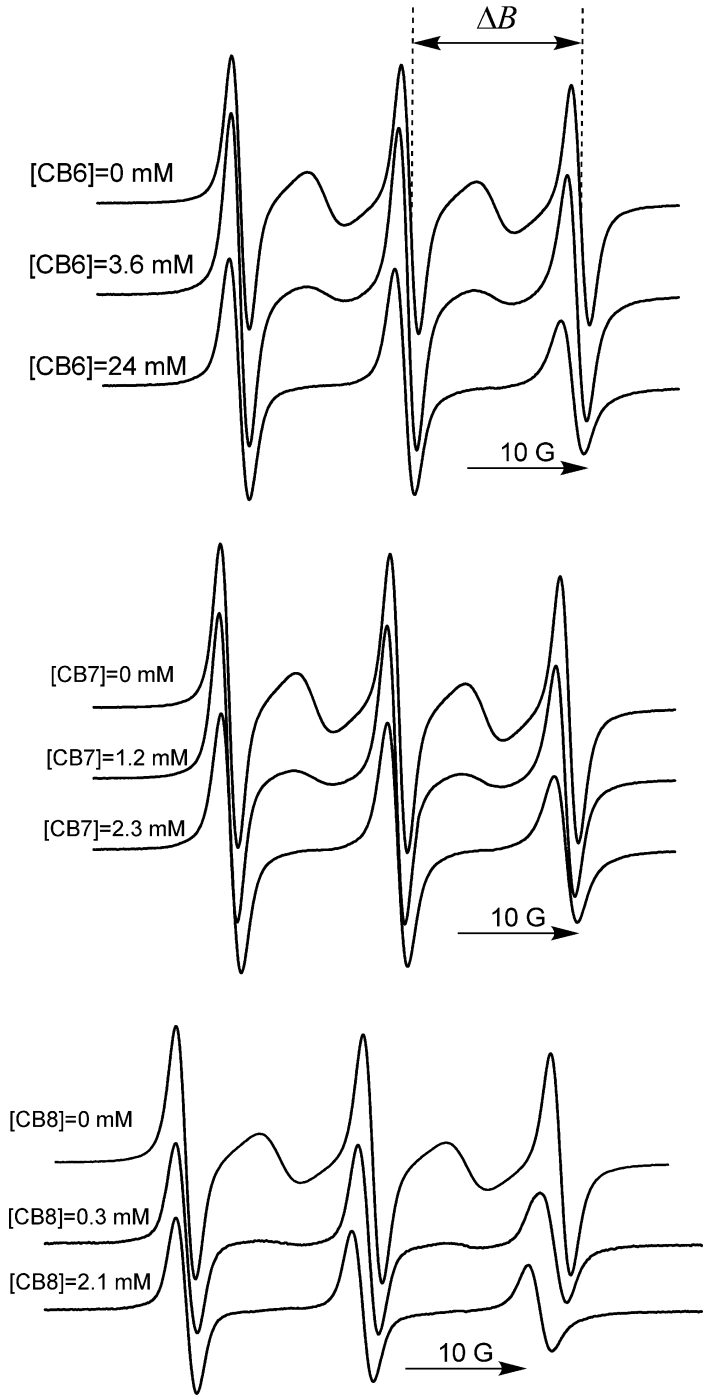

Figure 8. ESR spectra of **1a** (0.26 mM) in the presence of different amount of CB[*n*] in water at 298 K.

The disappearance of the exchange peaks is compatible both with the formation of a pseudorotaxane *i.e.* with a symmetric complex in which the ethylene glycol units are surrounded by the macrocycle and also with the inclusion of one or two nitroxide units (Scheme 2).

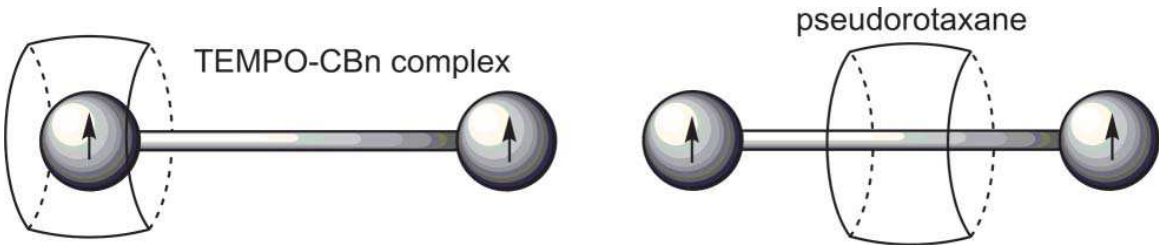

Scheme 2

In order to check if the observed changes in the ESR spectra are caused by formation of a pseudorotaxane or are simply due to a TEMPO–CB[*n*] interaction, the variation of field separation between the ESR central and high field lines (Δ*B*, see Figure 8) as a function of macrocyclic concentration was followed in water at 298 K (Figure 9).[61]

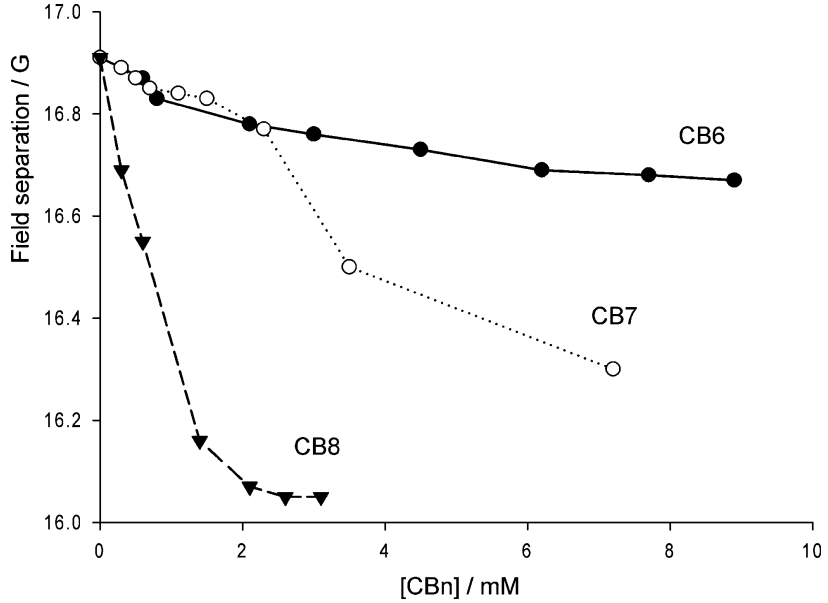

Figure 9. Field separation between the ESR central and high field lines (Δ*B*) for biradical **1a** in the presence of different amount of CB[6], CB[7] and CB[8] in water at 298 K. With CB[6] NaCl 0.1 M was added to the solution.

Different behaviours were observed depending on the size of the macrocycle. The addition of CB[6] to the biradical solution showed no significant changes in Δ*B* value even at high concentration (>20 mM). At these concentrations, however, the ESR spectra of the biradicals showed only three lines. This behaviour is consistent with a weak complexation of **1a** in which the nitroxide moiety is not included inside the hydrophobic cavity of CB[6], but is instead dissolved in the bulk water with the nitroxide function located among the carbonyl groups of the macrocylcle.

With CB[7], the exchange coupling is completely suppressed at 2.0 mM of macrocycle. At this concentration however, the field separation is still very close to the value measured in water (ΔΔ*B*= -0.15 G). Both observations strongly support the formation of a pseudorotaxane (see Scheme 2) in

which the macrocycle is located on the center of the linear chain, thus forcing the biradical to adopt an elongated conformation having TEMPO units exposed to the bulk water and suppressed spin exchange (J = 0). The formation of a strong complex between nitroxide **1a** and CB[7] is also expected on the basis of the strong interaction between the ammonium site and the carbonyl oxygens of CB[7], as already found with protonated amines.[62] This was confirmed by following the ESR spectral variations observed by changing the pH from 7 to 13.

Around pH 7, the ESR spectrum of a solution containing CB[7] (5.5 mM) and biradical **1a** (0.4 mM) showed the three line spectrum due to the paramagnetic pseudorotaxane. The increase of solution basicity to pH = 12 with NaOH reverted the ESR spectrum to the original five lines signals. This observation strongly suggests that the deprotonated diradical is released from the pseudorotaxane to the bulk water. The process is reversible: addition of HCl to give back pH 7 results in the formation of three lines spectrum and of the pseudorotaxane.

The thermodynamic stability of the pseudorotaxane was checked by measuring the equilibrium constant K for the association between the diamagnetic analogue (**1c**) of the diradica and CB7 by ^{1}H NMR. The signals of the free and bound guests protons are simultaneously observed, revealing that the rate of exchange between these species is slow in the NMR time scale. Integration of the separate signals as a function of CB[7] concentration provides the corresponding association equilibrium constant (K) as 1879 ± 256 M^{-1}.

This value is one order of magnitude smaller than the K value measured for the inclusion of TEMPO monoradical by the same host,[54] indicating that the presence of substituents on the piperidine ring results in a significant decrease in the stability of the complex.

Only in the presence of a large excess of CB[7] (>3 mM), complexes with higher CB[7]/**1a** stoichiometry, in which TEMPO units are included inside hydrophobic cavity of CB[7], are formed, as indicated by the significant decrease of ΔB in the corresponding ESR spectra.

Finally, with CB[8], a strong decrease of both field separation and intensity of exchange lines was observed when increasing macrocyle concentration in water solution. This behaviour indicated that complexation by CB[8] occurs preferentially in the immediacy of TEMPO radical units rather than on the ethylene glycol units.

It was previously shown[54-55] that, with CB[8], the larger size of the cavity and the presence of a strong interaction between the ammonium cation and the carbonyl groups should favour a geometry in which the longer axis of the nitroxide is parallel to the short principal axis of the macrocyle. This is not possible in the presence of the smaller macrocycle, CB[7], where TEMPO radical is forced to be inserted with the NO group lying on the plane passing through the equatorial carbon–carbon bonds of the host and with the geminal methyl groups pointing toward the carbonyl portals.

These observation led to the conclusion that TEMPO unit cannot pass through the CB[6] cavity, while with the larger member of the cucurbituril family the reversible formation of a pseudorotaxane or a complex between the tetramethylpiperidine ring and the cucurbituril is possible.

5.7.2. A CB[6]-based paramagnetic [3]-rotaxane

Once established that TEMPO could act as a stopper, a CB[6]-based rotaxane having the 2,2,6,6-tetramethylpiperidine-*N*-oxyl ring as the end-cap group was constructed. The synthesis of the rotaxane was achieved using CB[6] as catalyst in the 1,3-dipolar cycloaddition between suitably functionalized alkyne and azide groups to give 1,4-disubstituted triazole (see Section 5.6.2.).[63]
By this approach, the *N*-propargyl derivative of 4-amino-TEMPO **4** (0.18 mmol) and diazide **5** (0.09 mmol) were added to CB[6] (0.18 mmol) dissolved in aqueous HCl 6 M and the resulting solution was stirred at 60 °C for 24 h (Scheme 3). After reduced pressure solvent removal, the bis-*N*-hydroxy derivative of paramagnetic [3]rotaxane (**3b**) was obtained as a light yellow solid in 75% yield. The rotaxane diradical **3a** was recovered by treating **3b** in water solution with an excess of Ag_2O.[64]

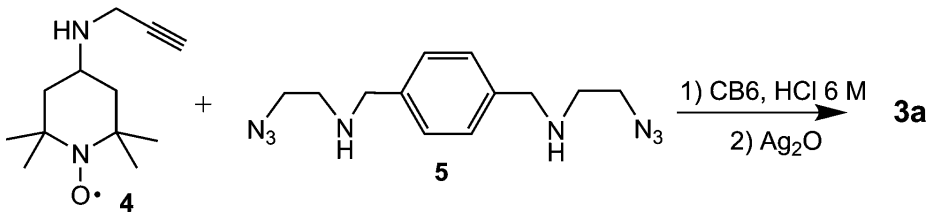

Scheme 3 Structures of the alkyne **4** and of the azide **5** used in the synthesis of the [3]rotaxane **3a**.

The formation of the interlocked molecule is evidenced when comparing ^{1}H NMR spectral data of the thread recorded in D_2O, with those of rotaxane.[65]
In the proton spectrum of the [3]rotaxane **3b** (see Figure 10, line b) the presence of the macrocycle wrapping the diradical thread is detected by significant complexation-induced chemical shifts (CIS) of the dumbbell with respect to the resonances of the free thread **2b** (Figure 10, line a). The sign of CIS ($\Delta\delta = \delta$bound - δfree) gives a rough indication of the position of the thread within CB, negative
$\Delta\delta$ revealing the part of the thread located inside the macrocycle, and the contrary being for positive values of CISs.[66] According with these assumptions, analysis of the CIS values reported in Figure 10 shows that the triazole moieties of the thread are positioned within the two CB[6] macrocycles,

as the consistent upfield shift (-1.64 ppm) displayed by the aromatic proton of the heterocycle is indicative of the strong involvement of the triazole proton in complexation.

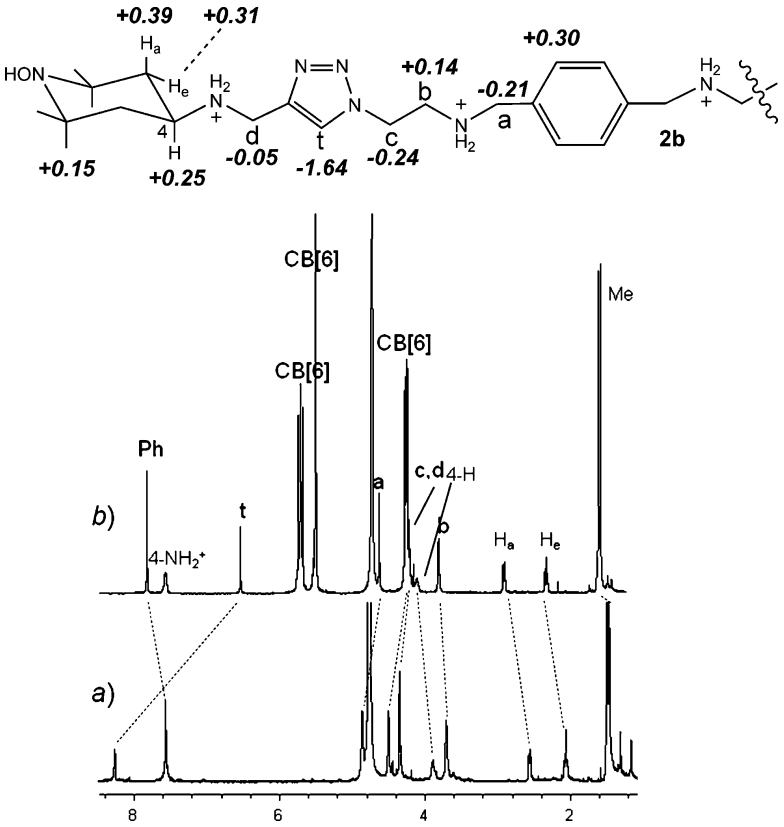

Figure 10. ^{1}H NMRspectrum in D_2O of *a*) thread **2b** (1 mM); *b*) [3]rotaxane **3b** (1 mM) with complexation induced chemical shifts ($\Delta\delta$ in ppm).

Considerable negative CISs are detected also for the adjacent protons labeled with **c** and **d** letters, while phenyl and piperidine ring protons exhibit positive shift, confirming their position outside the cavity near the carbonyl portals of the macrocycle. Unexpectedly, spectrum of **3b** shows an additional peak at 7.6 ppm, which, on the basis of ROESY experiments, was assigned to the ammonium protons linked to the 4-position of *N*-hydroxy TEMPO. The presence of such slow-exchangeable protons in deuterated water strongly supports that the ammonium protons linked to the 4-position of *N*-hydroxy TEMPO are hydrogen-bonded to the CB carbonyl-lined portal in the [3]rotaxane.[67]

The ESR spectrum of rotaxane **3a** in water (a_N = 16.75 G, g = 2.0057, see Figure 11b) consists of three lines as expected for a nitroxide biradical in the extended conformation in which the TEMPO fragments behave as two single nitroxide radicals. This spectrum is clearly different form that obtained under the same experimental condition with the free thread **2a** (a_N = 16.80 G, g = 2.0057), which is characterized by broaden exchange peaks, due to the exchange interaction between the

paramagnetic fragments (see Figure 11 a). The high field ESR line of **3a** is characterized by a lower height respect to that obtained with **2a**, this being due to the slower motion in solution of the rotaxane biradical, resulting in incomplete averaging of the anisotropic components of the hyperfine and *g*-tensors.

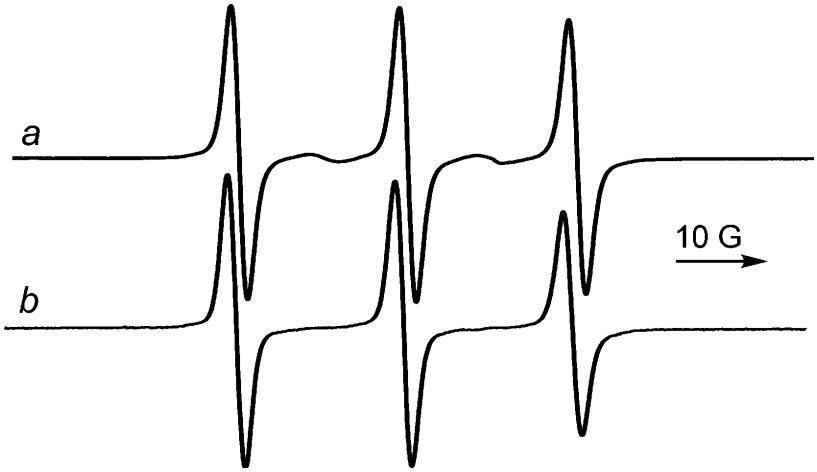

Figure 11. ESR spectra of free thread **2a** (a) and rotaxane **3a** (b) in water at 340 K.

This is the first example of a paramagnetic rotaxane containing CB[6] as wheel, in which it is possible to reversibly trigger spin exchange by simply changing the pH of the solution in the presence of nitroxide biradical **1a** and the larger CB[7] derivative.

However the intrinsic rigid structure (Figure 12) doesn't allow any movement of the rings, which remains over the triazole units.

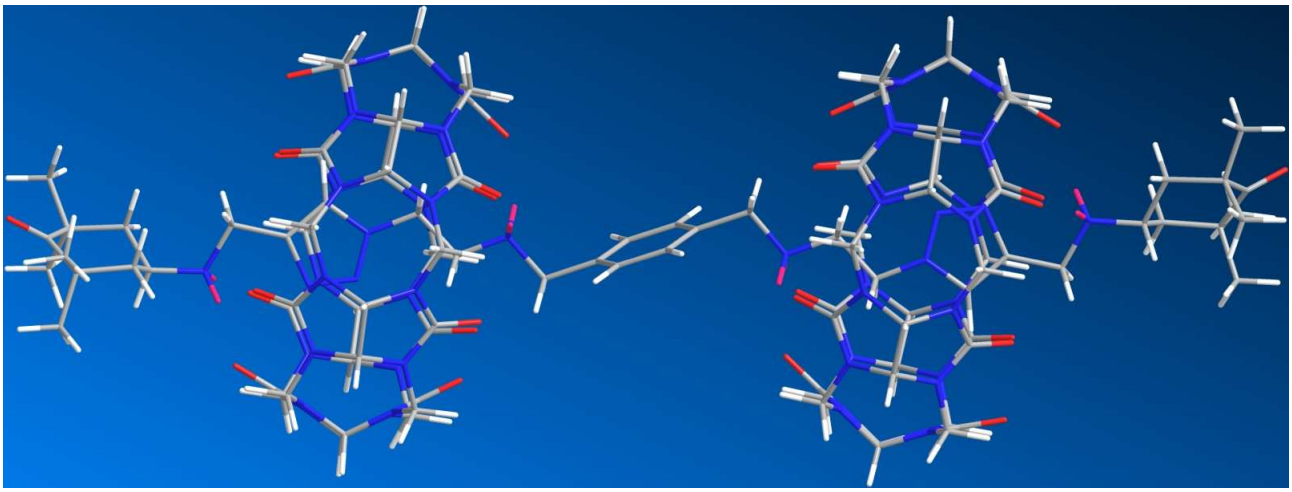

Figure 12. One of the possible 3D model of [3]-rotaxane **3a** obtained with *Macromodel (*AMBER Force Field*).*

PELDOR (pulsed electron double resonance) is actually an EPR technique that can provide distance measurement between spin labels. Because of the nature of the measurement and the relaxation properties of nitroxide spin labels, the distances available to this technique is described as being limited to between approximately 20 and 80 Å. In the case of biological molecules rather than synthetic model compounds, the upper distance limit for the acquisition of high quality experimental data, on a commercially available machine, has so far been about 55 Å (a reasonable definition of quality being that the data should have a large signal-to-noise ratio, show good depth of oscillation, and be acquired over such a time that at least one full oscillation is recorded).

Because of the presence of the two terminal nitroxide units in **3a**, it was possible to obtain for the first time, the exact distance between paramagnetic centers using PELDOR technique. The PELDOR trace (recorded by R. Pievo and M. Bennati at the Max Planck Institute for Biophysical Chemistry of Gottingen) is in agreement with a distance of 30.6 Å between the two terminal units; this makes suppose that the adopted geometry is the one in which the aromatic methylene groups point in the same direction, allowing a smaller distance between the two nitroxide groups.

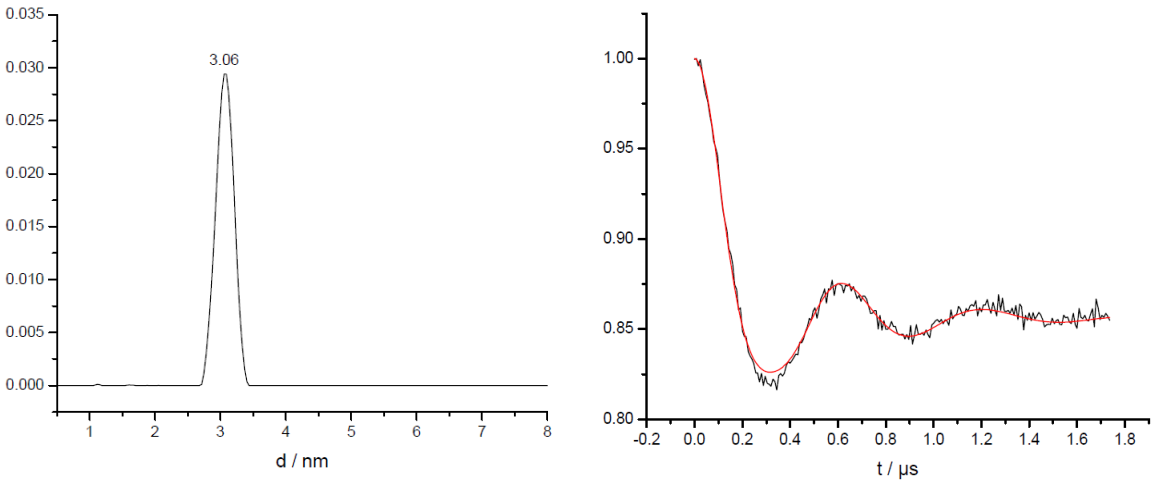

Figure 13. Left: PELDOR data for rotaxane **3a**; right: distance distribution derived by Tikhonov regularization.

The presence of persistent radical centers in pseudorotaxanes and rotaxanes not only allows for the first time to determine the exact distance between the stopper units but should also be considered as an attractive functionality that can be exploited to modulate the behaviour of molecular devices. Work in this field are actually in progress in the laboratory.

5.8. Towards a pH-driven reversibile molecular switch

Exploiting cucurbit[6]uril-catalyzed 1,3-dipolar cycloaddition between properly designed monomers and aiming at increasing the complexity of [3]-rotaxane **3a** previously obtained, a [3]-rotaxane containing a long aliphatic spacer was synthesized (**7a**).

The *N*-propargyl derivative of 4-amino-TEMPO **4** (0.26 mmol) and diazide **5** (0.13 mmol) were added to CB[6] (0.26 mmol) dissolved in aqueous HCl 6 M and the resulting solution was stirred at 60 °C for 24 h (Scheme 4). After reduced pressure solvent removal, the bis-*N*-hydroxy derivative of paramagnetic [3]-rotaxane (**7b**) was obtained as a light yellow solid in 80% yield. The rotaxane diradical **7a** was recovered by treating **7b** in water solution with an excess of Ag_2O.[64]

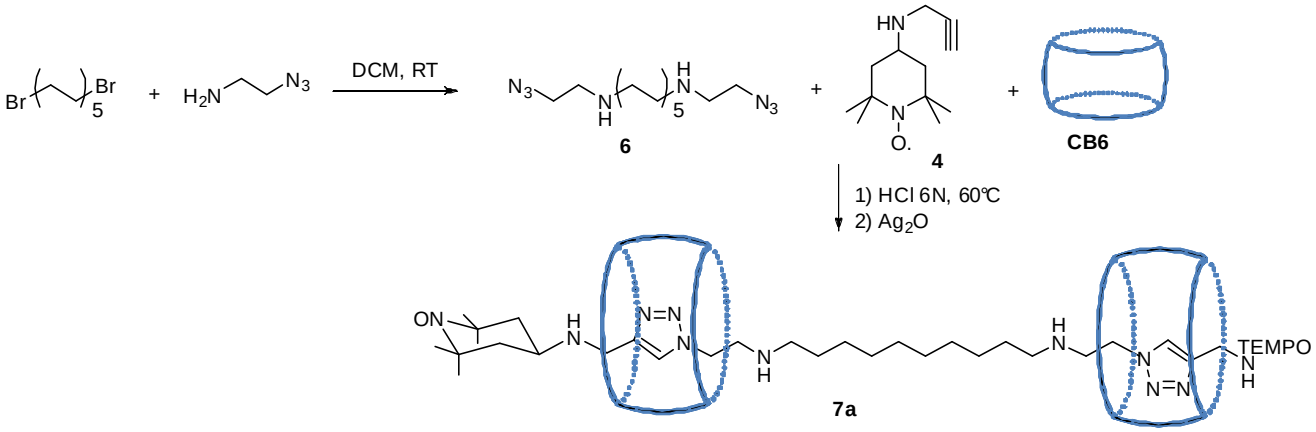

Scheme 4. Structures of the alkyne **4** and of the azide **6** used in the synthesis of the [3]rotaxane **7a**.

The formation of the rotaxane was evidenced by recording the H-NMR spectrum of **7b**. Actually, the NMR spectrum shows a resonance at 6.5 ppm which is diagnostic for the proton of a threaded triazole ring. In addition the signal of the terminal proton of alkyne at 2.9 ppm is not observed in the ^{1}H NMR spectrum of **7b**; this further indicates the formation of a triazole ring (Figure 14).

The ESR spectrum of rotaxane **7a** in water (see Figure 15b) is similar to the one of rotaxane **3a**, consisting of three lines as expected for a nitroxide biradical in the extended conformation in which the TEMPO fragments behave as two single nitroxide radicals. On the contrary, in the free thread **8a**, there is the appearance of broaden exchange peaks, due to the exchange interaction between the paramagnetic fragments (see Figure 15 a).

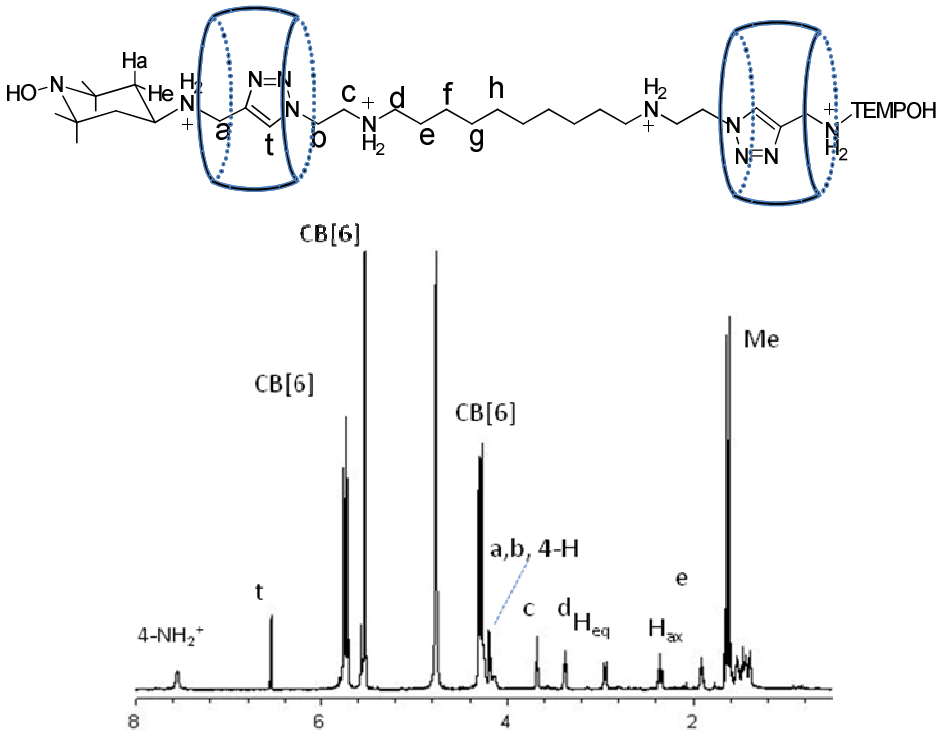

Figure 14. ^{1}H NMR spectrum in D_2O of [3]rotaxane **7b** (1 mM)

a)

b)

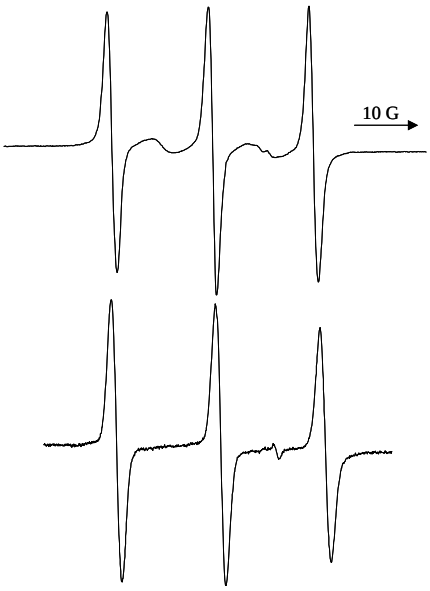

Figure 15. ESR spectra of free thread **8a** (a) and rotaxane **7a** (b) in water at 340 K.

In the axle there are two recognition sites, the decyl alkyl chain and two diammonium triazoles. The preferred sites for CB[6] is the triazole. However, NMR spectra recorded at different pH showed that it is possible to move reversibly the macrocyclic ring. At low pH, that is the starting state, as the reaction is carried out in very acidic medium, CB[6] rings have a greater affinity for the diammino triazole unit than for the diamino decamethylene site; the interaction between rings and

the diamino triazole unit is mainly ion-dipole interaction between carbonyl groups of CB[6]'s portals and the $–NH_2^+$ ions adjacent to the decyl spacer and to the stopper. However, since the cavity of CB[6] is hydrophobic, it is possible to force CB[6] to move over the hydrophobic part of the molecule, the decamethylene spacer, if the ion-dipole interaction is disrupted by a base. The resulting complex is stabilized by the hydrophobic effect and by H-bonding between the –NH adjacent to the decyl spacer and the oxygen of the carbonyl groups.

As mentioned before, this was confirmed by NMR spectra: the addition of NaOD directly in the NMR tube caused the decreasing of the indicative signal at 6.5 ppm due to the encapsulated triazole proton and the parallel appearance of a peak at around 8 ppm due to the unencapsulated triazole proton, stating that one of the macrocycles has enough space to move upon the axle. (Figure 16)

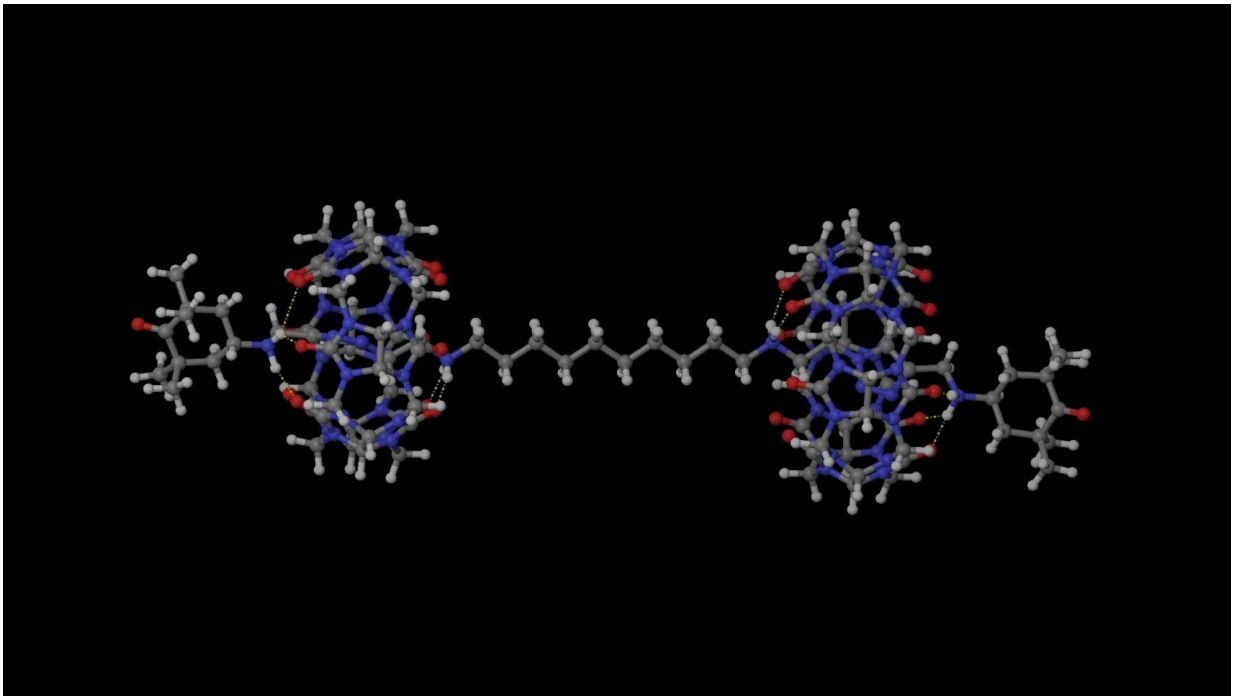

Figure 16. One of the hypothetical 3D model of [3]rotaxane showing that the decamethylene spacer offers the possibility for one ring to move upon the axle.

The following addition of acid caused the gradual disappearance of signal at 8 ppm and appearance of the peak at 6.5 ppm, demonstrating that this rotaxane behaves as a pH-driven reversible molecular switch and exhibits conformational changes caused by the movement of rings under base, acid and heat stimuli from one location to another. Further studies are in progress to fully characterised this pH-driven paramagnetic switch.

5.9. Experimental section

General

ESR spectra has been recorded by using the following instrument settings: microwave power 0.79 mW, modulation amplitude 0.04 mT, modulation frequency 100 kHz, scan time 180 s, 2 K data points.

^{1}H and 2D NMR spectra were recorded at 298 K on a Varian Inova spectrometer operating at 600 MHz in D_2O solutions using the solvent peak as an internal standard (4.76 ppm). ^{13}C NMR spectra were recorded on a Varian Mercury operating at 100 MHz in D_2O solutions using DSS (3 (trimethylsilyl)-1-propanesulfonic acid, sodium salt) as an external standard. Chemical shifts are reported in parts permillion (δ scale). ROESY data were collected using a 90° pulse width of 6.7 μs and a spectral width of 6000 Hz in each dimension, respectively. The data were recorded in the phase sensitive mode using a CW spin-lock field of 2 KHz, without spinning the sample. Acquisitions were recorded at mixing times 300 ms. Other instrumental settings were: 64 increments of 2 K data points, 8 scans per *t*, 1, 1.5 s delay time for each scan.

ESI-MS spectra were recorded with Micromass ZMD spectrometer by using the following instrumental settings: positive ions; desolvation gas (N_2) 230 L h^{-1}; cone gas (skimmer): 50 L h^{-1}; desolvation temp. 120° C; capillary voltage: 3.2 kV; cone voltage: 40 and 100 V; hexapole extractor: 3 V.

UV-Vis spectra were taken on a Jasco V-550 spectrometer.

All reagents were commercially available and were used without further purification. Compound **4** was synthesized according to literature procedure.[68]

Synthesis of *N,N'*-(1,4-phenylenebis(methylene))bis(2-azidoethanamine) (5)

A solution of 1,4-bis(bromomethyl)benzene (0.38 g, 1.45 mmol) in CH_2Cl_2 (10 ml) was added dropwise to freshly prepared azidoethylamine[69] (1.25 g, 14.5 mmol) at room temperature. The resulting solution was stirred at room temperature for 24 h. A white precipitate was obtained which was filtered and dissolved in HCl 2N. The solvent was removed under reduced pressure and the solid residue was recrystallised from ethanol/diethyl ether 2 : 1, obtaining the product (0.238 g, 60%) as white crystals.

M. p.: > 300° C (decomp).

Elemental analysis for $C_{12}H_{20}N_8$ Calc.: C, 52.16; H, 7.29; N, 40.55; Found: C, 52.21; H, 7.39; N, 40.40. ^{1}H NMR (600 MHz, D_2O): δ 3.26 (t, 4H, J = 6.0 Hz, CH_2), 3.75 (t, 4H, J = 6.0 Hz, CH_2), 4.30 (s, 4H, CH_2), 7.55 (s, 4H, Ph). ^{13}C NMR (100 MHz, D_2O, DSS): δ 48.48, 49.43, 53.15, 133.32, 134.58. Positive ESI-MS: m/z 274.9 $(M - H)^{+}$.

Synthesis of diradical (2a)

$CuSO_4$ (0.01 g, 0.04 mmol) and ascorbic acid (0.014 g, 0.08 mmol) were added to a solution of azide 5 (0.027 g, 0.1 mmol) and alkyne 4 (0.045 g, 0.21 mmol) in water (4 ml). The resulting suspension was stirred at room temperature overnight. The product was purified by gel filtration over a Sephadex G-15 column to yield a light orange solid (0.075 g, 50%). Positive ESI-MS: m/z 715.3 $(M+Na)^+$.

Elemental analysis for $C_{36}H_{60}N_{12}O_2$ Calc.: C, 62.31; H, 8.86; N, 24.22; Found: C, 62.50; H, 8.65; N, 23.94. UV-Vis (H_2O): λ 376 nm. EPR: (a_N = 16.85 G, g = 2.0057). ^{1}H NMR (600 MHz, D_2O): δ 3.30–3.80 (m, 4H, b), 3.80–4.50 (m, 4-H, c, d), 7.44 (bs, 4H, Ph), 8.00–8.60 (m, 2H, t).

The proton spectrum of 2b was obtained by $Na_2S_2O_4$ reduction of the NMR sample containing 2a to afford the corresponding bis-N-hydroxy amine.

^{1}H NMR (600 MHz, D_2O): δ 1.47 (s, 12H, CH_3), 1.50 (s, 12H, CH_3), 2.07 (t, 4H, J = 13.2 Hz, H_a), 2.56 (d, 4H, J = 13.2 Hz, H_e), 3.71 (bs, 4H, b), 3.89 (m, 2H, 4-H), 4.35 (s, 4H, d), 4.50 (bs, 4H, c), 4.87 (s, 4H, a), 7.57 (s, 4H, Ph), 8.27 (s, 2H, t).

Synthesis of [3]Rotaxane (3b)

CB6 (0.183 g, 0.18 mmol) was dissolved in HCl 6 M (3 ml) and the resulting solution was stirred for 30 min. Alkyne 4 (0.038 g, 0.18 mmol) and subsequently azide 5 (0.025 g, 0.09 mmol) were added under vigorous stirring at room temperature. The resulting solution was stirred at 60°C for 24 h. The solvent was removed under reduced pressure to obtain a light yellow solid (0.181 g, 75%). M. p.: > 300◦ C (decomp). Uv-Vis (H_2O): λ 312 nm.

^{1}H NMR (600 MHz, D_2O): δ 1.62 (s, 12H, CH_3), 1.65 (s, 12H, CH_3), 2.37 (t, 4H, J = 13.2 Hz, H_a), 2.95 (d, 4H, J = 13.2 Hz, H_e), 3.85 (t, 4H, J = 6.7 Hz, b), 4.15 (m, 2H, 4-H), 4.26 (t, 4H, J = 6.7 Hz, c), 4.30 (s, 4H, d overlapped with CB[6]), 4.29 (d, 12H, J= 15.6 Hz, CB[6]), 4.30 (d, 12H, J = 15.6 Hz, CB[6]), 4.66 (s, 4H, a), 5.54 (s, 24H, CB[6]), 5.73 (d, 12H, J = 15.6 Hz, CB[6]), 5.76 (d, 12H, *J* = 15.6 Hz, CB[6]), 6.57 (s, 1H, t), 7.61 (bs, 4H, NH_2^+), 7.85 (s, 4H, Ph). ^{13}C NMR (100 MHz, D_2O, DSS): δ 21.94, 29.94, 41.50, 42.96, 48.12, 48.45, 52.16, 53.67, 53.96, 54.17, 70.62, 72.97, 122.88, 133.06, 135.62, 141.21, 158.97, 159.43. Positive ESI-MS: *m/z* 672.6 $(M)^{4+}$, 897.2 $(M)^{3+}$.

The rotaxane diradical **3a** was recovered by treating **3b** in water solution with an excess of Ag_2O.

Synthesis of *N,N'*-bis(2-azido-ethyl)decane-1,10-diamine dihydrochloride (6)

A solution of 1,10-dibromodecane (0.42 g, 1.39 mmol) in CH_2Cl_2 (2.5 ml) was added to freshly prepared azidoethylamine[69] (1.2 g, 13.9 mmol) at room temperature. The resulting solution was stirred at room temperature for 48 h. 1M aqueous NaOH (2.7 ml) was added to reaction mixture and the mixture was stirred for 1 h to room temperature. The organic layer was separated by extraction and washed with saturated NaCl. After drying the organic layer over Na_2SO_4, the solvent was removed under reduced pressure. The light yellow liquide reisdue was dissolved in diethylether (2.7 ml) and the solution was cooled to 0°C in ani ce-bath. 0.1 M HCl solution in diethyl ether (2.7 ml) was added dropwise. The resulting mixture was stirred at room temperature for 4 h. The solvent was removed under reduced pressure and the residue was recrystallized from ethanol to obtain a white solid (0.302 g; 70 %).

^{1}H NMR (600 MHz, D_2O): δ 1.29 (m, 12H, f, g, h), 1.67 (m, 4H, e), 3.07 (t, 4H, J= 7.8 Hz, d), 3.21 (t, 4H, J= 5.4 Hz, b), 3.74 (t, 4H, J= 5.4 Hz, c).

Positive ESI-MS: *m/z* 311 $(M+H)^+$

Synthesis of [3]Rotaxane (7b)

CB6 (0.259 g, 0.26 mmol) was dissolved in HCl 6 M (6 ml) and the resulting solution was stirred for 30 min. Alkyne 4 (0.054 g, 0.26 mmol) and subsequently azide 6 (0.040 g, 0.13 mmol) were added under vigorous stirring at room temperature. The resulting solution was stirred at 60°C for 24

h. The solvent was removed under reduced pressure to obtain a light yellow solid (0.283 g, 80%). M. p.: > 300◦ C (decomp).
^{1}H NMR (600 MHz, D_2O): δ 1.39–1.53 (m, 12H, f, g, h), 1.62 (s, 12H, CH_3), 1.65 (s, 12H, CH_3), 1.91 (quint, 4H, J= 7.8 Hz, e), 2.36 (t, 4H, J= 13.2 Hz, H_{ax}), 2.95 (d, 4H, J= 14.4 Hz, H_{eq}), 3.38 (t, 4H, J= 7.2 Hz, d), 3.68 (t, 4H, J= 6Hz, c), 4.13 (m, 2H, 4-H), 4.18-4.20 (m, 4H, b), 4.27 (s, 4H, a overlapped with CB[6]), 4.29 (d, 12H, J= 15.6 Hz, CB[6]), 4.30 (d, 12H, J = 15.6 Hz, CB[6]), 5.53 (s, 24H, CB[6]), 5.73 (d, 12H, J = 15.6 Hz, CB[6]), 5.76 (d, 12H, *J* = 15.6 Hz, CB[6]), 6.55 (s, 1H, t), 7.56 (bs, 4H, NH_2^+).
The rotaxane diradical **7a** was recovered by treating **7b** in water solution with an excess of Ag_2O.

References

1. Lagona, J.; Mukhopadhyay, P.; Chakrabarti, S.; Isaacs, L. *Angew. Chem. Int. Ed.*, **2005**, *44*, 4844-4870.
2. Behrend, R.; Meyer, E.; Rusche, F. *Justus Liebigs Ann. Chem*. **1905**, *339*, 1–37.
3. Freeman, W. A.; Mock, W. L.; Shih, N.-Y. *J. Am. Chem. Soc.* **1981**, *103*, 7367–7368.
4. Kim, J.; Jung, I.-S.; Kim, S.-Y.; Lee, E.; Kang, J.-K.; Sakamoto, S.; Yamaguchi, K.; Kim, K. *J. Am. Chem. Soc.* **2000**, *122*, 540 – 541.
5. Day, A. I.; Arnold, P.; Blanch, R. J.; Snushall, B.; *J. Org. Chem.* **2001**, *66*, 8094–8100.
6. Day, A. I.; Blanch, R. J.; Arnold, A. P.; Lorenzo, S.; Lewis, G. R.; Dance, I. *Angew. Chem*. **2002**, *114*, 285–287; *Angew . Chem. Int. Ed.* **2002**, *41*, 275–277.
7. Mock, W. L. *Top. Curr. Chem*. **1995**, *175*, 1 – 24.
8. Hoffmann, R.; Knoche, W.; Fenn, C.; Buschmann, H.-J. *J. Chem. Soc. Faraday Trans*. **1994**, *90*, 1507 – 1511.
9..Lee, J. W.; Samal, S.; Selvapalam, N.; Kim, H.-J.; Kim, K. *Acc. Chem. Res*. **2003**, *36*, 621 – 630.
10. Kim, K. *Chem. Soc. Rev*. **2002**, *31*, 96 – 107.
11. Marquez, C.; Huang, F.; Nau, W. M.; *IEEE Trans. Nanobioscience* **2004**, *3*, 39 – 45.
12. Thiocarbonyl analogues of cucurbiturils have been discussed in the patent literature. For DFT calculations, see: Pichierri, F. *Chem. Phys. Lett*. **2004**, *390*, 214 – 219.
13. Marquez, C.; Hudgins, R. R.; Nau, W. M. *J. Am. Chem. Soc.* **2004**, *126*, 5806 – 5816.
14. Buschmann, H.-J. Jansen, K.; Meschke, C.; Schollmeyer, E.; *J. Solution Chem*. **1998**, *27*, 135 – 140.
15. Zhang, G.-L.; Xu, Z.-Q.; Xue, S.-F.; Zhu, Q.-J.; Tao, Z.; *Wuji Huaxue Xuebao* **2003**, *19*, 655 – 659.
16. Jansen, K.; Buschmann, H.-J.;.Wego, A.; Dopp, D.; Mayer, C.; Drexler, H. J.; Holdt, H. J.; Schollmeyer, E.; *J. Inclusion Phenom. Macrocyclic Chem*. **2001**, *39*, 357 – 363.

17. Honig, B.; Nicholls, A. *Science* **1995**, *268*, 1144 – 1149.
18. Houk, K. N.; Leach, G. L.; Kim, S. P.; Zhang, X. *Angew. Chem. Int. Ed.*, **2003**, *115*, 5020-5046; *Angew. Chem. Int. Ed.* **2003**, *42*, 4872-4897.
19. Buschmann, H.-J.; Jansen, K.; Schollmeyer, E. *Thermochim. Acta* **2000**, *346*, 33-36.
20. Fujiwara, H.; Arakawa, H.; Murata, S.; Sasaki, Y. *Bull. Chem. Soc. Jpn.* **1987**, *60*, 3891-3894.
21. Izatt, R. M.; Terry, R. E.; Haymore, B. L.; Hansen, L.D.; Dalley, N. K.; Avondet, A. G.; Christensen, J. J. *J. Am. Chem. Soc.* **1976**, *98*, 7620-7626.
22. Buschmann, H.-J.; Cleve, E.; Schollmeyer, E. *Inorg. Chim. Acta* **1992**, *193*, 93-97.
23. Buschmann, H.-J.; Cleve, E.; Jansen, K.; Schollmeyer, E. *Anal. Chim. Acta* **2001**, *437*, 157-163.
24. Buschmann, H.-J.; Cleve, E.; Jansen, K.; Wego, A.; Schollmeyer, E. *J. Inclusion Phenom. Macrocyclic Chem.* **2001**, *40*, 117-120.
25. Buschmann, H.-J.; Jansen, K.; Schollmeyer, E. *Inorg. Chem. Commun*. **2003**, *6*, 531–534.
26. Zhang, X. X.; Krakowiak, K. E.; Xue, G.; Bradshaw, J. S.; Izatt, R. Z. *Ind. Eng. Chem. Res.* **2000**, *39*, 3516–3520.
27. Mock, W. L.; Shih, N.-Y. *J. Org. Chem*. **1986**, *51*, 4440–4446.
28. Virovets, A. V.; Blatov, V. A.; Shevchenko, A. P. *Acta Crystallogr. B* **2004**, *60*, 350–357.
29. Xu, Z.-Q.; Yao, X.-Q.; Xue, S.-F.; Zhu, Q.-J.; Tao, Z.; Zhang, J.-X.; Wei, Z.-B.; Long, L.-S. *Huaxue Xuebao* **2004**, *51*, 1927 – 1934.
30. Mock, W. L.; Irra, T. A.; Wepsiec, J. P.; Adhya, M. *J. Org. Chem*. **1989**, *54*, 5302 – 5308.
31. Tuncel, D.; Steinke, J. H. G. *Chem. Commun*. **1999**, 1509 – 1510.
32. Tuncel, D.; Steinke, J. H. G, *Macromolecules* **2004**, *37*, 288 – 302.
33. Tuncel, D.; Steinke, J. H. G, *Chem. Commun*. **2002**, 496 – 497.
34. Tuncel, D.; Steinke, J. H. G.; *Polym. Prepr*. **1999**, *40*, 585 – 586.
35. Jeon, Y.-M.; Whang, D.; Kim, J.; Kim, K. *Chem. Lett*. **1996**, 503–504.
36. Meschke, C.; Buschmann, H.-J.; Schollmeyer, E. *Macromol. Rapid Commun*. **1998**, *19*, 59 – 63.
37. Meschke, C.; Buschmann, H.-J.; Schollmeyer, E. *Polymer* **1998**, *40*, 945 – 949.
38. Buschmann, H.-J.; Cleve, E.; Mutihac, L.; Schollmeyer, E. *Microchem. J*. **2000**, *64*, 99 – 103.
39. Buschmann, H.-J.; Jansen, K.; Schollmeyer, E. *Acta Chim. Slov*. **1999**, *46*, 405 – 411.
40. Buschmann, H.-J.; Wego, A.; Schollmeyer, E.; Dopp, D. *Supramol. Chem*. **2000**, *11*, 225 – 231.
41. Liu, S.-M.; Wu, X.; Huang, Z.; Yao, J.; Liang, F.; Wu, C.-T. *J. Inclusion Phenom. Macrocyclic Chem.* **2004**, *50*, 203 – 207.
42. He, X.; Li, G.; Chen, H. *Inorg. Chem. Commun*. **2002**, *5*, 633–636.
43. He, X.-Y.; Li, J.; Gao, Y.; Chen, H.-L. *Wuji Huaxue Xuebao* **2003**, *19*, 153 – 158.
44. Tan, Y.; Choi, S.; Lee, J. W.; Ko, Y. H.; Kim, K. *Macromolecules* **2002**, *35*, 7161 – 7165.

45. Tuncel, D.; Steinke, J. H. G. *Chem. Commun*. **2001**, 253 – 254.

46. Buschmann, H.-J.; Meschke, C.; Schollmeyer, E. *An. Quim. Int. Ed*. **1998**, *94*, 241 – 243.

47. Choi, S.; Lee, J. W.; Ko, Y. H.; Kim, K. *Macromolecules* **2002**, *35*, 3526 – 3531.

48. Lee, J. W.; Ko, Y. H.; Park, S.-H.; Yamaguchi, K.; Kim, K. *Angew. Chem.* **2001**, *113*, 768 – 771; *Angew. Chem. Int. Ed*. **2001**, *40*, 746 – 749.

49. Mock, W. L.; Irra, T. A.; Wepsiec, J. P.; Manimaran, T. L. *J. Org. Chem*. **1983**, *48*, 3619 – 3620.

50. Krasia, T. C.; Steinke, J. H. G. *Chem. Commun*. **2002**, 22 – 23.

51. Mileo, E.;Casati, C.; Franchi, P.; Mezzina, E.; Lucarini, M. *Org. Biomol. Chem.*, **2011**, DOI: 10.1039/c0ob01160f.

52. Mezzina, E.; Fanì, M.; Ferroni, F.; Franchi, P.; Menna, M.; Lucarini, M. *J. Org. Chem.*, **2006**, *71*, 3773.

53. *'Nitroxides: Applications in Chemistry, Biomedicine, and Materials Science'*, ed. Likhtenshtein, G.; Yamauchi, J.; Nakatsuji, S.; Smirnov, A. I.; Tamura, R. Wiley-VCH, Weinheim, **2008**.

54. Mezzina, E.; Cruciani, F.; Pedulli, G. F.; Lucarini, M. *Chem.–Eur. J.*, **2007**, *13*, 7223.

55. Mileo, E.; Mezzina, E.; Grepioni, F.; Pedulli, G. F.; Lucarini, M. *Chem.–Eur. J.*, **2009**, *15*, 7859.

56. Bardelang, D.; Banaszak, K.; Karoui, H.; Rockenbauer, A.; Waite, M.; Udachin, K.; Ripmeester, J. A.; Ratcliffe, C. I.; Ouari, O.; Tordo, P. *J. Am. Chem. Soc.*, **2009**, *131*, 5402.

57. Kirilyuk, I.; Polovyanenko, D.; Semenov, S.; Grigorev, I.; Gerasko, O.; Fedin, V.; Bagryanskaya, E. *J. Phys. Chem. B*, **2010**, *114*, 1719.

58. Jayaraj, N.; Porel, M.; Ottaviani, M. F.; Maddipatla, M. V. S. N.; Modelli, A.; Da Silva, J. P.; Bhogala, B. R.; Captain, B.; Jockusch, S.; Turro, N. J.; Ramamurthy, V. *Langmuir*, **2009**, *25*, 13820.

59. Luckurst, G. R.; Pedulli, G. F. *J. Am. Chem. Soc.*, **1970**, 92, 4738.

60. Ionita, G.; Meltzer, V.; Pincuc, E.; Chechik, V. *Org. Biomol. Chem.*, **2007**, *5*, 1910.

61. The choice to follow ΔB and not a_N was because the spectrum is the superimposition of different species due to the radical dissolved in the bulk water, and to the different complexes between **1a** and the macrocylic hosts.

62. Marquez, C.; Hudgins, R. R.; Nau, W. M. *J. Am. Chem. Soc.*, **2004**, *126*, 5806.

63. Tuncel, D; Katterle, M. *Chem.–Eur. J.*, **2008**, *14*, 4110 and references therein.

64. Das, K.; Pink, M.; Rajca, S.; Rajca, A. *J. Am. Chem. Soc.*, **2006**, *128*, 5334.

65. ^{1}H NMR spectrum of the thread **2b** was recorded at pH 4.

66. Wyman, I. W.; Macartney, D. H. *Org. Biomol. Chem.*, **2009**, *7*, 4045 and references therein.

67. The spectrum of the same sample recorded after 2 h shows a halved signal of the 4-NH_2^+ protons, which disappears after *ca.* 12 h.

68. Mason, B. P.; Bogdan, A. R.; Goswami, A.; McQuade, D. T. *Org. Lett.*, **2007**, *9*, 3449.

69. Angelos, S.; Yang, Y.-W.; Patel, K.; Stoddart, J.-F.; Zink, J. I. *Angew. Chem., Int. Ed.*, **2008**, *47*, 2222.

Chapter 6: The actinoid series: towards a new class of templates

6.1. Introduction

In the synthesis of mechanically interlocked molecules, templates became more and more important, orienting the reactants to produce permanent structures, as the result of new linkages.
Molecular recognition and self-assembly may be used with reactive species in order to pre-organize a system for a chemical reaction (to form one or more covalent bonds). It may be considered a special case of supramolecular catalysis. Non-covalent bonds between the reactants and a "template" hold the reactive sites of the reactants close together, facilitating the desired chemistry. This pre-organization is particularly useful for situations where the desired reaction conformation is thermodynamically or kinetically unlikely, such as in the preparation of large macrocycles. After the reaction has taken place, the template may remain in place, be forcibly removed, or may be "automatically" decomplexed on account of the different recognition properties of the reaction product.

6.2. Concepts and opportunities[1]

Since their inception, [2, 3] chemical templates have provided exciting new molecular topologies,[4,5] beginning with macrocycles and macropolycycles, and then proceeding to simple and complicated knots, monomeric and polymeric rotaxanes, simple and oligomeric catenanes and varieties of molecular switches.
A chemical template organizes an assembly of atoms, with respect to one or more geometric loci, in order to achieve a particular linking of atoms.[6, 7]
The ambition to create continuous and intricate molecular architectures requires that the achieving of a particular linking of atoms establish a permanent interlocking between the molecules. This will usually require formation of one or more chemical bonds while the template organizes the assembly of atoms.
Equally important, the template may involve components that, like catalysts, do not become permanent parts of the molecular architectures.

There are two classes of chemical templates: kinetic templates, of primary importance in generating molecularly interlocked structures, that influence the mechanistic pathway and thermodynamic or equilibrium templates that select and bind certain complementary structures from among an equilibrating mixture of structures.[2]

It is appropriate to judge the effectiveness of template synthesis by comparison with so-called statistical threading which provides the appropriate baseline methodology because it is what is left if a template is not used; it depends on the probability that a linear molecule will penetrate and occupy the space within a macrocycle without the benefit of any particular intermolecular attraction.

Further, threading is a simple elemental step of great importance to the formation of interlocked structures, and the first interlocked molecular structures were prepared by routes involving statistical threading.[8]

Early on, Wasserman estimated with experimental findings the statistical probability for threading a linear molecule through a macrocycle to be something less than 0.01. [9,10] Similarly, the classic study by Harrison and Harrison of rotaxane formation with the ring component bound to a Merrifield resin revealed that 70 successive applications of the statistical threading and blocking reactions resulted in only 6% of the rings being converted to rotaxane.[11] In contrast, template threading is based on mutually attracting participants (to form a template complex). Many studies involving single threadings using various templates give much higher yields — up to 92% in the best case.[12]

Gibson and co-workers [13-15] have pointed out the compelling fact that statistical threading can be used with most systems comprised of a linear molecule and a macrocyclic molecule. His work exemplified the use of statistical threading in the formation of polyester polyrotaxanes by polymerizing sebacoyl chloride and 1,10-decanediol in the presence of a crown ether followed by a capping reaction with 3,3,3-triphenylpropionyl chloride (Figure 1).

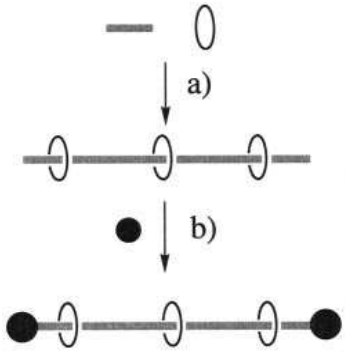

Figure 1. A cartoon example of statistical threading for polyrotaxane formation: (a) polymerization of linear segments in the presence of a macrocycle, (b) a stoppering reaction to trap the rings.

The resulting polymer had 16% by weight of the trapped macrocycle, showing the statistical method to be effective, since no template interaction occurs to aid threading. It is Gibson's view that the special functionalities and complementary geometries required for effective template threading greatly limit the applicable systems.

The disadvantages are great when the desired product involves a continuous structure such as a polyrotaxane or polycatenane because of the necessary repetition of many stages of complicated interactions. From the standpoint of the template enthusiast, this further emphasizes the need for simple templates having components that serve catalytic functions.

6.3. Components of chemical templates - anchors, turns, threadings, and cross-overs.

In order to achieve template-directed assembly of extremely complicated and/or highly extended, interlocked molecular architectures it is necessary to achieve an intimate understanding of how chemical templates function and how they can control vast cascading sequences of templating steps in polymerization processes.[7]

In any chemical template, an anchor constitutes the first component (a metal ion, ion pair

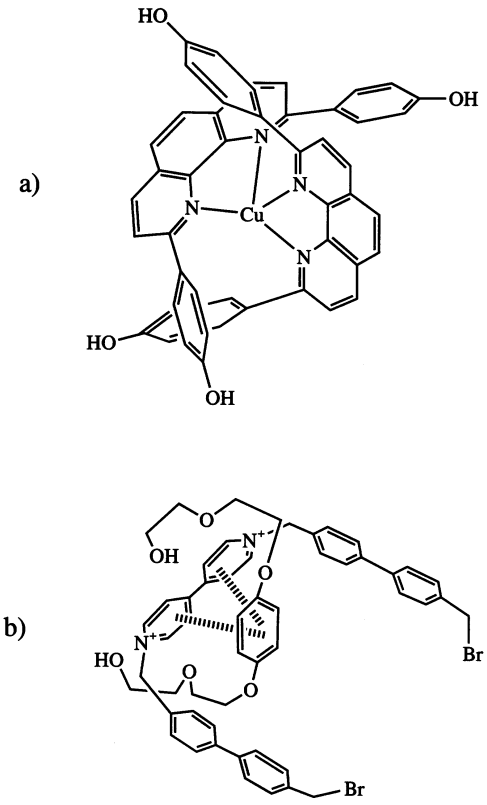

Figure 2. Examples of anchor/turn template complexes: (a) Sauvage's Cu^{I} anchor and phenanthroline turn, (b) Stoddart's π-donor and π-acceptor conjugate

complement, partial charge complement, or hydrogen bonded partner) which holds an appropriate conjugate component, or components.

The role performed is to build a turn into the emerging structure and such a component is called a molecular turn.

Molecular turns have two or more terminal, or near terminal, reactive groups, each pointed in a critical, often the same, direction. This simple kind of molecular template is composed of an anchor and a molecular turn, and the turn may be intrinsic in the structure of the conjugate component or, in the case of a more flexible conjugate component, it may be caused by the anchor (Figure 2). Examples of turns forced by the anchor include the first clearly demonstrated template synthesis[2,3], numerous studies on the synthesis of macrocycles [16–19], and, a variety of studies by Amabalino and Stoddart [20]. In contrast, the conjugates used by Dietrich-Buchecker and Sauvage[21] in their ground breaking studies of catenane and knots are themselves molecular turns.

The combination of an anchor with two non-parallel molecular turns produces a molecular cross-over (Figure 3). This template is one of the two that organizes elements essential for catenane and rotaxane synthesis.

Catenanes are produced by two ring closings on a molecular cross-over, each ring closing process making use of a single molecular turn.

Rotaxanes are produced by one ring closing on a single molecular turn and the addition of blocking groups to the other conjugate.

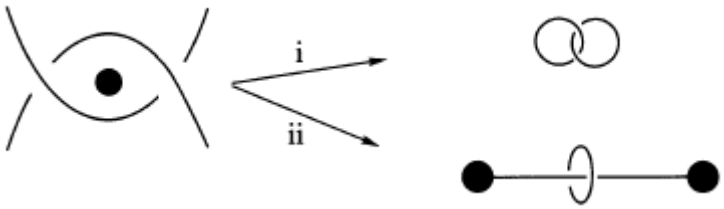

Figure 3. A simple cross-over gives (i) a catenane upon two ring closures or (ii) a rotaxane upon one ring closure and blocking

6.4. Metal ion templates

At the moment, the aim of the organic synthetic is to control intricate sequences of steps (threadings, cross-overs, ring closings, and other linkages) in order to form complicated orderly molecular entanglements. The many structural motifs achieved through chemical templates till now are displayed in Figure 4.

The power of chemical templates becomes obvious and even more fascinating realizing that the marvelous array of structural motifs so briefly summarized above has been achieved with a remarkably small number of distinct chemical templates.

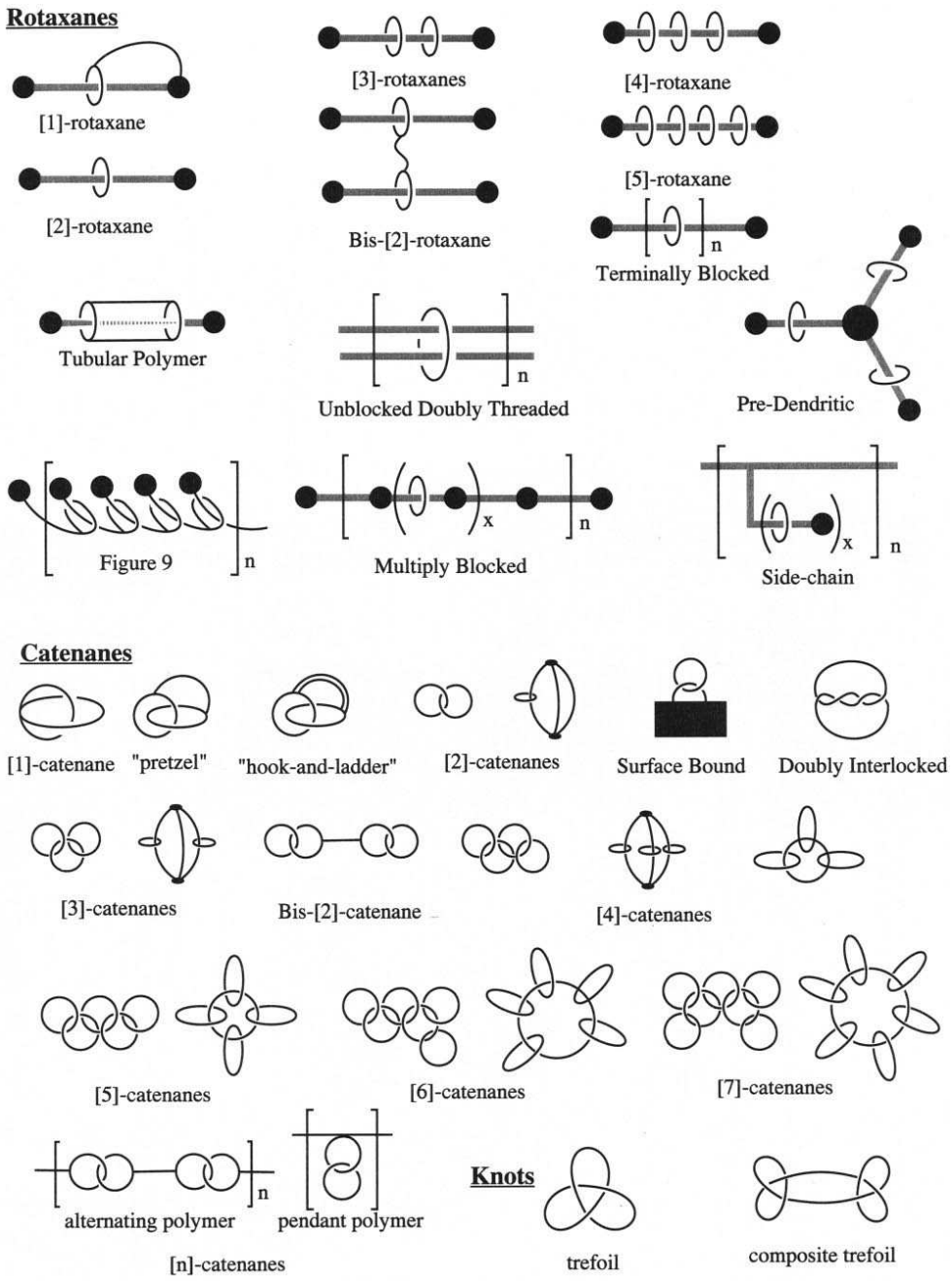

Figure 4. The various interlocked structures which have resulted from template syntheses: rotaxanes, catenanes, and knots.

Templates based on metal ion anchors are prototypical of the concept and historically important since they provided the seminal examples. A single metal ion anchor acts as a unique point around which the construction of new molecules that cannot be made by other known pathways can be achieved.

Metal ion templates played a key role in the development of macrocyclic ligand chemistry and its derivative chemistries, constituting a multifunctional center about which molecular turns of various kinds are readily oriented.

The Busch group, in the early 1960s, demonstrated the first rational synthesis of macrocycles around metal ion templates [2,3,22,23]. The planar nickel(II) ion in Figure 5 forces a tetradentate ligand into a turn, bringing its two reactive terminal groups into adjacent positions, facilitating cyclization by their reaction with a reagent that is a second molecular turn, α,α'-dibromo-*o*-xylene. This example demonstrates the meaning of the kinetic template effect, the ability of the metal ion anchor to predictably control the spatial orientation of reactive groups during the formation of critical linkages.

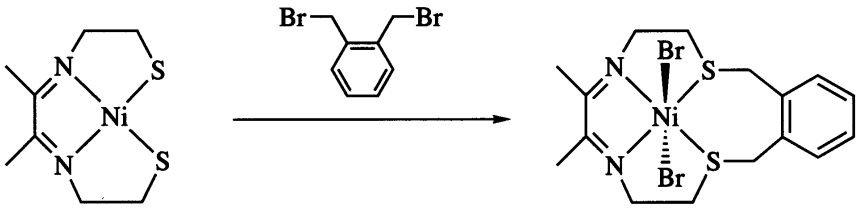

Figure 5. The seminal metal ion template macrocyclization

Metal ion anchors offer the additional advantage that they are often readily removed, leaving the interlocked structure intact, or as stated by Sauvage, ''The novelty of this approach… is that the chelating ligands collected by the metal, and organized in its coordination sphere, are not covalently linked to each other after the cyclization reaction''.[24]

The potential of metal ion templates for the production of interlocked structures was first widely recognized in the preparation of catenanes, molecules made up of two or more mechanically interlocked, or interpenetrating rings, the simplest being the two component [2]-catenane.

Several conceptually different routes for catenane synthesis were described, including statistical threading ,[8] direct organic synthesis ,[25] and various template methods, which have been by far the most successful.

There are multiple template routes to catenane formation:

a) the ring-turn approach (Fig. 6(a)), forms a macrocycle initially by reaction of a turn and a second difunctional reactant; complexation of this macrocycle with an anchor and another equivalent of the turn gives the threaded template, in effect a pseudorotaxane. The second ring can then be closed about the first to produce the [2]-catenate.[26]

b) the two-turn approach (Fig. 6(b)) cyclizes both turns of a template composed of a single cross-over, using difunctional reagents. The same pseudorotaxane is a likely intermediate. This method requires fewer steps, yet often leads to lower yields.[27]

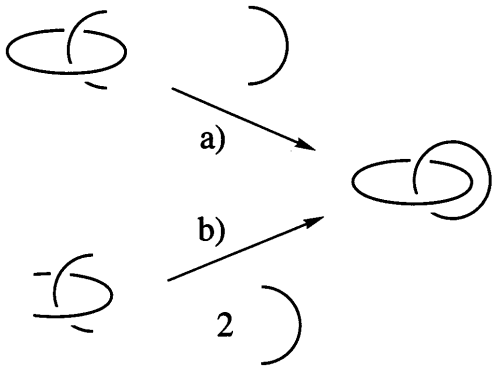

Figure 6. Two strategies for template catenane formation: (a) the ring-turn approach, (b) the two-turn approach.

In the 'three-dimensional' realm required for interlocked structures, non-planar geometries are templated by selection of appropriate nonplanar metal ions as anchors. By coordination, the metal ion anchors two conjugate molecular turns which are thereby oriented in accord with the metal ion coordination sites they occupy.

For a tetrahedral metal ion anchor, didentate ligands:molecular turns are held in mutually orthogonal positions with respect to each other. The molecular turn-ligand, 2,9-bis(*p* hydroxyphenyl)-1,10-phenanthroline (Fig. 7(a)), has critical structural features that have made it highly successful — it provides the necessary geometric control over terminal reactive groups that extend well beyond the metal center and can form the copper(I) complex (Fig. 7(b)), which was found to exhibit the geometry and binding strength needed.

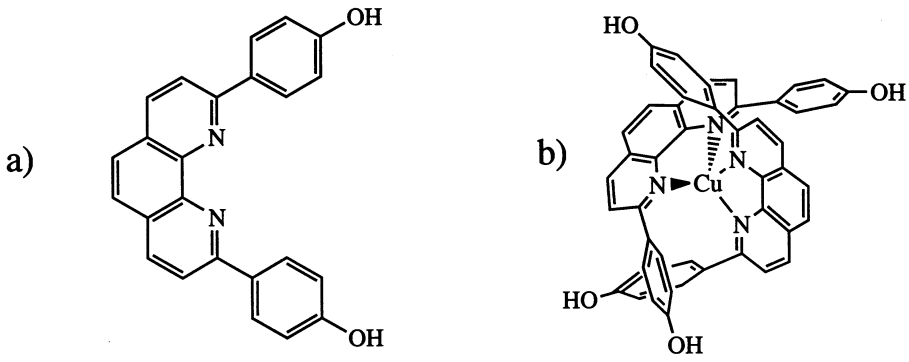

Figure 7. (a) Sauvage's molecular turn, (b) the resulting two-turn complex of CuI.

In the first reported template synthesis of catenanes, where the bifunctional ring closing reagents were pentaethylene glicol dihalides, only 27% of the product was obtained by the two-turn approach,[27] while the ring-turn approach yielded 42% .[26] Recently, using the Grubbs' ring closing

metathesis reaction and moving the ring closure reaction to a much greater distance for the metal-anchored cross-over, the Sauvage group has prepared simple [2]-catenanes in 92% yield.[28] From this and other examples it is apparent that for interlocking turns, choosing and locating the terminal functional groups so that no additional linking atoms (or a minimum number) are required to complete the ring greatly facilitates the efficiency of catenane formation.

The advantage probably derives in large part from the reduced competition between the formation of intramolecular and intermolecular linkages. Other advantages should stem from reclaiming the ability to use a large excess of a second reagent and the fact that no additional atoms are needed to form the final ring.

6.5. The actinides as new class of templates in catenanes' synthesis

6.5.1. Introduction

Metal ions with a range of different two- and three-dimensional coordination geometries (Figure 8a–d) have been used as a template for the synthesis of catenanes and rotaxanes.[29,30] The result is a rich tapestry of mechanically interlocked ligands and complexes that have been studied from the point of view of their electrochemistry,[31] photochemistry,[32] reactivity,[33] selectivity,[34] and as prototypes for molecular machines.[35] Some of these systems can be assembled under thermodynamic control,[36] others under kinetic control.[31-34,37] Some use sophisticated ligand systems,[38] others relatively simple ones.[36] Some feature homoleptic complexation modes,[31a, 36a,c,39,40] others heteroleptic ones.[37a,c,41,42]

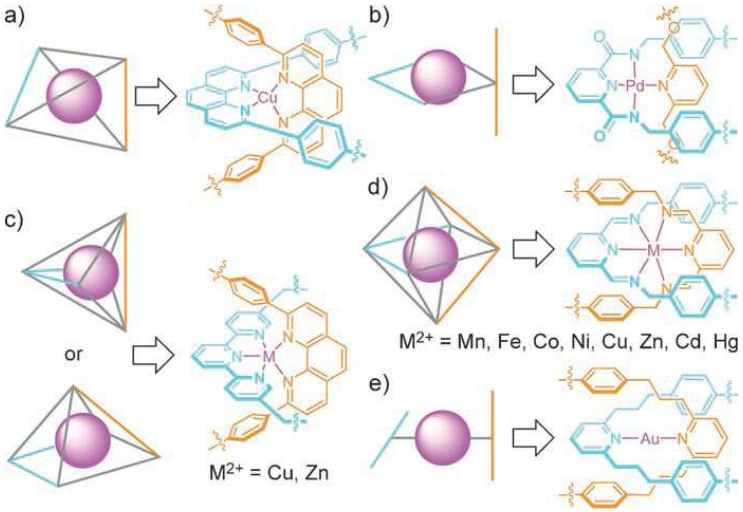

Figure 8. Metal coordination geometries successfully utilized in the metal-template synthesis of catenanes and rotaxanes. a) Four-coordinate (tetrahedral);[31a,32e,33a,b,34,36c,37a,b,39] b) four-coordinate (square planar);[33d,37c,41] c) five-coordinate (square-based pyramid/trigonal bipyramidal);[42] d) six-coordinate (octahedral);[36a,b,40] e) two-coordinate.[43]

With the exception of the case *e*, where the use of gold (I) was aimed to demonstrate the attractiveness of exploiting a linear coordination mode in synthesis because of its simplicity and the potential generality of a motif requiring just two monodentate ligands to bind the metal, all employ at least one multidentate ligand, to create a rigid coordination sphere around the metal.
The precursors of macrocycles, the so-called *U-shapes*, are so allowed to be in the right position forming a stable complex, as this approach relies on their supramolecular preorganization using non-covalent interactions to offset some of the entropic cost of association and help to position the components to form the desired product.

6.5.2. The Actinides[44]

The actinide (or actinoid, IUPAC nomenclature) series include the 15 chemical elements with atomic numbers from 89 to 103, actinium to lawrencium.
The actinide series derives its name from the first element of the series, actinium, and from the greek word “aktis”, which means ray, reflecting the elements’ radioactivity; although actinoid (actinide) means “actinium-like” and therefore should exclude actinium, it is usually included in the series for the purpose of comparison. Only thorium and uranium occur in more than trace quantities in nature; the other actinides are synthetic elements. All actinides are radioactive and release energy upon radioactive decay; uranium, thorium, and plutonium, the most abundant actinides on Earth, are used in nuclear reactors and nuclear weapons.
The actinides are usually considered to be *f-block elements*, belonging to hard elements, preferably bound in complexation reactions to the hard oxygen donor atoms, and they show much more variable valence than the lanthanides. Correspondingly, studies of complexation of these elements in solutions were until the 1980s performed with complexants bonding the complexed metal ion either exclusively to oxygen atoms or to both oxygen and nitrogen atoms. Such complexes may be very stable in solution, offering the possibility to exploit this property in the synthesis of mechanically interlocked architectures.
As the metal ion preorganizes reactive molecular fragments in a spatial controller manner to obtain preferentially the desired structure over many others (see Section 6.4), the use of a metal with the property of expanding the valence state gives hope to get a more stable intermediate complex.
A possible synthetic strategy of [2]-catenanes can be scehmatized in the following steps (Figure 9):

a) Synthesis of electron-rich ligands of the necessary geometry, containing donor atoms like oxygen, nitrogen or sulfur.

b) Reaction with an appropriate actinide salt in stoichiometric ratio of 2 to 1, to obtain a complex (cross-over), following the two turn-approach (see Figure 6*b*): the metal coordinates within the cavity of the ligand with coordination number beyond 6.

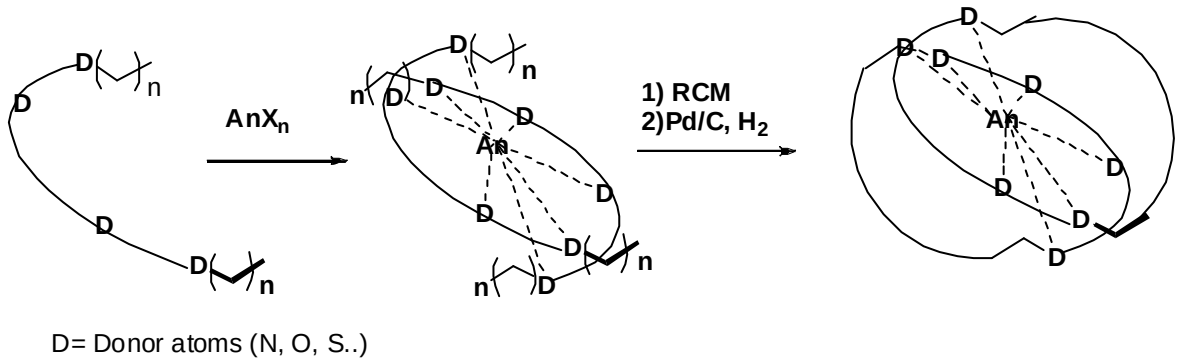

Figure 9. Synthetic strategy of [2]-catenanes

c) Once formed the complex 2:1 with the cation, a macrocyclization reaction affords the [2]-catenane.

6.5.3. Ring-closing metathesis

Ring-closing metathesis (or RCM) has emerged as a powerful tool for the construction of carbocyclic and heterocyclic ring systems; being basically a variation on olefin metathesis, it is the macrocyclization reaction which is usually used to generate 5 up to 30-membered cyclic alkenes; it allows the closing of previously hard to make rings (7-8 member rings in particular) and it makes use of a Grubbs' catalyst, yielding the cycloalkene and a volatile alkene, like ethene (Figure 10). The *E/Z*-selectivity depends on the ring strain.

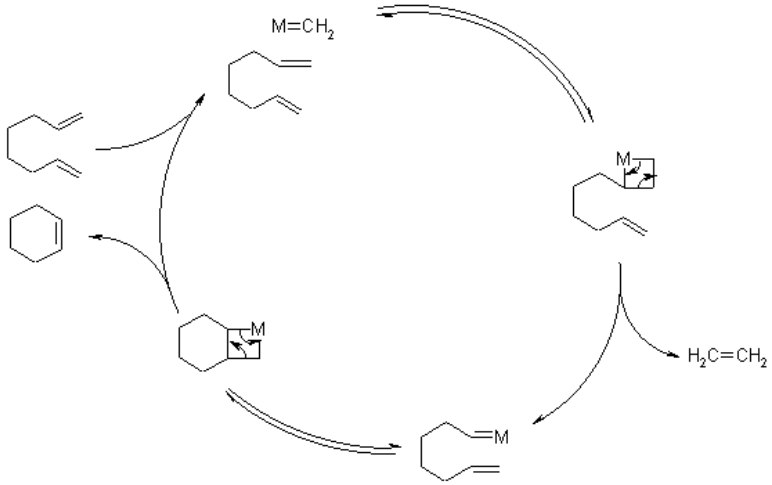

Figure 10. Chauvin's mechanism of Ring-closing metathesis

6.6. A pentadentate ligand based on 2,2';6',2"-terpyridine

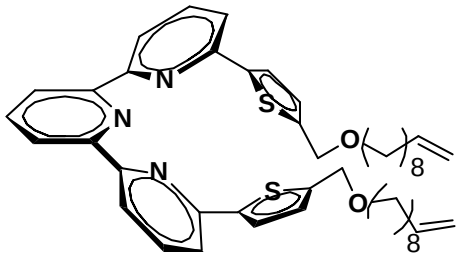

L1

The pentadentate ligand **L1** based on terpyridine exhibits the necessary features to create a complex 2:1 with a multivalent cation (e.g. actinides); nitrogen and sulfur atoms constitute the linking point for the metal, which is the multifunctional center about which 2 equivalents of molecular turns **L1** are readily oriented.

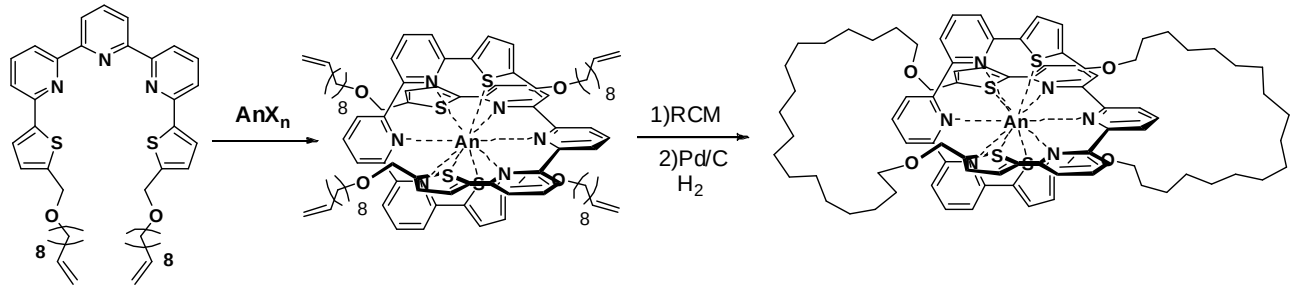

Figure 10. Formation of a ten-coordinate complex which allows the right position of the precursors of the macrocycles.

The cross-over between the two pentadentate *U-shapes* affords a ten-coordinate complex where the coordination sphere constitutes a rigid framework in which the metal is the center and allows the right orientation for the next rings' closing.

The ligand is composed of two main building blocks, the dibromo-terpyridine and an organo stannane based on thiophene ring, which are joined together through the *Stille coupling reaction*,[45,46] a chemical reaction which is very widely used in organic chemistry, coupling an organotin compound with an sp^2-hybridized organic halide catalyzed by palladium and with very few limitations on the R-groups.

The reaction mechanism of the Stille reaction has been well studied.[47] The first step in this catalytic cycle is the reduction of the palladium catalyst (**1**) to the active Pd(0) species (**2**). The oxidative addition of the organohalide (**3**) gives a cis intermediate which rapidly isomerizes to the trans intermediate **4**[45] Transmetalation with the organostannane (**5**) forms intermediate **7**, which produces

the desired product (**8**) and the active Pd(0) species (**2**) after reductive elimination. The oxidative addition and reductive elimination retain the stereochemical configuration of the respective reactants.

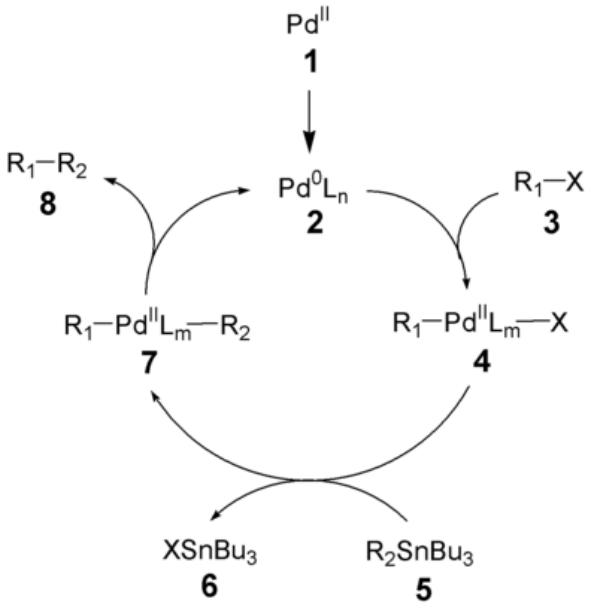

Figure 11. Suggested mechanism for the Stille reaction

The first building block, the di-halide, was obtained starting from glutaryl dichloride; the exchange with the amine afforded the corresponding Weinreb amide[48] **9**, N-Methoxy-N-methylglutamide, in quantitative yield, then the introduction of pyridine ring gave compound **10**,[48] 1,5-Di(6-Bromo-2-pyridil)pentane-1,5-dione, with 40% of yield; finally the condensation in presence of ammonium acetate afforded the 6, 6''-Dibromo-2,2':6', 2''-terpyridine[49] **11** with 50 % of yields (Scheme 1).

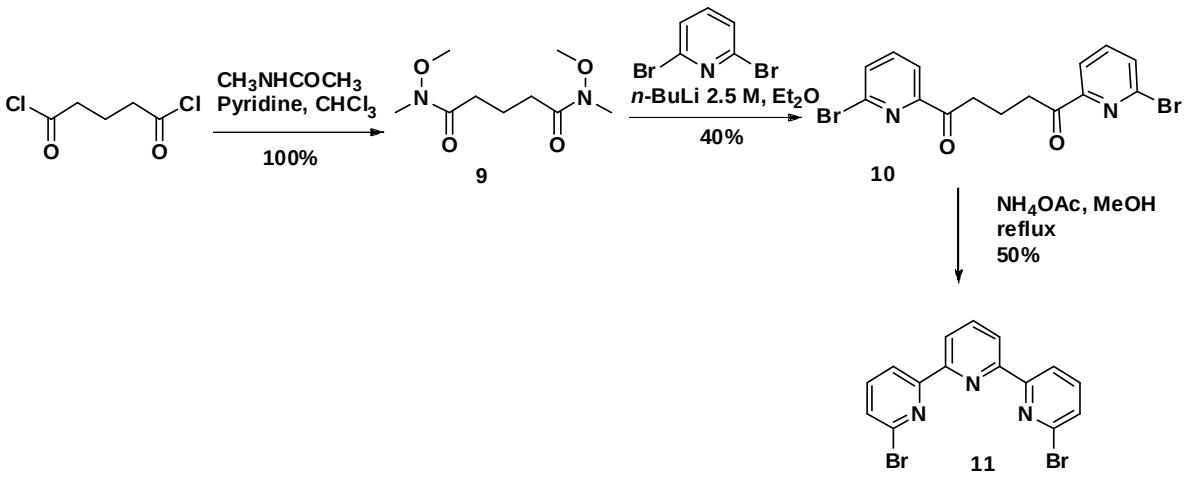

Scheme 1. Synthesis of 6, 6''-Dibromo-2,2':6', 2''-terpyridine.

The second building block (Scheme 2), the organo stannane, was obtained from the thiophene **12**, alkylated with 1-undecenol in quantitative yield, affording the 2-Bromo-5-dec-9-enyloxymethyl-thiophene **13**, which through transmetallation, afforded the tin compound **14**.

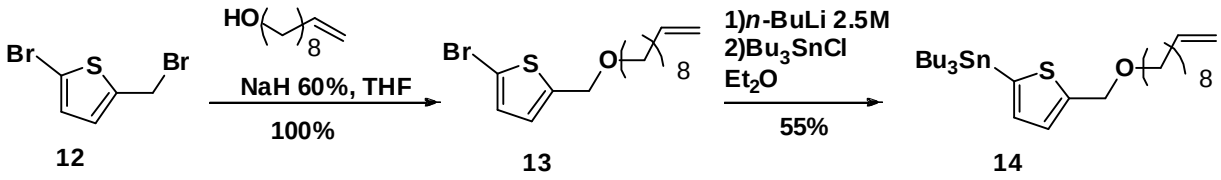

Scheme 2. Synthesis of Tributyl-(5-dec-9-enyloxymethyl-thiophen-2-yl)-stannane.

The coupling reaction between compound **11** and **14** afforded the ligand **L1** in good yield (53 %) (Scheme 4).

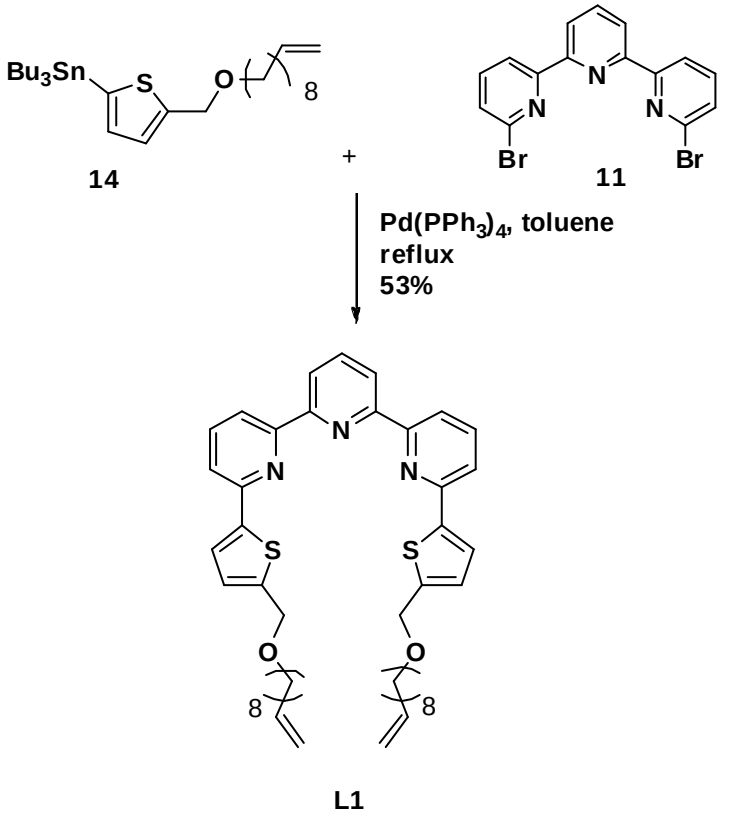

Scheme 4. Synthesis of pentadentate ligand **L1** with long aliphatic chain

In the first complexation studies, a more easily achievable ligand (less synthetic steps) was synthesized, the analogous U-shape with only one methyl group attached to thiophene (Scheme 5). The commercially available 2-methylthiophene **15**, after metallation, afforded the corresponding organo stannane **16** which, without any purification, was coupled with dibromoterpyridine **11** to afford the ligand **17**, the "model system" to be used in the first experiments with metal templates.

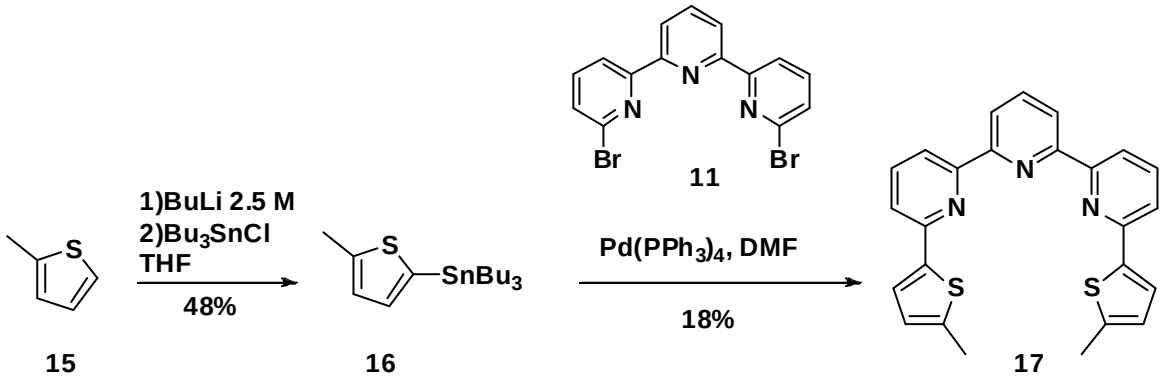

Scheme 5. Synthesis of pentadentate ligand (*model system*).

6.7. A tetradentate ligand based on dipyrromethane moiety

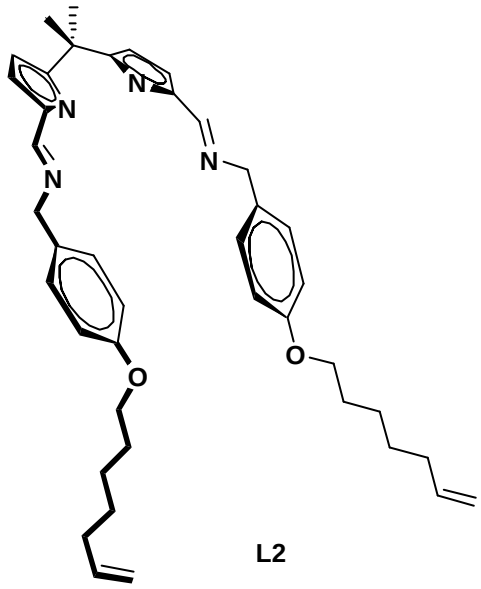

The tetradentate ligand **L2** is a very attracting compound, being electron rich and similar to the previous ligand **L1** for shape and skills in hydrogen bondings so it can be equally used to detect the complexation properties of Actinides metals.

It is composed as well of two building blocks, the dipyrromethane core carrying two halide groups and an aromatic amine joined through formation of an imine bond.

The aromatic amine (Scheme 6) was synthesized starting from the cyanoalcohole **18**, alkylated with good yield (73%) to **19;** the reduction of the nitrile group to amine to obtain the compound **20** was almost quantitative (94%).

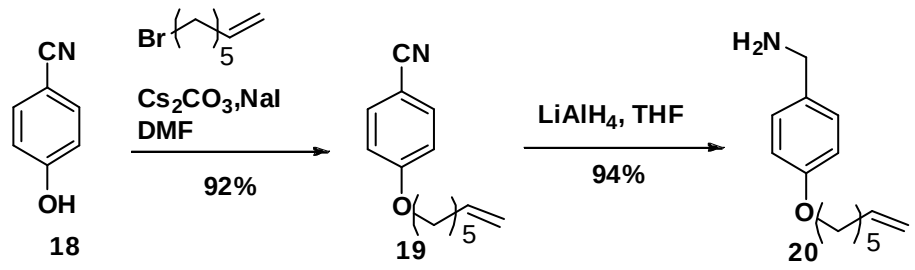

Scheme 6. Synthesis of the amine with the long aliphatic chain.

The formyldipyrromethane core was obtained (Scheme 7) starting from pyrrole passing for the 5,5'-dimethyldipyrromethane[50] (**21**) and then to get the 5,5'-diformyl-2, 2'-dimethyldipyrromethane[51] (**22**) through the Vilsmeier-Haack reaction, which allows the formylation of electron rich arenes, using the formylating agent which is formed in situ from DMF and $POCl_3$.

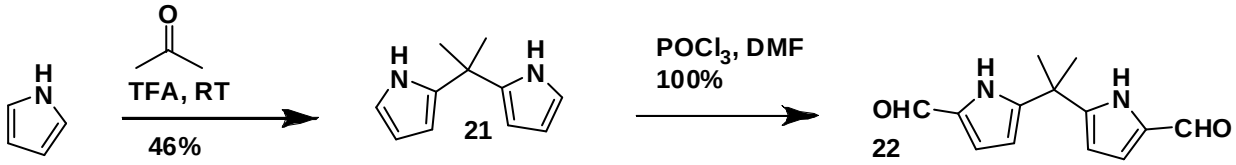

Scheme 7. Synthesis of the dimethyldipyrromethane core.

The reaction of the dihalide **22** with 2 equivalents of **20** afforded a new *U-shape* **L2**, based on the imine-motif, compatible for a rigid framework able to chelate metal ions. (Scheme 8)

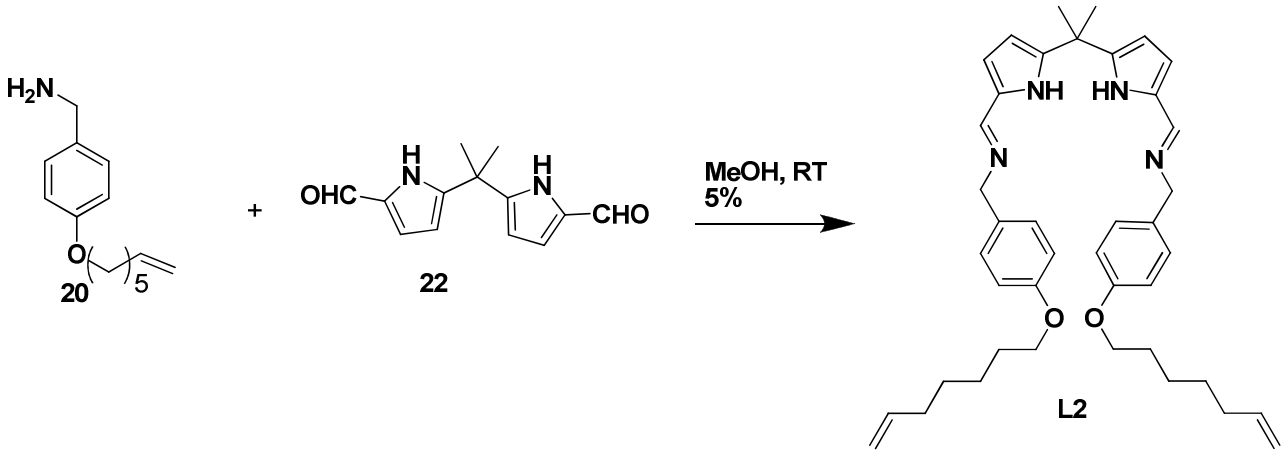

Scheme 8. Synthesis of tetradentate ligand **L2** with long aliphatic chain.

Like in the previous case, in order to carry out preliminary complexation studies, the analogous model system **23** was synthesized, carrying only a methyl group, starting from commercially available toluylbenzylamine; the product was obtained by precipitation from diethyl ether with quite good yield (65%). (Scheme 9)

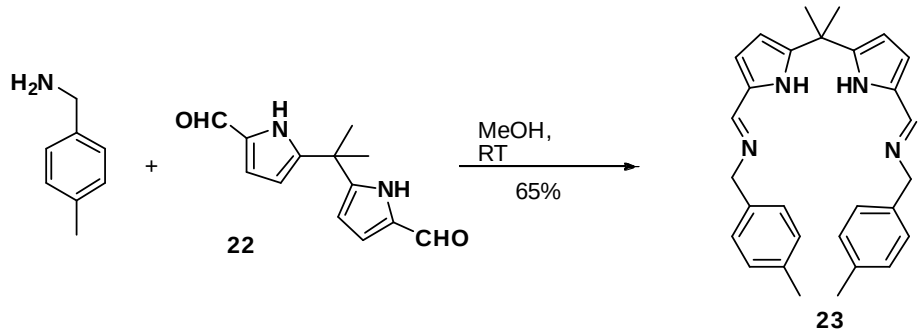

Scheme 9. Synthesis of tetradentate ligand (*model system*).

6.8. Preliminary results and conclusions

The first experiments were carried out with the model system **23** in presence of different amounts of $Ti(Cl)_4$.The choice of using Titanium, a *d-block element*, relies in his resemblance to Actinides' electronic properties and his capability of acting as a Lewis acid.

Mixing dried compound **23** with $Ti(Cl)_4$ in the ratio 1:1 (in presence of base DABCO, 1,4-diazabicyclo[2.2.2]octane) and recording NMR spectra in the time, (just after the addition of the

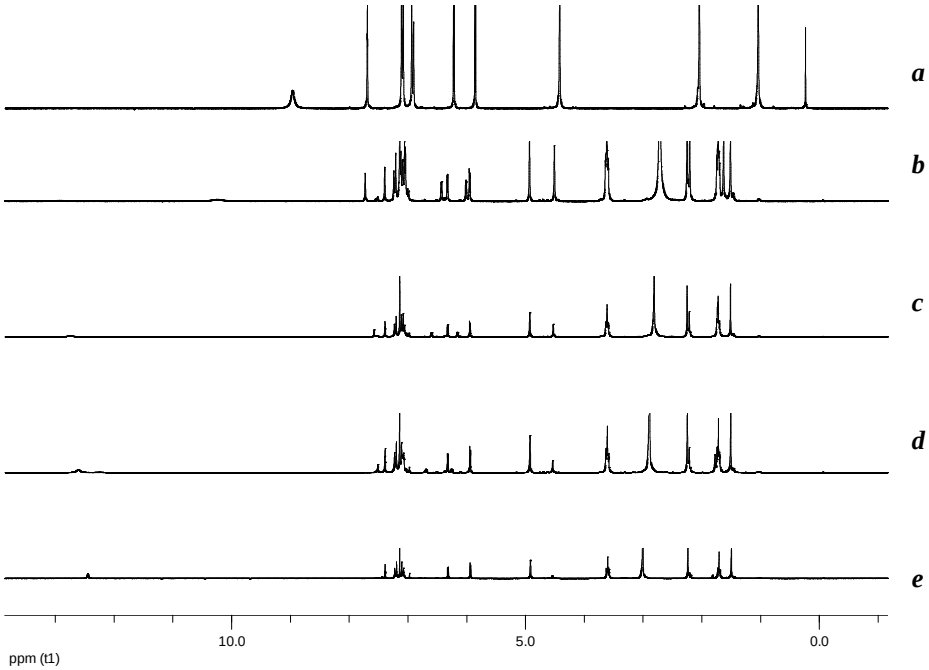

Figure 12. NMR spectra (dried $CDCl_3$, 400 MHz) of: *a*) the dried ligand **23** *b*) straight after the addition of $Ti(Cl)_4$ (t=0); *c*) after 1 hour; *d*) after 5 hours *e*) after 16 hours, heating at 75° C (stoichiometric ratio ligand/Ti 1:1)

salt, after 1, 5, 16 hours and heating at 75°C in the last case) it's evident the formation of two distinct patterns of signals, as in the case of a mixture of complexed and uncomplexed ligand, situation which develops into a new profile of signals, probably belonging to the complex, after 16 hours and heating (Figure 12).

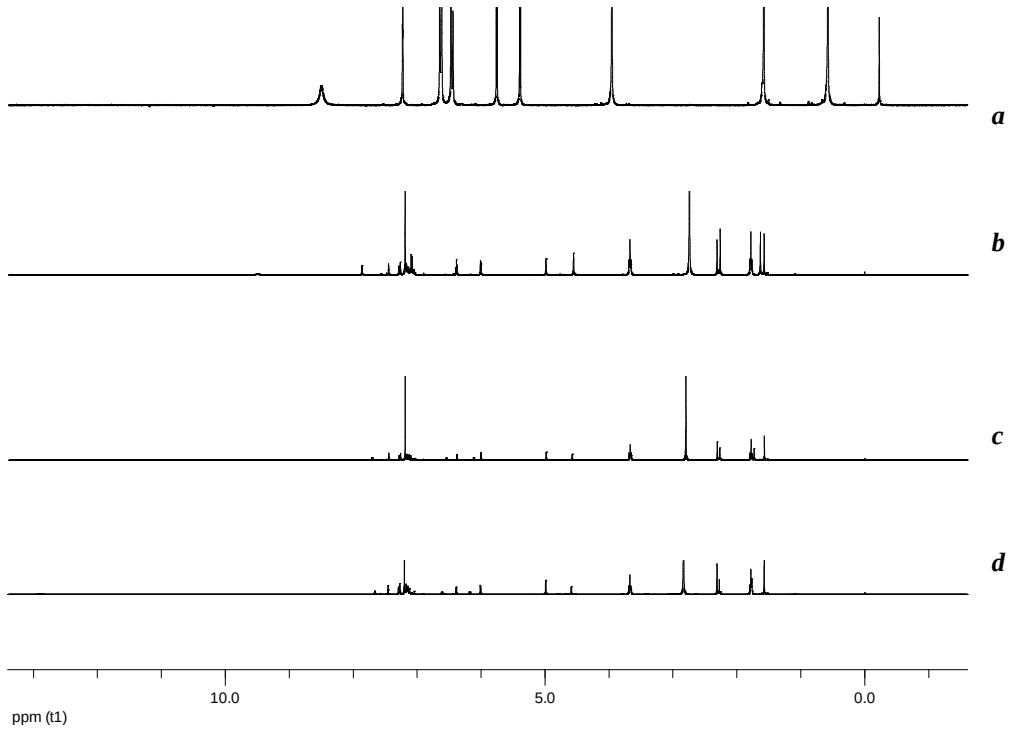

Figure 13. NMR spectra (dried $CDCl_3$, 400 MHz) of: *a*) the dried ligand **23** *b*) straight after the addition of $Ti(Cl)_4$ (t=0); *c*) after 5 hours; *d*) after 16 hours, heating at 75° C (stoichiometric ratio ligand/Ti 2:1)

In the Figure 13 as well, the spectrum of the dried ligand, at the top, is compared with the other ones straight after the addition of $TiCl_4$ (t=0) and after 5 and 16 hours (after 16 hours the sample was heated at 75°C), but now the ratio ligand/$TiCl_4$ is 2:1, according to the aim of the project to check the possibility of using actinides to template the formation of a [2]-catenane, after the formation of the complex (*cross-over*) of the corresponding two *U-shapes*. The profile of the spectra is very similar, as expected, to the previous ones, confirming the formation of the complex ligand/$TiCl_4$ 2:1, former step to the RCM, to obtain the [2]-catenane.

These preliminary experiments confirm the central role of metal cations which are able to preorganize reactive molecular fragments in a predictable manner, gathering macrocycles' precursors incorporating chelating subunits; the use of actinides, with the possibility of realising stable *cross-overs* with coordination number beyond 6, means the real opportunity to develop the synthesis of [2]-catenanes using even actinide-template effect.

6.9. Experimental section

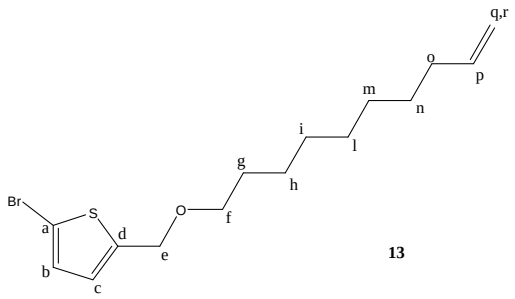

13

2-Bromo-5-dec-9-enyloxymethyl-thiophene (13): NaH 60% (400mg, 10 mmol) was added to a solution of 9-decen-1-ol (1.56g, 10 mmol) in THF (100ml), at 0°C. The reaction mixture was stirred for 20 minutes then allowed to warm to room temperature and stirred for further 45 minutes. 2-Bromo-5-bromomethylthiophene (2.68g, 10.5 mmol) was then added at 0°C, the reaction mixture is let to reach room temperature, then heated under reflux overnight.
The reaction mixture was quenched by addition of brine; after extraction with DCM, the organic layer was collected and dried over $MgSO_4$. Then solvent was removed and the crude product was purified by column chromatography (Petroleum ether/diethyl ether 95:5 v/v), obtaining 2.95g of the product (Yield: quantitative); ^{1}H NMR (400 MHz, $CDCl_3$) δ= 6.90 (d, 1H, *J*= 3.6 Hz, $H_{thiophene}$), 6.73 (d, 1H, *J*=3.6 Hz, $H_{thiophene}$), 5.86-5.76 (m, 1H, H_p), 5.02-4.91 (m, 2H, $H_{q,r}$), 4.56 (s, 2H, H_e), 3.45 (t, *J*= 6.5 Hz, 2H, H_f), 2.07-2.01 (m, 2H, H_o), 1.61-1.54 (m, 6H, $H_{alkyl\ chain}$), 1.38-1.33 (m, 6H, $H_{alkyl\ chain}$); ^{13}C NMR (400MHz, $CDCl_3$) δ= 139.2, 129.3, 126.3, 114.1, 70.3, 67.5, 33.8, 29.6, 29.42, 29.39, 29.1, 29.0.

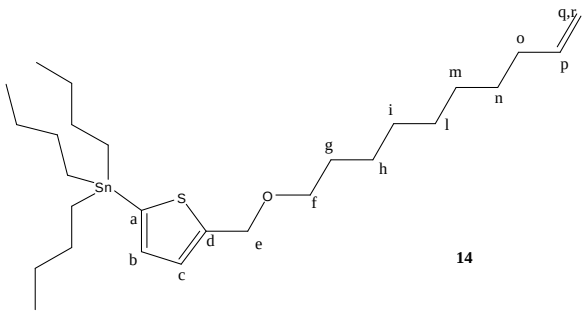

14

Tributyl-(5-dec-9-enyloxymethyl-thiophen-2-yl)-stannane (14): n-BuLi 2.5 M (2.24 ml, 5.6 mmol) was added dropwise to a solution of 2-Bromo-5-dec-9-enyloxymethyl-thiophene (1.41g, 5mmol) in diethyl ether (100ml) at -78°C. Tributyltinchloride (1.95g, 6mmol) was added dropwise after 2 hours of stirring and, after 30 minutes, the reaction mixture was allowed to go to room temperature and let under stirring overnight. The reaction mixture was quenched with addition of brine; after extraction with ethyl acetate, the organic layer was collected and dried over Na_2SO_4. Then solvent was removed and the crude product was purified by column chromatography (petroleum ether/diethyl ether 95:5 v/v), obtaining the product as a brown oil (1.32g, 53%); ^{1}H NMR (400MHz, $CDCl_3$) δ=7.10 (d, *J*=3.2 Hz, 1H, H_c), 7.02 (d, *J*=3.2 Hz, 1H, H_b), 5.86-5.76 (m, 1H, H_p), 5.01-4.90 (m, 2H, $H_{q,r}$), 4.69 (s, 2H, H_e), 3.48 (t, *J*= 6.6 Hz, 2H, H_f), 2.06-2.00 (m, 2H, H_o), 1.68-1.52 (m, 4H, $H_{g,h}$), 1.10-1.06 (m, 4H, $H_{i,l}$), 0.97-1.09 (m, 27H, stannane) 0.94-0.87 (m,4 H, $H_{m,n}$); ^{13}C NMR (400MHz, $CDCl_3$) δ= 146.8 (q, $C_{thiophene}$), 139.2 (CH, C_p), 137.3 (q, $C_{thiophene}$),

135.0 (CH, C_b), 127.4 (CH, C_c), 114.1 (CH_2, $C_{q,r}$), 70.2 (CH_2, C_f), 67.2 (CH_2, C_e), 33.8 (CH_2, C_o), 29.7 (CH_2), 29.4 (CH_2), 29.1 (CH_2), 28.9 (CH_2), 27.4 (CH_2), 27.3 (CH_2), 26.1 (CH_2).

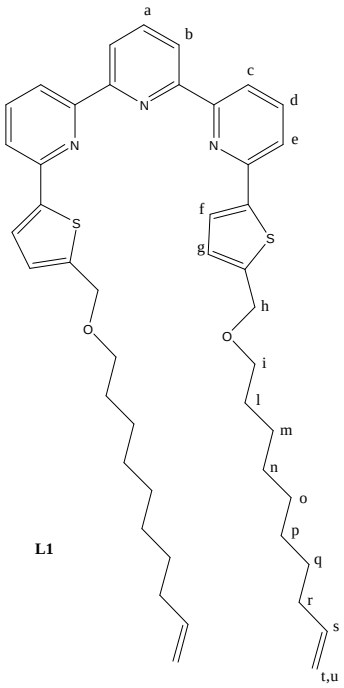

L1

Chemical Formula: $C_{45}H_{55}N_3O_2S_2$
Molecular Weight: 734.07
Elemental Analysis: C, 73.63; H, 7.55; N, 5.72; O, 4.36; S, 8.74

L1: $Pd(PPh_3)_4$ (0.017 g, 0.015 mmol) was added to a mixture of 5-tributylstannylalkylthiophene (0.149 g, 0.3 mmol) and 5,5'-dibromoterpyridine (0.039g, 0.1 mmol) in dry toluene (10 ml). The mixture reaction was stirred at reflux overnight.
After the mixture had cooled to room temperature, NaOH 0.1 M in MeOH was added and the solution was stirred for 30 minutes; after the addition of brine, the organic layers were extracted with ethyl acetate.
The organic layer was separated, and the aqueous layer was extracted with CH_2Cl_2. The combined organic layer was washed with water, dried over Na_2SO_4 and concentrated under reduced pressure.
The residue was purified by column chromatography on silica gel with petroleum ether/ethyl acetate (90:10 v/v) to yield the U-shape (0.059 g, 53 %) as a white-yellow solid.
^{1}H NMR (400 MHz, $CDCl_3$): δ= 8.63 (d, *J*=8 Hz, 2H, H_b), 8.51 (dd, *J*=0.8, 7.6 Hz, 2H, H_c), 8.00 (dd, *J*= 7.6, 8Hz, 1H, H_a), 7.85 (dd, *J*= 8, 7.6 Hz, 2H, H_d), 7.66 (dd, *J*=0.8, 8Hz, 2H, H_e), 7.54 (d, *J*= 3.6 Hz, 2H, H_f), 7.02 (d, *J*= 3.6 Hz, 2H, H_g), 5.85-5.75 (m, 2H, H_s), 5.00-4.90 (m, 4H, $H_{t,u}$), 4.70 (s, 4H, H_h), 3.53 (t, *J*= 6.8 Hz, 4H, H_i), 2.05-1.99 (m, 4H, H_r), 1.67-1.60 (m, 4H, H_l), 1.37-1.30 (m, 20H, $H_{alkyl\ chain}$); ^{13}C NMR (400 MHz, $CDCl_3$): δ= 155.6 (q), 154.9 (q), 151.7 (q), 145.2 (q), 143.9 (q), 139.2 (CH, C_s), 137.8 (CH, C_a), 137.5 (CH, C_d), 127.0 (CH, C_g), 124.1 (CH, C_f), 121.3 (CH, C_h), 119.0 (CH, C_c), 118.3 (CH, C_e), 114.1 ($CH\underline{C}H_2$, $C_{t,u}$), 70.3 (CH_2, C_i), 67.7 (CH_2, C_h), 33.8 (CH_2, C_r), 29.7 (CH_2, $C_{alkyl\ chain}$), 29.4 (CH_2, $C_{alkyl\ chain}$), 29.1 (CH_2, $C_{alkyl\ chain}$), 28.9 (CH_2, $C_{alkyl\ chain}$), 26.1 (CH_2, $C_{alkyl\ chain}$); LRESI-MS: *m/z* = 734; HRESI-MS: *m/z* = 734.38140 (calcd for $C_{45}H_{56}N_3O_2S_2$, 734.38324).

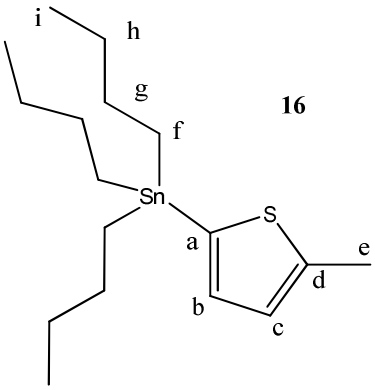

16

Tributyl-(5-methyl-thiophen-2-yl)-stannane (16): n-BuLi 2.5 M (15 ml, 37.5 mmol) was added dropwise to a solution of 2-methyl-thiophene (2.45g, 25mmol) in THF (100ml) at -78°C. After 30 min of stirring at room temperature, tributyltinchloride (12.2g, 37.5 mmol) was added dropwise at -78°C then the reaction mixture was allowed to go to room temperature and let under stirring overnight. The solvent was removed under reduced pressure then, after addition of water, the product was extracted with DCM; the organic layer was collected and dried over Na_2SO_4, obtaining the product as a yellow oil (4.65g, 48%); ^{1}H NMR (400MHz, $CDCl_3$) δ= 6.97 (d, *J*= 3.2Hz, 1H, H_b), 6.88 (d, *J*= 3.2 Hz, 1H, H_c), 2.54 (s, 3H, H_e), 1.32 (m, 2H, H_g), 1.29 (m, 2H, H_h), 0.87 (t, *J*= 6.4 Hz, 3H, H_i), 0.36 (t, *J*= 6.4 Hz, 3H, H_f); ^{13}C NMR (400MHz, $CDCl_3$) δ= 145.3 (q, $C_{thiophene}$), 135.4 (CH, C_b), 134.3 (q, $C_{thiophene}$), 126.6 (CH, C_c), 67.2 (CH_2, C_e), 29.7 (CH_2), 29.4 (CH_2), 29.1 (CH_2), 28.9 (CH_3).
LRESI-MS: *m/z* = 331 $[M+1]^+$- Bu; HRESI-MS: *m/z* = 388.12409 (calcd for $C_{17}H_{32}SSn$, 388.12412).

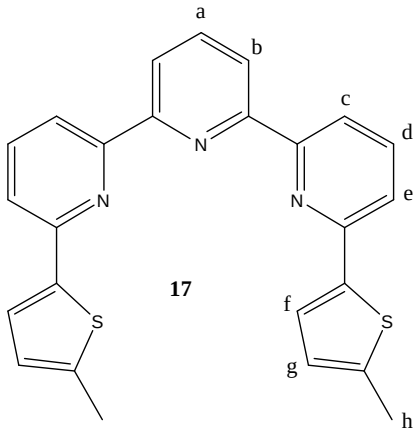

17

Chemical Formula: $C_{25}H_{19}N_3S_2$
Molecular Weight: 425.56846

17: $Pd(PPh_3)_4$ (0.27 g, 0.24 mmol) was added to a mixture of 5-tributylstannyl-2-methylthiophene (2.48 g, 6.4 mmol) and 5,5'-dibromoterpyridine (0.63 g, 1.6 mmol) in dry toluene (100ml). The mixture reaction was stirred at reflux overnight. After the mixture had cooled to room temperature, NaOH 0.1 M in MeOH was added and the solution was stirred for 30 minutes; after the addition of brine, the organic layers were extracted with ethyl acetate.
The organic layer was separated, and the aqueous layer was extracted with CH_2Cl_2. The combined organic layer was washed with water, dried over Na_2SO_4 and concentrated under reduced pressure.
The residue was purified by column chromatography on silica gel with petroleum ether/diethyl ether (80:20 v/v) to yield the U-shape (0.12 g, 17.5 %) as a yellow solid.

^{1}H NMR (400 MHz, $CDCl_3$): δ= 8.60 (d, *J*=8.0 Hz, 2H, H_b), 8.47 (d, *J*= 8.0 Hz, 2H, H_c), 7.99 (dd, *J*=8.0, 7.6 Hz, 1H, H_a), 7.82 (dd, *J*= 8.0, 7.6 Hz, 2H, H_d), 7.61 (d, *J*= 8.0 Hz, 2H, H_e), 7.47 (d, *J*=4.0 Hz, 2H, H_f), 6.80-6.79 (dd, *J*= 0.8, 4.0 Hz, 2H, H_g), 2.56 (s, 6H, H_h); ^{13}C NMR (400 MHz, $CDCl_3$): δ= 155.5 (q), 154.9 (q), 151.9 (q), 142.8 (q), 142.5 (q), 137.8 (PyrCH), 137.4 (PyrCH), 126.3 (PyrroleCH), 124.5 (PyrroleCH), 121.2 (PyrCH, C_b), 118.6 (PyrCH, C_c), 118.1 (PyrCH, C_e), 15.7 (CH_3, $C_{h'}$); LRESI-MS: *m/z* = 426 $[M+1]^+$; HRESI-MS: *m/z* = 426.10992 (calcd for $C_{25}H_{20}N_3S_2$, 426.10932).

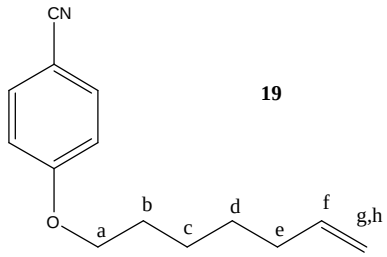

19

4-Hept-6-enyloxy-benzonitrile (19): Cs_2CO_3 (13.03g, 40mmol), 7-bromo-hepten-1-ene (3.54g, 20mmol), NaI (600mg, 4mmol) were added to a solution of 4-hydroxybenzonitrile (2.38g, 20mmol) in DMF (40ml). The reaction mixture was left under stirring overnight at 80°C. The solvent was removed under reduced pressure and, after addition of brine, the crude product was extracted with DCM; the organic layer was collected and dried over Na_2SO_4. Then the solvent was removed and the crude product was purified by column chromatography (petroleum ether/diethyl ether 60:40 v/v), obtaining the product in 92% of yield (3.95g); ^{1}H NMR (400MHz, $CDCl_3$) δ= 7.57 (d, *J*= 8.8 Hz, 2H, ArCH), 6.93 (d, *J*= 9.2 Hz, 2H, ArCH), 5.86-5.76 (m, 1H, H_f), 5.04-4.94 (m, 2H, $H_{g,h}$), 3.99 (t, *J*=6.8 Hz, 2H, H_a), 2.11-2.07 (m, 2H, CH_2), 1.84-1.77 (m, 2H, CH_2), 1.48-1.45 (m, 4H, CH_2); ^{13}C NMR (400MHz, $CDCl_3$) δ= 162.4 (q, C), 138.6 (CH, C_f), 133.9 (CH, ArCH), 119.3 (q, ArC), 115.1 (CH, ArCH), 114.6 (CH_2, $C_{g,h}$), 103.6 (q, ArC), 68.3 (CH_2), 33.6 (CH_2), 28.8 (CH_2), 28.5 (CH_2), 25.4 (CH_2).

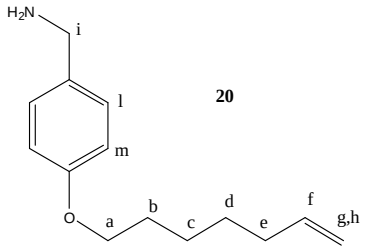

20

4-Hept-6-enyloxy-benzylamine (20): A solution of 4-Hept-6-enyloxy-benzonitrile (3.00g, 13.9 mmol) in THF (18ml) was added dropwise to a solution of $LiAlH_4$ (1.78g, 41mmol) in THF (41ml), at -78°C; the reaction mixture was then let going to room temperature and stirred for 45 minutes, after that it was heated to reflux for 3 hours. The reaction mixture was cooled at 0°C and diethyl ether (100 ml) was added, then it was quenched by successive dropwise additions of water (1.78 ml), 15% aqueous sodium hydroxide solution (1.78 ml) and finally water (5.4 ml). The reaction mixture was let under stirring at room temperature overnight then it was filtered through a sinter

and the solvent was removed under reduced pressure to give the product as a white solid (2.9g, 94%); ^{1}H NMR (400MHz, $CDCl_3$) δ= 7.21 (d, *J*= 8.8 Hz, 2H, H_l), 6.86 (d, *J*= 8.8 Hz, 2H, H_m), 5.87-5.78 (m, 1H, H_f), 5.04-4.93 (m, 2H, $H_{g,h}$), 3.94 (t, *J*= 6.6 Hz, 2H, H_a), 3.80 (s, 2H, H_i), 2.11-2.06 (m, 2H, H_e), 1.82-1.75 (m, 2H, H_b), 1.48-1.44 (m, 4H, $H_{c,}$d); ^{13}C NMR (400MHz, $CDCl_3$) δ= 158.0 (q, ArC), 138.8 (CH, C_f), 135.4 (q, ArC), 128.2 (CH, C_l), 114.5 (CH, C_m), 114.4 (CH_2, $C_{g,h}$), 67.9 (CH_2, C_a), 45.9 (CH_2, C_i), 33.7 (CH_2, C_e), 29.1 (CH_2, C_b), 28.6 (CH_2, C_{c-d}), 25.5 (CH_2, C_{c-d}); LRESI-MS: *m/z* = 220 $[M+1]^+$; HRESI-MS: *m/z* = 220.16960 (calcd for $C_{14}H_{22}ON$, 220.16959).

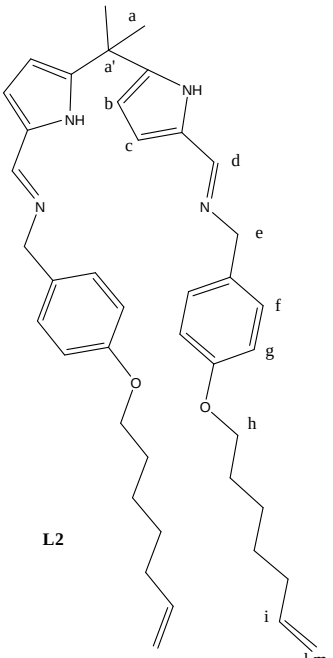

L2

Chemical Formula: $C_{41}H_{52}N_4O_2$
Molecular Weight: 632.87718

L2: 4-Benzylamine (3.11 g, 14.2 mmol) dissolved in MeOH (30 ml) was added dropwise to a solution of 5,5'-diformyl-2,2'-dimethyldipyrromethane (1.63 g, 7.1 mmol) in MeOH (120ml). The solution was stirred at room temperature overnight, then the solvent was removed under reduced pressure. The product was collected after precipitation from diethyl ether and filtration (180 mg, 5%).

^{1}H NMR (400 MHz, $CDCl_3$): δ= 8.00 (s, 2H, H_d), 7.16 (d, *J*= 8.0 Hz, 4H, H_f), 6.85 (d, *J*= 8.8 Hz, 4H, H_g), 6.37 (d, *J*= 3.6 Hz, 2H, H_c), 6.03 (d, *J*= 3.6 Hz, H_b), 5.87-5.76 (m, 2H, H_i), 5.03-4.93 (m, 4H, $H_{l,m}$), 4.58 (s, 4H, H_e), 3.93 (t, *J*= 6.6 Hz, 4H, H_h), 2.10-2.05 (m, 4H, H $_{alkyl\ chain}$), 1.81-1.74 (m, 4H, H $_{alkyl\ chain}$), 1.66 (s, 6H, H_a), 1.47-1.45 (m, 8H, $H_{alkyl\ chain}$); ^{13}C NMR (400MHz, $CDCl_3$): δ= 158.2 (q), 152.0 (CH, C_d), 142.8 (q), 138.8 (CH, C_i), 131.3 (q), 129.6 (q), 129.2 (CH, C_f), 114.8 (CH, $C_{pyrrole}$), 114.6 (CH, C_g), 114.4 (CH_2, $C_{l,m}$), 106.0 (CH, $C_{pyrrole}$), 67.9 (CH_2, C_h), 63.8 (CH_2, C_e), 35.8 (q, $C_{a'}$), 33.7 (CH_2, $C_{alkyl\ chain}$), 29.1(CH_2, $C_{alkyl\ chain}$), 28.8 (CH_2, $C_{alkyl\ chain}$), 28.7 (CH_3, C_a), 25.6 (CH_2, $C_{alkyl\ chain}$); LRESI-MS: *m/z* = 632.9 $[M+1]^+$, HRESI-MS: *m/z* = 633.41685 (calcd for $C_{41}H_{53}N_4O_2$, 633.41681).

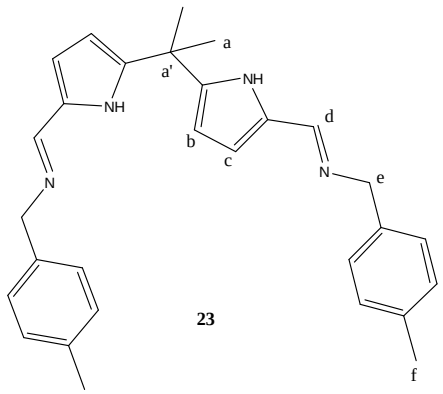

23

Chemical Formula: $C_{29}H_{32}N_4$
Molecular Weight: 436.59118

23: 4-Benzylmethylamine (2.42 g, 20 mmol) dissolved in MeOH (1 ml) was added dropwise to a solution of 5,5'-diformyl-2,2'-dimethyldipyrromethane (2.30 g, 10 mmol) in MeOH (120ml). The solution was stirred at room temperature overnight, then the solvent was removed under reduced pressure. The product was collected after precipitation from diethyl ether and filtration as a pink solid (2.83 g, 65%).
^{1}H NMR (400 MHz, $CDCl_3$): δ= 8.02-8.01 (m, 2H, H_d), 7.17-7.12 (m, 8H, $H_{phenylene}$), 6.37 (d, *J*= 3.6 Hz, 2H, H_c), 6.03 (d, *J*= 3.6 Hz, 2H, H_b), 4.60 (s, 4H, H_e), 2.33 (s, 6H, H_f), 1.66 (s, 6H, H_a); ^{13}C NMR (400MHz, $CDCl_3$): δ= 152.2 (CH, C_d), 142.8 (q), 136.6 (q), 136.4 (q), 129.6 (q), 129.2 (phenyleneCH), 128.0 (phenyleneCH), 114.9 (pyrroleCH), 106.0 (pyrroleCH), 64.1 (CH_2, C_e), 35.7 (q, $C_{a'}$), 28.7 (CH_3, C_a), 21.1 (CH_3, C_f); LRESI-MS: *m/z* = 437 $[M+1]^+$; HRESI-MS: *m/z* = 437.26931 (calcd for $C_{29}H_{33}N_4$, 437.26997).

References

1. Hubin, T. J.; Busch, D. H.; *Coord. Chem. Rev.* **2000**, *200-202*, 5-52.
2. Thompson, M. C.; Busch, D. H. *J. Am. Chem. Soc*. **1964**, *86*, 3651.
3. Thompson, M. C.; Busch, D. H. *Chem. Eng. News* **1962**, *17*, 57.
4. For a historical perspective, see: Busch, D. H.; Vance, A. L.; Kolchinski, G. in: J.-M. Lehn (Ed.), *Comprehensive Supramolecular Chemistry*, vol. 9, Elsevier Science, New York, **1996**, 1–42.
5. Hubin, T. J.; Kolchinski, A. G.; Vance, A. L.; Busch, D. H. in: G.W. Gokel (Ed.), *Advances in Supramolecular Chemistry*, vol. 5, JAI Press, Stanford, CT, USA, **1999**.
6. Busch, D. H. *J. Incl. Phen*. **1992**, *12* 389.
7. Busch, D. H.; Stephonson, N. A. *Coord. Chem. Rev*. 1990, *100*, 119.
8. Wasserman, E. *J. Am. Chem. Soc*. **1960**, *82*, 4433.
9. Frisch, H. L.; Wasserman, E. *J. Am. Chem. Soc*. **1961**, *83*, 3789.
10. Wasserman, E. *Sci. Am. 207* **1962**, 94.
11. Harrison, I. T.; Harrison, S. *J. Am. Chem. Soc.* **1967**, 89, 5723.
12. Mohr, B.; Weck, M.; Sauvage, J.-P.; Grubbs, R. H. *Angew. Chem. Int. Ed. Engl.* **1997**, *36*, 1308.

13. Gibson, H. W.; Engen, P. T.; Lee, S.-H.; Liu, S.; Marand, H.; Bheda, M. C. *Polym. Prepr. (Am. Chem. Soc. Div. Polym. Chem.)* **1993,** *34*, 64.
14. Shen, Y. X.; Xie, D.; Gibson, H. W. *J. Am. Chem. Soc*. **1994**, *116*, 537.
15. Gibson, H. W.; Liu, S.; Lecavalier, P.; Wu, C.; Shen, Y. X.; *J. Am. Chem. Soc*. **1995**, *117*, 852.
16. Lindoy, L. F.; *The Chemistry of Macrocyclic Ligand Complexes*, Cambridge University Press, Cambridge, **1989**.
17. Melson, G. *Coordination Chemistry of Macrocyclic Compounds*, Plenum, New York, **1979**.
18. Parker, C. (Ed.), *Macrocyclic Synthesis: A Practical Approach*, Oxford University Press, Oxford, UK, **1996**.
19. Bradshaw, J. S.; Krakowiak, K. E.; Izatt, R. M. *Aza-Crown Macrocycles*, Wiley, New York, **1993**.
20. Amabilino, D. B.; Stoddart, J. F. *Chem. Rev*. **1995**, *95*, 2725, and references therein.
21. Chambron, J.-C.; Dietrich-Buchecker, C.; Sauvage, J.-P. in: J.-M. Lehn (Ed.), *Comprehensive Supramolecular Chemistry*, vol. 9, Elsevier Science, New York, **1996**, pp. 43–83, and references therein.
22. Curry, J. D.; Busch, D. H. *J. Am. Chem. Soc.* **1964**, *86*, 592.
23. Melson, G. A; Busch, D. H. *J. Am. Chem. Soc*. **1965**, *87*, 1706.
24. Sauvage, J.-P. *Acc. Chem. Res*. **1990,** *23*, 319.
25. Schill, G. *Catenanes, Rotaxanes and Knots*, Academic Press, New York, **1971**.
26. Dietrich-Buchecker, C. O.; Sauvage, J.-P. *Tet. Lett.* **1983**, *24*, 5095.
27. Dietrich-Buchecker, C. O.; Sauvage, J.-P. *J. Am. Chem. Soc*. **1984**, *106*, 3043.
28. Mohr, B.; Weck, M.. Sauvage, J.-P.; Grubbs, R. H. *Angew. Chem. Int. Ed. Engl*. **1997,** *36*, 1308.
29. For reviews on the metal-template synthesis of mechanically interlocked molecules,see : a) MolecularCatenanes , Rotaxanes and Knots: A Journey Through theWorld of Molecular Topology (Eds.: J.-P. Sauvage,C . Dietrich-Buchecker),W iley-VCH,Weinheim, **1999**; b) Collin, J.-P.; Dietrich-Buchecker, C.; Gavina, P.; JimLnez-Molero, M. C.; Sauvage, J.-P. *Acc. Chem. Res*. **2001**, 34, 477 – 487; c) Menon, S. K.; Guha, T. B.; Agrawal, Y. K. *Rev. Inorg. Chem*. **2004**, *24*,97 – 133; d) Cantrill, S. J.; Chichak, K. S.; Peters, A. J.; Stoddart, J. F. *Acc. Chem. Res*. **2005**, *38*, 1 – 9.
30. For “active-metal-template” rotaxane synthesis,in which the metal acts as both a template and a catalyst for covalent-bond formation and thus generally changes oxidation state,coordination number,and/or geometry during the reaction, see: a) Aucagne, V.; Hanni, K: D.; Leigh, D. A.; Lusby, P. J.; Walker, D. B.; *J. Am. Chem. Soc*. **2006**, *128*,2186 – 2187; b) Saito, S.; Takahashi, E.; Nakazono, K. *Org. Lett*. **2006**, *8*,5133 – 5136; c) Berna, J.; Crowley, J. D.; Goldup, S. M.;

Hanni, K. D.; Lee, A.-L.; Leigh, D. A. *Angew. Chem*. **2007**, *119*,5811 – 5815; *Angew. Chem. Int. Ed.* **2007**, *46*,5709 – 5713; d) Aucagne, V.; Berna,J.; Crowley, J. D.; Goldup, S. M.; Hanni, K. D.; Leigh, D. A.; Lusby, P. J.; Ronaldson, V. E.; Slawin, A. M. Z.; Viterisi, A.; Walker, D. B.; *J. Am. Chem. Soc.* **2007**, *129*,11950 – 11963; e) Crowley, J. D.; Hanni, K. D.; Lee, A.-L.; Leigh, D. A. *J. Am. Chem. Soc*. **2007**, *129*, 12092 – 12093; f) Goldup, S. M.; Leigh, D. A.; Lusby, P. J.; McBurney, R. T.; Slawin, A. M. Z. *Angew. Chem*. **2008**, *120*,3429 –3432; *Angew. Chem. Int. Ed.* **2008**, *47*,3381 – 3384; g) Berna, J.; Goldup, S. M.; Lee, A.-L.; Leigh, D. A.; Symes, M. D.; Teobaldi, G.; Zerbetto, F.; *Angew. Chem*. **2008**, *120*,4464 – 4468; *Angew. Chem. Int. Ed*. **2008**, *47*,4392 – 4396.

31. a) Dietrich-Buchecker, C.; Sauvage, J.-P.; Kern, J.-M.; *J. Am. Chem. Soc*. **1989**, *111*,7791 – 7800; b) Armaroli, N.; Balzani, V.; Collin, J.-P; Gavina, P.; Sauvage, J.-P.; Ventura, B. *J. Am. Chem. Soc*. **1999**, *121*,4397 – 4408; c) Raehm, L.; Kern, J.-M.; Sauvage, J.-P. *Chem. Eur. J.* **1999**, *5*,3310 –3317.
32. a) Chambron, J.-C.; Harriman, A.; Heitz, V.; Sauvage, J.-P. *J. Am. Chem. Soc*. **1993**, *115*,6109 – 6114; b) Andersson, M.; Linke, M.; Chambron,J.-C.; Davidsson, J.; Heitz, V.; Hammarstrom, L.; Sauvage, J.-P. *J. Am. Chem. Soc.* **2002**, *124*,4347 – 4362; c) Mobian, P.; Kern,J.-M.; Sauvage, J.-P. *Angew. Chem*. **2004**, *116*,2446 – 2449; *Angew. Chem. Int. Ed*. **2004**, *43*,2392 – 2395; d) Collin, J.-P.; Jouvenot, D.; Koizumi, M.; Sauvage, J.-P. *Eur. J. Inorg. Chem*. **2005**, 1850 – 1855; e) Kwan, P. H.; Swager, T. M.; *J. Am. Chem. Soc*. **2005**, *127*,5902 – 5909; f) Bonnet, S.; Collin, J.-P. *Chem. Soc. Rev.* **2008**,*37*, 1207 – 1217.
33. a) Dietrich-Buchecker, C. O.; Kern, J.-M.; Sauvage, J.-P. *J. Chem. Soc. Chem. Commun.* **1985**,760 – 762; b) Albrecht-Gary, A.-M.; Saad, Z.; Dietrich-Buchecker, C. O.; Sauvage, J.-P *J. Am. Chem. Soc*. **1985**, *107*,3205 – 3209; c) Albrecht-Gary, A.-M.; Saad, Z.; Dietrich-Buchecker, C. O.; Sauvage, J.-P. *J. Am. Chem. Soc*. **1988**, *110*, 1467 – 1472; d) Leigh, D. A.; Lusby, P. J.; Slawin, A. M. Z.; Walker, D. B. *Angew. Chem*. **2005**, *117*,4633 – 4640; *Angew. Chem. Int. Ed.* **2005**, *44*,4557 – 4564.
34. Arnaud-Neu, F. A.; Marques, E.; Schwing-Weill, M.-J.; Dietrich-Buchecker, C. O.; Sauvage, J.-P.; Weiss, J. *New J. Chem*. **1988**, *12*, 15 – 20.
35. a) Champin, B.; Mobian, P.; Sauvage, J.-P. *Chem. Soc. Rev*. **2007**, *36*, 358 – 366; b) Kay, E. R.; Leigh, D. A.; Zerbetto, F. *Angew. Chem*. **2007**, *119*,72 – 196; *Angew. Chem. Int. Ed*. **2007**, *46*, 72–191.
36. a) Leigh, D. A.; Lusby, P. J.; Teat, S. J.; Wilson, A. J.; Wong, J. K. Y.; *Angew. Chem.* **2001**, *113*,1586 – 1591; *Angew. Chem. Int. Ed.* **2001**, *40*, 1538 – 1543; b) Hogg, L.; Leigh, D. A.; Lusby, P. J.; Morelli, A.; Parsons, S.; Wong, J. K. Y. *Angew. Chem*. **2004**, *116*, 1238 – 1241;

Angew. Chem. Int. Ed. **2004**, *43*, 1218 – 1221; c) Hutin, M.; Schalley, C. A.; Bernardinelli, C.; Nitschke, J. R. *Chem. Eur. J*. **2006**, *12*, 4069 – 4076.

37. a) Dietrich-Buchecker, C. O.; Sauvage, J.-P.; Kintzinger, J.-P. *Tet. Lett*. **1983**, *24*,5095 – 5098; b) Sauvage, J.-P *Acc. Chem. Res*. **1990**, *23*, 319 – 327; c) Fuller, A.-M. L.; Leigh, D. A.; Lusby, P. J. *Angew. Chem*. **2007**, *119*,5103 – 5107; *Angew. Chem. Int. Ed*. **2007**, *46*, 5015 – 5019.
38. a) JimLnez, M. C.; Dietrich-Buchecker, C. O.; Sauvage, J.-P. *Angew. Chem.* **2000**, *112*, 3422 – 3425; *Angew. Chem. Int. Ed.* **2000**, *39*,3284 – 3287; b) JimLnez-Molero, M. C.; Dietrich-Buchecker, C. O.; Sauvage, J.-P. *Chem. Eur. J.* **2002**, *8*, 1456 – 1466.
39. Mohr, B.; Weck, M.; Sauvage, J.-P.; Grubbs, R. H. *Angew. Chem*. **1997**, *109*,1365 – 1367; *Angew. Chem. Int. Ed. Engl*. **1997**, *36*, 1308 – 1310.
40. a) Sauvage, J.-P.; Ward, M. *Inorg. Chem*. **1991**, *30*, 3869 – 3874; b) Piguet, C.; Bernardinelli, G.; Williams, A. F.; Bocquet, B. *Angew. Chem***. 1995**, *107*,618 – 621; *Angew. Chem. Int. Ed. Engl.* **1995**, *34*,582 – 584; c) Mobian, P.; Kern, J.-M.; Sauvage, J.-P. *J. Am. Chem. Soc*. **2003**, *125*,2016 – 2017; d) Arico, F.; Mobian, P.; Kern, J.-M.; Sauvage, J.-P.; *Org. Lett.* **2003**, *5*,1887 – 1890; e) Chambron, J.-C.; Collin, J.-P.; Heitz, V.; Jouvenot, D.; Kern, J.-M.; Mobian, P.; Pomeranc, D.; Sauvage, J.-P. *Eur. J. Org. Chem*. **2004**, 1627 – 1638.
41. a) Fuller, A.-M.; Leigh, D. A.; Lusby, P. J.; Oswald, I. D. H.; Parsons, S.; Walker, D. B. *Angew. Chem*. **2004**, *116*,4004 – 4008; *Angew. Chem. Int. Ed.* **2004**, *43*, 3914 – 3918; b) Furusho, Y.; Matsuyama, T.; Takata, T.; Moriuchi, T.; Hirao, T.; *Tet. Lett*. **2004**, *45*, 9593 – 9597; c) Fuller, A.-M- L.; Leigh, D. A.; Lusby, P. J.; Slawin, A. M. Z.; Walker, D. B. *J. Am. Chem. Soc*. **2005**, *127*, 12612 – 12619.
42. Hamann, C.; Kern, J.-M.; Sauvage, J.-P. *Inorg. Chem*. **2003**, *42*, 1877 – 1883.
43. Goldup, S. M.; Leigh, D. A.; Lusby, P. J.; McBurney, R. T.; Slawin, A. M. Z. *Angew. Chem. Int. Ed.* **2008**, *47*, 6999-7003.
44. Kolarik, Z. *Chem. Rev.* **2008,** *108*, 4208–4252.
45. Kosugi, M. et al. *Chem. Letters* , **1977**, 301.
46. Milstein, D.; Stille, J. K. *J. Am. Chem. Soc.* **1978**, *100*, 3636.
47. Casado, A. L.; Espinet, P. *Organometallics* **1998**, *17*, 954–959.
48. Dai, Z.; Proni, G.; Mancheno, D.; Karimi, S.; Berova, N.; Canary, J. W. *J. Am. Chem. Soc.*, **2004**, *126*, 11760-11761.
49. Newkome, G. R.; Hager, D. C.; Kiefer, G. E. *J. Org. Chem.*, **1986**, *51*, 850-853.
50. Littler, B. J.; Miller, M. A.; Hung, C.-H.; Wagner, R. W.; O'Shea, D. F.; Boyle, P. D.; Lindsey, J. S. *J. Org.Chem.*, **1999**, *64* (4), 1391-1396.

51. Love, J. B.; Blake, A. J.; Wilson, C.; Reid, S. D.; Novak, A.; Hitchcock, P. B. *Chem. Comm.*, **2003**, 1682-1683.